Haptic Human Human Interaction

motor learning & haptic communication

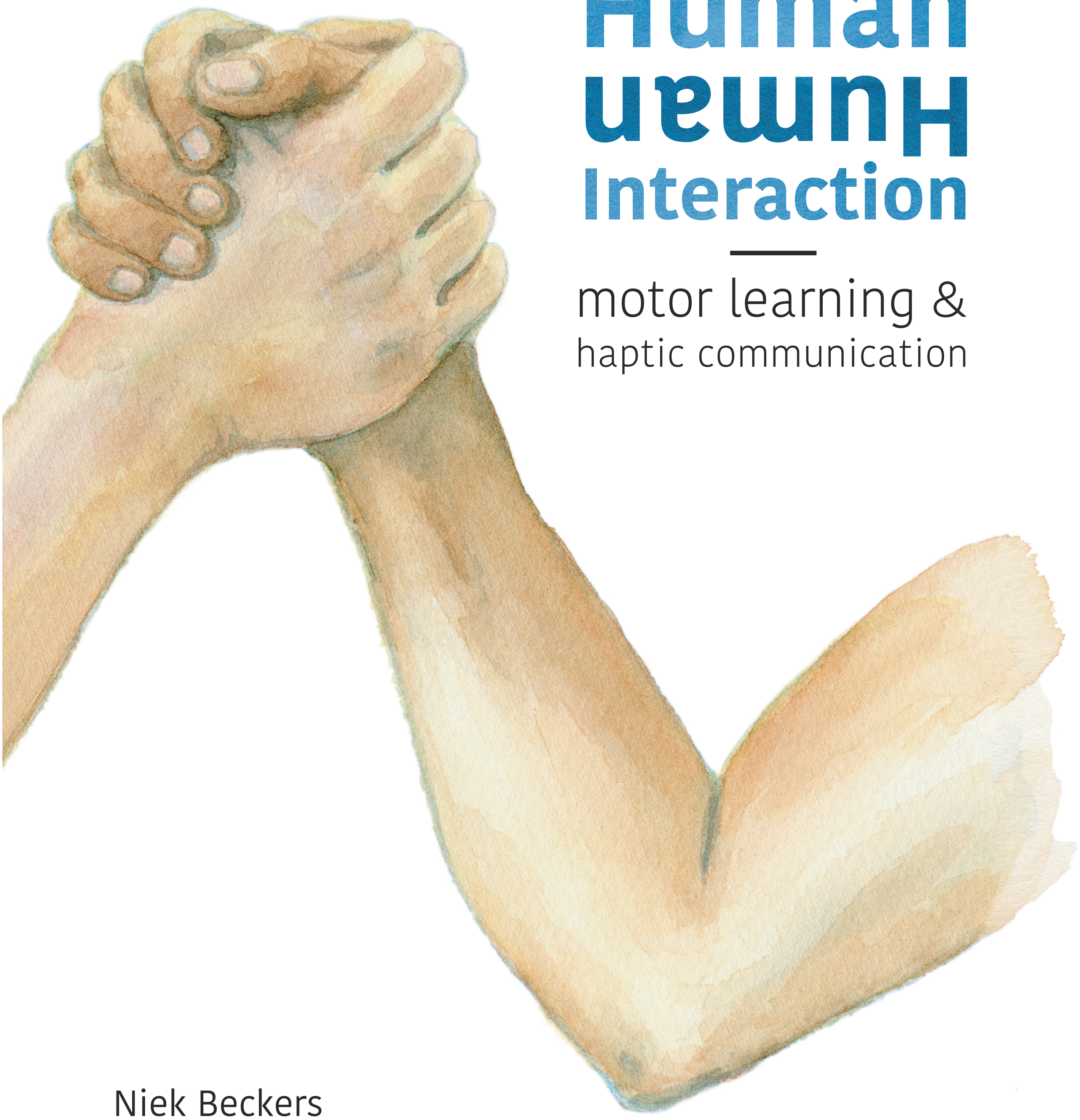

Niek Beckers

HAPTIC HUMAN-HUMAN INTERACTION
MOTOR LEARNING & HAPTIC COMMUNICATION

N.W.M. Beckers

HAPTIC HUMAN-HUMAN INTERACTION
MOTOR LEARNING & HAPTIC COMMUNICATION

PROEFSCHRIFT

ter verkrijging van
de graad van doctor aan de Universiteit Twente,
op gezag van de rector magnificus,
prof.dr. T.T.M. Palstra,
volgens besluit van het College voor Promoties
in het openbaar te verdedigen
op vrijdag 12 juli 2019 om 14.45 uur

door

Nicolaas Willem Maria Beckers

geboren op 28 februari 1986
te Nijmegen

Dit proefschrift is goedgekeurd door:

de promotor:	prof.dr.ir. H. van der Kooij
de co-promotor:	dr. E.H.F. van Asseldonk

Cover design: Brigit Hoogenberk, brgt. illustraties, brgt.nl
Printed by: Ipskamp printing
ISBN: 978-90-365-4807-6
DOI: 10.3990/1.9789036548076

PROMOTIE COMMISSIE:

Voorzitter Secretaris	prof.dr. G.P.M.R. Dewulf	Universiteit Twente
Promotor	prof.dr.ir. H. van der Kooij	Universiteit Twente
Co-promotor	dr. E.H.F. van Asseldonk	Universiteit Twente
Leden	prof.dr.ir. J.H. Buurke	Universiteit Twente
	prof.dr.ir. D.M. Brouwer, PDEng	Universiteit Twente
	prof.dr.ir. D.A. Abbink	Technische Universiteit Delft
	prof.dr. L. Marchal-Crespo	Universität Bern, Switzerland
	prof.dr. J.B.J. Smeets	Vrije Universiteit Amsterdam

This work is part of the research programme Symbionics (project number 13524) which is partly financed by the Netherlands Organisation for Scientific Research (NWO).

NWO
Applied and
Engineering Sciences

This research benefited from the advice and financial support of the following companies, whose support is thankfully acknowledged.

Hankamp
Rehab

Hocoma
a DIH brand

MOOG

FESTO

Publication of this thesis was partly financially supported by the department of Biomechanical Engineering, University of Twente.

UNIVERSITY
OF TWENTE.

Contents

Summary ix

Samenvatting xiii

1. Introduction 3

2. BROS: the admittance-controlled multiplayer haptic robot 19

3. Haptic interaction between humans neither facilitates nor interferes with learning novel dynamics 51

4. Haptic interaction does not improve motor learning of a visuomotor rotation 73

5. Motion plans of rigidly-coupled pairs change predictably in joint reaching 99

6. Haptically-interacting individuals do not need to exchange information through the interaction force to improve in a tracking task 123

7. General discussion 153

A. BROS – Supplementary information 183

B. Haptic interaction does not improve motor learning of a visuomotor rotation – Supplementary information 185

C. Motion plans of rigidly-coupled pairs change predictably in joint reaching – Supplementary information 193

D. Haptic communication in a tracking task – Supplementary information 199

Dankwoord 207

Summary

Haptic interaction with a partner – interaction by exerting forces onto each other directly or through an object – plays an important role in our lives. It can help us to coordinate our actions; dance partners can smoothly coordinate dance moves by communicating their intentions through interaction forces. Many new movement or *motor* tasks – referred to as motor learning – are also learned while haptically-interacting with someone else; parents physically support their child while it learns to ride a bicycle or therapists help individuals suffering from stroke to regain motor function through physical assistance. However, our knowledge of haptic human-human interaction and its implications on how we learn new motor tasks is still limited.

The goal of this thesis is to create a better understanding of *whether* haptic interaction between two humans improves individual motor learning in a collaborative motor task and *why* haptic interaction would improve motor performance and learning. We approached this goal in two main steps: (1) we performed two studies in which participants learned a new motor task while haptically interacting with each other; and (2) we investigated whether and how the interacting participants used the interaction force to coordinate actions or to improve their own task performance.

To investigate how two humans haptically collaborate, we designed and built BROS (Bi-partner RObotic Setup), a dual-manipulandum robotic setup (Chapter 2 and Fig. 1). BROS consists of two identical robotic manipulanda – one for each individual in a pair – that participants could move with their hand in a horizontal plane. We could generate many types of haptic interactions between the two partners, ranging from a stiff connection, similar to carrying a table together, to a compliant connection, such as holding a rubber band together.

Haptic interaction between humans does not improve individual motor learning in a collaborative motor task

We tested how haptic interactions between two humans learning the same motor task influenced their individual motor learning using two different learning tasks (Chapters 3 and 4). We assessed motor learning by analyzing which final performance they reached after sufficient practice and at what rate individuals improved their performance to their final performance level. The partners tracked the same randomly- and continuously-moving target in a plane as accurately as possible in both tasks (see Fig. 1). In the first experiment, we introduced a dy-

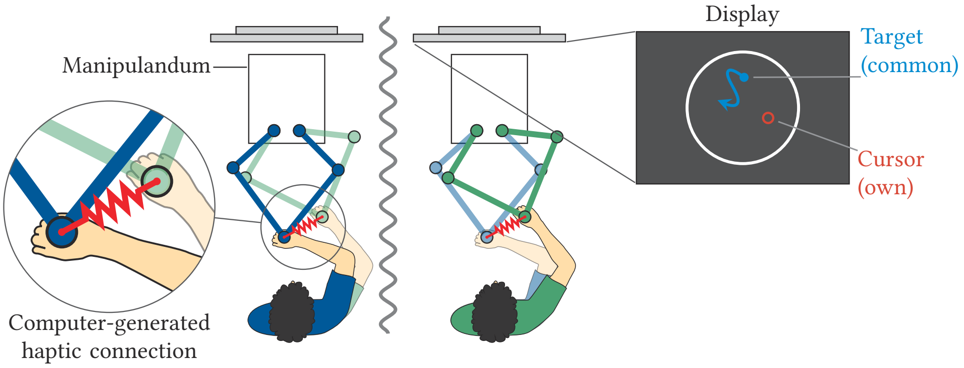

Figure 1. | BROS, the dual-manipulandum robotic setup. Participants were haptically-coupled using BROS.

namic perturbation using a velocity-dependent force field in the tracking task to increase the task difficulty and to elicit learning (Chapter 3). The force field perturbed the hand movements of each partner proportional to their own movement velocity. The force field initially degraded tracking performance, but participants learned how to compensate for the force field and gradually improved tracking performance over time. To study whether haptic interaction would influence motor learning, we intermittently connected the hands of both partners using a computer-generated compliant connection *without making the individuals explicitly aware of the interaction* while they performed the tracking task. Although haptic interaction improved performance *during* interaction, practicing together did not generalize to better tracking performance when doing the task alone. Haptic interaction also did not speed up learning.

It is possible that haptic interaction did not improve individual motor learning due to the force field learning task. In our force field experiment, the force field was superimposed on the interaction force; hence, the force field and interaction force were in the same sensory domain. The force field could have limited the usefulness of the interaction force to improve each individual's motor learning.

We, therefore, performed a second experiment using the same tracking task but introduced a visual perturbation – a visuomotor rotation – instead of a force field to evoke learning (Chapter 4). The visual feedback of the arm movement on the computer display is rotated with respect to the actual arm movement in a visuomotor rotation. Similar to the force field, humans gradually learn how to move in such a visual perturbation. To better understand why haptic interaction would improve learning, we also investigated how two important factors influenced individual motor learning: the amount of interaction time and the strength of the interaction (e.g., the strength of the connection between the partners). Consistent with our force field study, we still found no benefit of haptic human-human interaction on individual motor learning in a visuomotor rotation compared to individuals who practiced the task alone. Interaction led neither to a better motor skill performance nor an increased motor learning rate. Increasing the amount of interaction time or interaction strength also did not improve motor learning.

Combining the results of these two studies, we conclude that solely being haptically coupled to a partner who is learning the same tracking task does not improve individual motor learning in a visual or dynamic perturbation.

Haptic communication is not necessary to explain the motor behavior in collaborative motor tasks

Although haptic interaction does not lead to better motor performance when performing the tracking task alone, it does improve motor performance *during* interaction. More importantly, we found that interaction improves performance in a tracking task even when unconsciously being coupled to a worse-performing partner. How does haptic interaction with a worse-performing partner still improve performance?

To explain this result, we developed a computational model in which we mechanically coupled two simulated partners who both independently performed the same aforementioned continuous tracking task (Chapter 6). The model assumed that the partners were unaware of the haptic connection; the partners were only mechanically influenced by the interaction force originating from the coupling. Thus, the simulated partners did not exchange any information about each other or the task through the interaction force, such as estimating the actions or intentions of their partner, to improve their performance. We refer to such exchange of information through the interaction force as haptic communication. This ‘no haptic communication’ model accurately predicted the improvement due to interaction observed in the experimental data. Additional model analysis suggested that haptic interaction improved performance because the compliant connection between the participants partially compensated for each partner’s motor output variability, which includes tracking errors such as overshoots. The worse-performing partners in a pair additionally benefited from the haptic guidance provided by their better-performing partner. Hence, the model suggested that the participants did not necessarily need to haptically communicate to improve performance in a continuous tracking task.

This explanation is in contrast with a previous study[1], which proposed that partners estimated each others movement goals through the interaction force to improve their own estimate of the target location, which was subsequently used to improve their performance. This hypothesis assumed that the partners were able to accurately perceive the interaction force. However, when we impaired the perception of the interaction force by superimposing a force field on the tracking task and interaction force, participants still improved due to the haptic interaction similarly to when no force field was present. We showed that the interaction force was biased in direction and magnitude by the force field, even when assuming that the partners learned a substantial, but incomplete internal model of the force field. These results suggest that haptically-interacting partners do not need to have an accurate perception of the interaction force to yield similar performance improvements during interaction as when no force field was present. This further affirms that haptic communication was not necessary to improve performance during haptic interaction in a continuous tracking task.

Researchers suggested that the interaction force can be used to negotiate roles – such as leader-follower – between rigidly-coupled participants to improve performance in a point-to-point reaching task. How did the partners achieve such coordination and how did the roles emerge trial-by-trial? To answer these questions, we examined how two rigidly-coupled individuals coordinated their actions trial-by-trial during a collaborative reaching task to the same stationary target (Chapter 5). The joint reaching movements were remarkably consistent across the experiment and pairs also produced opposing forces between them that they did not minimize over trials. Using a computational model of the joint reaching task, we found that both partners executed their own pre-programmed motion plan that ignored their partner's behavior. The results suggest that the partners did not exchange information through the interaction force to coordinate actions, similar to our results in the continuous tracking task.

In conclusion, the results of haptic interaction in a collaborative tracking task and collaborative reaching task suggest that haptically coupling two partners does not guarantee that the partners will communicate or coordinate actions through the haptic connection.

---

[1] A Takagi, G Ganesh, T Yoshioka, M Kawato, and E Burdet. Physically interacting individuals estimate the partner's goal to enhance their movements. *Nature Human Behaviour*, 1(3):0054, 2017.

Samenvatting

Haptische interactie met een partner – interactie door krachten rechtstreeks of via een voorwerp op elkaar uit te oefenen – speelt een belangrijke rol in ons leven. Het kan ons helpen onze bewegingen te coördineren: danspartners kunnen bijvoorbeeld dansbewegingen op elkaar afstemmen door hun intenties te communiceren via interactiekrachten. Nieuwe bewegingstaken of *motorische taken* kunnen worden geleerd (ook wel motorisch leren genoemd) terwijl mensen haptisch samenwerken met een partner. Therapeuten helpen mensen bijvoorbeeld met het herstellen van hun motorische functies na een beroerte door hen fysiek te ondersteunen. Echter, onze kennis van haptische mens-mens interactie en hoe deze ons kan helpen om nieuwe motorische taken te leren, is beperkt.

Het doel van dit proefschrift is om te onderzoeken of haptische interactie tussen twee mensen helpt om het motorisch leren van beide partners in een gezamenlijke motorische taak te verbeteren. We onderzochten hoe haptische interactie met een partner, die dezelfde taak oefende, het motorisch leren beïnvloedde in twee aparte leertaken. Daarnaast bestudeerden we of en hoe de partners de interactiekracht gebruikten om de prestaties te verbeteren in de motor taak of om acties te coördineren.

Om te onderzoeken hoe twee mensen haptisch samenwerken hebben wij de Bipartner Robotic Setup (BROS) ontworpen (Hoofdstuk 2). BROS bestaat uit twee identieke robotische manipulanda – één voor iedere partner – elk met een handvat die de deelnemer kon bewegen in een horizontaal vlak (Fig. 1). BROS stelde ons in staat om verschillende haptische connecties tussen de twee partners te maken, zoals een stijve of een flexibele verbinding. Een stijve verbinding is vergelijkbaar met het samen dragen van een tafel. Een flexibele verbinding is vergelijkbaar met het samen vasthouden van een elastiek.

Haptische interactie tussen twee mensen leidt niet tot een verbeterd motorisch leren in een gezamenlijke motorische taak

We onderzochten hoe de haptische interactie tussen twee partners die dezelfde motorische taak uitvoerden het motorisch leren in deze taak van elke partner individueel beïnvloedde. We hebben dit in twee verschillende leertaken getest (Hoofdstukken 3 en 4). Wij analyseerden het motorisch leren door het uiteindelijke prestatieniveau te berekenen en te analyseren hoe snel dit niveau werd bereikt. De motorische taak bestond uit het volgen van een doel op een scherm dat voor beide partners hetzelfde was (zie Fig. 1). Dit doel bewoog continu en onvoorspel-

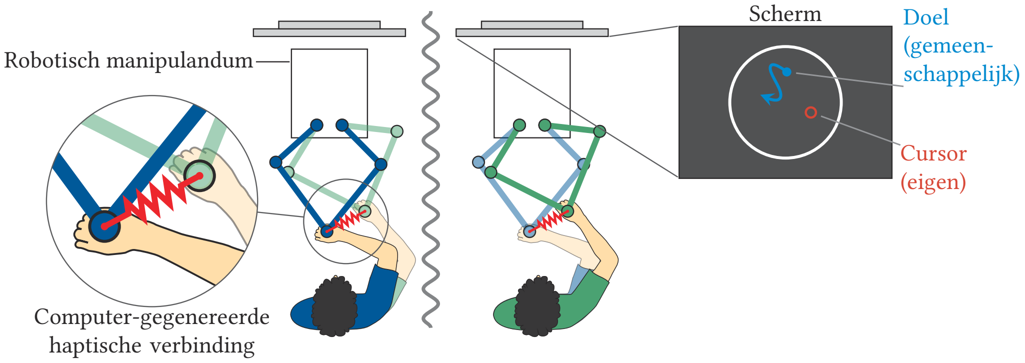

Figuur 1. | BROS, de dubbele robotische opstelling. De partners werden aan elkaar gekoppeld door BROS.

baar; de partners moesten dit doel zo precies mogelijk volgen. Om deze volgtaak moeilijker te maken en zo het motorisch leren te stimuleren introduceerden wij een dynamische verstoring met behulp van een snelheidsafhankelijk krachtveld in het eerste experiment. Het krachtveld verstoorde de handbewegingen als een functie van de bewegingssnelheid van beide partners. Deze verstoring verslechterde de prestaties in de volgtaak in eerste instantie, maar door oefening leerden de deelnemers om de krachtsverstoringen te compenseren en zo hun prestaties te verbeteren. We koppelden de twee deelnemers met een flexibele verbinding aan elkaar om te bestuderen of haptische interactie dit leerproces zou versnellen en tot betere eindprestaties zou leiden. *De twee partners werden niet op de hoogte gesteld van de koppeling*. Haptische interactie verbeterde de prestaties van beide partners *tijdens* de interactie, maar leidde niet tot betere prestaties wanneer de taak *alleen* werd uitgevoerd. Het leerproces werd ook niet versneld door haptische interactie.

Het is mogelijk dat het individuele leervermogen niet verbeterd werd door het krachtenveld. Het krachtveld werd toegevoegd aan de interactiekracht; de interactiekracht en het krachtveld bevonden zich dus in hetzelfde domein. Het is daarom mogelijk dat de bruikbaarheid van de interactiekracht om het leerproces te verbeteren werd beperkt door het krachtveld.

We voerden daarom een tweede studie uit met dezelfde volgtaak maar introduceerden nu een visuele verstoring: een visuomotor rotatie (Hoofdstuk 4). In een visuomotor rotatie wordt de visuele terugkoppeling van de handbewegingen op het computerscherm geroteerd ten opzichte van de echte handbewegingen. Dit resulteert in een fout tussen wat de deelnemer ziet waar zijn/haar hand is ten opzichte van waar hij/zij voelt waar de hand is, wat leidt tot een verslechtering van de volgprestaties. De visuomotor rotatie verslechterde de prestaties in de volgtaak, maar met voldoende oefening leren de deelnemers om de volgtaak accuraat uit te voeren door voor de visuele verstoring te compenseren. We onderzochten ook hoe twee belangrijke factoren invloed hadden op het individueel motorisch leren: de hoeveelheid interactietijd en de kracht van de haptische verbinding tussen de partners. Consistent met ons krachtveldexperiment vonden we geen voordeel van haptische interactie op individueel motorisch leren in een visuomotor rotatie vergeleken met individuen die de taak alleen leerden. Interactie leidde niet tot betere individuele prestaties, noch tot een sneller leerproces. Meer interactietijd of een hogere interactiesterkte had ook geen invloed op het leren.

Gebaseerd op deze twee experimenten concluderen we dat een haptische koppeling met een partner die dezelfde volgtaak leert niet leidt tot een verbeterd individueel motorisch leren in een dynamische of visuele verstoring.

Haptische communicatie is niet noodzakelijk om het gedrag tijdens haptische interactie te verklaren

Hoewel haptische interactie niet resulteerde in betere individuele prestaties wanneer de volgtaak vervolgens alleen werd uitgevoerd, werden de prestaties wel sterk verbeterd *tijdens* de haptische interactie. Wat nog interessanter was, was dat haptische interactie de prestaties verbeterde, zelfs als iemand gekoppeld was aan een slechter-presterende partner. Hoe kan haptische interactie met een slechtere partner je eigen prestaties verbeteren?

Om deze resultaten te verklaren ontwikkelden we een wiskundig model waarin we twee partners modelleerden die de volgtaak onafhankelijk van elkaar uitvoerden (Hoofdstuk 6). De twee gesimuleerde partners werden aan elkaar gekoppeld met een flexibele verbinding. Het model nam aan dat de partners zich niet bewust waren van de haptische koppeling; de partners werden alleen mechanisch beïnvloed door de interactiekracht afkomstig van de connectie. De partners wisselden dus geen informatie over elkaar of de taak uit via de interactiekracht in het model, zoals het schatten van elkaars acties of intenties om hun prestaties te verbeteren. Deze informatie uitwisseling via de interactiekracht wordt ‘haptische communicatie’ genoemd. Dit model voorspelde de prestatieverbeteringen door haptische interactie in de experimentele data nauwkeurig. Een aanvullende modelanalyse suggereerde dat haptische interactie prestaties verbeterde omdat de flexibele verbinding de motor variabiliteit, waaronder bewegingsfouten zoals het doel voorbij schieten, van beide partners gedeeltelijk compenseerde. De slechter-presterende deelnemer profiteerde bovendien van de haptische begeleiding van hun beter-presterende partner. Dus, het model suggereerde dat de partners niet haptisch hoefden te communiceren in een continue volgtaak om hun prestaties te verbeteren.

Deze verklaring staat lijnrecht tegenover een andere studie[1], waarin werd gesuggereerd dat partner elkaars bewegingsdoelen schatten via de interactiekracht om zo hun eigen inschatting van het doel te verbeteren, die vervolgens werd gebruikt om hun eigen volgprestaties te verbeteren. Hun hypothese veronderstelde onder andere dat de partners de interactiekracht nauwkeurig konden waarnemen. Wanneer we echter de waarneming van de interactiekracht bemoeilijkten door een krachtveld aan de volgtaak toe te voegen, verbeterden de deelnemers door haptische interactie net zoveel als toen er geen krachtveld aanwezig was. We toonden verder aan dat de waarneming van de interactiekracht in richting en grootte beïnvloed was door het krachtveld, zelfs als we aannamen dat de partners een substantieel maar incompleet model van het krachtveld hadden geleerd. Deze resultaten doen verder vermoeden dat partners de interactiekracht niet nauwkeurig hoefden waar te nemen om dezelfde prestatieverbeteringen te krijgen vergeleken met toen er geen krachtveld aanwezig was. Dit bekrachtigt dat haptische communicatie niet noodzakelijk was om de prestaties te verbeteren tijdens haptische interactie in een continue volgtaak.

In een andere taak, waarin twee haptisch-gekoppelde partners samen naar een gemeenschappelijk stilstaand doel reikten, zag een andere studie dat de partners verschillende rollen – zoals leider en volger – aannamen. De onderzoekers suggereerden dat de samenwerkende partners de interactiekracht gebruikten om deze rollen te verdelen en acties te coördineren. Maar hoe coördineerden de partners hun acties en hoe kwamen deze rollen tot stand tijdens de haptische interactie? We onderzochten hoe twee star-gekoppelde partners hun acties coördineerden in een gezamenlijke reiktaak om deze vragen te beantwoorden (Hoofdstuk 5). De meetdata liet zien dat de gezamenlijke reikbewegingen opmerkelijk consistent waren. Daarnaast produceerden de partners tegengestelde krachten op elkaar die ze niet minimaliseerden; een teken dat de partners hun acties niet per sé coördineerden. Met behulp van een wiskundig model van de gezamenlijke reiktaak zagen wij dat beide partners hun eigen voorgeprogrammeerde bewegingsplan uitvoerden waarin ze hun partner negeerden. Deze resultaten suggereerden dan de partners geen informatie uitwisselden via de interactiekracht om hun acties te coördineren, vergelijkbaar met de resultaten van de continue volgtaak.

Ten slotte, deze resultaten suggereren dat twee mensen haptisch met elkaar verbinden niet garandeert dat de partners de interactiekracht bewust en effectief gebruiken om bijvoorbeeld acties te coördineren of informatie uit te wisselen.

---

[1] A Takagi, G Ganesh, T Yoshioka, M Kawato, and E Burdet. Physically interacting individuals estimate the partner's goal to enhance their movements. Nature Human Behaviour, 1(3):0054, 2017.

Chapter 1.

Introduction

It is snowing heavily and the wind is howling as my climbing partner and I start to climb the Stüdlgrat, a famous ridge up Austria's highest peak – the Großglockner. The view on my partner is regularly obstructed by the rock as the route meanders up the ridge and the wind prevents us from communicating verbally. The only other way of communication is through our climbing rope. When my partner climbs faster than me, the tension in the rope increases, indicating that either I should speed up or he should slow down. By communicating through the rope we are still able to coordinate our climbing speed and safely climb to the top.

The ability to coordinate actions between individuals is an integral part of our lives and often determines how successful we are at a motor task, such as dancing or climbing [1]. Action coordination between humans can occur through many channels, for instance through verbal communication, facial expressions or imitation [2–4]. People can also coordinate actions by exerting forces onto each other. In the mountaineering example, we exerted forces onto each other through the climbing rope, facilitating motor coordination and task performance as long as the goal is properly understood by both climbers. This form of interpersonal interaction is referred to as physical human-human interaction or haptic human-human interaction. Figure 1.1 shows some examples of haptic interaction between humans. A therapist physically supports a patient to help regain motor function after stroke or injury. Movers can use haptic interaction to coordinate movements while carrying a heavy object. A team can physically assist each other to reach a common goal, like reaching the top of a climb.

Humans can haptically-interact in different ways, mainly depending on the task and roles of each partner [5, 6]. Jarrassé et al. [5] described a framework to classify interactive behaviors between two or more agents – including two humans, two robots, or a human and a robot – based on optimal control theory in which each agent minimizes their cost; the sum of effort and error. Optimal

Figure 1.1. | Examples of haptic human-human interaction in daily life. Photo credits: UK Stroke Association (left figure), Gainesville Movers (middle figure), Constantine Antoniades (right figure).

control theory is a common approach used to describe and predict human motor behavior [7, 8]. Jarrassé et al. [5] classified interactions into three main categories: competition, collaboration, and cooperation. During competitive haptic interaction, both partners only consider their own cost and, if necessary, impede the other partner's performance. In contrast, during cooperative and collaborative interactions, each partner considers his/her own cost function and that of their partner, attempting to work together to find a mutually beneficial solution to a common task. The main difference between cooperation and collaboration is how roles are assigned between the partners. In cooperation, roles are assigned a priori to each partner, such as leader-follower or teacher-student. This can result in partners performing different sub-tasks, while both work towards the same goal.

Jarrassé et al. [5] identified two forms of cooperation that are relevant for human-robot interaction: assistance and education. During assistance, both agents try to minimize only the effort and error of the individual who is receiving assistance. An example is an exoskeleton that assists a human with walking. During education, the teacher attempts to minimize his own effort in order to challenge the student, let the student perform according to his capabilities, and promote learning in the student [5]. The goal of the teacher is to become obsolete as soon as the student has reached a certain skill level and can execute the task independently.

During collaboration, roles are not assigned beforehand and are left to emerge spontaneously [5, 6] and can change while both partners work together toward the same goal. Each partner attempts to achieve the task themselves and could take the performance of the other partner into account. When collaborating, partners are equally responsible for reaching the goal. Collaboration also includes the interactions that can be described using differential game theory, in which each partner chooses a strategy such that no partner has anything to gain by changing only his/her strategy [5, 9] – a situation also known as a Nash equilibrium [10]. Another form of collaboration is co-activity, in which the partners interact without needing to know what the other partner is doing, but still succeed in the common task together [5]. An example of co-activity is when two interacting partners execute a motor task independently by ignoring the other partner, but were influenced by the haptic connection between them. Co-activity is the simplest form of interaction because no exchange of information through the interaction force is required.

Research on haptic interaction between humans has mostly focused on collaboration. These studies indeed found that collaborating partners adopt spontaneous roles depending on the task [11–16]. For example, Reed and Peshkin [11] found that two partners, who haptically collaborated to move a crank to a target as fast as possible, specialized into roles in which one partner took care of the acceleration of the crank and the other decelerated the crank. Interacting partners do not necessarily converge to global role distributions, but adopt strategies that are specific for each pair [13]. In addition, partners can change roles over time [13].

Collaborating partners can perform a task as well as [12] or better than [11, 17] either of the partners alone. Ganesh et al. [17] investigated how haptic interaction impacts the performance of two humans who were performing the same collaborative task – tracking a common continuously-moving target. They made two interesting observations: (1) haptic interaction between two humans leads to performance improvements during interaction for both partners, even when one partner is significantly worse at the tracking task than the other partner and (2) that haptic interaction improved individual motor learning compared to practicing the task alone.

Motivated by these promising results, we set out to investigate two aspects of haptic human-human interaction in collaborative tasks. First, we investigated whether and why haptic interaction with a human improves motor learning compared to practicing the task alone. Second, we studied how two humans both can improve performance during haptic interaction.

In this chapter, I will first discuss why gaining knowledge on haptic human-human interaction would be useful, for instance to complement the development of human-robot interaction strategies. I will then briefly summarize the most important research on two aspects of haptic human-human interaction: the performance improvement during interaction and the effect of interaction on motor learning. In the final sections, I will present the research questions and outline of this thesis.

1.1. Why investigate haptic human-human interaction?

We live in a time in which intelligent systems, such as robots, are rapidly becoming an integral part of our society: robotic devices are introduced in healthcare to assist therapists in neurorehabilitation and physical therapy [18–20]; exoskeletons are becoming increasingly capable of supporting gait or helping to regain motor function after stroke (e.g., [21, 22]); and industrial robots are starting to work in direct physical contact with human workers, such as wearable robots that assist the worker in lifting heavy objects [23]. Still, designing robots that can physically interact with a human to cooperatively perform motor tasks, aid in rehabilitation, or physically assist a human to learn a new motor task, is a complex challenge for roboticists [6].

A large body of literature – a detailed overview of which is beyond the scope of this introduction – exists describing different approaches on how to control robots that physically interact with humans. For additional information, see Marchal-Crespo and Reinkensmeyer [18] for a comprehensive review of robot-assisted rehabilitation approaches or Goodrich and Schultz [24] for a survey on human-robot interaction. Many of these approaches are implemented in an ad-hoc manner based on notions of what the desirable features of a robot interacting with a human should be [6, 18, 25]. The majority used cooperative interaction strategies in which the robot is at the full service to the human. For example, rehabilitation robots are controlled such that they guide the human over a pre-defined desired kinematic trajectory to eventually improve motor function – a form of haptic guidance [26, 27]. Other strategies tuned the amount of assistance based on the motor skill level of the participant or only supported certain sub-tasks of a movement to promote the active participation of the human [28–30]. However, there is evidence that haptically guiding a movement does not improve motor control, as demonstrated in rehabilitation after a stroke [18, 19]. Robots could also be used to augment movement errors or promote motor exploration to facilitate motor learning, yet the effectiveness of error augmentation to improve learning depends on the skill level of the participants and motor task characteristics [31–34].

To further promote effective, intuitive, and versatile interaction between humans and robots, researchers expressed the desire to develop human-robot interaction paradigms that resemble the haptic interactions between two humans [6, 18, 25, 35]. The research on haptic interaction between humans while they perform or learn a collaborative motor task, like the study of Ganesh et al. [17], could provide valuable information for the development of intuitive, flexible, and effective robotic control algorithms. Knowledge of haptic human-human interaction could help the human to better understand the intentions of the robot and vice-versa [6, 35]. Rehabilitation robots could interact with the patient similarly to how a physical therapist would during conventional therapy, alleviating the physical demands on the therapist, potentially minimizing the training time, and rehabilitation outcome [6]. Industrial robots could interact with their human colleagues in a way that is intuitive to the human, such that the robot's intentions are immediately understood, ensuring safe and efficient human-robot collaboration.

1.2. Learning better together through haptic interaction

Ganesh et al. [17] were the first to show that haptic interaction between two humans improves each partner's own motor learning. They used a tracking task that required both partners to follow the same randomly-moving target on a computer screen by moving the handle of their robotic manipulandum (Fig. 1.2B). Performance was the mean tracking error. The partners haptically-interacted in some trials through a compliant connection: a computer-generated spring with a small damping component that was rendered by each manipulandum (Fig. 1.2A), that coupled their hands. To elicit learning, Ganesh et al. [17] introduced a visuomotor rotation in which the visual feedback of the cursor was rotated clockwise with 80 deg with respect to the hand movement (Fig. 1.2C). Haptic interaction improved individual motor performance significantly more and, although not explicitly mentioned by the authors, initially faster compared to someone who practiced the task alone [17].

The reasons why haptic human-human interaction would improve motor learning in a collaborative task remain unknown. It is possible that participants 'coached' each other on how to move in the learning task through haptics. Moving in an 80 deg visuomotor rotation, the learning paradigm used by Ganesh et al. [17],

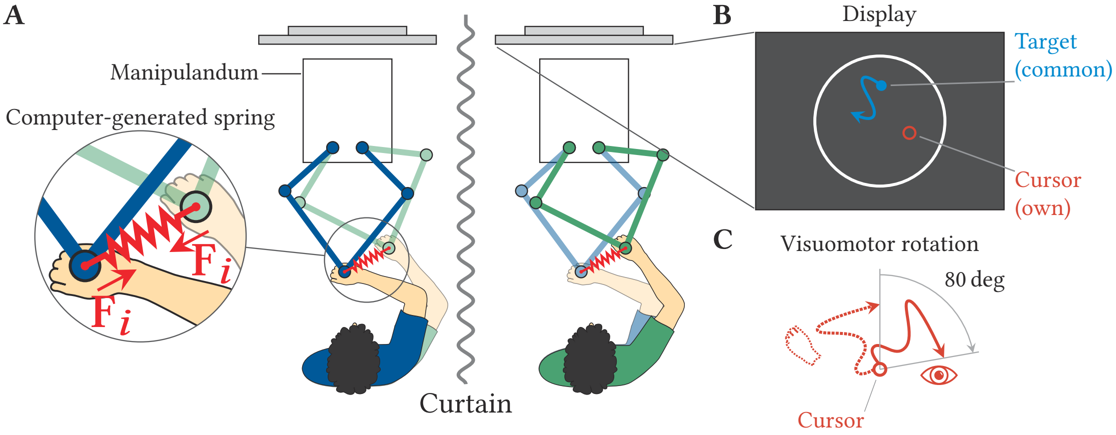

Figure 1.2. | Robotic setup and display and experiment design (taken from Chapter 4). **A** Each participant grasped the handle of one of the two manipulanda. Visual feedback was presented on a display mounted in front of each participant. **B** Participant received visual feedback of their own cursor position and a common target position. **C** Visuomotor rotation: the visual feedback of the cursor was rotated clockwise with 80 deg with respect to the hand movement.

likely required a change in movement strategy [36]. Haptically-interacting partners could have coached each other on how to move in the visual perturbation. Similarly, visually observing someone else learn a motor task has been shown to facilitate the observer's motor learning of the same task [37, 38]. Perhaps haptic interaction allowed for 'haptic observation' of how to move in the visuomotor rotation, improving motor learning. However, participants were not made explicitly aware of the interaction, so it is unknown whether such processes occurred.

Despite the promising results by Ganesh et al. [17], theirs remains the only study that found that haptic human-human interaction in a collaborative task benefits motor learning.

1.3. Performing better together through haptic interaction

As mentioned earlier, haptic interactions with another human consistently improve performance across several tasks, including reaching tasks [11] and tracking tasks [17, 39]. Specifically, Ganesh et al. [17] showed that haptic interaction also improved the performance of both partners tracking the same unpredictably-moving target. Ganesh et al. [17] used a compliant connection (Fig. 1.2A), which allowed the participants to move independently while still feeling an interaction force resulting from the haptic interaction. Remarkably, Ganesh et al. [17] found that haptic interaction even with a worse-performing partner resulted in performance improvements.

How did the haptically-interacting partners improve their performance in [17]? To explain their results, researchers from the same group hypothesized that the interacting partners extracted information about each other from the interaction force [40]. They proposed that partners estimate their partner's movement goal, use it to improve their estimate of the goal, and improve motor performance. In order to estimate their partner's movement goal, participants first estimated their partner's position through the interaction force. The partner's control actions are then estimated and used to estimate the partner's movement goal.

Haptic interaction has been shown to be useful for communicating movement intentions before (e.g., [14, 41–43]). However, most of these studies used less complex tasks than a fast-moving tracking task, for instance tasks that required movement in one dimension [41, 42], or assigned roles to the partners a priori [14]. Sawers et al. [14] reported that the leader in a dancing couple used small interaction forces to communicate the intended movement to the follower (i.e., they used cooperative tasks; participants were aware of the haptic connection). Takagi et al. [40] was the first to propose that haptic interaction improved motor performance in a collaborative task, because partners estimated their partner's state and movement intention, even though participants were not made explicitly aware of or had any other accurate knowledge of the haptic interaction with the other partner. The question remains whether the exchange of accurate information, as required by the goal integration model, is possible in a fast-moving tracking task.

1.4. Research questions

The goal of this thesis is to create a better understanding of whether and why haptic interactions between two humans improve individual motor learning and performance during interaction. If haptic interaction indeed leads to better individual motor learning compared to learning the motor task alone, then why would haptic interaction improve learning? It is possible that partners exchange information through the interaction force, for instance to coordinate motor actions or roles, like teacher-student, or to communicate information (e.g., 'tips or tricks') on how to learn the task better through haptics. Therefore, another crucial question in haptic human-human interaction is whether and how humans can exchange any information through the interaction force, in particular in a complex movement task such as a tracking task.

We investigated the following research questions:

1. Does haptic human-human interaction improve individual motor learning in a collaborative motor task and if so, why?
2. How do rigidly-coupled partners coordinate motor actions in a joint reaching task?
3. Do individuals improve performance during haptic interaction in a collaborative tracking task by exchanging information about each other through the interaction force? Is such haptic communication necessary to explain the observed improvements?

1.5. Thesis outline

This thesis consists of three parts: one chapter describing the hardware that we developed to study haptic interaction between humans and two research themes, see Fig. 1.3. Research theme I focuses on whether and how haptic interaction improves motor learning (research question 1). Theme II centers on the question of how people coordinate actions in haptic interaction and how people improve performance through haptic interaction (research questions 2 and 3).

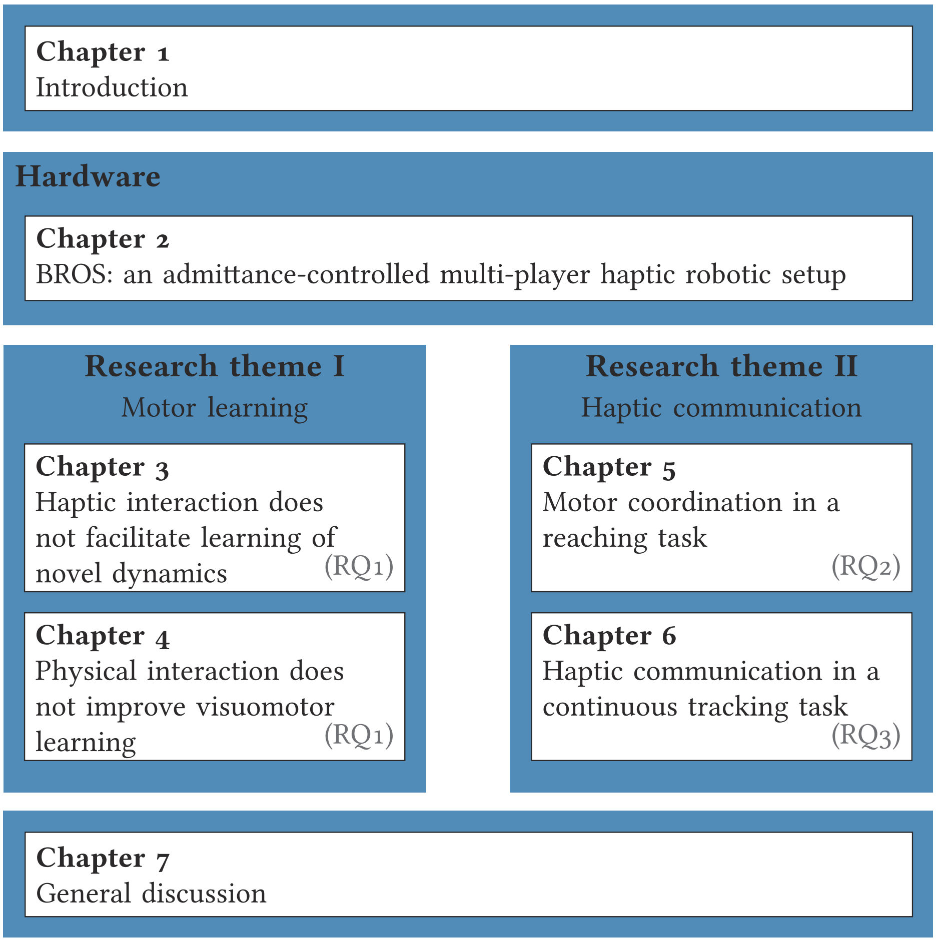

Figure 1.3. | Thesis outline. Each chapter, except for the hardware chapter, discusses one of the research questions indicated by RQ1, RQ2, or RQ3.

All chapters, excluding this introduction and the discussion, have been written as papers that were either presented at a scientific conference or (are to be) submitted in scientific journals. Therefore, each chapter can be read separately. A short description of each chapter is provided below.

Hardware

Chapter 2 describes the design and implementation of BROS: the Bi-partner RObotic Setup (see Fig. 1.4). BROS consists of two identical manipulanda that allow arm movement in a horizontal plane. Control of each manipulandum was implemented using an admittance controller, which renders desired dynamics (in our case a point mass of $0.3\,\mathrm{kg}$ with a damping component of $0.2\,\mathrm{N\,s\,m^{-1}}$) uniformly in the x- and y-directions over the workspace. The manipulanda can

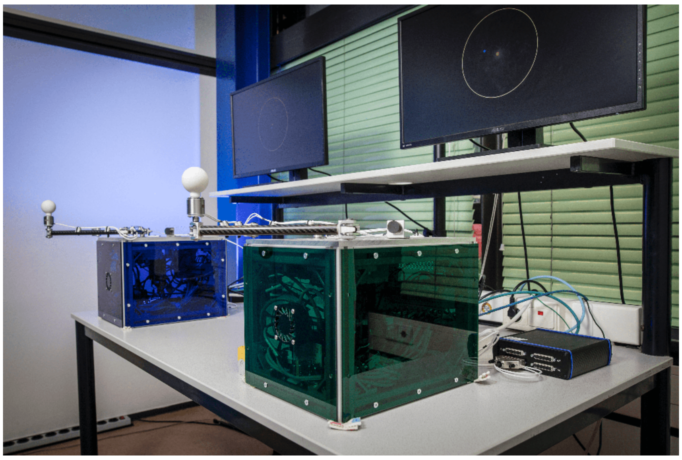

Figure 1.4. | The BROS dual-robotic setup for studying haptic human-human interaction.

be coupled through the control software, allowing for a wide variety of haptic interactions. We developed BROS specifically to study haptic interaction between two humans. This chapter also describes a detailed evaluation of the manipulanda, with extra attention to how the manipulandum renders constant dynamics across its workspace, essential for studying human motor control and haptic interaction.

Research theme I: motor learning

Ganesh et al. [17] showed that haptic interaction improved motor learning in a visuomotor learning task (see Fig. 1.2C). However, many new motor tasks we learn in real life involve learning new dynamics, for instance learning to stabilize yourself on a bicycle or swinging a tennis racket. We investigated whether haptic interaction improved motor learning of novel dynamics in **Chapter 3**. Participants performed a continuous tracking task while interacting with each other through a compliant connection. We then introduced a velocity-dependent force field perturbation as novel dynamics and investigated whether haptic interaction, now in the same sensory domain as the learning task, improved individual motor learning. Individual motor learning of the participant who intermittently haptically-interacted was not different from the participants who learned the task alone. Hence, we found that haptic interaction did not facilitate nor interfere with learning novel dynamics.

It is possible that haptic interaction did not improve the learning of novel dynamics because the learning task and interaction force were in the same sensory domain. To investigate whether the motor learning benefits of haptic interaction are task-specific, we also performed a motor learning experiment with the same visuomotor rotation learning task as used by Ganesh et al. [17]. We also investigated why haptic interaction would improve individual motor learning and tried to understand this process better by investigating two factors that could impact the learning process: the amount of interaction time and the strength of the interaction. **Chapter 4** describes the experiments and their results. Contrary to Ganesh et al. [17] but consistent with Chapter 3, we found no benefit of haptic human-human interaction on individual motor learning in a visuomotor rotation compared to individuals who learned the task alone. Interaction led neither to a better motor skill level nor an increased motor learning rate. Increasing the amount of interaction time or interaction strength did not improve motor learning.

Research theme II: haptic communication

Studies proposed that haptically interacting partners improved performance by coordinating roles through the interaction force [11, 12, 41]. Reed and Peshkin [11] proposed that participants improved performance by specializing into roles in which one partner took care of the acceleration and the other provided the deceleration of a movement. How did these roles emerge? **Chapter 5** describes an experiment and computational model to answer this question. We tested rigidly-coupled pairs in a joint reaching task to study the changes in the partner's movements. However, the joint reaching movements were surprisingly consistent across trials. A computational model demonstrated that the two partners had distinct motion plans, which did not change with time. These results suggest that rigidly-coupled pairs accomplished joint reaching movements by relying on a pre-programmed motion plan that was independent of their partner's behavior.

A continuous tracking task as the one used in Chapters 3 and 4 and [17, 40] and coupling the two partners through a compliant connection may be more suitable to examine haptic interaction and how haptic interaction improves performance than a reaching task with rigid coupling. Similar to Ganesh et al. [17], we found that haptic interactions though a compliant connection improves performance in a tracking task, even with a worse-performing partner (see **Chapter 6**). However, improvement benefits reduced when interacting with increasingly worse partners. Takagi et al. [40] proposed that interacting participants improved performance by exchanging accurate information through the interaction force. However, is such information exchange possible through haptics, in particular in a fast-moving tracking task? We provide an alternative explanation backed up by a computational model. A model that made as few assumptions as possible about the interaction – participants did not need to estimate their partner's state, actions or intentions through the interaction force – sufficiently described the performance improvements during interactions. In addition, we impaired the accurate perception of the interaction force by superimposing a force field (as in Chapter 3) on the tracking task. Even though the interaction force perception was biased by the force field, we still found the same improvement due to interaction. Our results suggest that no information exchange needs to occur to improve performance, challenging the goal integration hypothesis of Takagi et al. [40].

References

[1] N Sebanz, H Bekkering, and G Knoblich. Joint action: bodies and minds moving together. *Trends in Cognitive Sciences*, 10(2):70–76, February 2006.

[2] S Garrod and M J Pickering. Why is conversation so easy? *Trends in Cognitive Sciences*, 8(1):8–11, January 2004.

[3] C D Frith. Social cognition. *Philosophical Transactions of the Royal Society B: Biological Sciences*, 363(1499):2033–2039, June 2008.

[4] P E Keller, G Novembre, and M J Hove. Rhythm in joint action: psychological and neurophysiological mechanisms for real-time interpersonal coordination. *Philosophical Transactions of the Royal Society B: Biological Sciences*, 369(1658):20130394–20130394, November 2014.

[5] N Jarrassé, T Charalambous, and E Burdet. A Framework to Describe, Analyze and Generate Interactive Motor Behaviors. *PLoS ONE*, 7(11), 2012.

[6] A Sawers and L H Ting. Perspectives on human-human sensorimotor interactions for the design of rehabilitation robots. *Journal of NeuroEngineering and Rehabilitation*, 11(1), 2014.

[7] E Todorov and W Li. A generalized iterative LQG method for locally-optimal feedback control of constrained nonlinear stochastic systems. In *American Control Conference, 2005. Proceedings of the 2005*, pages 300–306 vol. 1, June 2005.

[8] S H Scott. Optimal feedback control and the neural basis of volitional motor control. *Nature Reviews Neuroscience*, 5(7):532–546, June 2004.

[9] D A Braun, P A Ortega, and D M Wolpert. Nash equilibria in multi-agent motor interactions. *PLoS Computational Biology*, 5(8):e1000468, August 2009.

[10] J F Nash. Equilibrium Points in N-Person Games. *Proceedings of the National Academy of Sciences of the United States of America*, 36(1):48–49, January 1950.

[11] K B Reed and M A Peshkin. Physical Collaboration of Human-Human and Human-Robot Teams. *IEEE Transactions on Haptics*, 1(2):108–120, 2008.

[12] R P R D van der Wel, G Knoblich, and N Sebanz. Let the Force Be With Us: Dyads Exploit Haptic Coupling for Coordination. *Journal of Experimental Psychology: Human Perception and Performance*, 37(5):1420–1431, October 2011.

[13] A Melendez-Calderon, V Komisar, and E Burdet. Interpersonal strategies for disturbance attenuation during a rhythmic joint motor action. *Physiology & Behavior*, 147:348–358, 2015.

[14] A Sawers, T Bhattacharjee, J L McKay, M E Hackney, C C Kemp, and L H Ting. Small forces that differ with prior motor experience can communicate movement goals during human-human physical interaction. *Journal of NeuroEngineering and Rehabilitation*, 14(1):8, January 2017.

[15] R Ikeura and H Inooka. Variable impedance control of a robot for cooperation with a human. *IEEE International Conference on Robotics and Automation*, 3:3097–3102 vol.3, 1995.

[16] R Groten, D Feth, H Goshy, and A Peer. Experimental analysis of dominance in haptic collaboration. *IEEE International Symposium on Robot and Human Interactive Communication. Proceedings*, pages 723–729, 2009.

[17] G Ganesh, A Takagi, R Osu, T Yoshioka, M Kawato, and E Burdet. Two is better than one: Physical interactions improve motor performance in humans. *Scientific Reports*, 4, 2014.

[18] L Marchal-Crespo and D J Reinkensmeyer. Review of control strategies for robotic movement training after neurologic injury. *Journal of NeuroEngineering and Rehabilitation*, 6(1), 2009.

[19] V Klamroth-Marganska, J Blanco, K Campen, A Curt, V Dietz, T Ettlin, M Felder, B Fellinghauer, M Guidali, A Kollmar, A R Luft, T Nef, C Schuster-Amft, W Stahel, and R Riener. Three-dimensional, task-specific robot therapy of the arm after stroke: a multicentre, parallel-group randomised trial. *The Lancet Neurology*, 13(2):159–166, February 2014.

[20] G Kwakkel, B J Kollen, and H I Krebs. Effects of robot-assisted therapy on upper limb recovery after stroke: A systematic review. *Neurorehabilitation and Neural Repair*, 22(2):111–121, 2008.

[21] A Esquenazi, M Talaty, A Packel, and M Saulino. The ReWalk Powered Exoskeleton to Restore Ambulatory Function to Individuals with Thoracic-Level Motor-Complete Spinal Cord Injury. *American journal of physical medicine & rehabilitation*, 91(11):911–921, November 2012.

[22] J Meuleman, E van Asseldonk, G van Oort, H Rietman, and H van der Kooij. LOPES II - Design and Evaluation of an Admittance Controlled Gait Training Robot with Shadow-Leg Approach. *IEEE Transactions on Neural Systems and Rehabilitation Engineering*, 24(3):352–363, March 2016.

[23] M P de Looze, T Bosch, F Krause, K S Stadler, and L W O'Sullivan. Exoskeletons for industrial application and their potential effects on physical work load. *Ergonomics*, pages 1–11, June 2016.

[24] M A Goodrich and A C Schultz. Human-Robot Interaction: A Survey. *Foundations and Trends in Human-Computer Interaction*, 1(3):203–275, 2007.

[25] P Morasso, M Casadio, P Giannoni, L Masia, V Sanguineti, V Squeri, and E Vergaro. Desirable features of a "humanoid" robot-therapist. *IEEE EMBS Conference proceedings: Annual International Conference of the IEEE Engineering in Medicine and Biology Society*, 2009:2418–2421, 2009.

[26] R B Gillespie, M O'Modhrain, P Tang, C Pham, and D Zaretsky. The virtual teacher. *Proceedings of ASME Dynamics Systems and Control Division, Symposium on Haptic Interface for Virtual Environment and Teleoperator Systems*, pages 171–178, 1998.

[27] J C Huegel and M K O'Malley. Progressive haptic and visual guidance for training in a virtual dynamic task. *IEEE Third Joint Eurohaptics Conference and Symposium on Haptic Interfaces for Virtual Environment and Teleoperator Systems*, pages 343–350, March 2010.

[28] H Vallery, E H F van Asseldonk, M Buss, and H van der Kooij. Reference Trajectory Generation for Rehabilitation Robots: Complementary Limb Motion Estimation. *IEEE Transactions on Neural Systems and Rehabilitation Engineering*, 17(1):23–30, February 2009.

[29] L L Cai, A J Fong, C K Otoshi, Y Liang, J W Burdick, R R Roy, and V R Edgerton. Implications of Assist-As-Needed Robotic Step Training after a Complete Spinal Cord Injury on Intrinsic Strategies of Motor Learning. *Journal of Neuroscience*, 26 (41):10564–10568, October 2006.

[30] B Koopman, E H F Van Asseldonk, and H van der Kooij. Selective control of gait subtasks in robotic gait training: Foot clearance support in stroke survivors with a powered exoskeleton. *Journal of NeuroEngineering and Rehabilitation*, 10(1):3, January 2013.

[31] E H F van Asseldonk, M Wessels, A H A Stienen, F C T van der Helm, and H van der Kooij. Influence of haptic guidance in learning a novel visuomotor task. *Journal of Physiology - Paris*, 103(3-5):276–285, September 2009.

[32] F C Huang, J L Patton, and F A Mussa-Ivaldi. Interactive priming enhanced by negative damping aids learning of an object manipulation task. *IEEE EMBS Conference proceedings: Annual International Conference of the IEEE Engineering in Medicine and Biology Society*, 2007:4011–4014, 2007.

[33] L Marchal-Crespo, J Lopez-Oloriz, L Jaeger, and R Riener. Optimizing learning of a locomotor task: Amplifying errors as needed. In *36th Annual International Conference of the IEEE Engineering in Medicine and Biology Society*, pages 5304–5307. IEEE, August 2014.

[34] L Marchal-Crespo, N Rappo, and R Riener. The effectiveness of robotic training depends on motor task characteristics. *Experimental Brain Research*, 235(12):3799–3816, December 2017.

[35] D A Abbink, T Carlson, M Mulder, J C F de Winter, F Aminravan, T L Gibo, and E R Boer. A Topology of Shared Control Systems—Finding Common Ground in Diversity. *IEEE Transactions on Human-Machine Systems*, 48(5):509–525, 2018.

[36] S Abeele and O Bock. Sensorimotor adaptation to rotated visual input: different mechanisms for small versus large rotations. *Experimental Brain Research*, 140(4): 407–410, October 2001.

[37] A G Mattar and P L Gribble. Motor Learning by Observing. *Neuron*, 46(1):153–160, 2005.

[38] C Granados and G Wulf. Enhancing motor learning through dyad practice: Contributions of observation and dialogue. *Research Quarterly for Exercise and Sport*, 78 (3):197–203, June 2007.

[39] D Feth, R Groten, A Peer, S Hirche, and M Buss. Performance related energy exchange in haptic human-human interaction in a shared virtual object manipulation task. In *WHC '09: Proceedings of the World Haptics 2009 - Third Joint EuroHaptics*

conference and Symposium on Haptic Interfaces for Virtual Environment and Teleoperator Systems. Technical University of Munich, IEEE Computer Society, March 2009.

[40] A Takagi, G Ganesh, T Yoshioka, M Kawato, and E Burdet. Physically interacting individuals estimate the partner's goal to enhance their movements. *Nature Human Behaviour*, 1(3):0054, 2017.

[41] R Groten, D Feth, R L Klatzky, and A Peer. The role of haptic feedback for the integration of intentions in shared task execution. *IEEE Transactions on Haptics*, 6 (1):94–105, January 2013.

[42] C E Madan, A Kucukyilmaz, T M Sezgin, and C Basdogan. Recognition of Haptic Interaction Patterns in Dyadic Joint Object Manipulation. 8(1):54–66, November 2015.

[43] D Feth, R Groten, A Peer, and M Buss. Control-theoretic model of haptic human-human interaction in a pursuit tracking task. In *Proceedings - IEEE International Workshop on Robot and Human Interactive Communication*, pages 1106–1111. Technische Universität München, Munich, Germany, IEEE, December 2009.

Chapter 2.

BROS: the admittance-controlled multiplayer haptic robot

Niek Beckers, Koen Heuver, Arvid Keemink,
Edwin van Asseldonk, and Herman van der Kooij

Manuscript in preparation

Abstract

Robotic manipulanda facilitate investigations on how two or more humans physically interact when performing a movement task together. Here we describe BROS, a robotic setup with two planar manipulanda designed specifically for studying physical human-human interaction. The design is based on a 5R closed-loop parallel pantograph and was optimized for low end-point mass. Control of each robotic device was implemented using an admittance controller, allowing isotropic dynamic behavior across the workspace. Furthermore, admittance control allows for stable coupling of the two manipulanda and a wide range of haptic interaction conditions. We evaluated the robotic devices in terms of stiffness rendering capabilities, force production, closed-loop position tracking performance and admittance rendering performance. We tested multiple degrees of virtual stiffness up to 400 $\mathrm{N\,m^{-1}}$, however higher stiffness rendering is possible, and the robots can produce over 50 N at the endpoint. The closed-loop position tracking bandwidth to the -3 dB point is approximately 21 Hz. The desired virtual mass-damper admittance could be rendered within a 10 % modulus deviation up to a frequency of 7.5 Hz. Finally, we validated the experimental capabilities of BROS with a human-human interaction experiment in which we varied the stiffness between the two interacting partners.

2.1. Introduction

Haptic robotic manipulanda are indispensable tools in studying human motor control, motor learning, physical rehabilitation and physical human-robot interaction. These robots range from lower-extremity exoskeletons, such as the LOPES [1], and full arm exoskeletons, like the ARMIN [2], to one degree of freedom (DOF) devices such as the Hi5 wrist manipulator [3]. Because many aspects of motor control can be studied using arm movements in a plane, most motor control studies predominantly used planar robotic manipulanda with a handle at the endpoint. Examples of planar robotic manipulanda include the vBOT [4], KINARM [5], Braccio di Ferro [6], PFM [7], Haptic Master [8] and 3DOM [9]. Planar endpoint robotic manipulanda have low complexity compared to multi-DOF devices like exoskeletons, allow for high-precision movement sensing and can provide a wide range of dynamic behaviors, such as minimal resistance to movement (e.g., low apparent impedance), rendering stiff objects or applying a velocity-dependent force field.

The existence of planar and similar robotic manipulanda facilitated the research on physical interaction between two humans (e.g. [10–13]). By studying the motor behavior when two partners are physically coupled to each other, for instance when carrying a table together, other researchers and we intend to determine the underlying mechanisms of physical interaction between two humans. One of the advantages of using robotic manipulanda for studying human-human interaction is the flexibility in generating different types of dynamic conditions, such as different physical connections between the interacting partners, ranging from rigid connections (carrying a table together) to compliant connections (for instance two people holding a rubber band).

Most robotic setups used in physical human-human interaction studies consist of two identical robotic manipulanda [3, 10, 14] whose endpoints can be virtually connected through the control software, similar to robotic setups used for bimanual control (e.g. [15]). For instance, Melendez-Calderon et al. [3] developed the Hi5 interface, which is a robotic setup with two 1 DOF wrist manipulanda, one for each partner, that allows wrist flexion and extension. While a dual 1 DOF robotic manipulandum alleviates the already complex analysis of human-human physical interaction, for motor learning purposes a manipulandum with at least two degrees of freedom and larger workspace is desirable. Ganesh et al. [10] and Braun et al. [16] both used two identical planar robotic devices: two PFM planar robotic manipulanda [7] and two vBOT manipulanda [4], respectively. While any dual robotic setup can be made by linking two (preferably identical) existing robotic manipulanda, most of the devices as mentioned earlier are built in-house and are not commercially available. On the other hand, off-the-shelf solutions usually do not fit budgetary constraints or desired specifications.

We developed the Bipartner RObotic Setup (BROS), which is a setup consisting of two identical robotic manipulanda designed explicitly for studying physical human-human interaction during sensorimotor tasks. Our goal was to develop a setup consisting of two compact planar robotic manipulanda with a highly configurable control and software architecture and low isotropic endpoint mass. Besides describing the design and implementation process of the robot, we emphasize the usefulness of admittance control for human motor control research. Most manipulanda use impedance control, sometimes with feedforward control for passive dynamics compensation [6, 9] which heavily depend on the accuracy of the estimated device dynamics. We evaluate the performance of the robot in terms of admittance control capabilities with a focus on its efficacy for human-robot interaction and motor control studies.

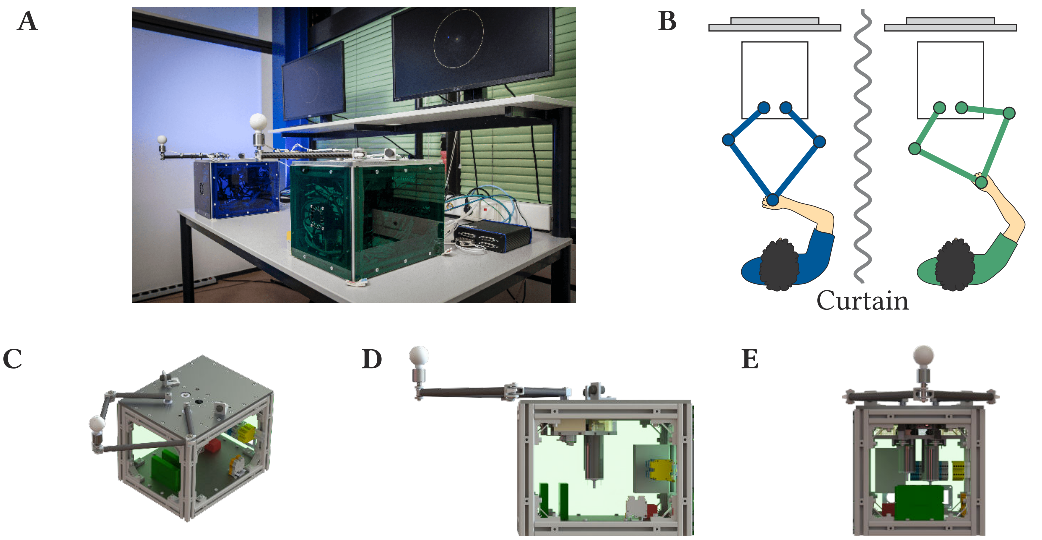

Figure 2.1. | Overview of BROS. (a) Overview photo of the BROS with the two robotic manipulanda and displays. (b) Schematic top view of the setup. (c–e) Isometric, side and front view renderings of the planar robotic manipulandum. The major mechanical and electronic components are built into the base of each manipulandum.

This paper first describes the robotic setup, design and implementation process, followed by the evaluation of the setup and its manipulanda. Lastly, we will assess its capabilities for performing physical human-human interaction experiments.

2.2. Design & Implementation

In this section, we first show an overview of the BROS, followed by a description of the design and implementation steps of the BROS. Because the main components are the two identical manipulanda, we will describe the design and evaluation for one robotic device, unless stated otherwise.

2.2.1. Overview

Figure 2.1 shows an overview of the BROS robotic setup and manipulandum. It comprises two identical planar parallel robotic manipulanda. Users hold the robot by the handle at the endpoint of the manipulandum, which is attached to the robot through a 6 DOF force/torque sensor. During experiments, a curtain is closed to isolate the participants so that they can only see their display and to minimize non-physical interaction.

2.2.2. Design requirements

The manipulanda of BROS are designed for the following requirements:

1. low endpoint mass such that the passive robot dynamics impede the user's arm movements as little as possible,
2. high structural rigidity such that high stiffness can be rendered,
3. a minimum elliptical workspace with a bounding box of $350 \times 200\,\text{mm}$ based on the typical movement magnitude in motor control work (e.g. [17]),
4. a global conditioning index (GCI) (the condition number κ integrated over the usable workspace) larger than 0.7 for good manipulability [18],
5. the apparent dynamics at the endpoint by the user should be isotropic across the workspace such that changing device dynamics do not influence the user's motor control and
6. the robot should be able to deliver 25 N at the endpoint across the workspace continuously and maximally 75 N at the nominal position, similar to [6].

2.2.3. Topology, kinematics and dynamics

The BROS planar robotic manipulanda are parallel robots using a 5R symmetric parallel robot topology (see Fig. 2.2). We chose this robot topology mainly for the high structural rigidity, needed to render high stiffness, in combination with low endpoint mass, necessary for rendering low impedance, and positioning and measurement accuracy [19]. A disadvantage of such a parallel kinematic chain is the increased computational complexity of kinematics and in particular dynamics [20]. Here we describe the kinematics and a simplified model of the device dynamics which we used for design optimization and device control. The actuators and position sensors are situated at joints 1 and 5 (the 'shoulder' joints, indicated by $\mathbf{P}_1$ and $\mathbf{P}_5$) and are fixed to the base frame; the endpoint is located at joint $\mathbf{P}_3$. Joints $\mathbf{P}_2$ and $\mathbf{P}_4$ are referred to as the 'elbow' joints. The links indicated by L_f and L_u are referred to as the 'forearm' links and 'upper arm' links, respectively. The origin of the Cartesian coordinate system is at the midpoint of the base segment L_b.

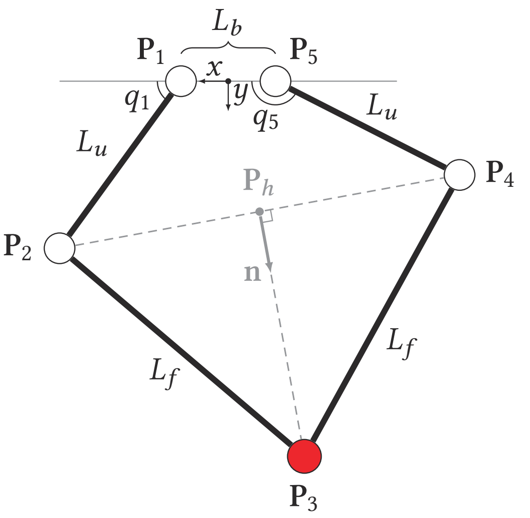

Figure 2.2. | Parallel 5R topology of the robotic device. The endpoint is at joint $\mathbf{P}_3$ and is indicated in red.

Direct kinematics

The Cartesian endpoint position $\mathbf{x} = [x_3, y_3]^T$ is directly related to the joint angles $\mathbf{q} = [q_1, q_5]^T$. The direct kinematics $\mathbf{x} = f(\mathbf{q})$ are derived using the approach as described in Klein et al. [9]. The positions of joints $\mathbf{P}_1, \mathbf{P}_2, \mathbf{P}_4, \mathbf{P}_5$ are:

$$\begin{aligned}
\mathbf{P}_1 &= \begin{bmatrix} \frac{L_b}{2} & 0 \end{bmatrix}^T, \\
\mathbf{P}_5 &= \begin{bmatrix} \frac{-L_b}{2} & 0 \end{bmatrix}^T, \\
\mathbf{P}_2 &= \begin{bmatrix} L_u \cos q_1 & L_u \sin q_1 \end{bmatrix}^T + \mathbf{P}_1 \text{ and} \\
\mathbf{P}_4 &= \begin{bmatrix} L_u \cos q_5 & L_u \sin q_5 \end{bmatrix}^T + \mathbf{P}_5.
\end{aligned} \tag{2.1}$$

Because both forearm links have length L_f, the triangle $\mathbf{P}_2\mathbf{P}_3\mathbf{P}_4$ is an isosceles triangle and therefore the projection of $\mathbf{P}_3$ should always be above the midpoint between $\mathbf{P}_2$ and $\mathbf{P}_4$. By defining point $\mathbf{P}_h$ that is midway of points $\mathbf{P}_2$ and $\mathbf{P}_4$, we can calculate the distance $||\mathbf{P}_h - \mathbf{P}_3||$ and corresponding normal vector $\mathbf{n}$ pointing from the midpoint $\mathbf{P}_h$ to $\mathbf{P}_3$:

$$\begin{aligned}
\mathbf{P}_h &= \frac{1}{2}(\mathbf{P}_2 + \mathbf{P}_4), \\
\mathbf{u} &= \mathbf{P}_4 - \mathbf{P}_2 = \begin{bmatrix} u_x \\ u_y \end{bmatrix} \text{ and} \\
\mathbf{n} &= \frac{1}{||\mathbf{u}||} \begin{bmatrix} u_y \\ -u_x \end{bmatrix}.
\end{aligned} \tag{2.2}$$

Because of the isosceles right triangle formed by $\mathbf{P}_2\mathbf{P}_h\mathbf{P}_3$ we know the distance from $\mathbf{P}_h$ to $\mathbf{P}_3$ to be $\sqrt{L_f^2 - \frac{1}{4}\left\|\mathbf{u}\right\|^2}$, such that the position $\mathbf{P}_3$ can be determined:

$$\mathbf{P}_3 = \mathbf{P}_h + \mathbf{n}\sqrt{L_f^2 - \frac{1}{4}\left\|\mathbf{u}\right\|^2}. \tag{2.3}$$

Because we are interested in the position of the endpoint $\mathbf{P}_3$ only, we denote the position of $\mathbf{P}_3$ as $\mathbf{x}$ from here on.

The geometric Jacobian $\mathbf{J}(\mathbf{q}) = \partial\mathbf{x}/\partial\mathbf{q}$ relating endpoint velocity to the joint velocity ($\dot{\mathbf{x}} = \mathbf{J}(\mathbf{q})\dot{\mathbf{q}}$) can be calculated analytically from 2.3. The Jacobian can be used to calculate the conditioning number κ [19]:

$$\kappa = \frac{1}{\left\|\mathbf{J}^{-1}\right\|\left\|\mathbf{J}\right\|}, \tag{2.4}$$

where a value of 0 and 1 indicate minimum and maximum dexterity (i.e. isotropy) respectively.

Dynamics

We derived a simplified model of the robot dynamics to optimize the design of the robot in terms of minimal passive device dynamics and for controller tuning. The joint-space dynamics of the robotic device can be written in the standard form

$$\begin{aligned} \mathbf{M}(\mathbf{q})\,\ddot{\mathbf{q}} + \mathbf{C}(\mathbf{q},\dot{\mathbf{q}})\,\dot{\mathbf{q}} + \mathbf{D}_c\mathrm{sign}(\dot{\mathbf{q}}) + \mathbf{D}_v\dot{\mathbf{q}} = \\ \boldsymbol{\tau}_q - \mathbf{J}^T(\mathbf{q})\,\mathbf{F}_e. \end{aligned} \tag{2.5}$$

where $\mathbf{M}(\mathbf{q})$ is the mass matrix, $\mathbf{C}(\mathbf{q},\dot{\mathbf{q}})$ includes the Coriolis and centripetal contributions, $\mathbf{D}_c$ and $\mathbf{D}_v$ are the Coulomb and viscous friction coefficients, $\boldsymbol{\tau}_q$ are actuator torques and $\mathbf{F}_e$ is an externally applied force at the endpoint [21].

Due to the coupling of the forearm links in the closed-loop kinematic chain, deriving the analytical solution of the device dynamics is complicated [19, 20]. Therefore, following the approach of Codourey [20], we used a simplified model which ignores the rotational inertia of the forearm links. To account for the mass of the left and right forearm links, we divided the mass m_f of each forearm link to the endpoint and corresponding elbow joints: $\frac{1}{3}m_f$ is added to the endpoint mass m_e at $\mathbf{P}_3$ and $\frac{2}{3}m_f$ is added to each elbow joint mass m_{el} at $\mathbf{P}_2$ and $\mathbf{P}_4$:

$$m_e' = m_e + \frac{1}{3}m_f \text{ and } m_{el}' = m_{el} + \frac{2}{3}m_f. \tag{2.6}$$

Due to these simplifications, the mass matrix now consists of two main components: (1) the rotational inertia $\boldsymbol{\Upsilon}_q$ of both shoulder joints, upper arm links and elbow joints and (2) the point-mass m_e' of the endpoint. The rotational inertia matrix $\boldsymbol{\Upsilon}_q$ is

$$\begin{aligned}\boldsymbol{\Upsilon}_q &= \begin{bmatrix}\Upsilon_{q,1} & 0\\ 0 & \Upsilon_{q,5}\end{bmatrix} \text{ with}\\ \Upsilon_{q,i} &= \Upsilon_m k_r^2 + \Upsilon_s + L_u^2\left(\frac{1}{3}m_u + m_{el}'\right), \quad i = 1, 5,\end{aligned} \tag{2.7}$$

where Υ_m is the actuator rotor inertia, k_r the transmission ratio, Υ_s the shoulder joint rotational inertia and m_u the upper arm link mass.

Contributions of the endpoint mass to the joint-space inertia and Coriolis and centrifugal terms are found by realizing that

$$\ddot{\mathbf{x}} = \mathbf{J}\ddot{\mathbf{q}} + \dot{\mathbf{J}}\dot{\mathbf{q}}. \tag{2.8}$$

Combining equations 2.5 to 2.8, the simplified dynamics are

$$\begin{aligned}\boldsymbol{\Upsilon}_q\ddot{\mathbf{q}} + m_e'\mathbf{J}^T\mathbf{J}\ddot{\mathbf{q}} + m_e'\mathbf{J}^T\dot{\mathbf{J}}\dot{\mathbf{q}} + \mathbf{D}_c\operatorname{sign}(\dot{\mathbf{q}}) + \mathbf{D}_v\dot{\mathbf{q}} &=\\ \boldsymbol{\tau}_q - \mathbf{J}^T\mathbf{F}_e&.\end{aligned} \tag{2.9}$$

2.2.4. Mechatronic design and implementation

Figure 2.3 shows an overview of the mechatronic implementation of one manipulandum.

Robot design

The link lengths L_b, L_u and L_f are the main design parameters, as they greatly determine workspace, manipulability and dynamics.

Due to the force requirements specified in Section 2.2.2 and because we used DC motors which can generate relatively low nominal torque output, a transmission was needed. We used a capstan wire transmission with transmission ratio k_r for two reasons, (1) a capstan wire transmission is highly back-drivable and (2) it has no backlash compared to a geared transmission. However, it does have a lower stiffness than gear-based transmissions.

The link lengths and transmission ratio are the results of an optimization of a cost function which included the requirements described above using a genetic algorithm in MATLAB (see the results in Table 2.1). The resulting link lengths and transmission ratio led to a robot design with an elliptical workspace with a

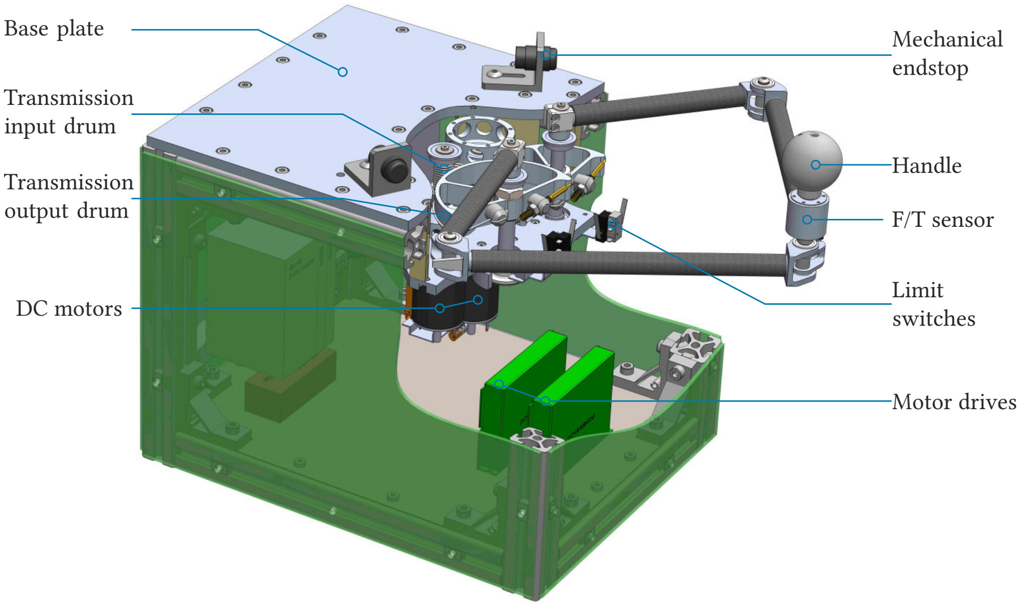

Figure 2.3. | Overview of the mechatronic implementation of one manipulandum.

bounding box of 355 by 215 mm, an average mass at the endpoint (averaged over the workspace) of 0.27 kg, maximum mass at the end of 0.55 kg at the usable workspace boundary and a global conditioning index of 0.74.

The condition number across the reachable workspace is given in Fig. 2.4A. Note that the usable workspace, indicated by the ellipse, is smaller than the total reachable workspace. We intentionally keep the robot's endpoint in the smaller usable workspace to avoid robot configurations with poor conditioning. The robot's nominal position – where the condition number is closest to 1 – is at $\mathbf{x}_{\text{nom}} = \left[0,\ 0.245\right]^T$ m.

The maximum translational mass at the endpoint over the reachable workspace (including all inertia contributions) is calculated by finding the largest eigenvalue of the mass matrix expressed in operational space at the endpoint (denoted as $\mathbf{M}_x$). We map the joint space mass matrix $\left(\mathbf{M}_q = \Upsilon_q + m_e'\mathbf{J}^T\mathbf{J}\right)$ to the endpoint operational space as follows [21]:

$$\mathbf{M}_x = \mathbf{J}^{-T}\mathbf{M}_q\mathbf{J}^{-1} = \mathbf{J}^{-T}\Upsilon_q\mathbf{J}^{-1} + m_e'\mathbf{I}^{2\times 2}. \qquad (2.10)$$

The mass of each component was estimated from CAD data, and the handle and force sensor were weighed.

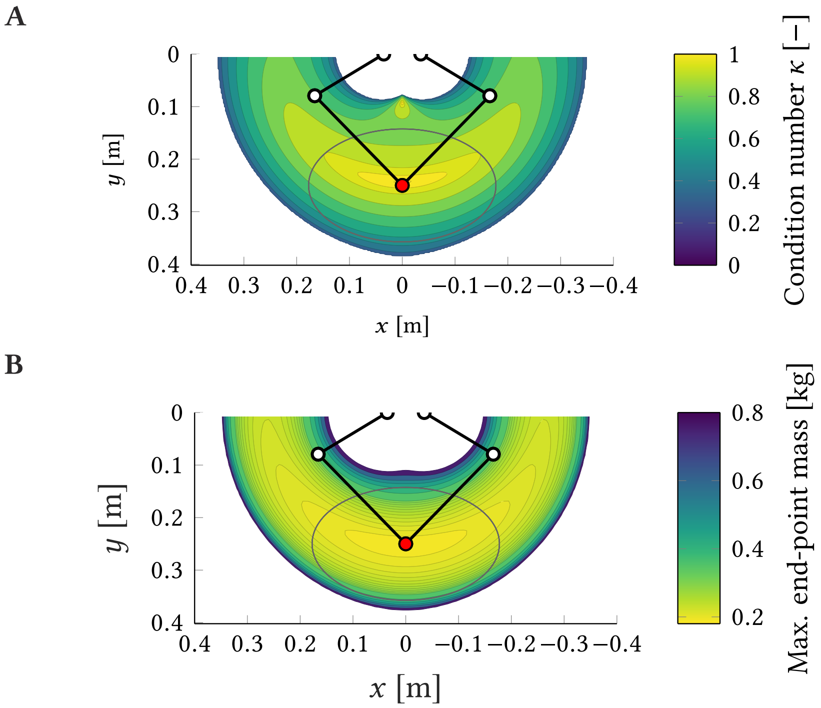

Figure 2.4. | Condition number and theoretical maximum endpoint mass, calculated using equation 2.10 across the workspace. **A** Theoretical condition number. **B** Theoretical maximum mass at the endpoint. Both figures show the robot configuration at the nominal position as well as the usable workspace.

Mechanical design

All links consist of circular carbon-fiber reinforced tubes with an outer diameter of 15 mm and 1 mm wall thickness (mass density of $65\,\mathrm{g\,m^{-1}}$ and a modulus of elasticity $E = 65\,\mathrm{GPa}$). At the most extended position of the robot with the arms clamped, we expect a structural deflection of the links of 0.2 mm at the endpoint when applying a force of 75 N at the endpoint.

Table 2.1. | Robotic device design parameters and values.

Parameter	Value	
L_b	0.07	[m]
L_u	0.238	[m]
L_f	0.153	[m]
k_r	7.3	[-]

Other parts, including joints and transmission, are machined from aluminum. We used low-friction ball-bearings (SKF) for all joints. The planar manipulandum is housed in a rigid support frame made out of extruded aluminum profiles (MISUMI). The housing contains most of the electronics (motor drive, sensors and other circuitry) and is closed using transparent covers (see Fig. 2.1).

The handle at the endpoint is a 3D-printed sphere that is comfortable to hold. The handle is connected to the 6 DOF force/torque sensor at the robot's endpoint and can freely rotate around the out-of-plane axis.

Actuation and sensors

The actuators at the shoulder joints are two Faulhaber 3890 H048CR brushed DC motors with a nominal torque of 0.24 N m and a stall torque of 2.9 N m. These motors have low rotor inertia ($1.71 \cdot 10^{-9}$ kg m^2) and no cogging due to them being coreless. The motors are connected to the transmission input shaft. Each motor is controlled by a Technosoft iPOS4808 BX-CAT motion controller in current control mode, which has a maximum continuous output current of 8 A, a peak output current of 20 A for a maximum of 2.5 s and a maximum nominal supply voltage of 48 V. Each motor drive has an EtherCAT controller and allows for multiple sensor read-outs directly onto the EtherCAT bus; in our case an incremental and an absolute encoder.

Position sensing is performed at each motor and each transmission output shaft. Each DC motor is equipped with an incremental encoder (Faulhaber IE3-1024L quadrature encoder, 1024 lines per revolution, 4096 counts in quadrature mode). An absolute encoder (MU1C, iCHaus) with a 16-bit per revolution resolution is connected to each transmission output shaft. Using these position sensors, we expect a worst-case measurement inaccuracy of $d\mathbf{x} \approx 26\,\mu\text{m}$ at the extreme of the workspace [19]. Joint velocity is calculated using a discrete-time differentiation of the position signals, followed by a second-order Butterworth low-pass filter with a 70 Hz cut-off frequency. The translational position and velocity of the endpoint are calculated using the direct kinematics and jacobian (see equations 2.1 to 2.3).

Forces and torques exerted onto the endpoint by the user are measured using a high-precision 6 DOF force/torque sensor (ME Meßsysteme K6D27 sensor with a custom 100 N and 2 N m range). The sensor's GSV-8DS EC amplifier (ME Meßsysteme) has 24-bit ADCs and an EtherCAT controller so that it can directly connect to the EtherCAT chain. We measured force sensor drift and measurement variance for 80 min. The force sensor measurement variances for the sensor's local x- and y-axes are similar and are in the range of $1.85 \cdot 10^{-5}\,\text{N}^2$ to $1.93 \cdot 10^{-5}\,\text{N}^2$. The drift of the x axis of the sensor was approximately $19.8\,\text{mN}\,\text{h}^{-1}$ (first-order linear regression).

Software implementation

The robots are controlled using the EtherCAT real-time control system (EtherCAT Technology Group), which is controlled through TwinCAT 3 (Beckhoff). The advantages of using the EtherCAT control system include low loop delay and jitter (< 100 ns) and simple reconfiguration of additional sensor slaves. Furthermore, any PC can serve as the EtherCAT master device. Physical processing cores can be isolated to be solely utilized for the EtherCAT real-time system execution, eliminating operating system-related timing delays. TwinCAT is capable of using compiled MATLAB Simulink (Mathworks) models for real-time control. Communication between the TwinCAT real-time kernel and the Windows operating system is performed using the TwinCAT Automation Device Specification (ADS) router.

The experiment control software, which handles the communication with the real-time EtherCAT system, is implemented in C^{++} on the same system. Experiment visualization is done using OpenFrameworks (version 0.10.0) which handles the low-level OpenGL programming for minimal latency and hardware-accelerated display of movements. Data for graphics visualization is polled from the real-time system and updated at 120 Hz. Complete experiment protocols can be programmed intuitively by human-readable XML files.

Safety

Multiple safety features are implemented: mechanical endstops, limit switches, emergency buttons, software limits and watchdog timers. To complement the mechanical endstops for each upper arm (see Fig. 2.1C), we implemented two limit switches per actuator at the extremes of their predefined range of motion. When pressed, the limit switches pull the enable circuits of both drives down, disabling both drives. Furthermore, each robotic device has an emergency button: when pressed, all motor drives of both robotic devices are disabled. We also implemented software limits for position, velocity and maximum force. When any of these parameters exceeds a threshold, all motor drives are disabled. Lastly, all EtherCAT slaves (the motor drives and the Beckhoff EtherCAT terminals) have built-in watchdog timers. These watchdog timers monitor the communication between the slave and the master computer. In case of a communication interruption (unplugging of a data cable or master computer crash), the watchdog timer in the motor drives will disable the drives after 50 ms. As a second layer of safety, the motor drive enable circuit is powered using a Beckhoff EL2008 digital out terminal which also includes a watchdog timer set to 50 ms. Once triggered, this watchdog timer will pull the digital output down, disabling the motor drive enable circuit and disabling the motor drives.

The electrical safety and electromagnetic compatibility are ensured by using a REOMED 2200 W medical isolator (REO) and redundant earthing. Where possible, shielded and screened electrical cabling is used. The covers of the support structure prohibit the user from touching any internal parts.

2.2.5. Manipulandum admittance controller

We chose an admittance control strategy for how a manipulandum reacts to the user's force input on the handle. In admittance control, the opposite of impedance control, the force exerted by the user onto the handle is measured and used to calculate a setpoint – through a model of desired virtual dynamics – for a lower-level position controller [22]. Figure 2.5 shows the basic control diagram of admittance control. The human exerts a force $\mathbf{F}_h$ onto the robot, which is used as an input to a virtual model $\mathbf{Y}_m$. This virtual model, for example, a mass-damper dynamic system, outputs a desired position $\mathbf{x}_d$ setpoint for the low-level controller $\mathbf{C}_p$. The controller $\mathbf{C}_p$ attempts to enforce $\mathbf{x}_d$ onto the robot $\mathbf{Y}_r$ using a controller force $\mathbf{F}_c$, resulting in the robot's motion $\mathbf{x}$.

For our application, admittance control has some advantages over impedance control which is often used in other devices (e.g. [4, 9]). Because the chosen robot configuration results in changing dynamics and conditioning across the workspace – for instance, the mass at the endpoint varies considerably over the workspace – admittance control allows us to make them isotropic. Although this can be achieved with impedance control, for instance by using feedforward dynamic compensation of the passive device dynamics, this heavily relies on how well the device dynamics can be estimated. Furthermore, for admittance control, it is more straightforward to render any dynamics, such as stiff objects and objects with high mass, which is more difficult in impedance control. For instance, when rendering a virtual wall in admittance, you only need to limit the desired position $\mathbf{x}_d$ to not cross the wall.

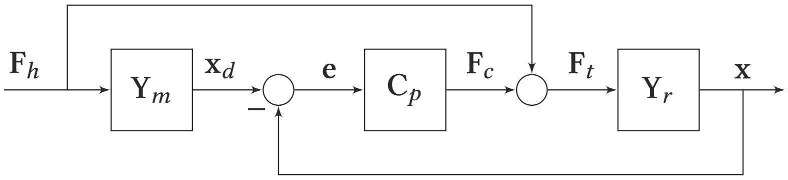

Figure 2.5. | Admittance control diagram for one manipulandum.

The apparent admittance $\mathbf{Y}_a(s)$ of the admittance controller shown in Fig. 2.5 is calculated by deriving the closed-loop transfer function from input $\mathbf{F}_h$ to $\mathbf{x}$:

$$\begin{aligned}\mathbf{Y}_a(s) = \begin{bmatrix} \frac{x(s)}{F_{h,x}(s)} & 0 \\ 0 & \frac{y(s)}{F_{h,y}(s)} \end{bmatrix} = \\ \left(\mathbf{I}^{2\times 2} + \mathbf{Y}_r(s)\mathbf{C}_p(s)\right)^{-1} \left(\mathbf{Y}_r(s) + \mathbf{Y}_r(s)\mathbf{C}_p(s)\mathbf{Y}_m(s)\right).\end{aligned} \tag{2.11}$$

The apparent admittance indicates the admittance the user feels during the interaction, taking the controller and robot dynamics into account.In the limit for high control gains, the apparent admittance converges to the desired admittance.

We set the virtual model dynamics of each robotic device to a mass ($m_v = 0.3\,\mathrm{kg}$) and damper ($b_v = 0.2\,\mathrm{N\,s\,m^{-1}}$) system. Although lower inertia is possible (e.g., the maximum mass of approximately 60 % of the usable workspace is smaller than 0.3 kg), these settings provide a good trade-off between apparent device dynamics and stability across dynamic conditions, such as rendering a rigid connection between the two robots' endpoints.

The low-level position control loop was closed using a PD controller ($\mathbf{C}_p$) in operational space [21]. The PD controller gains were tuned such that the endpoint position tracking behavior was stable across the usable workspace. The position gain k_p and differential gain k_d of controller $\mathbf{C}_p$ are set to $1500\,\mathrm{N\,m^{-1}}$ and $18\,\mathrm{N\,s\,m^{-1}}$, respectively. The controller gains are limited mainly due to mechanical constraints and the added phase lag in the closed loop due to velocity estimation, which we will analyze and discuss further in the next sections.

2.2.6. Teleoperation controller

A set of two coupled manipulanda is in principle a typical teleoperation setup. The two robotic devices can be coupled by interchanging the virtual spring force connecting both robots and adding the spring force to the virtual model force input. Figure 2.6 shows the control scheme of such a coupling: the difference in the desired robot position results in a spring force $\mathbf{F}_s$, which is added to the virtual model inputs. Admittance control allows for stable coupling of two robot devices compared to impedance control alternatives; the measured force can be interchanged directly as if both partners are applying force onto a common virtual model [23]. The low-level position control loop stiffness then limits the maximum render stiffness.

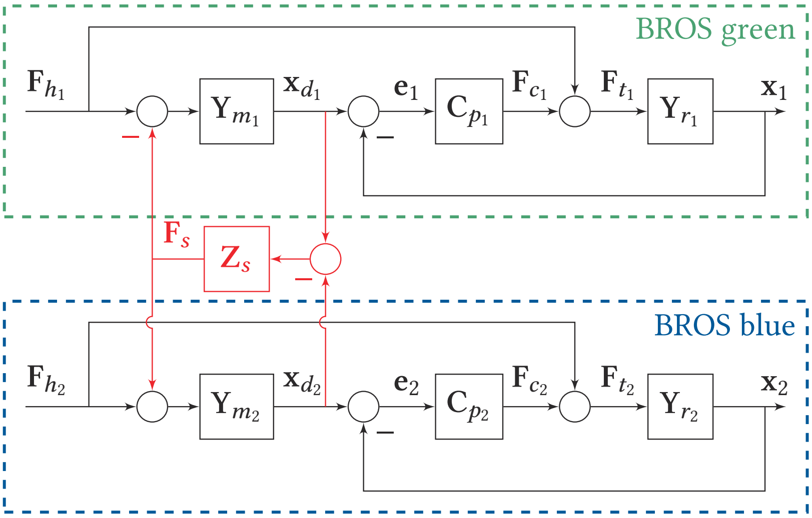

Figure 2.6. | Teleoperation controller diagram for two coupled manipulanda. The two coupled manipulanda are denoted by BROS green and BROS blue. $\mathbf{Z}_s$ denotes the connection dynamics coupling the two manipulanda, for instance a linear spring.

2.3. Evaluation

We performed some tests to evaluate the robotic device's performance. First, we tested the robot's low-level position control loop by measuring the robot's ability to render (closed-loop) stiffness and by its closed-loop position tracking bandwidth. Second, we evaluated the admittance control performance. Lastly, we evaluated the usability of the BROS for studying human-human interaction. We summarized the performance of a manipulandum in Table 2.2.

2.3.1. Closed-loop stiffness rendering and force production

The closed-loop stiffness at the handle was estimated at the nominal position in eight directions. We simulated nine springs in the virtual model, with the desired stiffness ranging from 20 N m^{-1} to 400 N m^{-1}. Per spring, we manually pulled the endpoint handle from the nominal position in eight directions. The measured force, handle position (as measured by the encoders) and handle velocity were recorded. We regressed a mass-spring-damper system in two dimensions to the measured data. The resulting stiffness in x and y was compared to the desired stiffness, see Fig. 2.7. Due to the high similarity in measured stiffness in x and y, we combined these stiffnesses in x- and y-direction in Fig. 2.7. When the desired stiffness of 200 N m is simulated, we measured a stiffness of 175 N m. The lower actual stiffness is due to the low-level position loop stiffness, which acts as a series compliance element with the desired stiffness $((1/1500 + 1/200)^{-1} =$

Table 2.2. | Performance measures of one manipulandum

Performance measure	**Value**
Usable workspace (ellipse with a bounding box of $L \times W$)	0.355 m × 0.215 m
Global conditioning index	0.74 –
Position resolution[□]	26 µm
Velocity resolution[□, ▽]	26 mm s^{-1}
Max. velocity (manual excitation)	1.05 m s^{-1}
Max. acceleration (closed-loop pos. input)	108.4 m s^{-2}
Max. acceleration (manual excitation)	16.7 m s^{-2}
Force/torque sensor range (in x and y)	100 N; 2 N m
Force sensor resolution (in x and y)	30 µN
Max. force production	50 N
Max. passive endpoint mass[□]	0.55 kg
Closed-loop position bandwidth (in x and y)	21 Hz
Admittance control bandwidth	6.5 Hz
Control frequency	1 kHz

□: The handle was at the position with lowest condition number (furthest away from the robot)
▽: Velocity resolution is calculated by dividing the position resolution by the sampling time (0.001 s)

175 N m^{-1}), see Fig. 2.7). This means that we need to compensate for the inner loop position control stiffness when setting the desired stiffness. Note that we did not take the structural stiffness of the device into account.

Each parallel manipulator of BROS is capable of generating over 50 N of force at the endpoint. We tested this by slowly increasing the generated force at the endpoint by open-loop control in eight directions. The user firmly held the handle at the endpoint. The force/torque sensor measured the force exerted by the robot onto the handle. We did not test forces over 50 N for safety reasons, because we do not expect to use such high forces during the intended human-human interaction experiments.

2.3.2. Closed-loop position bandwidth performance

The control bandwidth of the robot was assessed by analyzing the closed-loop position-position tracking performance at the endpoint *at the nominal position*. We used sum-of-sines excitation signals for the desired endpoint position $\mathbf{x}_d$ in operational space (see Chapter A for more information). The tracking performance was measured over five repetitions of 30 s with a sampling frequency of

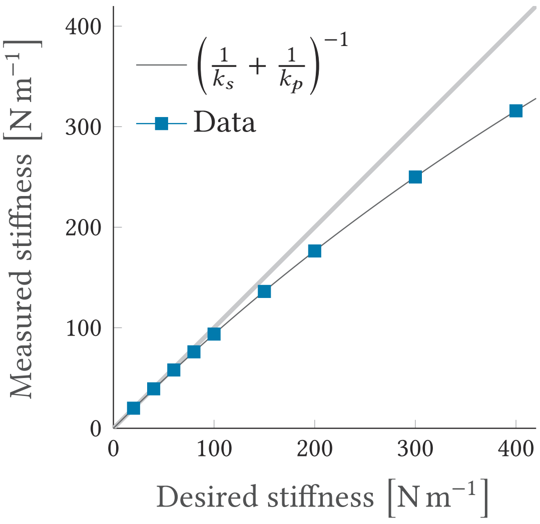

Figure 2.7. | Comparison of desired stiffness and measured stiffness. We evaluated several desired stiffness levels. The expected measured stiffness, based on the closed-loop position controller in series, is given as well. We measured the stiffness at each desired stiffness level five times, while moving the handle in eight directions. The markers indicate the mean measured stiffness, where the measured stiffness in x and y are combined. Although not visible, the small error bars (standard error of the mean) indicate that the measurements are highly repeatable.

1 kHz. The resulting robot endpoint position $\mathbf{x}$ was recorded. The measured frequency response $H_{\mathbf{x}_d,\mathbf{x}}$ for both the x and y axes are shown in Fig. 2.8. Our main observations are: (1) the frequency responses for both axes are very similar and show high consistency across repetitions, (2) the gain is approximately one up to 10 Hz for both axes, well above the expected human hand movement bandwidth, (3) a resonant peak occurs at approximately 17 Hz and (4) the frequency response crosses the -3 dB ($\sqrt{0.5}$) point at 21 Hz. Increasing the differential action of the low-level position loop PD controller should decrease the resonance peak; however, we were not able to increase damping and position gain further during tuning, most likely due to the second-order filter used for the velocity calculation and mechanical transmission resonance.

The sharp increase in the frequency response magnitude near 100 Hz in Fig. 2.8 is likely due to a mechanical resonance of the capstan transmission. To further analyze the capstan transmission dynamics, we clamped one of the upper arm links to the base of the robot (hence fixing the transmission output shaft) and sent a sum-of-sines torque excitation signal to the motor. We measured the angular motor position using the motor encoders, the (clamped) output shaft angular position using the absolute encoders and commanded and actual motor torque. The measured frequency response $H_{\tau_c,q_m}(j\omega)$ of the commanded torque τ_c to

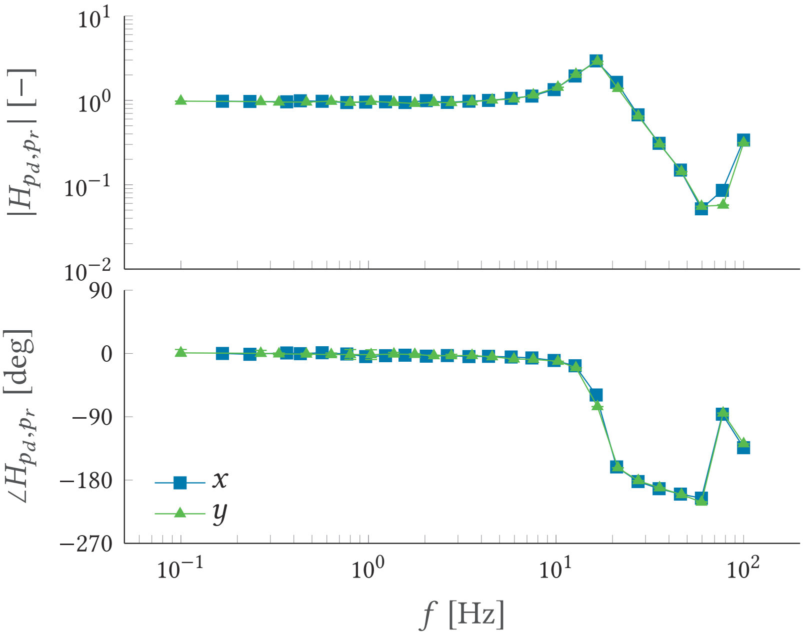

Figure 2.8. | Closed-loop position tracking frequency responses of the x and y directions at the nominal position. Markers and error bars indicate the mean and standard error of the mean, respectively. Note that the error bars are small and practically not visible, indicating that the frequency response results across the five repetitions was highly repeatable.

motor position q_m (see Fig. 2.9) indeed reveals a transmission resonance peak at $f_d \approx 110$ Hz. This low-frequency resonance most likely occurs due to the compliance in the cable transmission [24] and reduces stability margin, subsequently forcing controller gains down [25]. We will discuss options for curing the low-frequency resonance peak and its effect on stability limits in the discussion.

2.3.3. Admittance controller performance

We analyzed the performance of how well a robotic device can render the desired admittance using two metrics. First, we tested the isotropy of the rendered apparent admittance across the workspace and compared it to the passive device dynamics. Second, we analyzed the bandwidth over which the robotic device can render the desired admittance.

Isotropic apparent admittance

To compare the measured apparent dynamics and passive dynamics, we estimated the apparent endpoint mass and passive device endpoint mass to assess whether the admittance control approach indeed leads to isotropic dynamics

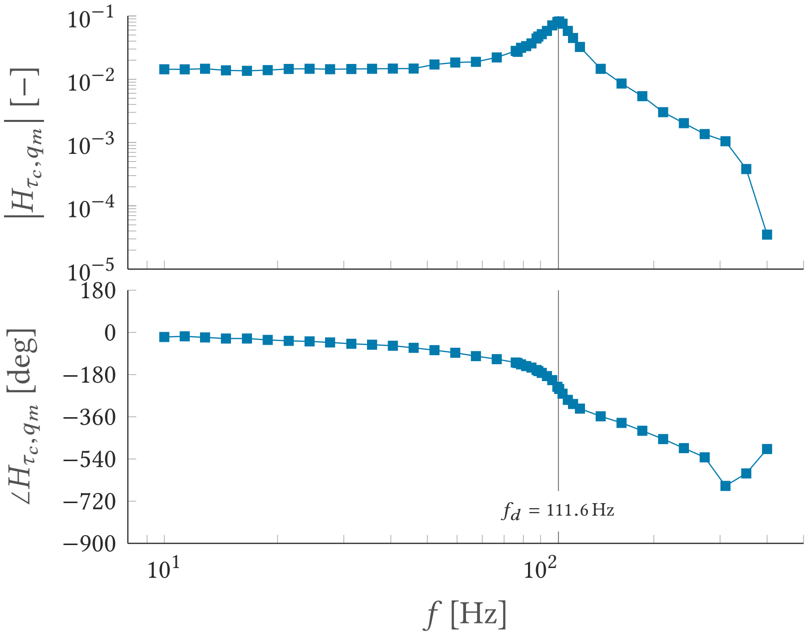

Figure 2.9. | Frequency response of the capstan transmission dynamics. The torque excitation signal consisted of 42 non-harmonic sines, equally spread over a bandwidth of 10 Hz to 400 Hz. Note that we decreased the frequency spacing between 90 Hz to 130 Hz to properly capture the resonance peak. The maximum absolute requested torque of the excitation signal was scaled to 0.2 N m.

across the workspace. To estimate the apparent admittance and passive device dynamics, we manually moved the handle at nine locations in all directions with different velocities and accelerations while staying close to the initial location for 60 s. This measurement was done twice: once when the admittance controller was switched on to measure the apparent mass and once when the device was switched off to measure the passive device mass. We recorded the force applied at the endpoint and the resulting robot movement and the endpoint position. Endpoint velocity and acceleration were obtained by time differentiation. To obtain the measured apparent mass, we fitted the desired dynamics $\mathbf{Y}_m$ (a mass-damper system in x- and y-directions) to the measured data. The resulting apparent mass matrix per location is shown in Fig. 2.10 including the expected apparent mass (e.g., $m_v = 0.3$ kg). To obtain the passive endpoint mass, we fitted the dynamic model (equation 2.9) to the measured data. The passive endpoint mass was then calculated using equation 2.10. All model fits were performed using MATLAB's `fmincon` algorithm and showed high R^2 values (> 0.9) indicating a good fit to the measurement data.

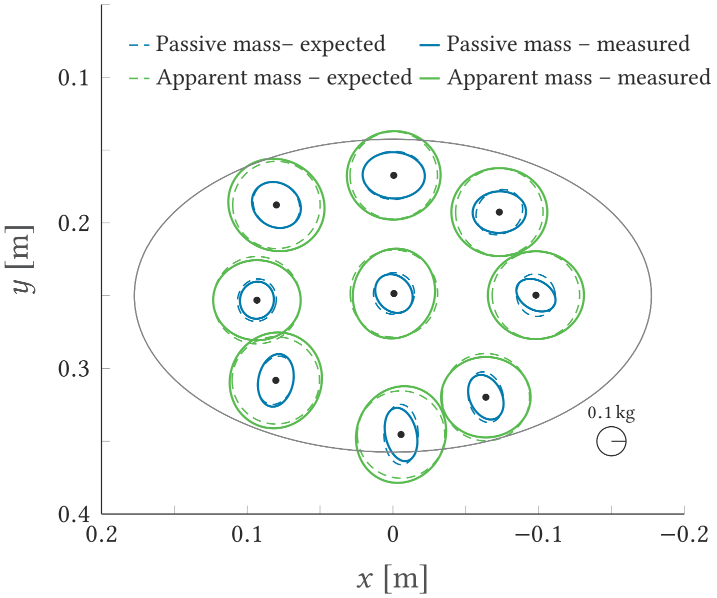

Figure 2.10. | Comparison of the expected versus measured passive and apparent mass across the workspace. The locations are the average positions of each measurement. The gray ellipse indicates the usable workspace. The admittance control approach leads to isotropic mass at different positions in the workspace.

Figure 2.10 compares the expected and measured apparent endpoint mass and expected and measured passive endpoint mass at the nine locations in the usable workspace. The apparent mass is mostly isotropic across the usable workspace compared to the passive endpoint mass. The advantage of the admittance control approach is evident for endpoint locations further away from the nominal position (i.e., locations with a smaller condition number). Dynamic feedforward compensation of the passive device dynamics could improve the passive device dynamics (e.g. [9]), however precisely identifying the passive device dynamics is not trivial. The admittance control approach 'solves' this problem for us. Small discrepancies are seen between the expected and measured endpoint masses; our manual excitation of the robot to measure these data is likely an important factor. Note that the desired apparent mass was set to 0.3 kg, which is higher than the maximum passive endpoint mass; this was done to ensure unconditional stability for all practical human-robot interaction scenarios expected during experiments.

Apparent admittance bandwidth

The bandwidth over which the desired dynamics can be rendered is examined by comparing the desired virtual dynamics Y_m with the apparent admittance inferred from Y_m, C_p and Y_r, denoted as Y_a, and felt or measured apparent admittance $\hat{\mathrm{Y}}_a$, where

$$\begin{aligned} \mathrm{Y}_a(s) &= \begin{bmatrix} \frac{x(s)}{F_{h,x}(s)} & 0 \\ 0 & \frac{y(s)}{F_{h,y}(s)} \end{bmatrix} = \begin{bmatrix} Y_x(s) & 0 \\ 0 & Y_y(s) \end{bmatrix} \text{ and} \\ \hat{\mathrm{Y}}_a(s) &= \begin{bmatrix} \hat{Y}_x(s) & 0 \\ 0 & \hat{Y}_y(s) \end{bmatrix}. \end{aligned} \tag{2.12}$$

We define the bandwidth as the lowest frequency at which the ratios of magnitude of the measured apparent admittance and the desired apparent admittance ($|\hat{\mathrm{Y}}_a|/|\mathrm{Y}_a|$) is smaller than 0.9 or larger than 0.9^{-1}.

The frequency response of the desired virtual dynamics Y_m is calculated with a mass of 0.3 kg and a damping of $0.2\,\mathrm{N\,s\,m^{-1}}$. We extracted the frequency response of the robot dynamics Y_r (from commanded torques to resulting robot position in x and y directions) using the data from the position control loop bandwidth evaluation, which means we can only evaluate Y_r at the frequencies given in Table A.1. The frequency response of the controller C_p was also evaluated at these frequencies, using the tuned position controller values. The inferred apparent admittance is then calculated using equation 2.11. The measured apparent admittance $\hat{\mathrm{Y}}_a$ was assessed by randomly applying forces onto the robot endpoint at different frequencies and in all directions for five repetitions of 120 s each at the nominal position. We took care to stay close to the nominal position while moving the endpoint. Note that the human user applying the forces was only able to provide frequencies in the range of approximately 0.2 Hz to 7.5 Hz.

Figure 2.11 shows the desired model dynamics Y_m, the inferred apparent admittance Y_a and measured apparent admittance $\hat{\mathrm{Y}}_a$. We see that the inferred and measured apparent admittance in both x- and y-directions match well. Furthermore, the inferred and measured apparent admittance results match the desired admittance at least up to 6 Hz. Above 6 Hz to 7.5 Hz the apparent admittance is still similar to the desired dynamics; however, the measured apparent admittance bandwidth already exceeds the bandwidth of typical human arm movements (for instance, the maximum frequency of human arm movements during tracking tasks is around 4 Hz [26]).

Because the apparent admittance is, among others, a function of the robot dynamics Y_r, the apparent admittance bandwidth varies over the workspace. To analyze this variation, we simulated the apparent admittance using equation 2.11

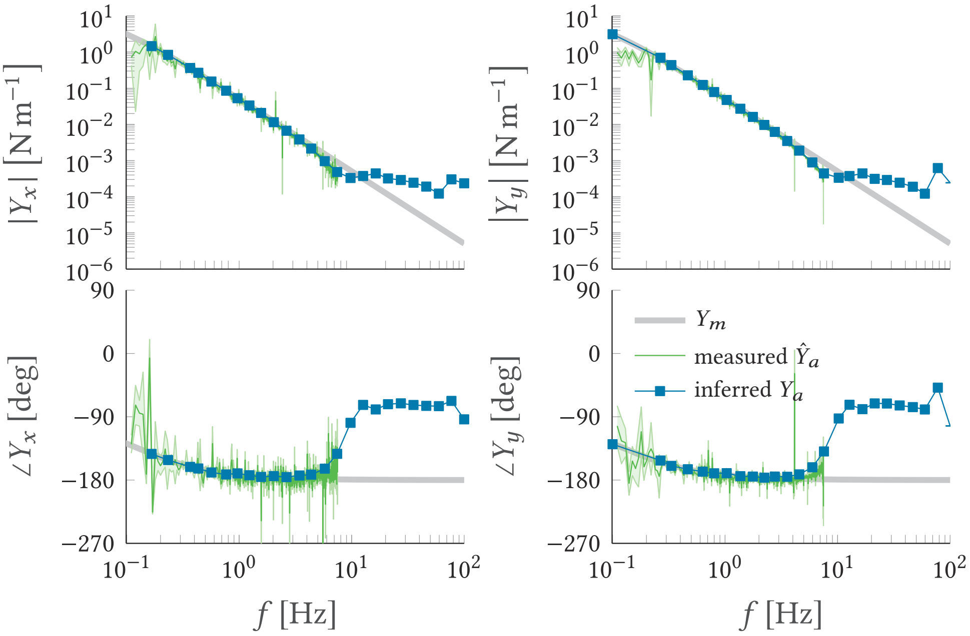

Figure 2.11. | Desired admittance versus inferred and measured apparent admittance. The left and right columns present the magnitude and phase of the desired, inferred and measured apparent admittance in the x- and y-directions at the nominal position, respectively. The measured apparent admittance shows the mean and standard error of the mean.

across the usable workspace. We estimated the parameters of the simplified dynamics (see equation 2.9) using a model fit as used for estimating the passive device dynamics as described above. The frequency response of the apparent admittance is then evaluated across the workspace and compared to the desired admittance. The apparent admittance bandwidth is defined as described above.

Figure 2.12 shows the simulated apparent admittance bandwidth across the usable workspace. The smallest bandwidth between the x- and y-directions was taken at each location. The further the endpoint is from the base of the robot, the lower the apparent dynamics bandwidth. The lowest bandwidth is approximately 4.8 Hz at the farthest position of the workspace, which is still above the expected bandwidth of human control and tracking behavior. Note that the simulated results are highly dependent on the estimated device dynamics parameters; as mentioned before, estimating the passive device dynamics yields results of varying quality. The bandwidth of the measured and inferred apparent admittance could be improved by improving the position control loop performance.

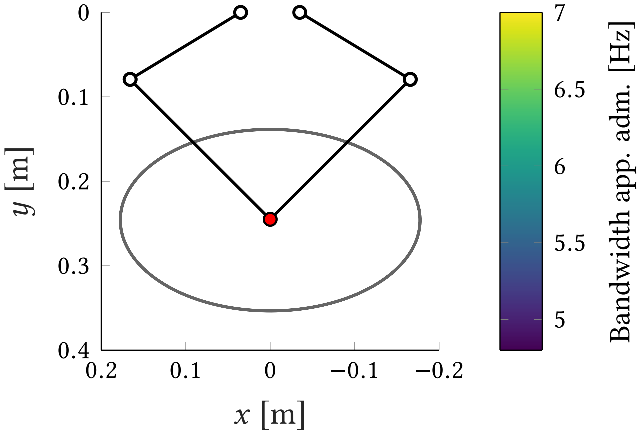

Figure 2.12. | Simulated bandwidth of the apparent admittance across the usable workspace. The shown bandwidth is the smallest frequency of the apparent admittance bandwidth in either the x- or y-direction.

2.3.4. Experimental evaluation

Here we present the results of an experiment to evaluate the performance of BROS for studying physical human-human interaction. This experiment also serves as a showcase of using an admittance control approach to teleoperation, in which the robots are coupled through a spring $\mathbf{Z}_s$ with different connection dynamics (see Fig. 2.6).

Ganesh et al. [10] showed that physical interaction through a compliant connection (a computer-generated spring) during a continuous tracking task leads to better tracking performance compared to performing the tracking task alone. More importantly, they found that you improve by interaction *regardless* of whether your partner is better or worse than you at the task. We performed a similar experiment to the one described by Ganesh et al. [10].

Experiment setup

We recruited 10 participants (aged 24.5 ± 2.2 years, four females and six males), which performed the experiment in five pairs. All participants performed the same planar tracking task. The goal was to track a target with a cursor as accurately as possible on a display. The cursor was controlled by moving the robot's handle. Each participant had a manipulandum and display, see Fig. 2.1.

The target moved continuously during trials of 48 s. The data of the first 3 s were discarded to remove any transient tracking behavior at the start of the trial. The target movement was always the same for both partners. The target movement was defined as sum-of-sines:

$$\begin{aligned}
x(t) &= 2.11\sin(0.63t + 4.86) + 2.05\sin(1.10t - 6.88)\\
&\quad + 1.91\sin(1.73t + 0.18) + 1.72\sin(2.67t - 8.49)\\
&\quad + 1.42\sin(4.24t + 3.75) + 1.31\sin(5.50t - 4.28)\\
&\quad + 1.13\sin(6.75t - 9.35) + 0.99\sin(8.01t - 0.54)\\
y(t) &= 1.95\sin(0.79t + 4.86) + 1.89\sin(1.26t - 6.88)\\
&\quad + 1.77\sin(2.04t + 0.18) + 1.59\sin(2.98t - 8.49)\\
&\quad + 1.31\sin(4.56t + 3.75) + 1.21\sin(5.18t - 4.28)\\
&\quad + 1.05\sin(6.44t - 9.35) + 0.91\sin(7.70t - 0.55)\,.
\end{aligned} \tag{2.13}$$

The tracking signal required hand movements over a circular workspace with a diameter of 18 cm, an average velocity of $13.9\,\mathrm{cm\,s^{-1}}$ and a maximum velocity of $28.9\,\mathrm{cm\,s^{-1}}$. Each pair performed 48 trials of the tracking task divided over six blocks.

Two types of trials were used in the experiment: *connected* and *single* trials. During some trials, the partners in a pair interacted with each other through a virtual spring; these trials are denoted as *connected* trials. The spring force allowed the partners to physically interact, while still being able to execute the tracking task independently. The computer-generated virtual spring (i.e., the connection dynamics $\mathbf{Z}_s$, see Fig. 2.2.6) consisted of a spring stiffness of $k_s = 120\,\mathrm{N\,m^{-1}}$ (same stiffness as used by Ganesh et al. [10]) and damping $b_s = 2.5\,\mathrm{N\,s\,m^{-1}}$:

$$\mathbf{F}_s = k_s\left(\mathbf{p}_p - \mathbf{p}_o\right) + b_s\left(\mathbf{v}_p - \mathbf{v}_o\right), \tag{2.14}$$

where $\mathbf{F}_s$ is the spring force exerted on a participant's hand, $\mathbf{p}_p$ and $\mathbf{v}_p$ and $\mathbf{p}_o$ and $\mathbf{v}_o$ are the partner's and the participant's own position and velocity, respectively. The elastic force was exerted onto both partners' hands by the robotic manipulanda. If a partner moved away from the other partner, they both experienced a force pulling them toward each other.

The partners were not connected during the remaining *single* trials. The sequence of single (S) and connected (C) trials was {[SCCSCSCS] [SCCSCSCS] [CSCSCSCC] [SCSSCSCS] [CSCSCSCC] [SSCSCSSC]}. Participants were not explicitly made aware whether the trial was a single or connected trial.

Participants gave informed consent to participation in the study. The study was designed following the principles of the Declaration of Helsinki.

An expedited assessment of the study by the Medical Ethical Review Board of the University of Twente (METC Twente) showed that the study poses minimal risk and under Dutch law does not need full ethical review.

Data analysis

We focus on the performance improvement due to physical interaction following the approach of Ganesh et al. [10] and Takagi et al. [11]. Motor performance was measured as the root-mean-square (RMS) of the tracking error, denoted by E (in cm), recorded at 1 kHz. We calculated performance for single trials (E_s) and connected trials (E_c). Since the compliant virtual springs still allowed independent tracking execution, E_c of each partner is not necessarily the same.

Similar to Ganesh et al. [10] and Takagi et al. [11], we examine the relationship between improvement due to the haptic interaction and the relative performance difference between partners. This allows us to study whether interaction with a better or worse partner results in differences in the benefits of the interaction for different skill levels. The improvement in performance due to interaction (I) is calculated as

$$I = 1 - \frac{E_c}{E_s}, \tag{2.15}$$

where E_c is the performance in a connected trial and E_s is the performance in the single trial following the connected trial. The relative performance (R) of the partner you interact with is calculated by

$$R = 1 - \frac{E_{s,p}}{E_s}, \tag{2.16}$$

where $E_{s,p}$ is the partner's performance during the single trial and E_s is the participant's own performance during the same single trial. To highlight the trends in the data, we calculated the mean performance improvement in bins that are 5 % of relative performance R wide.

To analyze whether physical interaction leads to significant improvement compared to performing the task alone, we used Wilcoxon sign-rank tests (one-sample) per bin to test whether the improvement per bin had a median larger than zero at a level of significance of 0.05.

Results

The improvement in task performance during a connected trial compared to both partners performing the task alone is plotted against the relative performance difference between the partners in Fig. 2.13.

Physical interaction generally leads to improvement in motor performance *during* interaction when connected to a better partner (top-right quadrant). We found significant improvement for all positive relative performance bins, i.e. when the relative partner performance is $R > 5\,\%$ (all sign-rank tests resulted in $p < 0.01$). Being connected to a worse partner did not significantly improve performance (top-left quadrant). All sign-rank tests for all bins $R < 0$ did not reveal significant differences except for the bin spanning the relative range $R = [-17.5, -12.5]\,\%$.

Although our evaluation experiment showed similar results to previous work [10] on physical human-human interaction, we could not confirm their main conclusion that physical interaction leads to improvement regardless of partner performance. Although we used similar spring dynamics, we found no significant improvement when interacting with a worse partner. Note that we used a different, more difficult target tracking sum-of-sine signal compared to Ganesh et al. [10]; however, we did not introduce a visual perturbation to during the tracking task (a visuomotor rotation), as Ganesh

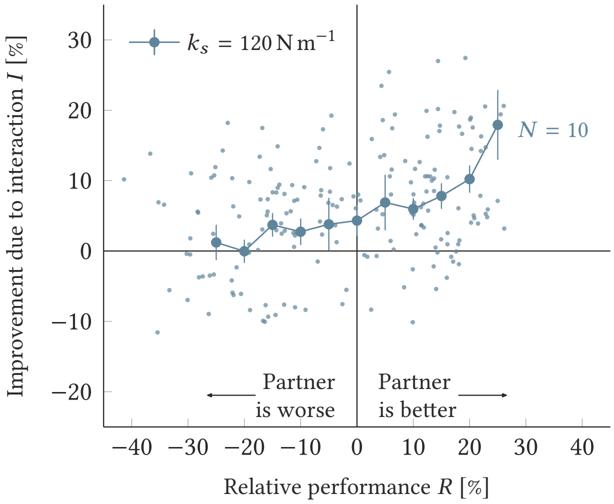

Figure 2.13. | Relative performance versus improvement due to physical interaction. The horizontal axis shows the relative performance R between interacting partners, the vertical axis shows the improvement I due to interaction: a positive improvement means that interaction helps. The error bars show the mean and standard error of the mean improvement per bin.

et al. [10] did. Nonetheless, the experiment demonstrated the capability of BROS to investigate physical human-human interaction.

2.4. Discussion

This paper described the design, implementation and evaluation of BROS, a robotic setup with two 2-DOF manipulanda designed for studying physical human-human interaction. We showed that the device can render the desired admittance across the workspace and can be used for studying human-human interaction. The compact design of the robotic manipulanda of BROS allows for multiple configurations of the setup (for instance two manipulanda for human-human interaction or bimanual motor control or one for unimanual motor control studies). Multiple safety features minimize the risk for the user.

Manipulandum evaluation

The main design parameters for the robotic devices were a minimal passive mass at the end-point, high force production and good robot conditioning while providing a sufficiently large workspace. BROS' capabilities to render admittance dynamics isotropically across the workspace allow for a useful tool to study human-human interaction. We assessed the uniformity in the x- and y-directions of the admittance dynamics by evaluating the apparent mass at several points across the workspace. Furthermore, we showed that the bandwidth with which the manipulanda can render the desired dynamics exceeds the typical bandwidth of human arm movements in a plane (e.g. [26]). The apparent passive mass at the end-point is relatively low compared to other devices and permits the stable rendering of low mass dynamics compared to other (impedance-controlled) devices (e.g. [4, 9]). The maximum force production of BROS is lower than other similar devices [4, 6, 9]; however, its force production is sufficient for our experimental goals.

Future hardware improvements

The evaluation test results suggest that some improvements can be made to improve BROS' performance. First, the position control loop performance can be improved in different ways. The velocity estimation is currently performed by using a discrete-time differentiation of the joint positions in combination with a second-order Butterworth filter with a cut-off frequency at 70 Hz. Other methods such as the first-order adaptive windowing (FOAW)

[27] or implementing a Kalman filter could yield better results. We could also use gyroscopes to measure the rotational rate of the joints directly. The position control loop can be further improved by implementing inverse dynamic control [21]. However, due to the uncertainty in the identified dynamic model parameters, such as identified static and viscous friction, we did not find significantly better performance using inverse dynamics compared to the (much simpler) PD controller we implemented instead; still, further research is warranted. Second, the low-frequency resonance mode originating in the capstan transmission reduces control stability margins. Acceleration feedback, for instance through inertial measurement units can help to cure low-frequency resonance [25]. At the moment we implemented a single PD controller; however, we could implement more complex control strategies, such as gain scheduling. Furthermore, the resonance frequency of the capstan transmission could be shifted to higher frequencies and thus reducing its impact by increasing the transmission stiffness, for instance by increasing the cable pretension or using cables with larger diameters [24].

In summary, the BROS provides a useful and versatile tool to study physical human-human interaction, bimanual motor control and upper-extremity impairment assessment [28, 29], other applications of teleoperation and motor control.

Acknowledgments

The authors would like to thank Arno Stienen for his contributions in the early design stages of BROS, Mattia d'Alessi for his help in collecting the data of the human-human interaction experiment and Hankamp Rehab for their support in building the devices.

References

[1] J Meuleman, E van Asseldonk, G van Oort, H Rietman, and H van der Kooij. LOPES II - Design and Evaluation of an Admittance Controlled Gait Training Robot with Shadow-Leg Approach. *IEEE Transactions on Neural Systems and Rehabilitation Engineering*, 24(3):352–363, March 2016.

[2] T Nef, M Mihelj, and R Riener. ARMin: A robot for patient-cooperative arm therapy. *Medical and Biological Engineering and Computing*, 45(9):887–900, September 2007.

[3] A Melendez-Calderon, L Bagutti, B Pedrono, and E Burdet. Hi5: a versatile dual-wrist device to study human-human interaction and bimanual control. In *2011 IEEE/RSJ International Conference on Intelligent Robots and Systems*, pages 2578–2583. IEEE, 2011.

[4] I S Howard, J N Ingram, and D M Wolpert. A modular planar robotic manipulandum with end-point torque control. *Journal of Neuroscience Methods*, 181(2):199–211, July 2009.

[5] S H Scott. Apparatus for measuring and perturbing shoulder and elbow joint positions and torques during reaching. *Journal of Neuroscience Methods*, 89(2):119–127, 1999.

[6] M Casadio, V Sanguineti, P G Morasso, and V Arrichiello. Braccio di Ferro: A new haptic workstation for neuromotor rehabilitation. *Technology and Health Care*, 14 (3):123–142, September 2006.

[7] H Gomi and M Kawato. Human arm stiffness and equilibrium-point trajectory during multi-joint movement. *Biological Cybernetics*, 76(3):163–171, March 1997.

[8] R Q van der Linde, P Lammertse, E Frederiksen, and B Ruiter. The HapticMaster, a new high-performance haptic interface. *Proceedings of Eurohaptics*, pages 1–5, 2002.

[9] J Klein, N Roach, and E Burdet. 3DOM: a 3 degree of freedom manipulandum to investigate redundant motor control. *IEEE Transactions on Haptics*, 7(2):229–239, April 2014.

[10] G Ganesh, A Takagi, R Osu, T Yoshioka, M Kawato, and E Burdet. Two is better than one: Physical interactions improve motor performance in humans. *Scientific Reports*, 4, 2014.

[11] A Takagi, G Ganesh, T Yoshioka, M Kawato, and E Burdet. Physically interacting individuals estimate the partner's goal to enhance their movements. *Nature Human Behaviour*, 1(3):0054, 2017.

[12] A Melendez-Calderon, V Komisar, and E Burdet. Interpersonal strategies for disturbance attenuation during a rhythmic joint motor action. *Physiology & Behavior*, 147:348–358, 2015.

[13] N Beckers, A Q L Keemink, E van Asseldonk, and H van der Kooij. Haptic Human-Human Interaction Through a Compliant Connection Does Not Improve Motor Learning in a Force Field. In D Prattichizzo, H Shinoda, H Z Tan, E Ruffaldi, and A Frisoli, editors, *11th International Conference, EuroHaptics 2018*, pages 333–344. Springer International Publishing, 2018.

[14] Y Che, G M Haro, and A M Okamura. Two is not always better than one: Effects of teleoperation and haptic coupling. *2016 6th IEEE ...*, pages 1290–1295, 2016.

[15] J Diedrichsen. Optimal task-dependent changes of bimanual feedback control and adaptation. *Current Biology*, 17(19):1675–1679, 2007.

[16] D A Braun, P A Ortega, and D M Wolpert. Nash equilibria in multi-agent motor interactions. *PLoS Computational Biology*, 5(8):e1000468, August 2009.

[17] D M Wolpert, J Diedrichsen, and J R Flanagan. Principles of sensorimotor learning. *Nature Reviews Neuroscience*, 12(12):739–751, November 2011.

[18] C M Gosselin and J Angeles. The Optimum Kinematic Design of a Planar Three-Degree-of-Freedom Parallel Manipulator. *Journal of Mechanisms Transmissions and Automation in Design*, 110(1):35, 1988.

[19] J-P Merlet. *Parallel Robots.* Springer Science & Business Media, January 2006.

[20] A Codourey. Dynamic modeling of parallel robots for computed-torque control implementation. *International Journal of Robotics Research*, 17(12):1325–1336, December 1998.

[21] B Siciliano, L Sciavicco, L Villani, and G Oriolo. *Robotics; Modelling, Planning and Control.* Springer Science & Business Media, London, January 2009.

[22] A Q L Keemink, H van der Kooij, and A H A Stienen. Admittance control for physical human–robot interaction. *International Journal of Robotics Research*, 1(2): 027836491876895–24, April 2018.

[23] P Lammertse. Admittance control and impedance control - a dual, with an application to master slave telemanipulation. Technical report, MOOG, November 2009.

[24] J Werkmeister and A Slocum. Theoretical and experimental determination of capstan drive stiffness. *Precision Engineering*, 31(1):55–67, December 2006.

[25] G Ellis. Cures for low-frequency mechanical resonance in industrial servo systems. *Conference Record of the IEEE Industry Applications Conference. th IAS Annual Meeting Cat. No.CH*, 1:252–258, 2001.

[26] P M T Zaal, D M Pool, M Mulder, and M M van Paassen. Multimodal pilot control behavior in combined target-following disturbance-rejection tasks. *Journal of Guidance, Control, and Dynamics*, 32(5):1418–1428, September 2009.

[27] F Janabi-Sharifi, V Hayward, and C-S J Chen. Discrete-time adaptive windowing for velocity estimation. *IEEE Transactions on Control Systems Technology*, 8(6):1003–1009, 2000.

[28] L Simmatis, J Krett, S H Scott, and A Y Jin. Robotic exoskeleton assessment of transient ischemic attack. *PLoS ONE*, 12(12), December 2017.

[29] T C Bourke, C R Lowrey, S P Dukelow, S D Bagg, K E Norman, and S H Scott. A robot-based behavioural task to quantify impairments in rapid motor decisions and actions after stroke. *Journal of NeuroEngineering and Rehabilitation*, pages 1–13, October 2016.

Chapter 3.

Haptic interaction between humans neither facilitates nor interferes with learning novel dynamics

Niek Beckers, Edwin van Asseldonk,
Arvid Keemink, and Herman van der Kooij

This chapter is based on the paper presented at Eurohaptics 2018 and is published in:
Prattichizzo D., Shinoda H., Tan H., Ruffaldi E., Frisoli A. (eds) Haptics: Science, Technology, and Applications. EuroHaptics 2018. Lecture Notes in Computer Science, vol 10893. Springer, Cham

Abstract

Humans have a natural ability to haptically interact with other humans, for instance during physically assisting a child to learn how to ride a bicycle. A recent study found that haptic human-human interaction can improve individual motor learning of tracking a continuously-moving target in a visuomotor rotation. We investigated whether haptic interaction also improved learning of a similar tracking task in a new dynamic environment. Pairs performed the tracking task and were intermittently connected to each other through a compliant connection. Motor learning was assessed by comparing each partner's individual performance during trials in which they were not connected to the performance of participants who learned the task alone. We found that haptic interaction did not lead to better individual motor performance or faster motor learning rates. Performance during haptic interaction was significantly better than when the partners were not interacting, even in the force field.

3.1. Introduction

Interaction with another human plays an important role when learning new motor tasks [1]. For example, visually observing someone else learn improves your own motor performance [2–4]. Haptic interaction – interaction by exerting forces onto each other – with a human partner who is learning the same collaborative motor task has also been shown to improve each participant's motor learning [5]. In Ganesh et al. [5]'s study, pairs learned to track a common randomly-moving target with their hands while being perturbed by a visuomotor rotation, in which the visual movement of the hand on a display was rotated with respect to the actual hand movement. Participants that haptically-interacted through a compliant connection improved more and faster compared to participants who practiced the same task without any interaction. However, to our knowledge, no studies other than [5] have shown the potential benefits of haptic interaction between humans on motor learning.

The benefits of haptic human-human interaction on individual motor learning could complement the design of robot-assisted motor learning paradigms. Other studies that used robotic assistance to help humans learn a new motor task showed mixed results. Haptic guidance – physically guiding a student through the desired movement – immediately improves performance while the student receives the assistance, but rarely results in improved individual motor learning [6–11]. To complement the design of human-robot interaction strategies that benefit the motor learning of the human, more research is needed to understand why haptic interaction with another human would improve learning and to investigate whether haptic interaction also improves learning in motor tasks other than a visuomotor rotation learning task as used by Ganesh et al. [5].

Here we tested whether haptic interaction between two humans, using the interaction paradigm from Ganesh et al. [5], improves the motor learning of novel dynamics. Many real-life motor tasks include (re)learning new task dynamics, for instance learning how to balance yourself on a bicycle. The novel dynamics consisted of a velocity-dependent force field, a well-known motor adaptation paradigm used in reaching tasks [12, 13] and tracking tasks [14].

When people move in a velocity-dependent force field for the first time, their movements are perturbed by the force field, which results in movement errors (e.g., [12–14]). People decrease these movement errors with practice – a process also referred to as motor adaptation – using at least two complementary mechanisms [15]. First, we can learn an internal model of the dynamics and use this model to predict and compensate for the perturbations [12, 16, 17]. Second, participants can modulate arm impedance through muscle co-contraction [18–20]. Studies found that both these mechanisms contribute to the early compensation of the force field; muscle co-contraction offers a temporary strategy to reduce errors while the internal model is learned [18, 21, 22].

Because the interaction forces originating from the haptic interaction are in the same sensory domain and plane as the force field, it is unknown how the haptic interaction will influence motor learning of the force field. Studies found that humans can learn to compensate for a velocity-dependent force field even when the force field is superimposed by a constant background force [23, 24]. These studies reported that participants had difficulty judging the force field strength when the background force was present, but the presence of aftereffects when the forces were removed indicated that participants learned an internal model of the forces to some extent despite the background force. Liu and Reinkensmeyer [24] also found that participants updated their internal model of the force field slower when the background force was present compared to the no background load condition. It is possible that the interaction force has a similar effect in our task; haptic interaction might slow down the motor learning of the force field.

In this study, we investigated whether haptic interaction between two partners facilitated or interfered with learning to track a randomly moving target in novel dynamics. Its primary goal is to investigate whether the promising improvement in learning a visuomotor task as reported by Ganesh et al. [5] also generalizes to a dynamic learning task. Contrary to Ganesh et al. [5], we found that haptic interaction neither facilitates nor interferes with learning to move in a velocity-dependent force field.

3.2. Methods

Forty participants (aged 19–35 years, 28 males and 12 females; all except four were right-handed according to the Edinburgh handedness inventory [25]) participated in the experiment. All participants were naive to the force field motor task. The study was designed following the principles of the Declaration of Helsinki. An assessment of the study by the Medical Ethical Review Board of the University of Twente (METC Twente) showed that the study posed minimal risk to the participants and therefore under Dutch law did not need full ethical review. All participants provided written informed consent. The experiment lasted approximately two hours; all participants received compensation for their participation.

3.2.1. Robotic setup

The experiments were performed using a dual robotic setup, see Fig. 3.1 and Chapter 2 for a full description. Participants held and moved their own robotic manipulandum. The manipulanda allowed arm movements in a horizontal plane. The manipulanda were admittance-controlled, such that the handle's dynamics (a mass of $0.3\,\mathrm{kg}$ and a damping of $0.25\,\mathrm{N\,s\,m^{-1}}$) were isotropic over the workspace. Each partner had their own display that showed the workspace, target and their own cursor (Fig. 3.1). Participants controlled the cursor by moving the handle of their own manipulandum. Cursor and target movements were scaled on the display to match the real-world movement of the manipulandum. A curtain obstructed the view of the other partner and the partner's display. A panel obstructed a direct view of the arm and hand of each participant. Participants were not allowed to communicate verbally during the experiment.

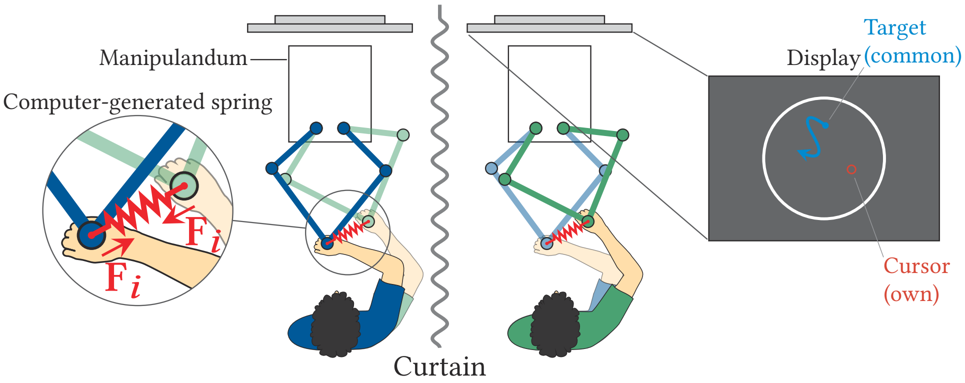

Figure 3.1. | Manipulanda and display. Each participant had their own display showing a cursor and target. The participants could control their own cursor by moving the handle. The target movement was the same for both partners. The detail shows how the partners were haptically coupled through a compliant computer-generated spring.

3.2.2. Task and interaction paradigm

Tracking task

All participants performed the same collaborative planar tracking task. The goal was to track a target as accurately as possible on a display. The participants tracked the continuously moving target during trials of 23 s followed by a 20 s break. The target movement was always the same for both partners in a pair. The target movement $\mathbf{T}$ in x- and y-direction (in mm) was defined as a sum-of-sines:

$$\begin{aligned} T^{(x)}(t) &= 28.7\sin(0.94t-7.77)+27.1\sin(1.26t-8.53)\\ &\qquad +23.5\sin(1.89t-4.36)+18.0\sin(2.83t-3.79)\\ T^{(y)}(t) &= 27.1\sin(1.26t-0.71)+25.3\sin(1.57t-3.45)\\ &\qquad +21.6\sin(2.20t+3.92)+16.4\sin(3.14t+4.93)\,. \end{aligned} \tag{3.1}$$

The tracking signal required hand movements over a circular workspace with a radius of 10 cm, an average velocity of $79\,\mathrm{mm\,s^{-1}}$ and a maximum velocity of $139\,\mathrm{mm\,s^{-1}}$. To prevent fast learning or other cognitive tracking strategies, we chose a uniformly random start time for the signals ($t \in [t_0, t_0+23]\,\mathrm{s}$, $t_0 \sim \mathcal{U}(0,20)$) and we rotated the tracking signal randomly from a set of six predefined rotations: $\left[0, \frac{1}{3}\pi, \frac{2}{3}\pi, \pi, \frac{4}{3}\pi, \frac{5}{3}\pi\right]$rad.

Connected and single trials

Two types of trials were used in the experiment: *connected* (C) and *single* (S) trials. A single trial is a trial in which the partners in a pair performed the task alone (they were not connected). During a connected trial, partners physically interacted through a compliant connection that connected the handles of the two partners (see the detail in Fig. 3.1). The connection was a computer-generated spring, which generated a force

$$\mathbf{F}_i = k_s \left(\mathbf{p}_p - \mathbf{p}_o\right) + b_s \left(\mathbf{v}_p - \mathbf{v}_o\right), \tag{3.2}$$

where k_s is the connection stiffness, b_s a damping contribution, $\mathbf{p}_p$ and $\mathbf{v}_p$ and $\mathbf{p}_o$ and $\mathbf{v}_o$ are the partner's and the participant's own position and velocity, respectively. The force was exerted onto both partners' hands by the manipulanda. If a partner moved away from the other partner, they both experienced a force pulling them toward each other. We also refer to the spring force $\mathbf{F}_i$ as the interaction force.

We set the stiffness and damping to $k_s = 150\,\mathrm{N\,m^{-1}}$ and $b_s = 2\,\mathrm{N\,s\,m^{-1}}$, respectively. The stiffness was similar to previous work [5], and we added a small damping coefficient for spring stability, but small enough to only minimally interfere with the velocity dependent force field. The compliant connection allowed the partners to haptically interact while being able to execute the tracking task independently. Active task execution was required; participants could not completely relax and let the force pull their hand along.

3.2.3. Experiment design and force field

All participants performed the experiment in pairs. Each pair performed four blocks of 21 trials, see Fig. 3.2A. Between blocks, participants had a four-minute break. Block 1 served as a baseline, in which participants practiced the tracking task without a perturbation. A velocity-dependent force field was introduced in blocks 2 and 3, which generated a planar force $\mathbf{F}_c$ given by

$$\mathbf{F}_c = \mathbf{D}\mathbf{v} \equiv \begin{bmatrix} F_\mathrm{c}^{(x)} \\ F_\mathrm{c}^{(y)} \end{bmatrix} = \begin{bmatrix} 0 & -15 \\ 15 & 0 \end{bmatrix} \begin{bmatrix} v^{(x)} \\ v^{(y)} \end{bmatrix} \tag{3.3}$$

on the hand of each participant, similar to previous work (a clockwise perturbation) [12, 26]. The force field was removed in block 4 to observe aftereffects, if present. The force field generated a force that was always perpendicular to the movement, see Fig. 3.2B. During the connected trials, the force field was superimposed on the interaction force; hence the participants would feel a total force $\mathbf{F}_t$, which is the sum of the force field $\mathbf{F}_c$ and the interaction force $\mathbf{F}_i$ (see Fig. 3.2C). The participants were informed that a force field would disturb their movements and they were instructed to track the target as accurately as possible at all times. We asked participants not to stop tracking to learn the force field.

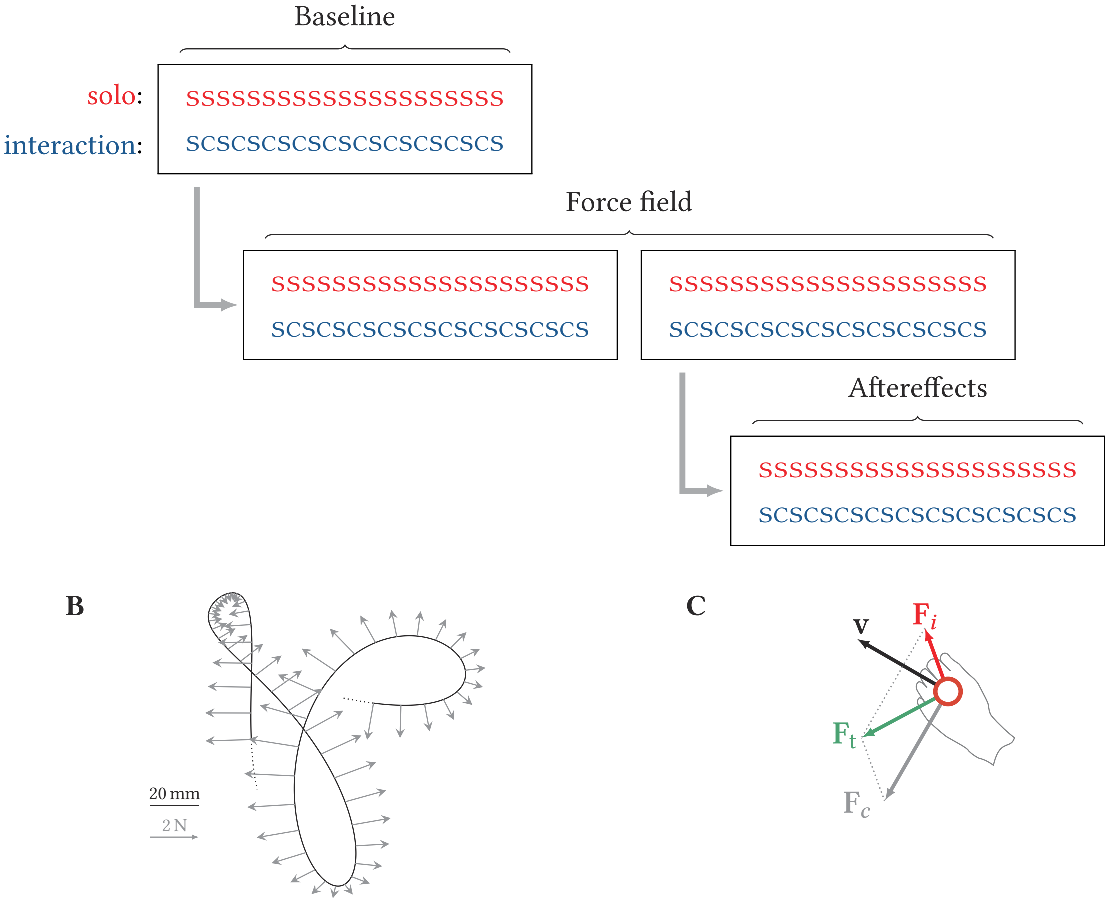

Figure 3.2. | Experiment design, force field and forces on the handle. **A** The four experiment blocks, including the trial sequences for the interaction and solo group. **B** The force field introduces forces perpendicular to the movement. Here we show part of the tracking signal and the ideal force compensation, if the target was tracked perfectly. **C** Forces at the robot handle during the force field blocks. The participant feels a total force $\mathbf{F}_t$, which is the sum of the force field force $\mathbf{F}_c$ (proportional to the own hand velocity $\mathbf{v}$) and interaction or spring force $\mathbf{F}_i$. The forces originating from the robot's dynamics are omitted.

We equally divided the forty participants over two groups: an interaction group and a solo group. They performed an alternating sequence of single and connected trials in each block (that is, {SCSCSCSCSCSCSCSCSCSCS}), see Fig. 3.2A. Hence, the partners in the interaction group intermittently interacted with each other while performing the tracking task in the baseline, force field and aftereffect blocks. Participants were not explicitly made aware of the haptic interaction.

The participants in the solo group only performed single trials (see Fig. 3.2A). We included a solo group for comparison and to analyze whether physical interaction would interfere with adapting to the force field [27].

3.2.4. Analysis

Data, including handle position and velocity, interaction force and total force exerted by each participant onto the handle were sampled and logged at 1 kHz. We used MATLAB R2017B to parse the data and perform additional analysis. Statistical analysis was done using the R statistical software package (version 3.5.1).

Motor performance and motor learning

The primary measure of motor performance is the root mean square of the tracking error E (the distance between the target and cursor) of the last 20 s of each trial. The lower the tracking error E, the better the motor performance. We calculated the motor performance for each partner and each trial. The performance during a single trial and connected trial are denoted by E_s and E_c, respectively. Partners could still perform the tracking task independently during the connected trials due to the connection compliance; hence the tracking errors in the connected trials are not necessarily the same for both partners.

The effect of haptic interaction on motor learning is assessed by comparing the individual learning curves of the baseline and force field blocks. Unless stated otherwise, we focus on individual motor learning based on the single trial performance per participant. Motor learning was quantified using four measures: (1) the performance after learning $E_{s,\mathrm{al}}$, (2) the initial motor performance $E_{s,0}$ when first exposed to the visuomotor rotation, (3) the motor improvement from the initial performance to the error after learning and (4) the rates at which each participant improved motor performance. We calculated the motor performance after learning, denoted by $E_{s,\mathrm{al}}$ as the mean performance of the last five single trials of the baseline and the force field blocks. The motor improvement in the baseline and force field blocks is the difference between the error after learning and the initial performance in the first trial of the baseline block and force field blocks $\left(E_{s,0} - E_{s,\mathrm{al}}\right)$.

The learning rate was extracted by fitting a single exponential function

$$E_s = a + be^{-\lambda(t-1)} \tag{3.4}$$

(where t is the trial number, λ the learning rate and a and b are constants) to each participant's single performance curves using MATLAB's FMINCON. We also extracted the rates of each participant's performance during the connected trials for comparison. We used R^2 as a goodness-of-fit measure. Fits that had an $R^2 < 0.25$ were not taken into account. We removed two fits in the solo group and one fit of the interaction group. Fitting a double exponent function or a power function to the learning curves did not yield significantly better R^2 values.

Force field compensation factor

People can use complementary mechanisms to compensate for a force field perturbation [15, 18]. Participants can increase arm impedance by muscle co-contraction [18, 19] as a compensation strategy. Furthermore, participants can learn and use an internal model of the force field to predict the force field forces based on their current hand velocity [12, 16, 26, 28, 29]. We calculated the force field compensation factor α, which served as a measure of how much each participant on average compensated for the force field forces in every single trial and reflects the combination of the aforementioned mechanisms [15, 26].

Following the approach of previous work [15, 26, 28], we regressed the *actual* compensation forces $\mathbf{F}_{c,a}$ generated by the participants to compensate for the force field on the *ideal* forces $\mathbf{F}_{c,i}$ that would fully compensate for the force field. The actual compensation force is preferably measured in error-clamp trials, in which the movements perpendicular to the desired movement are restricted such that the measured forces only describe the (feedforward) force field compensation [28]. However, error-clamp trials are mainly used in reaching tasks that involved discrete and fast reaching movements in which the force field is compensated for in a feedforward manner [26, 28]. In contrast, we used a continuous tracking task that required feedback control such that error-clamp trials are not as useful. Instead, to compensate for the forces resulting from moving the manipulandum, we calculated the the actual forces $\mathbf{F}_{c,a}$ during a single trial ($\mathbf{F}_i = 0\,\mathrm{N}$) per participant as follows:

$$\mathbf{F}_{c,a} = \mathbf{F}_t - (m_r \ddot{\mathbf{x}}_r + b_r \dot{\mathbf{x}}_r)\,, \tag{3.5}$$

where $\mathbf{F}_t$ is the measured total force, m_r and b_r are the mass and damping of each manipulandum's admittance model, and $\ddot{\mathbf{x}}_r$ and $\dot{\mathbf{x}}_r$ are the manipulandum's measured acceleration and velocity.

To calculate the ideal compensation forces $\mathbf{F}_{c,i}$, we assumed that participants would return to their tracking trajectories in the no force field blocks after extensive practice in the force field, based on previous work [14]. The ideal force profile was calculated using each participant's hand velocity of the average tracking trajectory of the last eight single trials of both the baseline and aftereffects blocks using equation 3.3. We then computed the compensation factor α as:

$$\alpha = \frac{1}{N} \sum_{k=1}^{N} \frac{\|\mathbf{F}_{c,a}\|}{\|\mathbf{F}_{c,i}\|}, \tag{3.6}$$

where k is the time step and N is the number of time steps in a trial. The resulting α reflects how much each participant compensated for the force field in a single trial.

Statistical analysis

All data and statistical model fit residuals were checked for normality using the Shapiro-Wilk normality test and visual inspection. We used dependent-samples t-tests to compare the performance between the single and connected trials of the interaction group. Independent-samples t-tests are used to compare performance between the solo and interaction groups. We compared the improvement improvement between solo and interaction groups using ANCOVA, with initial performance $E_{s,0}$ as covariate and group as factor. We used the Kruskal-Wallis test and Wilcoxon signed-rank test for paired samples and Mann-Whitney U tests for unpaired samples to compare the learning rates within and between groups. We analyzed the compensation factor using ANCOVA, with the single trial number as covariate and group as factor. We log-transformed the compensation factor such that the model fit residuals were normally distributed. We set the level of significance for all tests to 0.05; the Bonferonni correction was applied when making multiple comparisons. Unless explicitly stated, all data are reported as the mean ± standard error of the mean (s.e.m.).

3.3. Results

We investigated whether learning to move in novel dynamics – a velocity dependent force field – is facilitated by haptic interaction with a partner who is learning the same collaborative task, or whether haptic interaction interfered with learning. Participants tracked a randomly-moving target in a plane and were intermittently connected with a compliant spring. A force field was introduced to elicit motor learning. Performance – the root-mean-square of the tracking error – was calculated for single trials, in which participants performed the task alone, and connected tasks, in which the participants were haptically connected. We compared their single performance (i.e., when they were not connected) to a group who never haptically interacted.

Figure 3.3 shows the motor performance of the single trials for both the interaction and solo groups over the experiment. Both groups reached the same error after learning in the baseline block (see Fig. 3.3B; no significant difference between the interaction and solo group $t(38) = 0.13$, $p = 0.90$). When first exposed to the force field, individual motor performance was significantly worse compared to the performance of the last five single trials in the baseline block (dependent-samples t-tests; interaction group: $t(19) = 5.86$, $p = 1.2 \cdot 10^{-5}$; solo group: $t(19) = 6.66$, $p = 2.3 \cdot 10^{-6}$). The performance in the first force field trial was similar between the interaction and solo group (independent-samples t-test $t(38) = -0.72$, $p = 0.475$). Participants in the interaction and solo groups also improved significantly with respect to the initial performance in the force field (interaction group: $t(19) = 7.05$, $p = 1.0 \cdot 10^{-6}$; solo group: $t(19) = 5.78$, $p = 1.4 \cdot 10^{-5}$). Both groups learned to track the target in the force field equally well; the error after learning in the force field blocks was not significantly different between groups ($t(38) = -0.20$, $p = 0.84$), see Fig. 3.3B. In addition, the error after learning in the force field block was similar for both the solo and interaction groups (dependent-samples t-tests, within each group; interaction: $t(19) = 0.98$, $p = 0.338$; solo: $t(19) = 0.42$, $p = 0.680$).

3.3.1. Initially less-skilled participants do not benefit more from haptic interaction

It is possible that physical interactions resulted in more motor improvement for participants who are initially less skilled at the task [30]. Figure 3.3C shows each participant's improvement versus his/her initial performance $(E_{s,0})$ for all groups. The initial performance significantly predicted improvement (ANCOVA with $E_{s,0}$ as covariate and interaction group as a

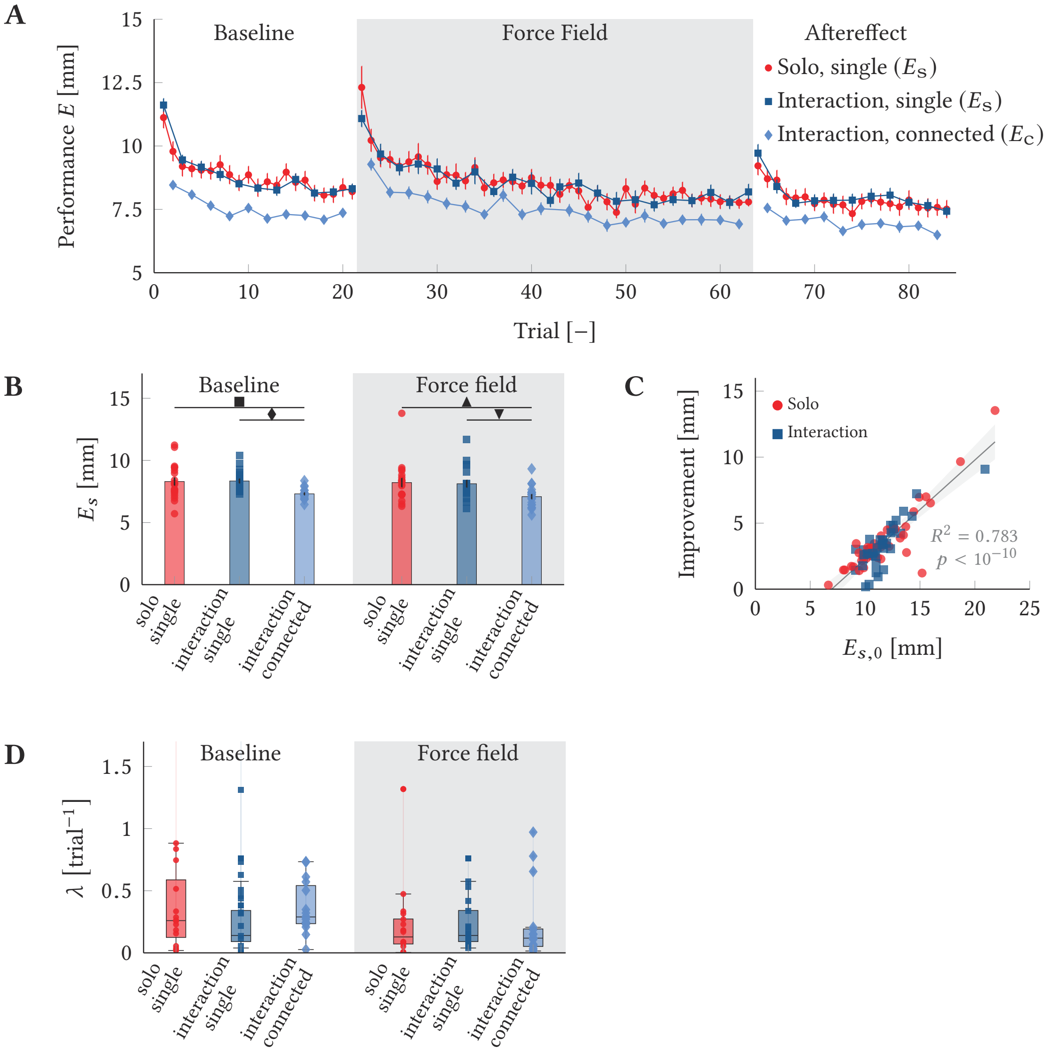

Figure 3.3. | Motor performance over the course of the experiment. **A** The learning curves of the single trials of both interaction and solo groups are similar. The performance during interaction is shown as well. **B** Individual performance after learning. Performance during interaction is significantly better than doing the task alone (■: independent-samples t-test, $t(38) = 3.05$, $p = 0.004$. ♦: dependent-samples t-test, $t(19) = 8.65$, $p < 10^{-7}$. ▲: independent-samples t-test, $t(38) = 2.79$, $p = 0.008$. ▼: dependent-samples t-test, $t(19) = 7.11$, $p < 10^{-6}$). We found no differences between baseline and force field performance after learning. **C** Motor improvement versus initial performance for the solo and interaction groups. **D** Individual learning rates λ, extracted from the fitted exponential learning curves of the force field blocks. No significant differences between the solo and interaction groups were found. All error bars indicate mean and standard error.

factor, slope $\beta_1 = 0.75$, $F(1, 76) = 146.19$, $p < 10^{-10}$, $\omega^2 = 0.78$). However, there were no significant differences in improvement between the solo and the interaction group (interaction group as a factor, $F(1, 76) = 0.02$, $p = 0.90$). Hence, haptic interaction did not lead to more motor improvement compared to practicing the force field alone.

3.3.2. Haptic interaction does not speed up individual motor learning

The learning rates of the baseline and force field blocks are shown in figures 3.3D. We found no significant differences in learning rates of the single trials between the solo and interaction groups, both in the baseline and force field blocks (see Fig. 3.3D). Furthermore, the learning rates in the connected trials were not significantly different compared to the single trial learning rates of both groups.

3.3.3. Performance is improved during haptic interaction, also in the force field

Haptic interaction led to a substantial improvement in motor performance *during* interaction in the baseline block. We compared the mean error of the last five single trials to the mean error of the last five connected trials of the interaction group. Motor performance improved significantly during interaction for all interaction groups compared to the single trials, see Fig. 3.3B. Furthermore, the performance during the connected trials was also significantly better than the single performance of the solo group.

Remarkably, haptic interaction also improved performance in the force field blocks (Fig. 3.3B). The force field generated an time-average force of 1.31 N in a trial; the measured interaction force was smaller (time-average of 0.44 N). Hence, even though the average interaction force during the connected trials was significantly smaller compared to the average force field force, interaction in the force field still improved performance (see Fig. 3.3B).

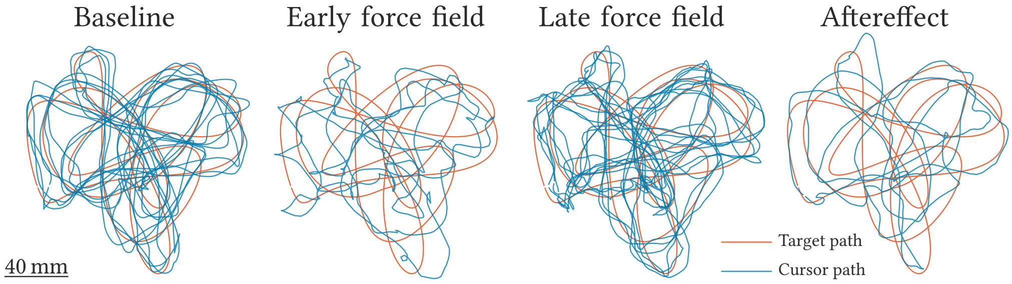

Figure 3.4. | Examples of a participant's cursor paths during single trials. Shown are the cursor paths of the last three single trials of the baseline block, first single trial in the force field, the last three trials of the force field blocks, and the first trial in the aftereffect block for one participant.

3.3.4. Evidence that participants learned an internal model of the force field

Immediately after the force field was removed, both groups showed significant aftereffects as reflected by the tracking performance. Performance in the first single trial in the aftereffect block was significantly worse than each participant's error after learning in the last single trial in the force field blocks (dependent-samples t-tests comparing performance per participant; interaction group: $t(19) = 3.64$, $p = 1.75 \cdot 10^{-3}$; solo group: $t(19) = 4.14$, $p = 5.57 \cdot 10^{-4}$), see Fig. 3.3A. The performance in the first single trial of the aftereffect block was the same for both groups ($t(38) = 1.41$, $p = 0.167$).

Figure 3.4 shows an example of the tracking paths of one participant to illustrate the aftereffect. On initial exposure to the force field, the tracking behavior is different compared to the baseline paths. The lateral deviations that are typical for force field perturbations are visible in the early exposure phase (most notable are the top and bottom loops and the leftmost loop). At the end of the force field blocks, the cursor paths are similar to the baseline behavior. The first single trial when the force field was removed shows aftereffects opposite the velocity-dependent force field, for example in the bottom and top loops.

Furthermore, participants already compensated for a substantial amount of the force field in the first single trial (~72 % to 77 %) and improved the accuracy of the internal model to approximately 86 %. The force field compensation factor α in the single trials (see Fig 3.5) increased significantly for both the interaction group and solo group with increasing exposure to the force field (ANCOVA, effect of trial covariate: $F(1, 876) = 123.78$, $p < 10^{-16}$). Furthermore, the compensation factor was not significantly different between

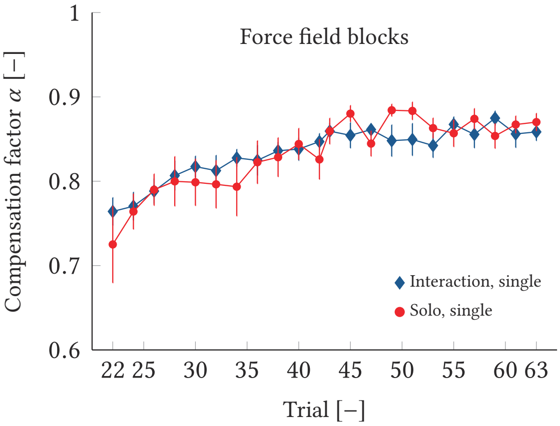

Figure 3.5. | Average force field compensation factor in the single trials across the force field blocks for the solo and interaction groups.

groups (group factor: $F(1, 876) = 0.08$, $p = 0.79$). The initial performance decrease in the aftereffect block, observed after effects, and the increasing compensation factor suggest that participants learned an internal model of the force field to some extent.

3.4. Discussion

We investigated whether haptic human-human interaction facilitated or interfered with learning to move in a new dynamic environment: a velocity-dependent curl force field. Participants intermittently interacted through a compliant connection with a partner who was learning the same collaborative motor task: tracking a randomly-moving target in the force field. Participants were not made explicitly aware of the interaction. Haptic interaction neither improved nor impeded *individual* motor learning (learning rate and performance after learning) compared to participants who practiced the learning task alone.

Haptic interaction does not improve individual motor learning

Physically assisting, or haptically guiding, someone who is learning a new motor task has been shown to improve performance while receiving the assistance, but these improvements are rarely retained when performing the task alone [7–9, 31, 32]. Haptic guidance may give the participants an erroneously good impression of their performance, suppress the detection of errors and the correction processes, and participants may rely on the haptic guidance for improved motor performance. Movement errors are a key training signal for motor learning [33]. Similarly, we found that haptic interaction significantly reduced movement errors during haptic interaction, even in the force field, which could explain why haptic interaction did not improve individual motor learning.

The force field only resulted in a relatively small reduction in tracking performance (the tracking error increased with ~5 mm compared to the final performance in the baseline block) and participants rapidly improved in the following trials. However, visual inspection of the cursor paths indicated that the force field substantially affected the tracking behavior. Still, we found that the participants in the interaction and solo group improved performance significantly and equally with practice in the force field. Furthermore, these results are consistent with a similar study by Conditt and Gandolfo [14], who found that participants improve performance in the same order of magnitude when tracing shapes in a velocity-dependent force field.

Force field compensation

The compensation factor showed that participants already compensated for a substantial amount of the force field in the first single trial ($\alpha \approx 72\,\%$). It is likely that participants rapidly minimized the additional movement errors due to the force field, in particular in the first trial, by increasing arm impedance through muscle co-contraction [15, 18]. With longer practice in the force field, participants compensated ~86 % on average, which is consistent with other studies that found that people learn approximately 80–82 % of similar force fields [15, 26, 28]. The compensation factor, similar to the adaptation factor used in other force field studies, reflects the combination of multiple complementary mechanisms that could be used to compensate for the force field, including increasing arm impedance and using an internal model of the force field [15]. We cannot distinguish between these mechanisms in our data, but the observed aftereffects indicated that participants, besides counteracting the force field using muscle co-contraction, also learned an incomplete internal model of the field [12, 14, 24].

Haptic interaction does not interfere with learning a force field

Although the haptic interaction was in the same sensory domain as the force field, which could have altered the task dynamics, we found no interference on individual motor learning; both the individual tracking performance and the force field compensation in the single trials of the participants in the interaction group were similar in magnitude and rate to those of the solo participants. Humans have been shown to adapt to velocity-dependent force field even when a background force was superimposed [23, 24], though the background force slowed learning down [24]. Our data showed that the intermittent haptic interaction did not slow down learning compared to the solo group.

To explain why a velocity-dependent force field was still learned despite the background force, Kurtzer et al. [23] suggested that people were able to discriminate between the static background force and dynamic velocity-dependent force. However, the interaction force in our haptic human-human interaction experiment was not constant in direction and magnitude, as it depends on the movements of both partners. The interaction force was also substantially smaller than the force field force, possibly making it more difficult to discriminate from the force field force. Yet haptic interaction still led to significantly better motor performance during the interaction. It, therefore, remains unknown whether the interacting partners were able to differentiate between the interaction force and force field accurately; we will analyze and discuss this further in Chapter 6.

This study compared to Ganesh et al. [5]

Our results are in contrast with the findings of Ganesh et al. [5], who found that haptic human-human interaction improves motor learning in a visuomotor rotation task. Although our experimental design and haptic interaction paradigm were similar to those of Ganesh et al. [5], it is possible that the type of learning task – force field or visuomotor rotation – plays an important role in why we did not see better motor learning during haptic interaction. The learning task of Ganesh et al. [5] was in a different sensory domain than the haptic interactions. Superimposing the interaction forces with a velocity-dependent force field might have limited the potential to learn from the other partner. The benefits of haptic interaction on motor learning could thus be task-specific. However, when we repeated the study of Ganesh et al. [5] using the same visuomotor rotation perturbation, we did not see benefits of haptic interaction on motor learning (see the next chapter), in line with the results of this study.

Limitations

Our study has limitations. First, the absolute magnitude of learning is in the order of millimeters. Ganesh et al. [5] showed greater individual performance improvements (in the order of centimeters). However, the motor improvement in the force field task still was significant and similar to previous studies who also tracked in a force field [14]. Second, although we believe that learning to move in novel dynamics has a higher out-of-the-lab validity than a visuomotor rotation learning task, the applicability to real-life learning tasks is still limited. Third, we did not make the participants explicitly aware of the haptic interaction. Presumably, assigning teacher-student roles in haptic interaction would have more potential to improve individual learning.

In conclusion, we found that haptic interaction between humans performing the same collaborative tracking task neither facilitated nor interfered with learning to move in a new dynamic environment. Interestingly, haptic interaction improved performance during the interaction, even when the perception of the interaction force was impaired by the force field. How did the participants still improve performance through the haptic interaction? We discuss this question in more detail in Chapter 6.

References

[1] N Sebanz, H Bekkering, and G Knoblich. Joint action: bodies and minds moving together. *Trends in Cognitive Sciences*, 10(2):70–76, February 2006.

[2] C H Shea, G Wulf, and Chad Whitacre. Enhancing Training Efficiency and Effectiveness Through the Use of Dyad Training. *Journal of Motor Behavior*, 31(2): 119–125, 1999.

[3] C Granados and G Wulf. Enhancing motor learning through dyad practice: Contributions of observation and dialogue. *Research Quarterly for Exercise and Sport*, 78 (3):197–203, June 2007.

[4] A G Mattar and P L Gribble. Motor Learning by Observing. *Neuron*, 46(1):153–160, 2005.

[5] G Ganesh, A Takagi, R Osu, T Yoshioka, M Kawato, and E Burdet. Two is better than one: Physical interactions improve motor performance in humans. *Scientific Reports*, 4, 2014.

[6] R A Schmidt and R A Bjork. New Conceptualizations of Practice: Common Principles in Three Paradigms Suggest New Concepts for Training. *Psychological Science*, 3(4):207–218, 1992.

[7] C J Winstein, P S Pohl, and R Lewthwaite. Effects of Physical Guidance and Knowledge of Results on Motor Learning: Support for the Guidance Hypothesis. *Research Quarterly for Exercise and Sport*, 65(4):316–323, December 1994.

[8] E H F van Asseldonk, M Wessels, A H A Stienen, F C T van der Helm, and H van der Kooij. Influence of haptic guidance in learning a novel visuomotor task. *Journal of Physiology - Paris*, 103(3-5):276–285, September 2009.

[9] M K O'Malley, A Gupta, M Gen, and Y Li. Shared Control in Haptic Systems for Performance Enhancement and Training. *Journal of Dynamic Systems, Measurement, and Control*, 128(1):75–11, 2006.

[10] L Marchal-Crespo, J Lopez-Oloriz, L Jaeger, and R Riener. Optimizing learning of a locomotor task: Amplifying errors as needed. In *36th Annual International Conference of the IEEE Engineering in Medicine and Biology Society*, pages 5304–5307. IEEE, August 2014.

[11] H Heuer and J Lüttgen. Robot assistance of motor learning: A neuro-cognitive perspective. *Neuroscience & Biobehavioral Reviews*, 56:222–240, 2015.

[12] R Shadmehr and F A Mussa-Ivaldi. Adaptive Representation of Dynamics During Learning of a Motor Task. *Journal of Neuroscience*, 14(5):3208–3224, May 1994.

[13] R Shadmehr and T Brashers-Krug. Functional stages in the formation of human long-term motor memory. *Journal of Neuroscience*, 17(1):409–419, 1997.

[14] M A Conditt and F Gandolfo. The motor system does not learn the dynamics of the arm by rote memorization of past experience. *Journal of Neurophysiology*, 1997.

[15] J B Heald, D W Franklin, and D M Wolpert. Increasing muscle co-contraction speeds up internal model acquisition during dynamic motor learning. *Scientific Reports*, 8(1):3270, 2018.

[16] J R Lackner and P DiZio. Rapid adaptation to Coriolis force perturbations of arm trajectory. *Journal of Neurophysiology*, 72(1):299–313, July 1994.

[17] O Donchin, J T Francis, and R Shadmehr. Quantifying Generalization from Trial-by-Trial Behavior of Adaptive Systems that Learn with Basis Functions: Theory and Experiments in Human Motor Control. *The Journal of Neuroscience*, 23(27): 9032–9045, October 2003.

[18] D W Franklin, R Osu, E Burdet, M Kawato, and T E Milner. Adaptation to stable and unstable dynamics achieved by combined impedance control and inverse dynamics model. *Journal of Neurophysiology*, 90(5):3270–3282, October 2003.

[19] E Burdet, R Osu, D W Franklin, T E Milner, and M Kawato. The central nervous system stabilizes unstable dynamics by learning optimal impedance. *Nature*, 414 (6862):446–449, November 2001.

[20] E Burdet, K P Tee, I Mareels, T E Milner, C M Chew, D W Franklin, R Osu, and M Kawato. Stability and motor adaptation in human arm movements. *Biological Cybernetics*, 94(1):20–32, January 2006.

[21] T E Milner and D W Franklin. Impedance control and internal model use during the initial stage of adaptation to novel dynamics in humans. *The Journal of Physiology*, 567(2):651–664, September 2005.

[22] D W Franklin, E Burdet, K P Tee, R Osu, C M Chew, T E Milner, and M Kawato. CNS Learns Stable, Accurate, and Efficient Movements Using a Simple Algorithm. *Journal of Neuroscience*, 28(44):11165–11173, 2008.

[23] I Kurtzer, P A DiZio, and J R Lackner. Adaptation to a novel multi-force environment. *Experimental Brain Research*, 164(1):120–132, April 2005.

[24] J Liu and D J Reinkensmeyer. Motor adaptation to a small force field superimposed on a large background force. *Experimental Brain Research*, 178(3):402–414, November 2006.

[25] R C Oldfield. The Assessment and Analysis of Handedness: the Edinburgh Inventory. *Neuropsychologia*, 9(1):97–113, 1971.

[26] M A Smith, A Ghazizadeh, and R Shadmehr. Interacting adaptive processes with different timescales underlie short-term motor learning. *PLOS Biology*, 4(6):1035–1043, June 2006.

[27] P M Bays, J R Flanagan, and D M Wolpert. Interference between velocity-dependent and position-dependent force-fields indicates that tasks depending on different kinematic parameters compete for motor working memory. *Experimental Brain Research*, 163(3):400–405, April 2005.

[28] R A Scheidt, D J Reinkensmeyer, M A Conditt, W Z Rymer, and F A Mussa-Ivaldi. Persistence of motor adaptation during constrained, multi-joint, arm movements. *Journal of Neurophysiology*, 84(2):853–862, July 2000.

[29] J Izawa, T Rane, O Donchin, and R Shadmehr. Motor adaptation as a process of reoptimization. *Journal of Neuroscience*, 28(11):2883–2891, March 2008.

[30] L Marchal-Crespo, M van Raai, G Rauter, P Wolf, and R Riener. The effect of haptic guidance and visual feedback on learning a complex tennis task. *Experimental Brain Research*, 231(3):277–291, September 2013.

[31] J C Huegel and M K O'Malley. Progressive haptic and visual guidance for training in a virtual dynamic task. *IEEE Third Joint Eurohaptics Conference and Symposium on Haptic Interfaces for Virtual Environment and Teleoperator Systems*, pages 343–350, March 2010.

[32] H Heuer and J Lüttgen. Motor learning with fading and growing haptic guidance. *Experimental Brain Research*, 232(7):2229–2242, July 2014.

[33] R Shadmehr, M A Smith, and J W Krakauer. Error Correction, Sensory Prediction, and Adaptation in Motor Control. *Annual Review of Neuroscience*, 33(1):89–108, June 2010.

Chapter 4.

Haptic interaction does not improve motor learning of a visuomotor rotation

---

Niek Beckers, Edwin van Asseldonk, and Herman van der Kooij

Under review

Abstract

Haptic interaction between two humans, for instance a therapist physically supporting a patient during recovery, could facilitate motor learning. Haptic interaction through a compliant connection with another human who is learning the same motor task has been shown to improve your own motor learning. These results are remarkable given that physically guiding someone with a robot rarely improves motor learning. Studies have found that such haptic guidance reduces movement execution errors, which are the main driver for motor learning. Haptic human-human interaction significantly reduces movement execution errors, so why would it improve motor learning? Here we investigated whether and, if so, why haptic human-human interaction would improve individual motor learning. We found that haptic human-human interaction through a compliant connection did not improve individual motor learning. Furthermore, neither more interaction time nor a higher interaction strength facilitated motor learning. Although haptic human-human interaction leads to immediate performance improvement during interaction, it does not improve individual motor learning beyond the skill level when practicing the task alone, which is in line with existing robot-assisted motor learning paradigms.

4.1. Introduction

During physical rehabilitation after a stroke, therapists physically move the patient's limbs to promote relearning of lost motor skills. Similarly, parents physically support their children while they are learning to take their first steps. Physical or *haptic* interactions like these, in which two partners exchange forces while performing and learning a motor task together, are common in our lives. Research has shown that haptically interacting partners adopt roles [1–4], such as leader-follower, that interactions can be used to communicate intentions [5, 6] and that haptic interaction improves motor performance during the interaction [1, 7]. Interestingly, Ganesh et al. [7], published in this journal, found that haptic interaction between two human partners improves each partner's own motor learning. Individuals who haptically interacted with another person performing the same task improved their *individual* motor performance significantly *more* and, although not explicitly mentioned by the authors, initially *faster* compared to someone who practiced the task alone. Despite these encouraging results, theirs is currently still the only study which found that haptic interaction benefits motor learning. In addition, the reasons why haptic human-human interaction benefits motor learning remain unknown.

Why would haptic human-human interaction improve individual motor learning? Since a theoretical framework explaining the benefits on motor learning specifically for haptic human-human interaction is lacking, we will approach this question from two different perspectives. First, we attempt to explain these results from a motor learning point of view. Many motor learning studies showed that learning to move in the presence of a perturbation, referred to as motor adaptation, is predominantly driven by errors between the planned and actual movements. A well-known motor adaptation paradigm is a visuomotor rotation perturbation, in which the visual feedback of the hand movement is rotated with respect to the actual hand movement, generating motor execution errors [8, 9]. These motor execution errors are used to develop an internal model of the perturbation, which then updates our motor commands to compensate for the perturbation [9–11]. The larger the experienced error, the more you learn to compensate for the error [12]. Robotic motor learning paradigms that reduce movement executions errors while learning a novel motor skill rarely improve motor learning [13–18]. For instance, haptic guidance to demonstrate the desired movement or changing the task dynamics to encourage the correct behavior does not improve motor learning [15, 16, 19–22]. Ganesh et al. [7] showed that haptic interaction with a human partner significantly reduced movement execution error while learning to move in a visuomotor rotation perturbation compared to someone practicing the task without interaction. Thus, from an error-based motor learning perspective no beneficial effects of haptic human-human interaction on motor adaptation would be expected.

Second, findings from other haptic human-human interaction studies could explain the improvement in motor learning. Haptically interacting humans can coordinate actions and adopt specialized roles by exchanging forces [1, 2, 4, 5], which could facilitate motor learning of both partners. For instance, participants could 'coach' each other on how to move in the learning task by exchanging forces. Moving in an 80 deg visuomotor rotation, the learning paradigm used by Ganesh et al. [7], likely requires a change in movement strategy [23]. Participants could haptically help each other to change their movement strategy to compensate for the visuomotor rotation, resulting in quicker learning compared to someone learning alone. Similarly, visually observing someone else learn facilitates your own motor learning [24, 25]. Perhaps haptic interaction allows for 'haptic observation' of how to move in the visuomotor rotation, improving motor learning. Note that the participants in the Ganesh et al.'s study were not aware of the physical connection, so we wonder whether they could have effectively used the haptic information of the interaction, especially in the early stages of the learning process.

The goal of this paper is to investigate whether haptic interactions with a partner who is learning the exact same motor task, using the same interaction paradigm and visuomotor rotation learning task as Ganesh et al. [7], indeed improves individual motor learning. Note that we use 'motor learning' to refer to the motor adaptation process to the visuomotor rotation in this paper. We hypothesize, based on error-based motor learning findings, that haptic human-human interaction in which the partners are unaware of the physical connection does not improve motor learning. However, it is possible that haptic interaction allows for exchange of information about the learning task which facilitates learning.

To further differentiate between these two explanations, beside repeating Ganesh et al. [7]'s study, we varied the amount of interaction time and the strength of the interaction. First, we tested a group which *continuously* interacted while learning the visuomotor rotation, resulting in more interaction time and consistency of interaction compared to the main experiment, in which partners *intermittently* interacted (e.g. in one trial partners interacted while in another they performed the task alone). We also expect that continuous haptic interaction does not improve motor learning; more interaction means even less experienced error for both partners while learning. However, if we observe improved motor learning as a result of continuous interaction compared to intermittent interaction or learning the task alone, it provides evidence that some aspect of haptic human-human interaction indeed plays an important role for facilitating motor learning.

Second, we investigated how the strength of the haptic interaction affects learning by increasing the stiffness of the compliant connection. A stronger connection could provide the partners with more haptic information about the learning task, however it also limits independent movement. Increased interaction stiffness results in additional improvement for the inferior performing partner in a pair during interaction [26]. Following our hypothesis, we would expect that motor learning of the inferior performing partner would not be improved and even impeded due to the haptic interaction, following the results of haptic guidance studies [14–16, 21].

Contrary to Ganesh et al. [7], we found no benefit of haptic human-human interaction on individual motor learning compared to individuals who learned the task alone. Interaction led neither to a better motor skill level nor increased motor learning rate. Increasing the amount of interaction time or interaction strength did not improve motor learning. Our data show that haptic human-human interaction through a compliant connection in which the participants are not aware of the interaction is not effective for improving individual motor learning.

4.2. Methods

Sixty healthy participants (34 men and 26 women; age 22.0 ± 2.1 yr; all except two participants were right-handed according to the Edinburgh handedness inventory [27]) were recruited to participate in the study. All participants had not previously performed any experiments involving a visuomotor rotation. The study was designed following the principles of the Declaration of Helsinki. An assessment of the study by the Medical Ethical Review Board of the University of Twente (METC Twente) showed that the study posed minimal risk to the participants and therefore under Dutch law did not need full ethical review. All participants provided written informed consent. The experiment lasted approximately two hours; all participants received a compensation for their participation.

4.2.1. Robotic setup

All experiments were performed using a dual robotic setup (Fig. 4.1A). Participants held a handle at the endpoint of their own manipulandum with their preferred hand. Each manipulandum allowed arm movements in a horizontal plane. A panel obstructed direct view of the arm and hand of each participant. Each partner had their own display that showed the workspace, a target and their own cursor which they could control by moving the manipulandum handle (Fig. 4.1B). Cursor and target movement were scaled to match the real-world movement of the manipulandum. A curtain obstructed view of the other partner and the partner's display. Participants were not allowed to verbally communicate during the experiment.

4.2.2. Task and interaction paradigm

All participants performed a task in which they tracked a continuously moving target with the cursor as accurately as possible, similar to Ganesh et al. [7]. The participants tracked the target during trials of 23 s. The target movement (in mm) was defined as a sum-of-sines (see Section B.1 for more

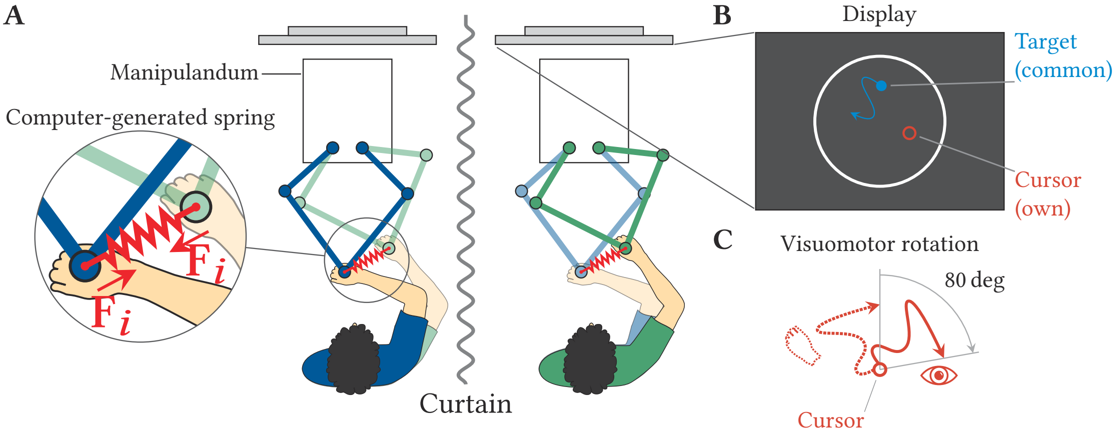

Figure 4.1. | Robotic setup and display and experiment design. **A** Each participant grasped the handle of one of the two identical manipulanda. Visual feedback was presented on a display mounted in front of each participant. A panel (not shown) obstructed the view of the hand and arm for each participant. **B** Participant received visual feedback of their own cursor position and a common target position. **C** Visuomotor rotation: the visual feedback of the cursor was rotated clockwise with 80 deg with respect to the actual hand movement.

details on the target signal design):

$$\begin{aligned} x(t) = {} & 28.7\sin(0.94t - 7.77) + 27.1\sin(1.26t - 8.53) \\ & +23.5\sin(1.89t - 4.36) + 18.0\sin(2.83t - 3.79), \\ y(t) = {} & 27.1\sin(1.26t - 0.71) + 25.3\sin(1.57t - 3.45) \\ & +21.6\sin(2.20t + 3.92) + 16.4\sin(3.14t + 4.93). \end{aligned} \tag{4.1}$$

The tracking signal required hand movements over a circular workspace with a radius of approximately 10 cm, an average velocity of 7.9 $\mathrm{cm\,s^{-1}}$ and a maximum velocity of 13.9 $\mathrm{cm\,s^{-1}}$. To prevent fast learning or other cognitive strategies, we generated the 23 s signal using a time offset t_0 which was sampled from a uniform distribution ($t \in [t_0, t_0 + 23]$ s, $t_0 \sim \mathcal{U}(0, 23)$s). We generated the tracking signals for all trials beforehand, such that all participants tracked the exact same target signal per trial. Each trial was followed by a 15 s rest break.

The participants performed 84 trials of the tracking task divided over four blocks with five minutes of rest between blocks. The first block (21 trials) served to measure the baseline tracking skill level of the participants. We introduced a visuomotor rotation by visually rotating the cursor movement clockwise with 80 deg (same as Ganesh et al. [7]) with respect to the actual hand movement (see Fig. 4.1C) in the remaining three blocks. We explained the concept of a visuomotor rotation to the participants and told them that their goal was to track the target as accurately as possible using continuous and smooth movements but not to estimate the magnitude of the rotation.

The haptic human-human interaction paradigm is the same as [7]. Two types of trials were used in the experiment: *single* (S) and *connected* (C) trials. The partners in a pair haptically interacted through a compliant connection in the connected trials. The connection was a computer-generated spring between the participant's hands (see the detail in Fig. 4.1A). The spring generated a force

$$\mathbf{F}_i = k_s \left(\mathbf{p}_p - \mathbf{p}_o\right) + b_s \left(\mathbf{v}_p - \mathbf{v}_o\right), \tag{4.2}$$

where k_s is the connection stiffness, b_s a damping contribution, $\mathbf{p}_p$ and $\mathbf{v}_p$ and $\mathbf{p}_o$ and $\mathbf{v}_o$ are the partner's and the participant's own position and velocity, respectively. The force was exerted onto both partners' hands by the manipulanda. If a partner moved away from the other partner, they both experienced a force pulling them toward each other. The stiffness and damping of the spring were chosen to be the same as the stiffness used by Ganesh et al. [7]: $k_s = 120\,\mathrm{N\,m^{-1}}$ and $b_s = 7\,\mathrm{N\,s\,m^{-1}}$. The compliant connection allowed the partners to haptically interact, while being able to independently execute the tracking task. Active task execution was required; participants could not completely relax and let the interaction force pull their hand along. We informed participants that the forces they experienced during the connected trials "involved external forces that would sometimes help the task and sometimes disturb it", but we did not provide explicit information about the connection. The trials in which the partners were not connected are denoted as single trials. The single trials were used to analyze individual motor performance and learning.

4.2.3. Experiments

We performed three experiments: (1) a 'main intermittent interaction' experiment in which we repeated Ganesh et al.'s interaction experiment, (2) a 'continuous interaction' experiment and (3) a 'stiff connection' experiment. The sixty participants were divided over four groups: a solo group ($N = 20$), an interaction group ($N = 20$, divided over 10 pairs), the 'continuous interaction' group ($N = 10$, 5 pairs) and the 'stiff connection' group ($N = 10$, 5 pairs). All pairs were gender-matched to avoid gender-related effects. We also matched partners on age as much as possible to avoid age-related effects on motor learning. All groups performed the same tracking task and learned the same visuomotor rotation with the same number of trials; we only changed how pairs interacted with each other per group. All participants received the same instructions.

The main interaction experiment consisted of the solo and interaction groups. The solo participants also performed experiment in pairs, but performed the motor learning task by themselves (they only performed single trials (S)). The interaction group *intermittently* interacted while performing the tracking task; single (S) and connected (C) trials alternated in each block, resulting in the following trial sequence across the four blocks: [{SCSCSCSCSCSCSCSCSCSCS} {**S**CSCSCSCSCSCSCSCSCSCS}, {SCSCSCSCSCSCSCSCSCSCS}, {SCSCSCSCSCSCSCSCSCSCS}] (see Fig. 4.2A).

The partners in each pair in the continuous interaction group were always connected to each other while learning to move in the visuomotor rotation. The first block consisted of single trials only. The second and third blocks consisted of connected trials only. The first nine trials in block 4 were connected trials and the last 12 trials were single trials to measure the *individual* motor performance after learning (see Fig. 4.2B). The trial sequence for the continuous interaction group was [{SSSSSSSSSSSS**S**SSSSSSSS} {CCCCCCCCCCCCCCCCCCCCC}, {CCCCCCCCCCCCCCCCCCCCC}, {CCCCCCCCC SSSSSSSSSSSS}]. To assess the *individual* motor performance on initial exposure to the visuomotor rotation $E_{s,0}$, we introduced the visuomotor rotation for one trial (trial 13, see the bold **S** in the trial sequence) in the baseline block.

The stiff connection group performed the same experiment as the interaction group, using the same alternating sequence of single and connected trials per block. We increased the connection stiffness k_s to $250\,\mathrm{N\,m^{-1}}$ and kept the damping constant. The higher connection stiffness increased the amount of interaction force with respect to the main interaction experiment, yet still allowed for independent movement.

4.2.4. Analysis

Kinematics of each partner were logged at 1 kHz. We used MATLAB R2017B and the R statistical software (version 3.5.1) for analysis. The main measure of motor performance is the root mean square of the tracking error E (the distance between the target and cursor in mm) of the last 20 s of each trial; the lower the tracking error E, the better the motor performance. We studied motor learning by analyzing the reduction of tracking error while learning to track the target in the visuomotor rotation. We are interested in each participant's *individual* motor learning; we therefore focus on each participant's performance in the single trials (E_s). Unless explicitly mentioned otherwise, when referring to motor learning, we mean *individual* motor learning. Motor learning was quantified using four measures: (1) the performance after learning $E_{s,\mathrm{al}}$, (2) the initial motor performance when first exposed to the visuomotor rotation $E_{s,0}$, (3) the motor improvement from the initial performance to the error after learning and (4) the rates at which each participant improved motor performance. The performance after learning $\left(E_{s,\mathrm{al}}\right)$ was calculated by taking the mean of the last five single trials of each participant in block 4. The initial motor performance $E_{s,0}$ was the performance in the first single trial of block 2 for the solo, interaction and stiff connection groups and trial 13 in the baseline block for the continuous interaction group. The motor improvement is the difference between $E_{s,0}$ and $E_{s,\mathrm{al}}$: $\left(E_{s,0} - E_{s,\mathrm{al}}\right)$.

The rates at which each participant improved his/her own motor performance were extracted by fitting exponential functions to each participant's motor performance curves. Short-term motor learning in error-based paradigms consists of multiple learning processes, each with their own learning rate [11]. We fitted a function with two exponents – one exponent that modeled a 'slow' learning process and one that modeled a 'fast' learning process [11] – to the motor performance curves of the visuomotor rotation learning blocks (blocks 2, 3 and 4):

$$E_s = a_\infty + a_s e^{-\lambda_s (t-1)} + a_f e^{-\lambda_f (t-1)}, \tag{4.3}$$

where t is the trial number, λ_s and λ_f are the slow and fast learning rates $\left(\lambda_s < \lambda_f\right)$, respectively, and a_∞, a_s and a_f are constants. We fitted equation 4.3 to the single trials of each participant to estimate their slow and fast learning rates. We also fitted equation 4.3 to the connected trials to estimate how fast performance increased for each participant in the connected trials. The fits resulted in a minimum and mean R^2 of 0.84 and 0.95, respectively, for all participants. Using a function with a single exponent led to a significantly worse fit; R^2 of a single exponent was worse (Wilcoxon signed-rank test, $Z = 741$, $p < 1 \cdot 10^{-7}$) and led to lower Akaike Information Criterion values (Wilcoxon signed-rank test, $Z = 45$, $p < 1 \cdot 10^{-5}$). This justifies our use of a double exponent function to analyze individual participant learning rates.

To investigate whether haptic interaction indeed improves motor performance compared to a partner's single performance, we also calculated the performance error in the connected trials (E_c) for all interacting partners. Partners could still perform the tracking task independently during the connected trials because of the connection compliance; hence the tracking errors during interaction are not necessarily the same for both partners. The connected performance (E_c) was compared to the individual performance (E_s) for each participant.

We performed one-way and linear mixed-effect ANOVA and post-hoc tests to identify differences in motor skill performance after learning, initial motor skill level, motor improvement and baseline skill level. We analyzed the effect of initial skill level E_0 as a covariate on motor improvement and learning rates using ANCOVA. All data and statistical model fit residuals were checked for normality using the Shapiro-Wilk normality test and for equality of variance with the Levene's test. In case of non-normality or when the sample size was < 10 in each group, we used the Kruskal-Wallis test and Wilcoxon signed-rank test for paired samples and Mann-Whittney U tests for unpaired samples. The level of significance for all tests was set to 0.05. Post-hoc tests were performed using the Holm-Bonferroni method to correct for the number of pairwise comparisons. Unless explicitly stated, all data are reported as the mean ± standard error of the mean (s.e.m.). The data files of two participants in the solo group (they performed the experiment in the same session) were corrupted and are therefore not taken into account in the analysis.

4.3. Results

We investigated whether haptic interaction improved individual motor learning. Participants learned how to track a moving target while being perturbed by a visuomotor rotation. Two partners were intermittently connected to each other through a compliant computer-generated spring. Their motor learning performance when performing the task without interacting with their partner was compared to a solo group who practiced the task always alone. Furthermore, we studied whether the amount of interaction time and interaction strength influenced motor learning. Motor learning was assessed by comparing the performance after learning, motor improvement and motor learning rates of each participant during trials when they were not interacting with their partner. The performance curves for all groups are shown in Fig. 4.2.

The motor learning task consisted of two components: the tracking task and the visuomotor rotation perturbation. We first checked that the baseline tracking performance was the same between groups. We found no significant difference in individual motor performance (E_s) between groups at the end of the baseline block (solo: 8.0 ± 0.3 mm, interaction: 8.3 ± 0.2 mm, continuous interaction: 7.7 ± 0.3 mm and stiff connection: 8.2 ± 0.3 mm, between-subject ANOVA, $F(3, 54) = 0.89$, $p = 0.451$, $\omega^2 = -0.006$). In addition, the visuomotor rotation initially degraded performance equally across groups. Motor performance at the initial exposure to the visuomotor rotation ($E_{s,0}$) was not significantly different between groups (solo: 48.0 ± 3.0 mm, interaction: 46.6 ± 2.9 mm, continuous interaction 48.5 ± 4.1 mm and stiff connection 50.4 ± 4.1 mm, between-subject ANOVA $F(3, 54) = 0.21$, $p = 0.89$, $\omega^2 = -0.044$). Because we established that baseline tracking performance and initial performance in the visuomotor rotation is equal across groups, any observed differences in motor learning in the visuomotor rotation blocks are likely due to the haptic interaction.

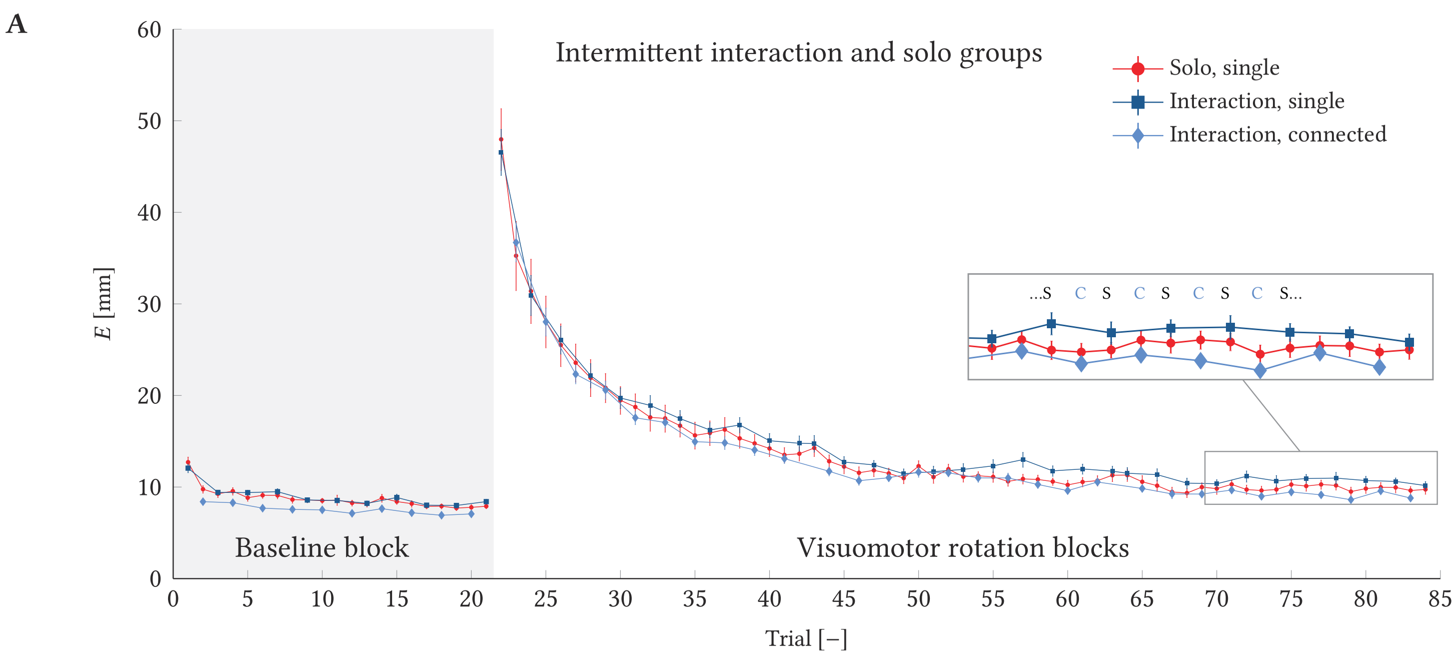

Figure 4.2. | Motor performance over the course of the experiment. **A** Interaction and solo groups. We show the performance of all single trials of the solo group (red ●) and the single trials (dark blue ■) and connected trials (light blue ♦) of the interaction group. The single and connected trials alternated for the interaction group. All data show the mean ± s.e.m. per group. See Fig. B.3 for all individual learning curves.

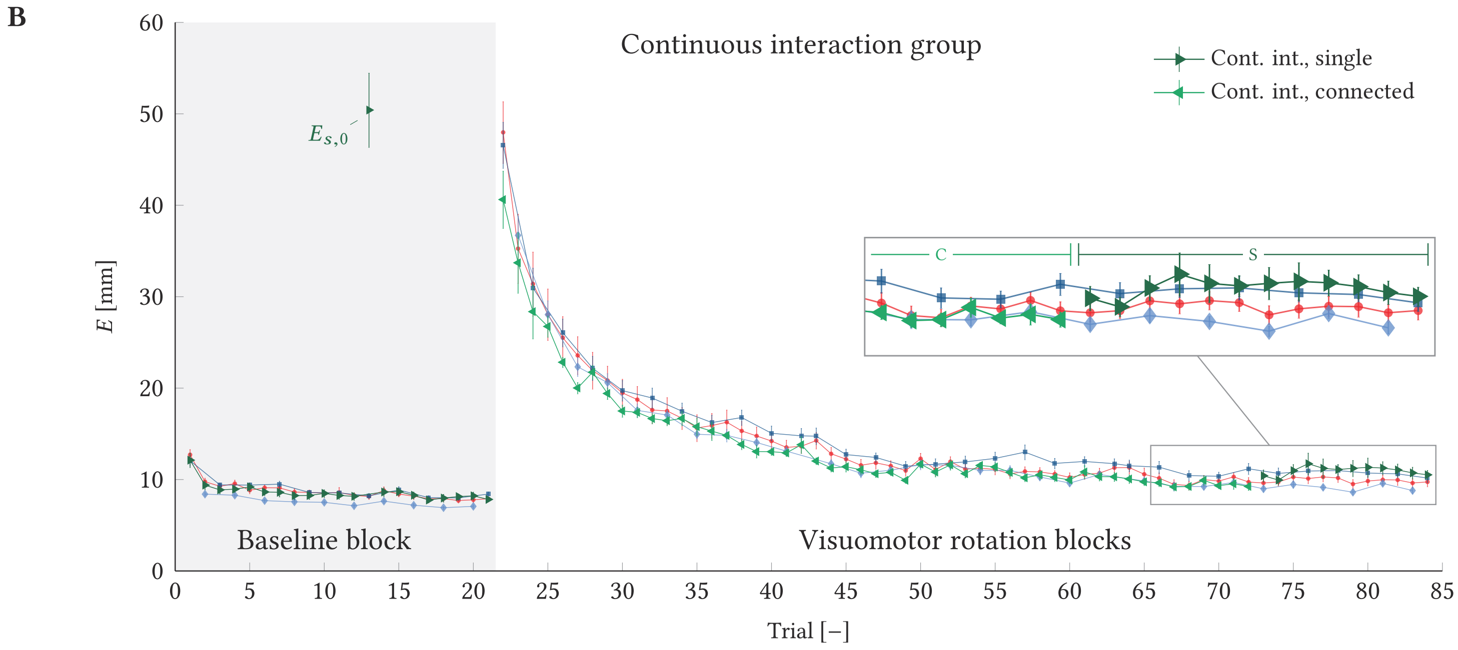

Figure 4.2. | Motor performance over the course of the experiment (continued). **B** Continuous interaction group: single trials (dark green ▸) and the connected trials (light green ◂). The visuomotor rotation was introduced in trial 13 in the baseline block to measure the participant's initial performance in the visuomotor rotation $E_{s,0}$. The solo and interaction group data are included for comparison. All data show the mean ± s.e.m. per group. See Fig. B.3 for all individual learning curves.

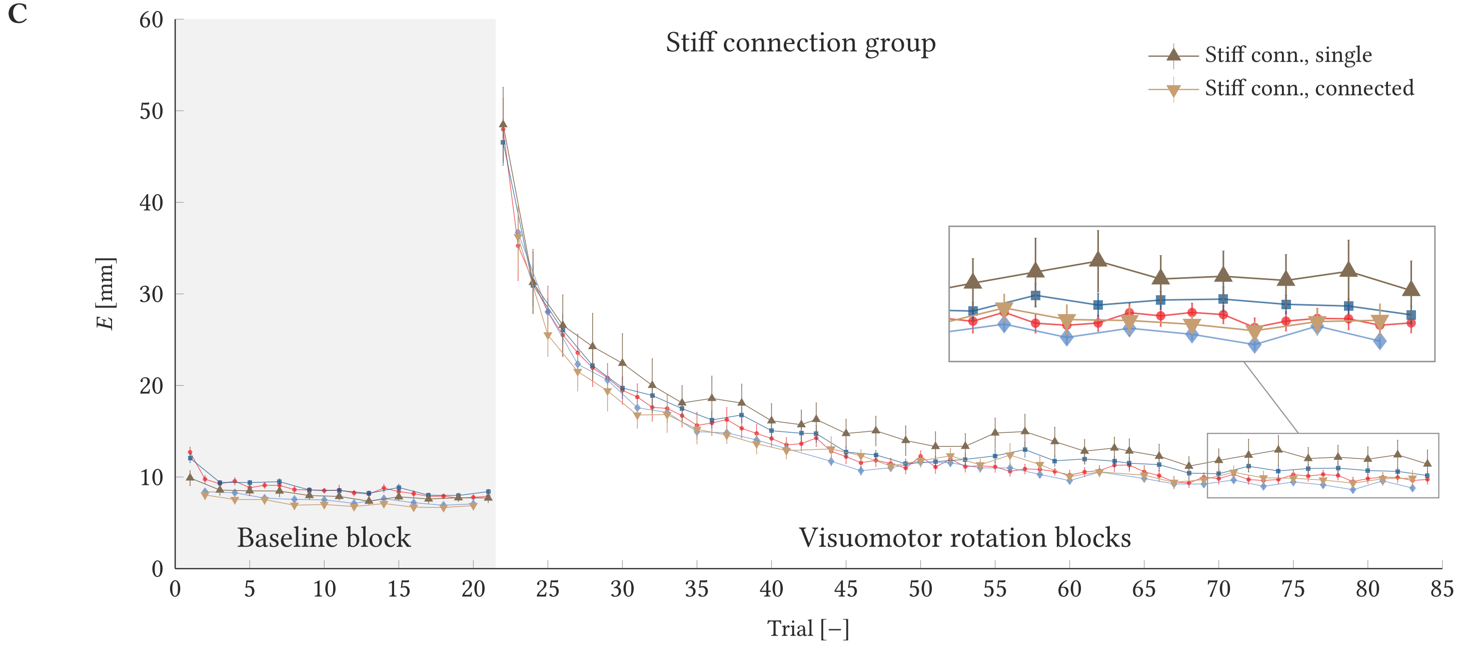

Figure 4.2. | Motor performance over the course of the experiment (continued). **C** Stiff connection group: single trials (dark brown ▲) and connected trials (light brown ▼). The solo and interaction group data are included for comparison. All data show the mean ± s.e.m. per group. See Fig. B.3 for all individual learning curves.

4.3.1. Haptic human-human interaction does not improve individual motor performance

Our results show that haptic human-human interaction does *not* improve motor performance after learning in the visuomotor rotation compared to the solo group (see the highlighted sections in Fig. 4.2). Figure 4.3A shows the group mean±s.e.m. of error after learning for the single trials $\left(E_{s,\mathrm{al}}\right)$ and connected trials $\left(E_{c,\mathrm{al}}\right)$. A between-subject ANOVA comparing only the individual performances across all groups revealed no significant differences in individual performance after learning $E_{s,\mathrm{al}}$ (solo: $10.0 \pm 0.6\,\mathrm{mm}$, interaction: $10.7 \pm 0.6\,\mathrm{mm}$, stiff connection $12.0 \pm 0.8\,\mathrm{mm}$, continuous interaction: $11.2 \pm 0.8\,\mathrm{mm}$, between-subject ANOVA $F(3, 54) = 1.44$, $p = 0.242$, $\omega^2 = 0.022$). Hence, we found no evidence that human-human interaction improves motor performance level beyond the skill level that a solo participant would reach. Interaction with a better partner also did not significantly affect the error after learning (see Fig. B.1A). Furthermore, increasing the time spent interacting (continuous interaction) or interaction strength (stiff connection) did not significantly change individual performance after learning.

It is possible that the haptic interactions resulted in more motor improvement for participants who are initially bad at the task; for instance, haptic human-human interaction could benefit an inferior participant through coaching. Figure 4.3B shows each participant's improvement versus his/her initial performance $\left(E_{s,0}\right)$ for all groups. The initial performance significantly predicted improvement (ANCOVA with $E_{s,0}$ as covariate and interaction group as factor, slope $\beta_1 = 0.970$, $F(7, 50) = 186.10$, $p < 1 \cdot 10^{-10}$, $\omega^2 = 0.96$). However, there were no significant differences in improvement between the solo and all interaction groups (interaction group as factor, $F(3, 50) = 0.56$, $p = 0.647$, $\omega^2 = 0.032$). Haptic interaction with a better partner did not lead to significantly more motor improvement (see Fig. B.1B). Hence, haptic human-human interaction does not lead to more motor improvement compared to the solo group.

A common finding of many studies on haptic human-human interaction is that interaction improves individual motor performance *during* interaction for both partners [1, 7, 26, 28]. We compared the mean error of the last five single trials to the mean error of the last five connected trials for the interaction and stiff connection group and the last five connected trials and last five single trials of the continuous interaction group. Motor performance improved significantly during interaction for all interaction groups compared to the single trials, see Fig. 4.3A (mixed-effect ANOVA on all interaction groups, main effect of single versus connected trial and participant as random

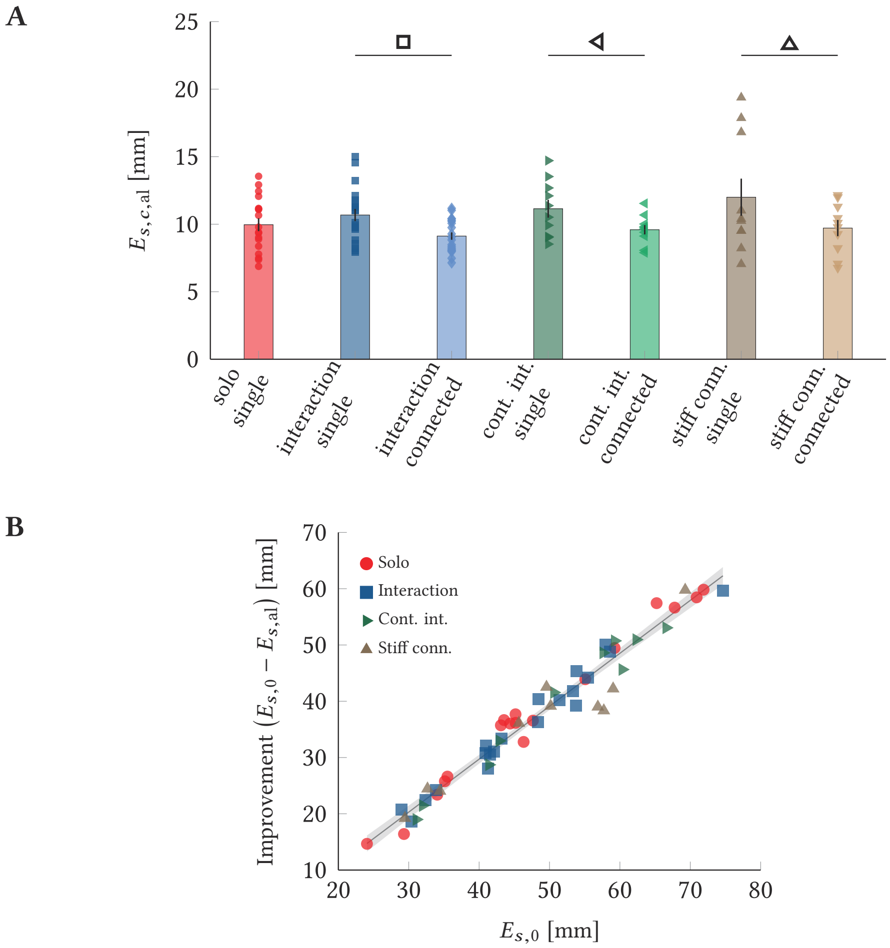

Figure 4.3. | Motor performance after learning and motor improvement. **A** Mean±s.e.m. of the individual error after learning (average error of the last five single trials in block 4) and the connected error after learning (average error of the last five connected trials in block 4). Post-hoc contrasts on performance difference between single and connected trials per group, paired tests: □: $t(37) = 3.82, p = 0.001$, ◁: $t(37) = 3.95, p = 0.001$, △: $t(37) = 2.69, p = 0.011$. **B** Motor improvement versus initial motor performance $E_{s,0}$ for each participant in all groups. The shaded area shows 95 % confidence interval for the fitted linear model.

factor, $F(1, 37) = 36.27,\ p < 1 \cdot 10^{-6}$). On average, interaction increased performance with 1.6 ± 0.4 mm (~15 % improvement) for the interaction group, 1.6 ± 0.6 mm (~14 % improvement) for the continuous interaction group and 2.3 ± 0.6 mm (~20 % improvement) for the stiff connection group. We found no significant difference between the connected trial performance across the interaction groups (mixed-effect ANOVA main effect of interaction group, $F(2, 37) = 0.78,\ p = 0.465$).

4.3.2. Haptic human-human interaction does not increase individual motor learning rate

Figure 4.4A compares the slow (λ_s) and fast (λ_f) learning rates of each participant's motor performance curves (fitted to the single trials) of the solo, interaction and stiff connection groups. We also included the learning rates of the connected trials. We found no significant differences in slow or fast learning rates between the solo, interaction and stiff connection groups (Kruskal-Wallis tests on the single trials only; slow learning rate: $\chi^2(2) = 0.17$, $p = 0.920$, fast learning rate: $\chi^2(2) = 2.48$, $p = 0.290$). Note that because the participants in the continuous interaction group did not perform any single trials while learning the visuomotor rotation, we cannot extract their individual motor learning rates. Instead, we compared the slow and fast learning rates during the connected trials between groups and the connected trial learning rates of the continuous interaction group to the individual learning rates of the other groups. The slow and fast learning rates of the connected trials were not significantly different between the interaction, continuous interaction and stiff connection groups (Kruskal-Wallis tests, slow learning rate: $\chi^2(2) = 5.65$, $p = 0.059$, fast learning rate: $\chi^2(2) = 0.44$, $p = 0.805$). Furthermore, comparing the connected slow and fast learning rate of the continuous group to the single learning rates of the other groups revealed no significant differences (Kruskal-Wallis tests; slow learning rate: $\chi^2(3) = 5.63$, $p = 0.131$, fast learning rate: $\chi^2(3) = 4.78$, $p = 0.189$). In summary, haptic interaction does not speed up motor learning compared to learning the task alone, with no effect of more interaction time or connection stiffness on learning rates.

Similar to the motor improvement, we investigated how the learning rates depended on initial motor performance. Research has shown that individuals with higher levels of motor variability, which in a tracking task like ours presumably results in larger motor performance errors, show higher learning rates [12, 29]. The slow and fast learning rates are plotted against each participant's initial performance for the solo, interaction and stiff connection group in Fig. 4.4B. We performed ANCOVA with initial performance as covariate and interaction group as factor on the slow and fast learning rates. The fast learning rate was not significantly influenced by the initial motor performance or the interaction group (initial performance: $F(1,42) = 0.56$, $p = 0.459$, interaction group: $F(2,42) = 2.46$, $p = 0.097$). However, we found that the slow learning rate is significantly affected by the initial motor performance (ANOVA, effect of $E_{s,0}$ on λ_s: $F(1,42) = 4.70$, $p = 0.036$) and interaction group (ANOVA, effect of interaction group on λ_s: $F(2,42) =$

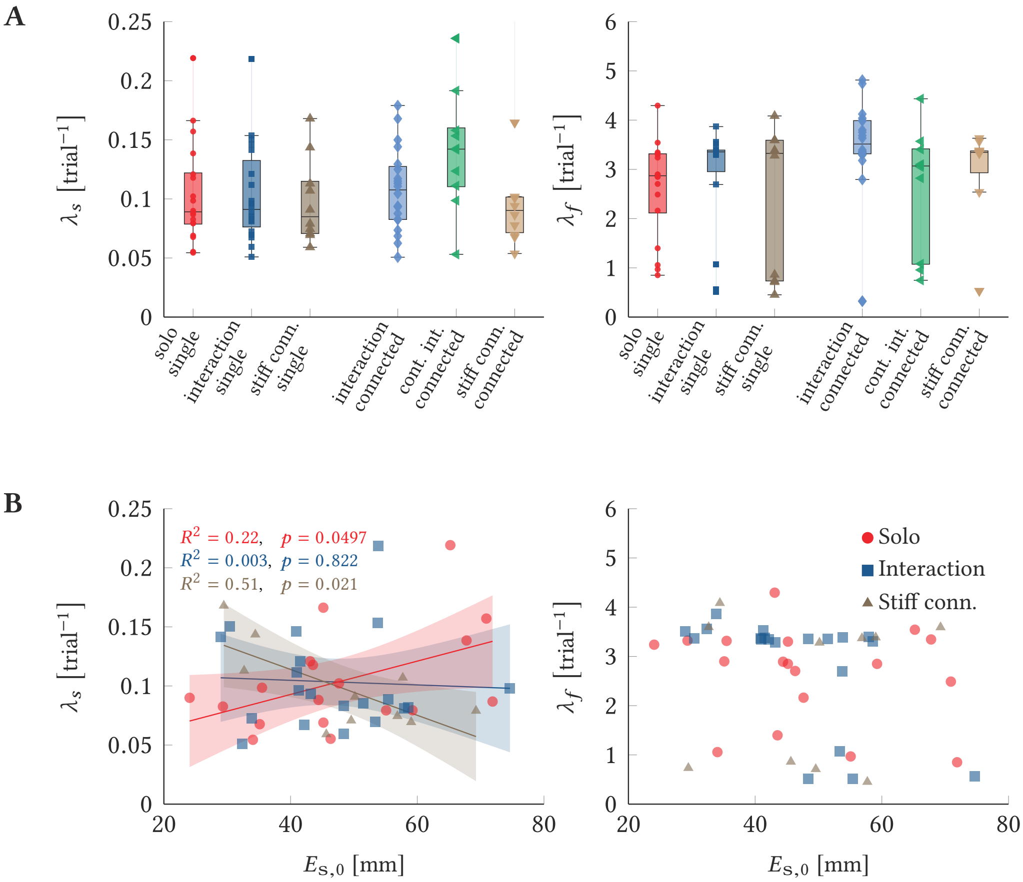

Figure 4.4. | Slow (λ_s) and fast (λ_f) learning rates. **A** Fast and slow learning rates of the single and connected learning curves. **B** Slow and fast learning rates versus initial performance $E_{s,0}$. The linear regression lines per interaction group are shown as well as the 95 % confidence intervals for the fitted linear model.

3.66, $p = 0.034$). More importantly, further analysis showed that the slopes (β_1) of the regression lines for the solo, interaction and stiff connection groups are significantly different (between group ANOVA, $F(2,42) = 4.22$, $p = 0.021$). We plotted the regression lines for each group in Fig. 4.4B to show these differences in slope. The slow learning rate of the solo group increased significantly with decreasing initial motor performance (slope $\beta_1 = 1.41 \pm 0.66$, $t(16) = 2.12$, $p = 0.0497$, $R^2 = 0.22$). The slow learning rate of the interaction group did not significant change with initial motor performance (slope $\beta_1 = -0.20 \pm 0.86$, $t(18) = -0.23$, $p = 0.822$, $R^2 = 0.003$; this slope was not different from the solo group: $t(42) = 1.54$, $p = 0.132$). Interestingly, the slow learning rate of the individuals in the stiff connection group decreased with decreasing initial motor performance (slope $\beta_1 = -1.94 \pm 0.68$, $t(8) =$

-2.86, $p = 0.021$, $R^2 = 0.51$). This trend was significantly different compared to the solo group's trend ($t(42) = -2.84$, $p = 0.0069$). These results suggest that haptic human-human interaction with a stiffer connection significantly slows down learning for initially less skilled participants.

4.4. Discussion

We examined whether haptic interactions between two humans performing the same motor task improved their own motor learning. This work was motivated by the results of Ganesh et al. [7], who were the first to report that haptic human-human interaction improved motor learning significantly compared to learning the motor task alone. We repeated their study by using the same interaction paradigm and motor learning task. We also studied the influence of interaction time and interaction strength on motor learning. The participants who intermittently interacted with another person did not yield better motor performance after learning or motor improvement compared to the participants who practiced the task alone. Physical interaction did not speed up motor learning. Neither the amount of interaction time nor the strength of the connection influenced individual motor learning. Our results contradict the observations of Ganesh et al. [7]. Unfortunately, the authors do not discuss why haptic human-human interaction would benefit motor learning. Here we discuss some key observations from error-based motor learning and robot-assisted motor learning research which support our results, but not those of Ganesh et al. [7].

Why is motor learning not improved by haptic interaction?

Our results are in line with observations in error-based learning and robot-assisted motor learning. Movement execution errors are a key training signal for motor learning [9, 10, 12, 30]. Since haptic human-human interaction reduces the experienced motor error for both partners, it was expected that we would see no benefits on motor learning. This is also consistent with many studies in robot-assisted motor learning. Several studies found that physically assisting a person in a movement task by providing guiding forces temporarily improved motor performance while the participant received the haptic guidance, but did not improve individual motor learning [13–16, 19–21, 31]. Physical human-human interaction may be seen as a compliant guidance that allows each participant to independently perform the task, but still benefit from the error-correcting guidance of the other partner.

This gives the interacting partners an incorrect good impression of their performance, but reduces error as driving factor for motor learning [32].

According to the challenge point theorem, 'optimal' learning is achieved when the difficulty of the task is appropriate for the participant's level of expertise [33]. Haptic guidance could benefit less skilled participants, whereas increasing error would be more beneficial for skilled participants [34]. Similarly, haptic interaction with a superior partner makes the task easier and could benefit initially less skilled participants, whereas interacting with an inferior performing partner temporarily could make the task more difficult. So based on this this theorem, haptic human-human interaction could have a beneficial effect on the performance of both partners, in particular when both partners differ in skill level. However, our analysis on the effect of initial performance on motor improvement and learning rates did not show any benefits of haptic interaction. Interaction with a better or worse partner also did not result in more improvement.

Although we found no benefit of haptic interaction on learning, interaction generally did not impede motor learning. The participants in the continuous interaction group only learned to move in the visuomotor rotation with haptic interaction and consistently experienced less error than the solo participants. They could have relied more heavily on the interaction forces for error correction, which could have impaired motor learning. Though when we removed the physical connection in the last trials, their individual performance was immediately similar to the individual performance of other participants. We did observe that motor learning seemed to be impeded for some participants in the stiff connection group. These participants interacted with a superior partner and showed relatively worse performance after learning and lower slower learning rates, indicating that these participants' individual learning process was hindered by the haptic interaction. Stiff haptic guidance in a visuomotor rotation learning task has been shown to impede motor learning [15]. Our results seem to be in agreement with the observations on stiff haptic guidance.

A contrasting explanation as to why haptic human-human interaction could improve motor learning is through some form of coaching or another type of motor coordination by exchanging forces. A large visuomotor rotation likely requires a change in movement strategy [23], so partners could have improved learning the visuomotor rotation by coaching each other through interaction. Our results do not support this hypothesis. Motor learning rates of the interacting partners of any interaction group were not faster and motor performance was not better than solo participants. If any form of motor coordination or coaching in haptic interaction would have been a driving factor for motor learning, we probably would have seen differences for the continuous interaction group, since the participants received the most interaction time. A strong physical connection even seemed to impede learning for some participants. Furthermore, all but six participants responded in a post-experiment questionnaire that they were unaware of the nature of the forces; they did not know that the forces originate from haptic interaction with their partner. It is therefore unlikely that the haptic interaction led to conscious motor coordination or coaching in the motor learning task.

It is possible that the benefits of haptic human-human interaction on motor learning are task-dependent like they are for haptic human-robot interaction [35]. Recently, we investigated the effect of haptic human-human interaction on motor adaptation to novel dynamics (a velocity-dependent force field). Interacting partners did not show faster learning or better motor performance in the force field compared to the solo participants [28]. Perhaps haptic human-human interaction could be useful in tasks in which timing is of importance [35, 36] or in tasks in which both partners need to learn subtasks [37]; haptic interaction could be used to support one subtask, possibly allowing for more effective learning of another subtask.

Our study compared to Ganesh et al. [7]

Although we used the same interaction paradigm and learning task as Ganesh et al. [7], there are small differences in the experimental design. First, due to the smaller workspace of our robotic setup (our workspace had a radius of 10 cm, Ganesh et al.'s workspace had a radius of 15 cm), we designed a different tracking signal which had a lower average and maximum velocities as their tracking signal. This resulted in lower performance error magnitudes, which could be a reason why we did not see a significant improvement in motor learning for the interaction group compared to the solo group. However, we found that haptic interaction resulted in significantly better performance *during* interaction, in particular for the inferior performing partners (see Fig. B.2), indicating that there was still significant room to improve motor performance. Furthermore, pilot tests showed that more difficult tracking signals, achieved by adding frequencies to the sum-of-sine target signal, did not yield better individual motor performance of the interacting partners. Second, we alternated the connected and single trials (e.g. SCSCS...), whereas Ganesh et al. [7] used a slightly less predictable semi-random sequence (e.g. SSCCSC...). We posit that our trial sequence did not significantly impact motor learning because always being connected (our continuous interaction group) also had no effect on individual motor performance.

Study limitations

Our study has a number of limitations. First, we make inferences on motor learning using a visuomotor rotation learning paradigm. A visuomotor rotation is a error-based motor adaptation paradigm which has been used in many motor learning studies [8, 9], but one could contest its applicability to real-world learning scenarios [38, 39]. Second, we studied motor learning during haptic human-human interaction without explicitly making participants aware of the interaction and without assigning roles. Assigning roles, such as educator-student, or making partners aware of the connection could influence motor learning of the interacting partners [25], warranting further research.

In conclusion, we showed that haptic human-human interaction through a compliant connection does not improve individual motor learning in a continuous movement task in a visuomotor rotation. If we recall the examples in which parents physically help their child to walk or a therapist assisting a patient to relearn arm movements, it is still likely that haptic human-human interaction can play a role in motor learning. Even though we studied two aspects of haptic human-human interaction, interaction time and interaction strength, further investigation into what role haptic human-human interaction and the interaction forces play in motor learning is necessary. Furthermore, to foster motor learning through haptic human-human interaction, we need to take important interaction aspects such as (conscious) motor coordination and role assignment into account.

Acknowledgments

We thank Jeanine van Bruggen en Frits Wiersma for their assistance with the experiments. We also thank Jared Atkinson and Victor Sluiter for their useful comments on the manuscript.

References

[1] K B Reed and M A Peshkin. Physical Collaboration of Human-Human and Human-Robot Teams. *IEEE Transactions on Haptics*, 1(2):108–120, 2008.

[2] R P R D van der Wel, G Knoblich, and N Sebanz. Let the Force Be With Us: Dyads Exploit Haptic Coupling for Coordination. *Journal of Experimental Psychology: Human Perception and Performance*, 37(5):1420–1431, October 2011.

[3] A Melendez-Calderon, V Komisar, and E Burdet. Interpersonal strategies for disturbance attenuation during a rhythmic joint motor action. *Physiology & Behavior*, 147:348–358, 2015.

[4] A Sawers, T Bhattacharjee, J L McKay, M E Hackney, C C Kemp, and L H Ting. Small forces that differ with prior motor experience can communicate movement goals during human-human physical interaction. *Journal of NeuroEngineering and Rehabilitation*, 14(1):8, January 2017.

[5] R Groten, D Feth, R L Klatzky, and A Peer. The role of haptic feedback for the integration of intentions in shared task execution. *IEEE Transactions on Haptics*, 6 (1):94–105, January 2013.

[6] A Kucukyilmaz, T M Sezgin, and C Basdogan. Intention recognition for dynamic role exchange in haptic collaboration. *IEEE Transactions on Haptics*, 6(1):58–68, October 2013.

[7] G Ganesh, A Takagi, R Osu, T Yoshioka, M Kawato, and E Burdet. Two is better than one: Physical interactions improve motor performance in humans. *Scientific Reports*, 4, 2014.

[8] J W Krakauer, M F Ghilardi, and C Ghez. Independent learning of internal models for kinematic and dynamic control of reaching. *Nature Neuroscience*, 1999.

[9] R Shadmehr, M A Smith, and J W Krakauer. Error Correction, Sensory Prediction, and Adaptation in Motor Control. *Annual Review of Neuroscience*, 33(1):89–108, June 2010.

[10] K A Thoroughman and R Shadmehr. Learning of action through adaptive combination of motor primitives. *Nature*, 407(6805):742–747, 2000.

[11] M A Smith, A Ghazizadeh, and R Shadmehr. Interacting adaptive processes with different timescales underlie short-term motor learning. *PLOS Biology*, 4(6):1035–1043, June 2006.

[12] K Wei and K P Körding. Relevance of error: what drives motor adaptation? *Journal of Neurophysiology*, 101(2):655–664, January 2009.

[13] R A Schmidt and R A Bjork. New Conceptualizations of Practice: Common Principles in Three Paradigms Suggest New Concepts for Training. *Psychological Science*, 3(4):207–218, 1992.

[14] C J Winstein, P S Pohl, and R Lewthwaite. Effects of Physical Guidance and Knowledge of Results on Motor Learning: Support for the Guidance Hypothesis. *Research Quarterly for Exercise and Sport*, 65(4):316–323, December 1994.

[15] E H F van Asseldonk, M Wessels, A H A Stienen, F C T van der Helm, and H van der Kooij. Influence of haptic guidance in learning a novel visuomotor task. *Journal of Physiology - Paris*, 103(3-5):276–285, September 2009.

[16] M K O'Malley, A Gupta, M Gen, and Y Li. Shared Control in Haptic Systems for Performance Enhancement and Training. *Journal of Dynamic Systems, Measurement, and Control*, 128(1):75–11, 2006.

[17] L Marchal-Crespo, J Lopez-Oloriz, L Jaeger, and R Riener. Optimizing learning of a locomotor task: Amplifying errors as needed. In *36th Annual International Conference of the IEEE Engineering in Medicine and Biology Society*, pages 5304–5307. IEEE, August 2014.

[18] H Heuer and J Lüttgen. Robot assistance of motor learning: A neuro-cognitive perspective. *Neuroscience & Biobehavioral Reviews*, 56:222–240, 2015.

[19] R B Gillespie, M O'Modhrain, P Tang, C Pham, and D Zaretsky. The virtual teacher. *Proceedings of ASME Dynamics Systems and Control Division, Symposium on Haptic Interface for Virtual Environment and Teleoperator Systems*, pages 171–178, 1998.

[20] D Feygin, M Keehner, and F Tendick. Haptic Guidance: Experimental Evaluation of a Haptic Training Method for a Perceptual Motor Skill. In *Proceedings 10th Symposium on Haptic Interfaces for Virtual Environment and Teleoperator Systems. HAPTICS 2002*, pages 40–47. IEEE Computer Society, March 2002.

[21] J C Huegel and M K O'Malley. Progressive haptic and visual guidance for training in a virtual dynamic task. *IEEE Third Joint Eurohaptics Conference and Symposium on Haptic Interfaces for Virtual Environment and Teleoperator Systems*, pages 343–350, March 2010.

[22] H Heuer and J Lüttgen. Motor learning with fading and growing haptic guidance. *Experimental Brain Research*, 232(7):2229–2242, July 2014.

[23] S Abeele and O Bock. Sensorimotor adaptation to rotated visual input: different mechanisms for small versus large rotations. *Experimental Brain Research*, 140(4): 407–410, October 2001.

[24] A G Mattar and P L Gribble. Motor Learning by Observing. *Neuron*, 46(1):153–160, 2005.

[25] C Granados and G Wulf. Enhancing motor learning through dyad practice: Contributions of observation and dialogue. *Research Quarterly for Exercise and Sport*, 78 (3):197–203, June 2007.

[26] A Takagi, F Usai, G Ganesh, V Sanguineti, and E Burdet. Haptic communication between humans is tuned by the hard or soft mechanics of interaction. *PLoS Computational Biology*, 14(3):e1005971–17, March 2018.

[27] R C Oldfield. The Assessment and Analysis of Handedness: the Edinburgh Inventory. *Neuropsychologia*, 9(1):97–113, 1971.

[28] N Beckers, A Q L Keemink, E van Asseldonk, and H van der Kooij. Haptic Human-Human Interaction Through a Compliant Connection Does Not Improve Motor Learning in a Force Field. In D Prattichizzo, H Shinoda, H Z Tan, E Ruffaldi, and A Frisoli, editors, *11th International Conference, EuroHaptics 2018*, pages 333–344. Springer International Publishing, 2018.

[29] H G Wu, Y R Miyamoto, L N Gonzalez Castro, B P Ölveczky, and M A Smith. Temporal structure of motor variability is dynamically regulated and predicts motor learning ability. *Nature Neuroscience*, 17(2):312–321, January 2014.

[30] M Kawato, K Furukawa, and R Suzuki. A Hierarchical Neural-Network Model for

Control and Learning of Voluntary Movement. *Biological Cybernetics*, 57(3):169–185, 1987.

[31] J Liu, S C Cramer, and D J Reinkensmeyer. Learning to perform a new movement with robotic assistance: comparison of haptic guidance and visual demonstration. *Journal of NeuroEngineering and Rehabilitation*, 3:20–20, 2006.

[32] L Marchal-Crespo, M Bannwart, R Riener, and H Vallery. The effect of haptic guidance on learning a hybrid rhythmic-discrete motor task. *IEEE Transactions on Haptics*, pages 1–16, January 2013.

[33] M A Guadagnoli and T D Lee. Challenge point: a framework for conceptualizing the effects of various practice conditions in motor learning. *Journal of Motor Behavior*, 36(2):212–224, June 2004.

[34] L Marchal-Crespo, P Wolf, N Gerig, G Rauter, L Jaeger, H Vallery, and R Riener. The role of skill level and motor task characteristics on the effectiveness of robotic training: first results. In *IEEE International Conference on Rehabilitation Robotics ICORR*, pages 151–156. Uniklinik Balgrist, Zurich, Switzerland, August 2015.

[35] L Marchal-Crespo, N Rappo, and R Riener. The effectiveness of robotic training depends on motor task characteristics. *Experimental Brain Research*, 235(12):3799–3816, December 2017.

[36] M Milot, L Marchal-Crespo, C S Green, S C Cramer, and D J Reinkensmeyer. Comparison of error-amplification and haptic-guidance training techniques for learning of a timing-based motor task by healthy individuals. *Experimental Brain Research*, 201(2):119–131, February 2010.

[37] J van Oosterhout, C J M Heemskerk, M R de Baar, F C T van der Helm, and D A Abbink. Tele-Manipulation with Two Asymmetric Slaves: Two Operators Perform Better Than One. *IEEE Transactions on Haptics*, 11(1):128–139, January 2018.

[38] G Wulf and C H Shea. Principles derived from the study of simple skills do not generalize to complex skill learning. *Psychonomic Bulletin & Review*, 9(2):185–211, May 2002.

[39] T Kitago and J W Krakauer. Motor learning principles for neurorehabilitation. *Handbook of clinical neurology*, 110:93–103, 2013.

Chapter 5.

Motion plans of rigidly-coupled pairs change predictably in joint reaching

Atsushi Takagi•, Niek Beckers•, and Etienne Burdet

PLoS ONE, 11(12):e0167314, 2016

• These authors contributed equally to this work.

Motion plans of rigidly-coupled pairs change predictably in joint reaching

Abstract

Parents can effortlessly assist their child to walk, but the mechanism behind such haptic coordination is still unknown. Studies have suggested that haptic coordination is achieved by interacting humans who update their movement or motion plan in response to the partner's behavior. Here, we tested rigidly coupled pairs in a joint reaching task to observe such changes in the partners' motion plans. However, the joint reaching movements were surprisingly consistent across different trials. A computational model that we developed demonstrated that the two partners had a distinct motion plan, which did not change with time. These results suggest that rigidly coupled pairs accomplish joint reaching movements by relying on a pre-programmed motion plan that is independent of the partner's behavior.

5.1. Introduction

From a parent coordinating movements to help a child learn to walk, to a therapist supporting a patient during recovery of their motor functions after injury or disease, we rely on haptic interaction while performing tasks with a common goal. Despite its importance, haptic coordination has only recently been investigated [1–9]. These studies use a variety of metrics such as distance from a goal [1, 4, 5], ad-hoc roles [2, 6, 7], magnitude of interaction force from the haptic coupling [3], the energy exchanged between partners [8] and dominance measures [9] to quantitatively analyse haptic interaction. Importantly, these studies measured only the outcome of haptic interaction and could only speculate as to the cause of these outcomes, which explains why we still have limited understanding of how two people complete a common task.

To understand how pairs or dyads haptically *coordinate* motion behaviors, which we define as the outcome of partners who change their movement or motion plan dependent on the partner's actions, we examined haptically connected partners whose task was to reach a common target from the same initial position. Since the reaching movement is discrete, we can measure trial-by-trial change in the kinematic trajectory and the interaction force. To interpret these changes in kinematics and force, we need a computational model of two coupled partners control. Without a model, the kinematics and interaction force alone cannot differentiate between one partner attempting to move faster or the other to move slower [10].

However, a computational model can resolve this redundancy as each dyad simulated by two coupled controllers yields a unique trajectory and interaction force pattern that can be compared with data. By using our experimental protocol and computational model together, we address the limitations of a previous study that purported that the interaction force is used to negotiate changes in motion plan, but could not support this claim [2].

If coupled partners do haptically coordinate the interaction force sensed through *haptics*, the sensory modality of touch and proprioception, in what manner would they change their motion plan? Reaching movements in humans have been shown to minimize error, e.g. distance of the hand from a target, and effort [11]. This can be modelled as the minimization of a cost function, which yields a motion plan. We hypothesize that dyads haptically coordinate by reducing effort in the form of interaction force that does not contribute to the movement [7]. However, other studies have suggested that the interaction force is critical to haptic coordination [2]. Do partners update their motion plan to reduce interaction force in order to conserve effort, or increase it to improve coordination? To answer this question, we also tested dyads who were constrained to produce a constant interaction force prior to the initiation of the reaching movement. If partners coordinate by minimizing force, their motion plans should update trial-by-trial to decrease this interaction force. The results suggest that the two partners use distinct motion plans unmodified throughout the trials.

5.2. Methods

5.2.1. Participants

Sixteen healthy participants (eight males, eight females; mean age: 25.9 years, age range: 22–33 years) were recruited in pairs to form eight *dyads*. Pairs were matched on sex to avoid any large differences in physical strength. All participants were right-handed, as assessed using the Edinburgh Handedness Inventory [12]. All participants gave informed consent prior to participation, and the experiment was conducted in accordance with the Declaration of Helsinki and approved by the Imperial College Research Ethics Committee.

5.2.2. Robotic setup

The experiments were performed in dyads using the Hi5 dual one degree-of-freedom wrist robotic manipulandum described in [13] (see Fig. 5.1A). Each participant placed his or her right wrist in the Hi5 robotic manipulandum, which allowed flexion and extension of the wrist. The wrist movement controlled a cursor on one's own computer display [13] (see Fig. 5.1B). The robotic interface can generate a stiff connection between both wrist interfaces with a torsional stiffness of $23\,\mathrm{N\,m\,rad^{-1}}$, which is equivalent to a linear stiffness of approximately $2300\,\mathrm{N\,m^{-1}}$ when assuming the pivot arm is 0.1 m from the centre of the wrist (centre of rotation) to the middle of the palm. Participants were separated by a heavy curtain, which prohibited them from seeing each other's movements, displays, and eliminated social interaction.

5.2.3. Experiment protocol

In each trial, participants made point-to-point reaching movements using the dual robotic interface with wrist flexion/extension. The movement's start and target positions were fixed at 10 deg extension and 30 deg flexion, respectively. To synchronize the movement start, participants initiated their movement after a 3 s countdown, which was shown on the display (see Fig. 5.1C). The trial ended when the cursor was held in the target for 0.5 s. Dyads performed 135 trials in seven blocks in which their wrists were alternately not connected (one *training* and three *solo* blocks) and connected (one *coupled* and two *push-pull blocks*), see Fig. 5.1B.

We constrained movement time during the training and solo blocks between 900 ms and 1200 ms for two reasons: (1) to allow for more time for interaction to occur compared to previous studies that showed variable movement times smaller than 800 ms [2, 3] and (2) to return partners to their baseline reaching movement such that the dyads started each coupled and push-pull block from the same condition. For this purpose, participants received feedback on the display using the messages “too fast” or “too slow” after a movement with duration smaller than 900 ms or larger than 1200 ms, respectively. Movement time was not constrained during the coupled and push-pull blocks since our aim is to investigate changes in coordination due to interaction forces, not due to changes in movement behavior to adjust for too short or too long movement durations.

Dyads first performed a *training block* of 15 trials to familiarize themselves with the interface and the reaching task, including the countdown and movement time constraint. During this training block, participants' wrists were not connected such that the participants independently reached towards the target (training & solo panel of Fig. 5.1C).

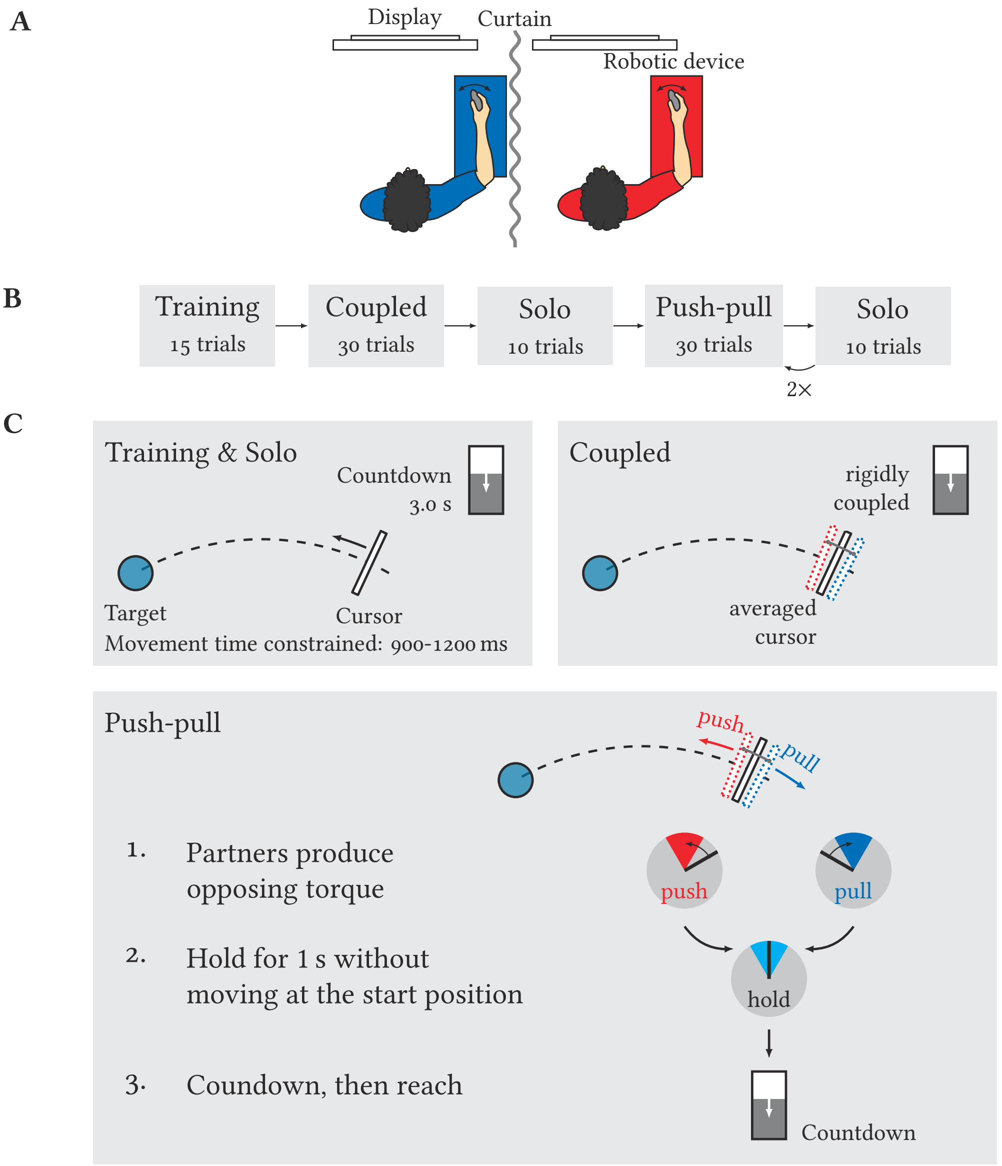

Figure 5.1. | Dyadic reaching manipulandum and protocol. **A** Schematic of the dual-wrist manipulandum setup. **B** The experiment was split up into three types of blocks: training and solo blocks, a coupled block and push-pull blocks. Dyads were alternately disconnected (training and solo blocks) and connected (coupled and push-pull blocks). After the first push-pull block and subsequent solo block, dyads performed another push-pull block and solo block. **C** In the training and solo blocks, partners are disconnected and reach the target alone. In the coupled and push-pull blocks the partners were rigidly coupled. In the coupled block, partners were rigidly coupled and moved the averaged cursor to the target. In the push-pull block, dyads were constrained to produce a torque of 0.7 N m prior to the reaching movement. One partner pushed towards the target and the other pulled away; once the initial opposing torque was balanced and the average cursor position at 0 deg, the 3 s countdown was initiated. Partners switched the pushing and pulling instructions in the second push-pull block.

After training, the partners experienced a *coupled block* of 30 trials, where their wrists were rigidly coupled by the computer-generated rigid connection. Instructions and procedure per trial in the coupled block were the same as in the training block; participants had to make reaching movements after a 3 s countdown (coupled panel of Fig. 5.1C). Although the connection was very stiff, the connection could still result in very small differences in cursor position between the partners. Therefore, the average wrist position was displayed as the common cursor. Through the rigid coupling, participants could exert torques onto each other.

Following the coupled block, participants performed a *solo block* of 10 trials, which was used to allow the participants to return to their baseline reaching behavior.

Dyads then experienced two *push-pull blocks* (30 trials per block) in which each reaching movement started with an initial opposing torque while being rigidly coupled (see Fig. 5.1C). Partners were instructed to produce an initial constant torque of 0.7 N m whilst remaining stationary at the starting position prior to the movement onset only. Once the torque was held for 1 s, the 3 s countdown was initiated and partners were instructed to reach to the target at the end of the countdown. During the countdown, dyads had to maintain the initial opposing torque and remain stationary at the starting position. No further instructions were given concerning the opposing torque during the reaching movement itself. In one push-pull block, one partner was assigned to *push towards* the target (i.e. produce a positive torque) and the other to *pull away* from it (i.e. produce a negative torque). In the next push-pull block, the instructions of pushing and pulling were switched. The order of which partner pushed towards the target was counterbalanced and randomly assigned to dyads. Each push-pull block was followed by a solo block.

5.2.4. Data analysis

Trajectory and interaction torque data was recorded at 100 Hz. Data was recorded from the start of the countdown until the cursor was in the target for 0.5 s. All trajectory and torque data were aligned on the start of a trial, which was defined as the time the wrist velocity exceeded $5\,\mathrm{deg\,s^{-1}}$. Data was then truncated after 1.2 s, which was the slowest permissible movement time as constrained during the solo trials. The trajectory and torque patterns of all trials were resampled to 256 time samples. Trajectory and torque patterns were filtered using a zero-phase sixth-order low-pass Butterworth filter with a cut-off frequency of 6 Hz.

Changes in haptic coordination throughout the coupled and both push-pull blocks were analysed per block by comparing the trial-by-trial changes in trajectory and torque patterns within each block. In addition, since we observed dyad-specific torque patterns, this analysis was performed for each dyad separately. To compare the trajectory and torque patterns we used wavelet-based ANOVA following the method described by McKay et al. (see [14] for a detailed description). By performing the time-series analysis in the wavelet domain, statistical power is increased relatively to time domain ANOVA, since differences between curves tend to be represented by a few wavelets and hence results in fewer comparisons. Furthermore, this method does not sacrifice temporal resolution which occurs when dividing the trajectory or torque patterns into time windows [14].

All trajectory and torque patterns were transformed to the wavelet domain using the MATLAB wavelet toolbox (third-order coiflets, decomposition level 4). This resulted in 256 wavelet coefficients for the trajectory and torque patterns for each trial. We grouped the 30 trials per coupled or push-pull block into six bins of five trials each in chronological order (e.g. bin 1: trials 1–5, bin 2: trials 6–10, etc.). By performing a wavelet-based ANOVA on the binned data with bin as single factor, we can test whether the trajectory and torque patterns change across bins and hence throughout each connected block. Significant differences in trajectory or torque patterns between bins could indicate changes in haptic coordination. A fixed-effect single-factor ANOVA model with bin as factor at a significance level of 0.05 was performed for each wavelet coefficient across bins, resulting in 256 F tests per block and per dyad. Post hoc multiple pairwise comparisons between bins using Scheffé's method were performed on the wavelet coefficients corresponding to the significant F tests. Post hoc tests were performed at significance level of 0.05 which was Bonferroni-adjusted for the number of significant initial F tests. Significantly different wavelet coefficients were transformed back to the time domain for visualization and analysis. This results in time-domain curves describing the mean differences of trajectory and torque patterns and temporal location of these differences between all combinations of bins, per connected block and per dyad [14]. Point-wise ANOVA were also performed in the time domain to corroborate the findings of the wavelet-based ANOVA. Figure C.3 shows an example of the mean difference curves as a result of the wavelet-domain and time-domain analysis for the coupled block of dyad VIII. All significant differences and temporal location of the differences in torque curves are summarized in Table C.1 for all connected blocks and all dyads.

5.2.5. Model of dyadic reaching

A participant reaching in one dimension using their wrist with state

$$\mathbf{x} = \begin{bmatrix} \theta, & \dot{\theta}, & \tau, & f \end{bmatrix}^T, \tag{5.1}$$

composed of the angle, angular velocity, torque and an auxiliary variable, evolves in discrete time through the state space model

$$\mathbf{x}_{k+1} = \mathbf{A}\mathbf{x}_k + \mathbf{B}u_k + \mathbf{C}\left(\mathbf{x}_k^p - \mathbf{x}_k\right), \tag{5.2}$$

where $\mathbf{x}_k^p$ is the state of the partner, k the time index,

$$\mathbf{A} = \begin{bmatrix} 1 & \delta & 0 & 0 \\ 0 & 1 & \frac{\delta}{I} & 0 \\ 0 & 0 & 1-\frac{\delta}{\tau_u} & \frac{\delta}{\tau_u} \\ 0 & 0 & 0 & 1-\frac{\delta}{\tau_u} \end{bmatrix}, \tag{5.3}$$

$$\mathbf{B} = \begin{bmatrix} 0 & 0 & 0 & \frac{\delta}{\tau_u} \end{bmatrix}^T, \tag{5.4}$$

$$\mathbf{C} = \begin{bmatrix} 0 & 0 & 0 & 0 \\ k_s\frac{\delta}{I} & b_s\frac{\delta}{I} & 0 & 0 \\ 0 & 0 & 0 & 0 \\ 0 & 0 & 0 & 0 \end{bmatrix}, \tag{5.5}$$

with the moment of inertia of the wrist I, time step δ and the stiffness and damping of the spring k_s and b_s that connects partners. The musculoskeletal system of the wrist is modelled using a second-order muscle-like filter with a time constant of $\tau_u = 40\,\text{ms}$ [15]. The connection matrix $\mathbf{C} = \mathbf{0}_{4\times4}$ if the partners are disconnected, as in the solo block. The motor command u_k sent to the wrist is

$$u_k = -\mathbf{L}\left(\mathbf{x}_k - \mathbf{t}\right), \tag{5.6}$$

where the target vector $\mathbf{t}$ is

$$\mathbf{t} = \begin{bmatrix} \theta_t, & 0, & 0, & 0 \end{bmatrix}^T \tag{5.7}$$

during reaching, with θ_t is the target angle of the movement. In addition, for the push-pull blocks, the target vector prior to the reaching movement in the push-pull blocks is

$$\mathbf{t}_0 = \left[\theta_0, \quad 0, \quad \tau_0, \quad 0\right]^T, \tag{5.8}$$

where θ_0 and τ_0 are the initial angle and the interaction torque imposed prior to the movement in the push-pull blocks, respectively. The controller gain $\mathbf{L}$ is computed by minimising the cost

$$\sum_{k=0}^{\infty} \mathbf{x}_k^T \mathbf{Q} \mathbf{x}_k + u_k R u_k, \tag{5.9}$$

where the matrix $\mathbf{Q}$ is positive semi-definite and R is positive. The solution of this infinite horizon linear quadratic regulator (LQR) is [16]

$$\mathbf{S} = \mathbf{Q} + \mathbf{A}^T \left[\mathbf{S} - \mathbf{S}\mathbf{B}\left(R + \mathbf{B}^T\mathbf{S}\mathbf{B}\right)^{-1} \mathbf{B}^T\mathbf{S}\right] \mathbf{A} \tag{5.10}$$

and the iterative solution of equation 5.10 yields the optimal gain

$$\mathbf{L} = \left(R + \mathbf{B}^T\mathbf{S}\mathbf{B}\right)^{-1} \mathbf{B}^T\mathbf{S}\mathbf{A}. \tag{5.11}$$

A pair of the human-like controllers were simulated in parallel, only interacting through the connection matrix $\mathbf{C}$. Thus, each partner was affected by the interaction forces alone, and did not plan a joint movement with another partner, yielding *co-activity* [17]. We assume that participants know the state of their own wrist with fidelity. For all simulations, the parameters were set to

$$k_s = 0.4\,\mathrm{N\,m\,deg^{-1}}, \; b_s = 0.05\,\mathrm{N\,m\,s\,deg^{-1}}, \; R = 0.5, \; \delta = 0.01\,\mathrm{s}, \; I = 0.1\,\mathrm{kg\,m^2},$$

where k_s is from the experiment and damping b_s is added to model the natural damping properties of the wrist. The inertia I and the control cost R were set to match the average speed and torque observed in the data such that the motion plan identification (described in the next section) converged within reasonable time for each dyad. The initial and target angles and initial opposing torque were set to

$$\theta_0 = -10\,\mathrm{deg}, \; \theta_t = 30\,\mathrm{deg},$$
$$\tau_0 = 0.7\,\mathrm{N\,m} \text{ or } -0.7\,\mathrm{N\,m},$$

as in the experiment.

5.2.6. Identifying the motion plan

To identify the parameters of the cost function $\mathbf{Q}$ (in equation 5.9) and the final target angle of each partner (equations 5.7 to 5.8), we conducted a tree-search of the 6 parameters $\mathbf{Q}_1(1,1)$, $\mathbf{Q}_1(2,2)$, $\theta_{t,1}$ and $\mathbf{Q}_2(1,1)$, $\mathbf{Q}_2(2,2)$, $\theta_{t,2}$ to identify their values that minimized the normalized squared distance from the trajectory and force pattern in the data

$$M = \frac{1}{2L}\sum_{i=0}^{L}\left[\frac{\left(\overline{\theta}_i - \theta_i\right)^2}{\sigma^2_{\theta_i}} + \frac{\left(\overline{\tau}_i - \tau_i\right)^2}{\sigma^2_{\tau_i}}\right] \tag{5.12}$$

where L is the length of data, $\overline{\theta}_i$ is the mean angle of the data over all trials in one block, $\overline{\tau}$ is the mean torque in one block, σ^2_θ and σ^2_τ are the variance of the angle and torque along the trajectory, and θ and τ are the angle and torque in the simulation. The parameters were initialized with the values

$$\mathbf{Q} = \mathrm{diag}\left(2, 0.1, 0, 0\right), \ \theta = 30\,\mathrm{deg}$$

which were incrementally altered in step sizes of $\delta Q_{\mathrm{pos}} = 2$, $\delta Q_{\mathrm{vel}} = 0.1$ and $\delta\theta_t = 1\,\mathrm{deg}$ (for position cost, velocity cost and final target angle) to minimize the magnitude of the metric in equation 5.12. The algorithm goes as follows: first, we simulated the 64 permutations of

$$\begin{aligned}
&\mathbf{Q}_1(1,1) \pm \delta Q_{\mathrm{pos}},\\
&\mathbf{Q}_1(2,2) \pm \delta Q_{\mathrm{vel}},\\
&\theta_{t,1} \pm \delta\theta_t,\\
&\mathbf{Q}_2(1,1) \pm \delta Q_{\mathrm{pos}},\\
&\mathbf{Q}_2(2,2) \pm \delta Q_{\mathrm{vel}},\\
&\theta_{t,2} \pm \delta\theta_t.
\end{aligned}$$

Out of these permutations, the parameters that minimized the metric of equation 5.12 was selected as the starting point again, and the process was repeated for 200 iterations for each dyad in the coupled and push-pull blocks. We then compared the relative changes in the position and velocity cost terms in the cost matrix $\mathbf{Q}$ between the coupled and push-pull blocks to examine any consistent change due to the torque prior to movement onset.

5.3. Results

We first examined the trajectories and interaction torques from the coupled block. The trajectories of the average cursor from all binned trials in the coupled block are shown in Fig. 5.2A, where each bin consists of five trials. The trajectories were different between dyads, but a statistical analysis showed no significant differences between the binned trials within dyads (for all F tests, $p > 0.05$, see Methods for a description of the analysis). Figure 5.2B shows the torque patterns from all dyads in the coupled block. Similar to the kinematics, we observed dyad-specific torque patterns. The partners in dyad II, for example, have specialized into pure acceleration (blue partner) and deceleration (red partner) of the coupled movement. Some statistical differences were found between within-dyad binned torque patterns; dyad III showed a difference in torque between bins 2 and 3 for only a small time window (0.38 s to 0.45 s; one significant F test, $p < 0.05$), see Table C.1. However, we observed no consistent trial-by-trial changes in the torque patterns for any dyad in the coupled block, with the exception of dyad VIII. Dyad VIII showed significantly higher torques in bin 1 compared to bins 2 to 6 (see Fig. C.3 and Table C.1 for details). Although the torques in bin 1 were higher, the torques in the other bins were consistent and showed no significant differences between bins. These data suggest that dyad VIII changed their motion plan after bin 1, but did not coordinate during bins 2 to 6, i.e. they did not change their motion plan to reduce effort.

5.3.1. Dyadic reaching with torque at movement onset

Next, we examined the torque patterns of all dyads in the push-pull blocks. The representative dyads I–IV are shown in Fig. 5.3, while dyads V-–VIII are plot in Fig. C.2. It appears that the torque patterns are unchanging from one trial to the next in each push-pull block. The wavelet-based ANOVA did reveal some significant differences in between bins for dyads I, VI, VII and VIII, see Table C.1. For instance, dyad I showed differences in torque between bin 1 and bins 5 and 6, but only briefly, and dyad VII's torque pattern in bin 2 was different compared to bins 4 and 5 in the last 0.5 s of the reaching movement (see Table C.1 for details). Importantly, the significant differences were not consistent across the push-pull bins for all dyads and across both push-pull blocks. There are three noticeable outcomes in the push-pull condition. First, partners in the same dyad do not have identical torque patterns when switching between pushing and pulling roles. Second, the torque pattern predominantly remains in the same direction throughout

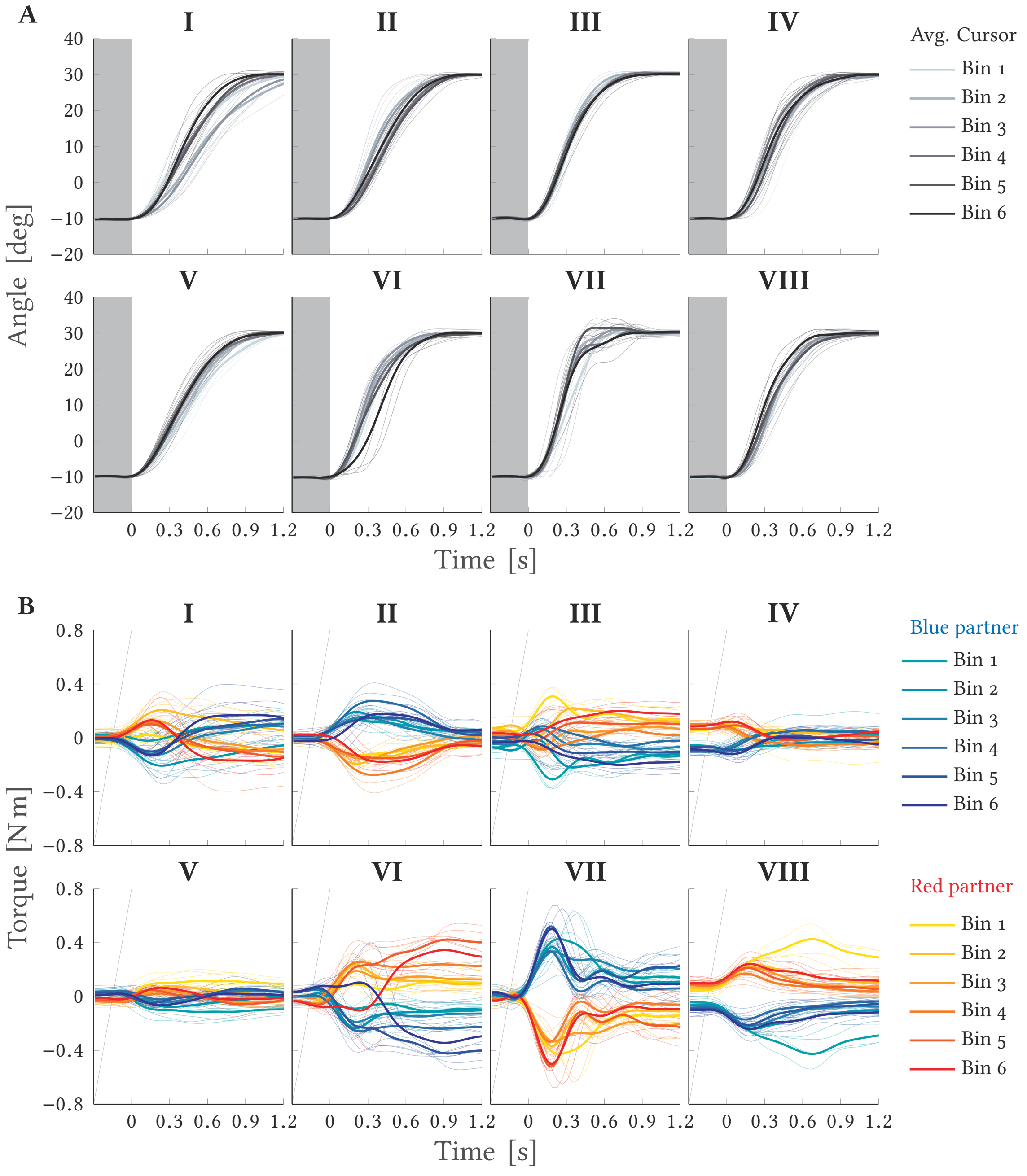

Figure 5.2. | Trajectory and torque data for the coupled block. **A** Trajectories of the average cursor for all dyads in the coupled block. The bold lines indicate the average trajectory of each bin; the thin lines show the individual trials. **B** Torque from all eight dyads, where each bold trace corresponds to the average of each bin; the bins progress chronologically from green to blue for the blue partner and from yellow to red for the red partner. With the exception of dyad VIII, no consistent trial-by-trial change in the torque was observed within dyads. Different dyads displayed specific torque patterns.

the whole movement, i.e. a partner constrained to push at movement onset keeps pushing and vice versa. Third, the torque at movement onset caused all dyads, in at least one push-pull block, to end the movement with constant (e.g. non-zero) opposing torque (paired-sampled t-test on the opposing torque at $t = 1.2\,\mathrm{s}$, $t(15) = 46.80$, $p < 0.001$). The constant opposing torque at movement end is possible due to the redundancy of the task, but is functionally superfluous and energy inefficient. Partners could have updated their motion plans between trials to reduce this superfluous torque, but they did not.

5.3.2. Simulation of dyadic reaching

Why do the trajectory and torque patterns remain relatively stable from trial-to-trial within each block? Why is the torque pattern dyad-specific, and how can the same dyad exhibit different trajectories and torque patterns between the coupled and push-pull blocks? To address these questions, we developed a computational model of dyadic reaching. The experimental results suggest that partners do not update their motion plan from trial-to-trial, but may have differing motion plans in each block. Thus, we assume that the torque patterns are a by-product of two rigidly coupled participants who planned their motion independently, corresponding to the mechanism of co-activity [17]. Each participant was modelled as a controller with muscle-like dynamics that minimized the difference in position and velocity between the cursor and target using a linear quadratic regulator [18]. Dyadic reaching was simulated with two of these controller agents who planned and executed their movements independently with movement affected by the torque of the rigid coupling.

As the trajectory and torque pattern in different block conditions was different for each dyad, partners may have had different motion plans between block conditions that did not change within each block. To identify the motion plans in each block for each partner, we modified each partner's state cost matrix $\mathbf{Q}$, which has two diagonal terms that prioritize the difference between the current and desired position and velocity (see Methods for details). How do these two terms in the state cost matrix affect the motion plan? A position-priority controller, with a large term in $\mathbf{Q}(1,1)$ and a small term in $\mathbf{Q}(2,2)$, will aggressively reach to the target, resulting in large overshoot (blue decoupled controller in Fig. 5.4A). A velocity-priority controller, with a small term in $\mathbf{Q}(1,1)$ and a large term in $\mathbf{Q}(2,2)$, will slowly converge to the target without overshooting (red decoupled controller in Fig. 5.4A).

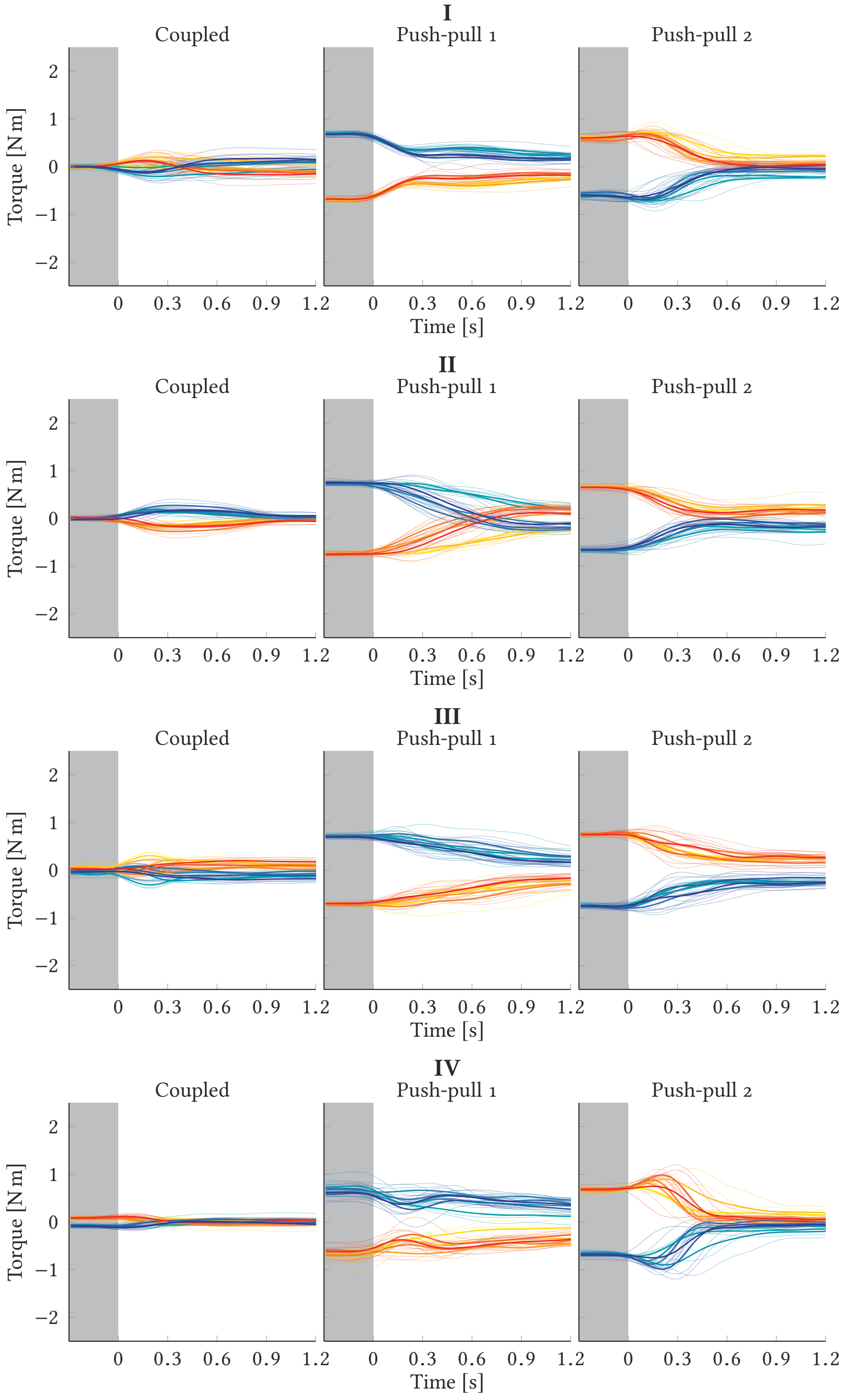

Figure 5.3. | Dyadic reaching with initial opposing torque prior to movement. Torque from dyads I–IV in the coupled and both push-pull blocks; each bold trace is the average trajectory of each bin. In all dyadic reaching blocks, the torque was unchanging between trials within each block.

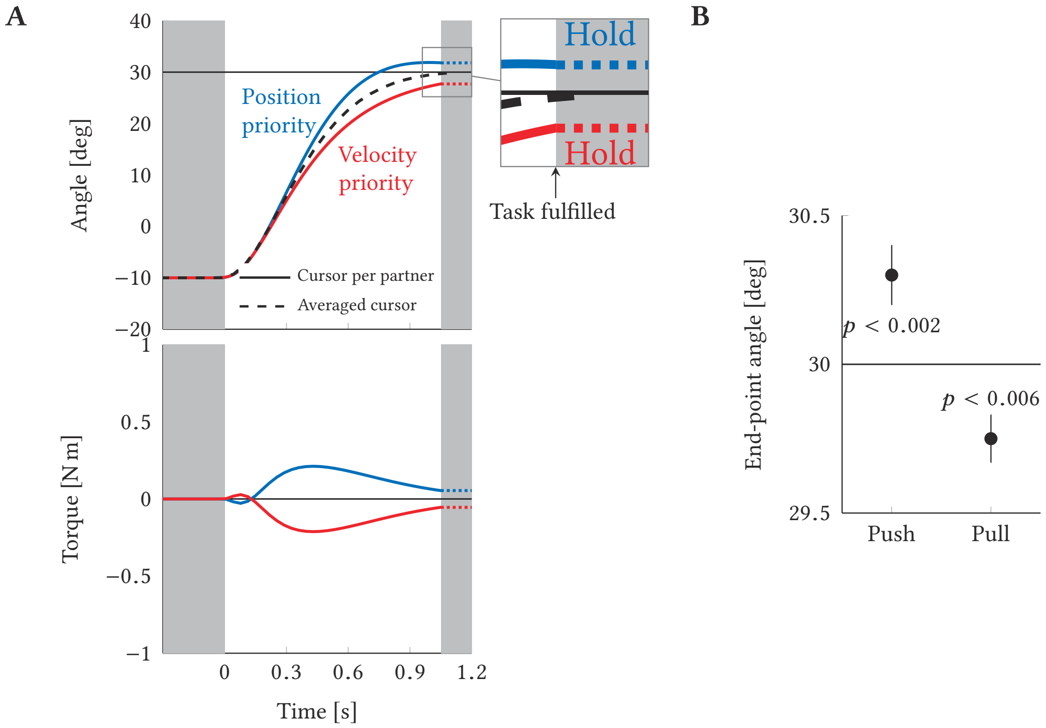

Figure 5.4. | Position and velocity priority in the motion plan explains endpoint bias. **A** The (decoupled) blue controller prioritizes position, which causes it to overshoot the target. The (decoupled) red controller prioritizes velocity such that it converges to the target without any overshoot. When the position-priority and velocity-priority controllers are coupled (dashed black trace), a force pattern is observed (dashed blue and red traces). The only manner in which the controllers would end the movement with constant torque is if they decide to hold their position once the reach is fulfilled. **B** Endpoint bias at the end of the reaching movement from all 16 partners. Partners, at movement onset, who pushed towards the target overshot it, and those who pulled away undershot it.

When these two controllers, one position-priority and the other velocity-priority, are rigidly coupled, an interaction torque pattern is observed (see dashed torque traces in Fig. 5.4A) that appears similar to dyad II's coupled reaching (Fig. 5.3). However, the simulated torque pattern decays, whereas dyad II ends the movement with a constant torque. The (optimal) controllers will never end the movement with wasteful torque, unless they decide to stick to their current position once the task is fulfilled. Looking back at the decoupled controllers (solid traces in Fig. 5.4A), the joint movement ends when the driving controller (blue) has overshot the target and the braking controller (red) is undershooting it. If both controllers maintain their respective positions once their average position reaches the target, the position-priority and velocity-priority controllers will end the movement with constant torque as dyad II did (zoomed plot in Fig. 5.4A). Upon examining the data (Fig. 5.4B), the partner pushing towards the target at movement onset overshot it (overshoot significantly different from zero; one-sample t-test on the pushing partner's position; $t(15) = 3.73$, $p < 0.002$) and the pulling partner undershot the target ($t(15) = -3.20$, $p < 0.006$). Thus, we suspected that pushing at movement onset altered the motion plan to prioritize position, and pulling to prioritize velocity.

We used a Monte Carlo tree-search to identify the underdetermined system of the motion plan priority and final reach position of both partners such that the simulated trajectories and torque pattern matched the data, which were averaged in each block, as closely as possible (see Methods for details). We modified each partner's state cost matrix $\mathbf{Q}$ incrementally in the direction that reduced the discrepancy between the simulation and the data. As each pair of controllers yield a unique trajectory and torque pattern, there is no issue in resolving the redundancy while interpreting a torque pattern. Since the trajectory and torque pattern was different between blocks even for the same dyad, we conducted the tree-search for each block separately for every dyad. We could then compare the identified motion plans in the push-pull blocks with those from the coupled block to assess how each partner's motion plan changed due to their pushing or pulling role in the push-pull block.

Figure 5.5 compares the data (solid trace) and the simulations (dashed trace) of the mean trajectories and torques of all trial from dyads I–-IV in both coupled and push-pull conditions. Taking dyad I as an example, in the first coupled block the red partner prioritized position more than blue. This is also evident from the solo blocks where the red partner was found to reach faster than the blue partner (see Table C.2). We simulated the different push-pull conditions using the motion plans identified in the coupled block, but the predicted trajectory and torque were different from the data. Clearly, the partners had different motion plans in the push-pull blocks than in the coupled block. So how had the partners' motion plan changed? Simulations revealed that in the first push-pull block, the (pushing) red partner prioritized position even more than in the coupled block, and the blue partner prioritized velocity. In the last push-pull block, the (pushing) blue partner prioritized position and the (pulling) red partner prioritized velocity. This pattern of change in the partners' motion plan was consistent in all dyads. Every partner pushing towards the target prioritized position, and those pulling away prioritized velocity (Fig. 5.5B–D for dyads I–IV, and Fig. C.2 for dyads V–VIII, see Table C.2 for identified state cost terms). This explains why pushing partners, who prioritized position, overshot the target and pulling partners, who prioritized velocity, undershot the target, just as predicted by the computational model (Fig. 5.4A and Fig. 5.4B).

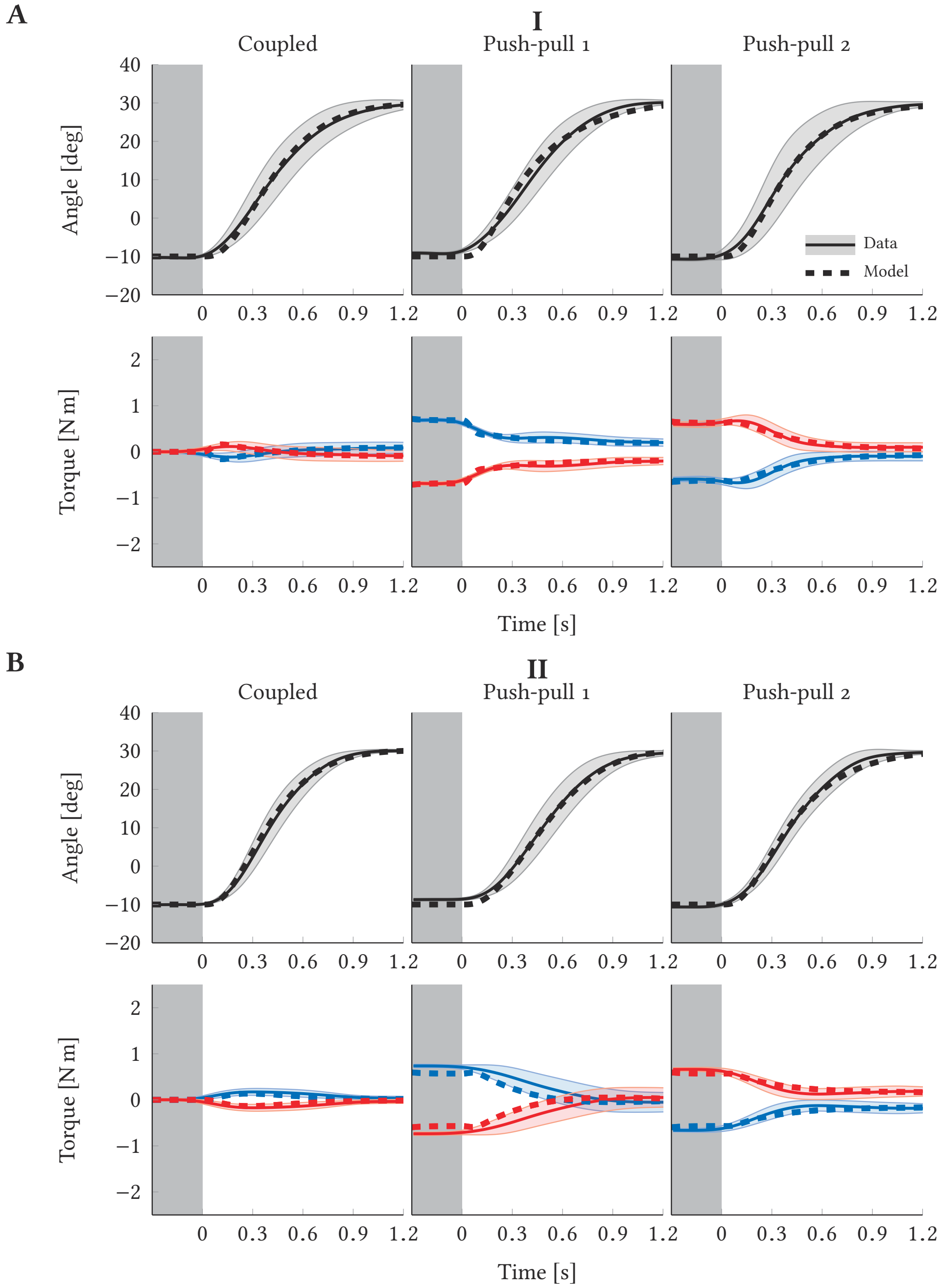

Figure 5.5. | Simulation of dyadic reaching. Trajectories and torques from dyads I to IV (**A**–-**D**) in the coupled and push-pull blocks. Solid trace is from the data showing the mean of all trials and the shaded area is the standard deviation; the dashed traces are from simulations. First, we identify the state costs of both partners in coupled reaching, then identify the state cost in the push-pull blocks to see what effect the opposing torques prior to movement onset had. In all dyads, the initial opposing torque had a consistent effect: partners pushing towards the target prioritized position and overshot the target; those pulling away prioritized velocity and undershot the target.

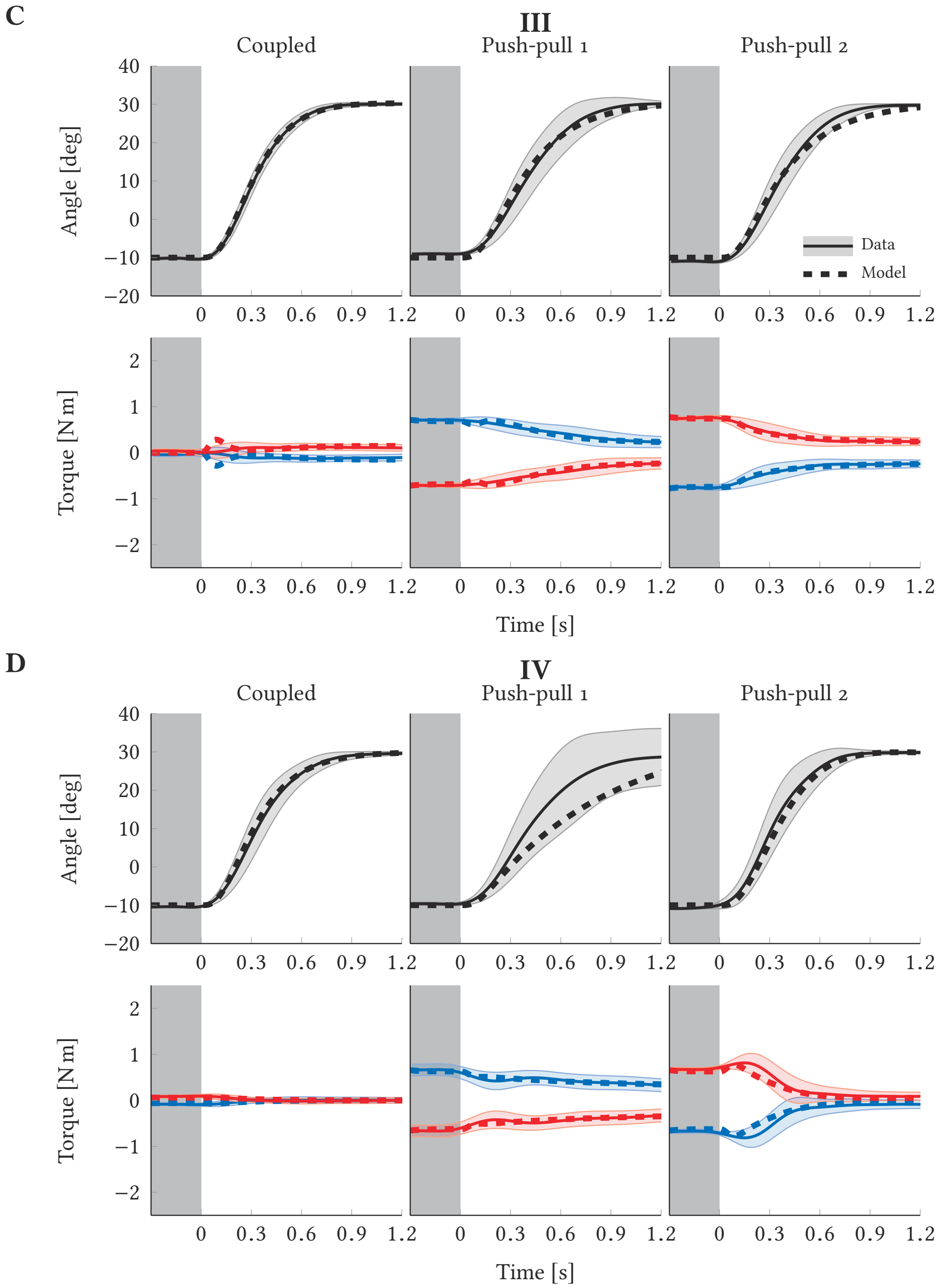

Figure 5.5. | Simulation of dyadic reaching (continued). Trajectories and torques from dyads I to IV (**A**–-**D**) in the coupled and push-pull blocks. Solid trace is from the data showing the mean of all trials and the shaded area is the standard deviation; the dashed traces are from simulations. First, we identify the state costs of both partners in coupled reaching, then identify the state cost in the push-pull blocks to see what effect the opposing torques prior to movement onset had. In all dyads, the initial opposing torque had a consistent effect: partners pushing towards the target prioritized position and overshot the target; those pulling away prioritized velocity and undershot the target.

5.4. Discussion

We systematically examined rigidly coupled dyadic reaching movements to observe the trial-by-trial emergence of coordination. We developed a computational model of the reaching movement to identify each partner's motion plan, thereby resolving the redundancy in interpreting kinematic and torque data. Our experiment revealed that dyads did not change their motion plan, i.e. did not coordinate their behavior, even after 30 movements. However, their motion plan was different when dyads were constrained to produce a constant opposing torque prior to movement onset. This modification of the motion plan was predictable and dependent on which direction the partner was producing the interaction torque.

Rigidly-coupled partners do not coordinate during a joint reaching task

Our study provides evidence that dyads do not coordinate during joint reaching movements towards the same target. This result stands in contrast with Reed and Peshkin [2] who argued that the interaction torque was used by dyads to negotiate specialized roles, like one partner who only accelerates and the other who purely decelerates. Indeed, we also observed dyads employing such a 'strategy' in our study, but this specialization can be explained by two reasons. First, partners may reach towards a common target at different speeds or initiate the movement with different reaction times as the authors did not implement a countdown [10]. When we examined the solo blocks where partners were decoupled, the partner who applied torque in the direction of the movement was also reaching faster in the solo trials. Second, the condition at movement onset can affect the specialization; partners who push towards the target prior to movement onset will tend to keep applying such torque throughout the movement. Reed and Peshkin [2] reported that their dyads were applying such opposing torques whilst waiting for the next target to appear, which explains the specialization they observed. Thus, the trajectory and torque patterns that these authors documented are the result of different movement speeds, reaction times and varying movement onset conditions.

Using computational modeling to understand haptic interaction

Our computational model resolved the redundancy in interpreting the trajectory and torque patterns observed during joint reaching. This is in contrast with previous studies [2, 6] that employed ad-hoc roles defined by the authors to classify the coordination strategies. Such an approach is limited and may be unwise as differences in natural movement speed may account for differences between dyads [10]. Furthermore, the use of a metric like the magnitude of interaction torque [3] is prone to misinterpreting the results of our study as it would suggest greater coordination in push-pull blocks in comparison to coupled blocks, which is evidently not the case as our computational model suggests. Interestingly, our computational model can be implemented in real-time on a robotic manipulandum to interact with a human partner. Future studies can employ this model to test if a robot partner, whose motion plan is programmed to minimize interaction torque on a trial-by-trial basis, may induce the human partner to do the same.

Our experimental results and computational model suggest that joint reaching may not be a suitable task when examining the emergence of haptic coordination, as partners do not seem to update their motion plan on a trial-by-trial basis. So how should future works study haptic coordination and its emergence? Comparing the simulation predictions from co-activity with the experimental results may yield clues as to whether partners coordinate their actions. For example, the study by Ganesh et al. [5], which examined tracking in dyads connected by an elastic band, cannot be explained by co-activity, and suggests a change in one's behavior with the haptic coupling. Our findings suggest that a joint reaching task is a suitable paradigm to compare with a computational model to identify each partner's motion plan, but is not sufficient to observe systematic trial-to-trial changes in the motion plans. A continuous task such as a pursuit tracking may be more suitable to examine haptic coordination [5, 8].

References

[1] N Sebanz, H Bekkering, and G Knoblich. Joint action: bodies and minds moving together. *Trends in Cognitive Sciences*, 10(2):70–76, February 2006.

[2] K B Reed and M A Peshkin. Physical Collaboration of Human-Human and Human-Robot Teams. *IEEE Transactions on Haptics*, 1(2):108–120, 2008.

[3] R P R D van der Wel, G Knoblich, and N Sebanz. Let the Force Be With Us: Dyads Exploit Haptic Coupling for Coordination. *Journal of Experimental Psychology: Human Perception and Performance*, 37(5):1420–1431, October 2011.

[4] S Gentry, E Feron, and R Murray-Smith. Human-human haptic collaboration in cyclical Fitts' tasks. In *2005 IEEE/RSJ International Conference on Intelligent Robots and Systems*, pages 3402–3407. IEEE, 2005.

[5] G Ganesh, A Takagi, R Osu, T Yoshioka, M Kawato, and E Burdet. Two is better than one: Physical interactions improve motor performance in humans. *Scientific Reports*, 4, 2014.

[6] N Stefanov, A Peer, and M Buss. Role determination in human-human interaction. In *EuroHaptics conference, 2009 and Symposium on Haptic Interfaces for Virtual Environment and Teleoperator Systems. World Haptics 2009. Third Joint*, pages 51–56. IEEE, 2009.

[7] A Melendez-Calderon, V Komisar, and E Burdet. Interpersonal strategies for disturbance attenuation during a rhythmic joint motor action. *Physiology & Behavior*, 147:348–358, 2015.

[8] D Feth, R Groten, A Peer, S Hirche, and M Buss. Performance related energy exchange in haptic human-human interaction in a shared virtual object manipulation task. In *WHC '09: Proceedings of the World Haptics 2009 - Third Joint EuroHaptics conference and Symposium on Haptic Interfaces for Virtual Environment and Teleoperator Systems*. Technical University of Munich, IEEE Computer Society, March 2009.

[9] R Groten, D Feth, H Goshy, and A Peer. Experimental analysis of dominance in haptic collaboration. *IEEE International Symposium on Robot and Human Interactive Communication. Proceedings*, pages 723–729, 2009.

[10] A Sawers and L H Ting. Perspectives on human-human sensorimotor interactions for the design of rehabilitation robots. *Journal of NeuroEngineering and Rehabilitation*, 11(1), 2014.

[11] D W Franklin, E Burdet, K P Tee, R Osu, C M Chew, T E Milner, and M Kawato. CNS Learns Stable, Accurate, and Efficient Movements Using a Simple Algorithm. *Journal of Neuroscience*, 28(44):11165–11173, 2008.

[12] R C Oldfield. The Assessment and Analysis of Handedness: the Edinburgh Inventory. *Neuropsychologia*, 9(1):97–113, 1971.

[13] A Melendez-Calderon, L Bagutti, B Pedrono, and E Burdet. Hi5: a versatile dual-wrist device to study human-human interaction and bimanual control. In *2011 IEEE/RSJ International Conference on Intelligent Robots and Systems*, pages 2578–2583. IEEE, 2011.

[14] J L McKay, T D J Welch, B Vidakovic, and L H Ting. Statistically significant contrasts between EMG waveforms revealed using wavelet-based functional ANOVA. *Journal of Neurophysiology*, 109(2):591–602, December 2012.

[15] J M Winters and P E Crago. *Biomechanics and Neural Control of Posture and Movement.* Springer, September 2011.

[16] R F Stengel. *Optimal Control and Estimation.* Dover Publications, New York, 1994.

[17] N Jarrassé, T Charalambous, and E Burdet. A Framework to Describe, Analyze and Generate Interactive Motor Behaviors. *PLoS ONE*, 7(11), 2012.

[18] E Todorov and M I Jordan. Optimal feedback control as a theory of motor coordination. *Nature Neuroscience*, 5(11):1226–1235, November 2002.

Chapter 6.

Haptically-interacting individuals do not need to exchange information through the interaction force to improve in a tracking task

---

Niek Beckers, Edwin van Asseldonk,
Arvid Keemink, and Herman van der Kooij

Manuscript in preparation

Abstract

Two is better than one: haptic interaction between two individuals in a continuous tracking task has been shown to improve performance for both partners. Researchers proposed that the interacting partners improved performance by estimating their partner's movement goal from the interaction force and using it to improve their own tracking performance. In contrast, we have a simpler explanation and provide evidence that no such haptic communication was necessary to improve performance in a similar tracking task. First, we show that the partners did not need to accurately perceive the interaction force to improve performance. We impaired the perception of the interaction force by superimposing a velocity-dependent force field on the task and found that individuals improved similarly during haptic interaction compared to when no force field was present. Second, we could accurately explain the improvements with a computational model that assumed no haptic communication to occur. Haptic interaction improves performance because the mechanical coupling between the two partners reduces motor variability and provides haptic guidance to the worse-performing partner in the pair.

6.1. Introduction

When carrying a couch up a flight of stairs together, movers can coordinate their movements by exerting forces onto each other through the couch. Haptic interactions between humans like these play an important role in motor coordination [1, 2]. Interestingly, haptic interaction with a partner who is performing the same task can also improve your motor performance, regardless of how good he/she is at the task [3–5]. Reed and Peshkin [4] showed that rigidly-coupled pairs were faster at reaching to a target compared to each participant doing the same task alone. Ganesh et al. [3] found that haptic interaction through a compliant connection, a computer-generated spring and damper, improved tracking performance for both partners during a collaborative tracking task, which required following a randomly-moving target. More importantly, they found that individuals still improved during interaction even when they interacted with a worse-performing partner.

How does haptic interaction with a worse-performing partner still improve motor performance? This finding is remarkable, as you might expect that being physically connected to a worse-performing partner would impede performance. To explain the results of [3], Takagi et al. [6] proposed a computational model in which the two haptically interacting partners infer each other's movement goal from the information transmitted in the interaction force. The estimated partner goal is then used to improve their own visual estimate of the target to enhance their tracking performance. So, Takagi et al. [6]'s goal integration model assumed that partners exchanged or extracted information from the interaction force, which is also referred to as *haptic communication*.

However, the tracking task in [3, 6] required following an unpredictably-moving target. In addition, both partners were still able to move independently due to the compliance of the haptic connection. Consequently, the interaction force changed magnitude and direction continuously for both partners. However, humans seem to have systematic errors in the perception of force magnitude [7–11] and direction [8, 9, 12], in particular when the forces are small. So, we ask whether accurate and unbiased interaction force perception and thus accurate haptic communication – such as estimating the goal of the partner – is possible in such a fast-moving tracking task.

Here we show, using both a model-based and an experimental approach, that haptic communication is not required to improve motor performance during haptic interaction in a tracking task, challenging Takagi et al. [6]'s goal estimation hypothesis. Instead, we hypothesize that the partners independently executed the tracking task and did not haptically communicate through the connection; they were only mechanically influenced by the interaction force of the connection. Specifically, we propose that the improvements are because the compliant connection primarily compensates for the motor output variability – the variability of the hand position during tracking, including errors due to focus lapses such as overshoots – of each partner. Furthermore, the mechanical connection provides haptic guidance for the worse-performing partner.

First, we used a computational model which assumed no haptic communication to occur to describe the improvements due to haptic interaction in a tracking task similar to the one used by Ganesh et al. [3]. This model consisted of two moving agents who tracked the target alone and were only influenced by the interaction force of the compliant connection. We did not model any exchange of information to occur through the interaction force.

Second, we impaired the perception of the interaction force by superimposing a velocity-dependent force field on the tracking task and interaction force. To haptically communicate through the interaction force, partners now had to discriminate the interaction force from the force-field force. If the accurate perception of the interaction force to exchange information is indeed essential to yield improvements, we would expect no or less improvement due to interaction while moving in the force field compared to when no force field was present.

The results and model showed that no exchange of information through the interaction force has to occur to explain the improvement during haptic interaction. Even when we superimposed a force field onto the task, impairing the perception of the interaction force, interaction still led to the same performance benefits as when no force field was present. Our study showed that the improvement benefits of haptic interaction in a fast-moving tracking task can primarily be explained by the motor variability-reducing nature of the compliant connection, challenging the hypothesis that partners haptically communicate by estimating each other's goals through the interaction force to improve performance.

6.2. Methods

The data used in this chapter are from the study presented in Chapter 3, which included a solo and interaction group. Because we are interested in how two humans haptically interact, we only used the data from the interaction group. The materials and methods are similar except for the analysis and interaction model.

Twenty participants (aged 19–35 years, 12 males and 8 females; all except one were right-handed according to the Edinburgh handedness inventory [13]) participated in the experiment. All participants were naïve to the force field motor task and interaction task. The study was designed following the principles of the Declaration of Helsinki. An expedited assessment of the study by the Medical Ethical Review Board of the University of Twente (METC Twente) showed that the study posed minimal risk to the participants and therefore under Dutch law did not need full ethical review. All participants provided written informed consent. The experiment lasted approximately two hours; all participants received compensation for their participation.

6.2.1. Robotic setup

The experiments were performed using a dual-robotic setup, see Fig. 6.1. Participants held and moved their own planar robotic manipulandum. The manipulanda were admittance-controlled, such that the manipulandum dynamics (simulating a mass of $m_r = 0.3\,\mathrm{kg}$ and a damping of $b_r = 0.25\,\mathrm{N\,s\,m^{-1}}$) were uniform in the x- and y-directions over the workspace. Each partner had their own display that showed the workspace, target and their own cursor

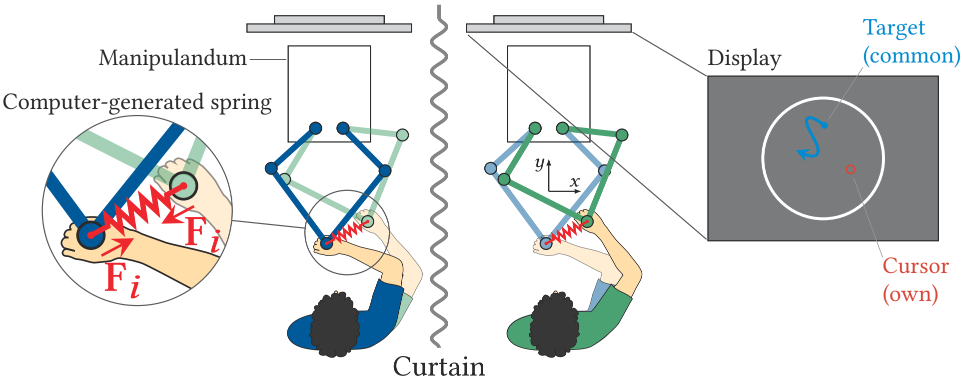

Figure 6.1. | Dual robotic setup. Each participant held their own manipulandum and tracked the same target. The displays showed the common target and each participant's own cursor. We indicated the local coordinate frame for one manipulandum. The partners were haptically coupled through a compliant computer-generated spring in the connected trials.

(see Fig. 6.1). Participants controlled the cursor by moving the handle of their manipulandum. Cursor and target movement were scaled to match the real-world movement of the manipulandum. A curtain obstructed the view of the other partner and the partner's display. A panel obstructed a direct view of the participant's own arm and hand. Participants were not allowed to communicate verbally.

6.2.2. Task and interaction paradigm

Tracking task

All participants performed the same planar tracking task. The goal was to track a target as accurately as possible on a display. The participants tracked the same unpredictably-moving target in trials of 23 s long followed by a 20 s break. The target movement $\mathbf{T} = \left[T^{(x)}\ T^{(y)}\right]^T$ (in cm) was defined as two sum-of-sines:

$$\begin{aligned} T^{(x)}(t) &= 2.87 \sin(0.94t - 7.77) + 2.71 \sin(1.26t - 8.53) \\ &\qquad + 2.35 \sin(1.89t - 4.36) + 1.80 \sin(2.83t - 3.79) \\ T^{(y)}(t) &= 2.71 \sin(1.26t - 0.71) + 2.53 \sin(1.57t - 3.45) \\ &\qquad + 2.16 \sin(2.20t + 3.92) + 1.64 \sin(3.14t + 4.93)\,. \end{aligned} \tag{6.1}$$

The tracking signal required hand movements over a circular workspace with a diameter of 20 cm, an average velocity of 7.9 $\mathrm{cm\,s^{-1}}$ and a maximum velocity of 13.9 cm s^{-1}. To prevent fast learning or other cognitive tracking strategies, we chose a uniformally random start time for the signals ($t \in [t_0, t_0 + 20]$ s, $t_0 \sim \mathcal{U}(0, 20)$) and we rotated the tracking signal randomly from six predefined rotations: $\left(\varphi = \left[0, \frac{1}{3}\pi, \frac{2}{3}\pi, \pi, \frac{4}{3}\pi, \frac{5}{3}\pi\right]\text{rad}\right)$.

Connected and single trials

Two types of trials were used in the experiment: *connected* (C) and *single* (S) trials. The participants tracked the target alone in a single trial (they were not connected). In a connected trial, the partners haptically interacted through a computed-generated compliant connection that connected the handles of the two partners (see the detail in Fig. 6.1), which generated an interaction force

$$\mathbf{F}_i = k_s\left(\mathbf{p}_p - \mathbf{p}_o\right) + b_s\left(\mathbf{v}_p - \mathbf{v}_o\right), \tag{6.2}$$

where k_s is the connection stiffness, b_s a damping contribution, and $\mathbf{p}_p$, $\mathbf{v}_p$, $\mathbf{p}_o$, and $\mathbf{v}_o$ are the partner's and the participant's own position and velocity, respectively. We set the stiffness and damping to $k_s = 150\,\text{N}\,\text{m}^{-1}$ and $b_s = 2\,\text{N}\,\text{s}\,\text{m}^{-1}$, respectively. The stiffness was similar to previous work [3] and a small damping was added for spring stability, but small enough to only minimally interfere with the velocity dependent force field. The force was exerted onto both partners' hands by the manipulanda. If a partner moved away from the other partner, they both experienced a force pulling them toward each other. The compliant connection allowed the partners to haptically interact while being able to execute the tracking task independently. Active task execution was required; participants could not completely relax and let the force pull their hand along.

6.2.3. Experiment design

The twenty participants performed the experiment in ten pairs. Each pair performed four blocks of 21 trials with a four-minute break between blocks for a total of 84 trials. Participants tracked the target without a force field in the first and last blocks, which we also refer to as *null field blocks*. We introduced a counterclockwise velocity-dependent curl force field in blocks 2 and 3, which generated a planar force $\mathbf{F}_c$ given by

$$\mathbf{F}_c = \mathbf{D}\mathbf{v} \equiv \begin{bmatrix} F_c^{(x)} \\ F_c^{(y)} \end{bmatrix} = \begin{bmatrix} 0 & -15 \\ 15 & 0 \end{bmatrix} \begin{bmatrix} v^{(x)} \\ v^{(y)} \end{bmatrix} \tag{6.3}$$

on the hand of each participant, where $\mathbf{v}$ is the participant's own hand velocity. The force field generated a force that was perpendicular to the movement

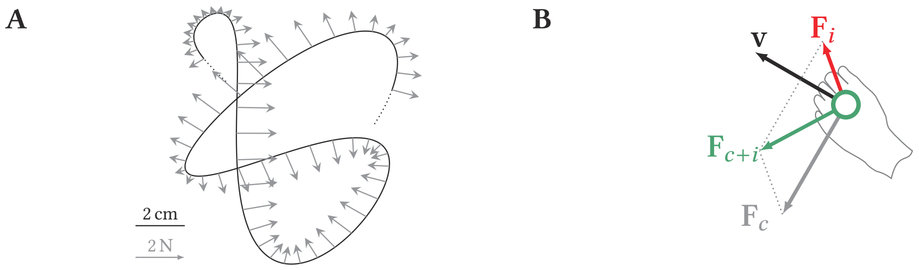

Figure 6.2. | Force field example and forces on the handle. **A** The force field introduces forces $\mathbf{F}_c$ perpendicular to the movement. The forces shown in this figure are based on perfect tracking of the target. **B** The participant feels a total force $\mathbf{F}_{c+i}$, which is the sum of the force field force $\mathbf{F}_c$ (in the force field blocks, proportional to velocity $\mathbf{v}$) and interaction $\mathbf{F}_i$.

(Fig. 6.2A). During the connected trials, the force field was superimposed on the interaction force; the participants would feel a force $\mathbf{F}_{c+i}$ that is the sum of the force field $\mathbf{F}_c$ and the interaction force $\mathbf{F}_i$ (see Fig. 6.2B). The participants were informed that a force field would disturb their movements and they were instructed to track the target as accurately as possible at all times. We asked them not to stop tracking to learn the force field. We refer to blocks 2 and 3 as the *force field blocks*.

The participants performed an alternating sequence of single and connected trials in each block ({S CS CS CS CS CS CS CS CS CS CS}). Hence, the partners intermittently interacted with each other while performing the tracking task in all blocks.

6.2.4. Analysis

Data, including handle position $\mathbf{p}$ and velocity $\mathbf{v}$, interaction force $\mathbf{F}_i$ and total force $\mathbf{F}_t$ exerted by each participant onto the handle, were sampled at 1 kHz. We used MATLAB R2018B to parse the data and perform additional analyses.

Motor performance is computed as the root mean square of the tracking error E (the distance between the target and cursor in cm) of the last 20 s of each trial – the lower the tracking error E, the better the motor performance. We calculated the motor performance for each partner in each trial. The performance during a single trial and connected trial are denoted by E_s and E_c, respectively. The tracking performances in the connected trials were not necessarily the same for both partners because they could still move independently because of the compliant connection.

We analyzed the time-averaged motor output variability – the variability of the hand position across trials – of each participant in the 'no force field' blocks (baseline and aftereffects). We used the last eight single trials of both null field blocks (so 16 single trials in total per participant) in which tracking performance was constant to avoid learning effects. The variance $\Sigma_{\mathbf{p}}$ of the hand position $\mathbf{p}$ is:

$$\Sigma_{\mathbf{p}} = E\left[(\mathbf{p} - E[\mathbf{p}])^2\right] \tag{6.4}$$

$$= \begin{bmatrix} \sigma_x^2 & \rho\sigma_x\sigma_y \\ \rho\sigma_x\sigma_y & \sigma_y^2 \end{bmatrix}. \tag{6.5}$$

We assumed that the participants tracked the target in the x- and y-directions independently. Consequently, the variances in x- and y-directions were assumed to be uncorrelated ($\rho = 0$). We used σ_x^2 as a scalar representative of the total motor output variability. We calculated the time-averaged variance of the hand position as follows:

$$\bar{\sigma}_x^2 = \frac{1}{N}\sum_{k=1}^{N} \sigma_{x,k}^2, \tag{6.6}$$

where $\sigma_{x,k}^2$ is the variance of the x-direction at time step k across the sixteen single trials and N is the number of time steps in each trial.

Motor improvement due to interaction

Ganesh et al. [3] found that the amount of performance improvement due to haptic interaction depended on the relative performance of the partner. Following [3, 6], we calculated the improvement due to interaction I and the relative partner performance R. The interaction group performed sets of connected and single trials (*CS*) in each block. The performance improvement due to interaction (I) is calculated per participant using the performance of the connected and single trial in each set (E_c and E_s, respectively):

$$I = 1 - E_c/E_s. \tag{6.7}$$

The relative performance of your partner (R) is calculated by

$$R = 1 - E_{s,p}/E_s, \tag{6.8}$$

where $E_{s,p}$ is the partner's performance during the single trial and E_s is your own performance during the same single trial.

Force analysis

We logged the total force $\mathbf{F}_t$ exerted by the participant on the handle measured by a force transducer as well as the true interaction force $\mathbf{F}_i$.

We analyzed how the force-field force impaired the perception of the interaction force. To estimate the interaction force $\hat{\mathbf{F}}_i$, participants primarily had to differentiate between the actual interaction force $\mathbf{F}_i$ and the force-field force $\mathbf{F}_c$. People can learn an internal model of the force field with extended practice [14–16], which could be used to estimate the current force-field force based on the current hand velocity (equation 6.3). However, studies found that humans only learn to compensate for a fraction α of the imposed field ($\alpha \approx 0.8$) [15–17]. If the participants indeed used an incomplete internal model of the force field to estimate the interaction force, they would underestimate the force-field force. The remaining, uncompensated, force-field force $\mathbf{F}_{c,u} = (1-\alpha)\,\mathbf{Dv}$ would bias the perceived interaction force:

$$\hat{\mathbf{F}}_i = \mathbf{F}_i + (1-\alpha)\,\mathbf{Dv}, \tag{6.9}$$

where $\mathbf{F}_i$ is the actual interaction force, α is the fraction of the force field that is learned (also referred to as the compensation factor), $\mathbf{D}$ is the force field, and $\mathbf{v}$ is the hand velocity.

We computed a compensation factor α as the amount of the force field that was compensated for in each single trial for every participant (i.e., when $\mathbf{F}_i = 0\,\mathrm{N}$). Following the approach of previous work [15, 16, 18], we regressed the *actual* compensation forces $\mathbf{F}_{c,a}$ generated by the participants to compensate for the force field on the *ideal* forces $\mathbf{F}_{c,i}$ that would fully compensate for the force field. The actual compensation force is preferably measured in error-clamp trials, in which the movements perpendicular to the desired movement are restricted such that the measured forces only described the (feedforward) force field compensation [15]. However, error-clamp trials are mainly used in reaching tasks that involved discrete and fast reaching movements in which the force field is compensated for in a feedforward manner [15, 18]. In contrast, we used a continuous tracking task that required feedback control such that error-clamp trials are not as useful. Instead, to compensate for the forces resulting from moving the manipulandum, we calculated the the actual forces $\mathbf{F}_{c,a}$ during a single trial ($\mathbf{F}_i = 0\,\mathrm{N}$) per participant as follows:

$$\mathbf{F}_{c,a} = \mathbf{F}_t - (m_r\ddot{\mathbf{x}}_r + b_r\dot{\mathbf{x}}_r)\,, \tag{6.10}$$

where $\mathbf{F}_t$ is the measured total force, m_r and b_r are the mass and damping of the manipulandum's dynamics, and $\ddot{\mathbf{x}}_r$ and $\dot{\mathbf{x}}_r$ are the manipulandum's endpoint acceleration and velocity.

To calculate the ideal compensation forces $\mathbf{F}_{c,i}$, we assumed that participants would return to their tracking trajectories in the null field blocks after extensive practice in the force field, based on previous work [19]. The ideal force profile was calculated using each participant's hand velocity of the average tracking trajectory of the last eight single trials of both the baseline and aftereffects blocks using equation 6.3. We then computed the compensation factor α as:

$$\alpha = \frac{1}{N} \sum_{k=1}^{N} \frac{||\mathbf{F}_{c,a}||}{||\mathbf{F}_{c,i}||}, \tag{6.11}$$

where k is the time step and N is the number of time steps in a trial. The resulting α reflects how much each participant compensated for the force field in a single trial. We assume that the compensation factor during connected trials was the same as in the single trials.

The compensation factor reflects a combination of multiple possible mechanisms that people could use to compensate for the force field. These complementary mechanisms include increasing arm impedance [16, 20, 21], learning an internal model of the force field that could be used in feedforward control (e.g., predictive force compensation based on the current hand velocity) [14, 16, 22, 23] and feedback control (e.g., reacting to tracking errors) [24].

Statistical analysis

Statistical analysis was done using the R statistical software package (version 3.5.2).

We compared the improvement due to interaction versus relative performance curves between the force field and null field blocks using the linear model

$$I = \beta_0 + \beta_1 R + \beta_2 F + \beta_3 (RF) + \epsilon, \tag{6.12}$$

where R is the relative performance (continuous predictor), F a factor indicating force field or no force field. The coefficients $\beta_{0,\ldots,3}$ are the intercept, coefficients for R, F and the interaction term (RF), respectively and ϵ is the unexplained variance of the data. We used the same model to compare the interaction model predictions with the data.

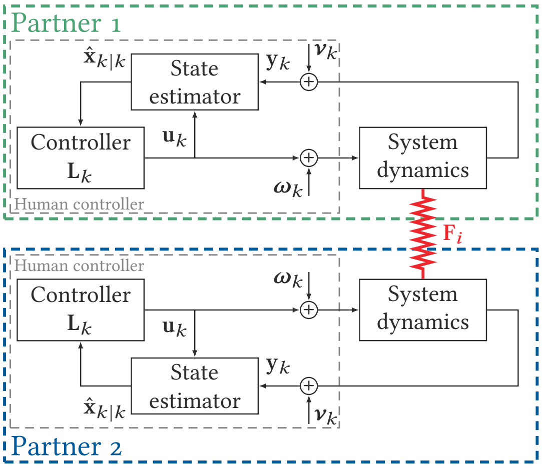

Figure 6.3. | Model of two partners tracking a target independent while under the influence of the interaction force $\mathbf{F}_i$. Each partner was modeled as a controller which generates a control input $\mathbf{u}_k$ to the system dynamics. A state estimate $\hat{\mathbf{x}}_{k|k}$ is obtained with a state estimator using an internal model of the system dynamics, a copy of the control input $\mathbf{u}_k$ and sensory observation $\mathbf{y}_k$. Partners were only connected through a compliant connection that exerted an interaction force $\mathbf{F}_i$ onto each partner; no other exchange of information was modeled.

All data and statistical model fit residuals were checked for normality using the Shapiro-Wilk normality test and visual inspection (QQ plots). The level of significance for all tests was set to 0.05. Unless explicitly stated, all data are reported as the mean ± standard error of the mean (s.e.m.).

6.2.5. Tracking model

We developed a model based on a Linear-Quadratic Gaussian controller (LQG) to describe each participant's tracking behavior in the single trials (e.g., their individual tracking behavior) in the null field blocks [25]. The tracking models of the partners in a pair are then coupled with a compliant connection (see Fig. 6.3), which will be described later.

System dynamics

We modeled the dynamics of each partner as a point mass in Cartesian coordinates. The combined action of all muscles is represented with a force $\mathbf{f}$ acting on the point mass. The muscle control signal $\mathbf{u}$ is transformed into force $\mathbf{f}$ by the muscle activation dynamics, which are modeled by a second-order low-pass filter [25]. The system dynamics were discretized with time step $\delta = 0.01\,\mathrm{s}$. The discrete-time state vector is given by

$$\mathbf{x}_k = \left[p_k^{(x)}\; p_k^{(y)}\; v_k^{(x)}\; v_k^{(y)}\; f_k^{(x)}\; f_k^{(y)}\; g_k^{(x)}\; g_k^{(y)}\; T_k^{(x)}\; T_k^{(y)}\; \dot{T}_k^{(x)}\; \dot{T}_k^{(y)}\right]^T, \tag{6.13}$$

where p is the hand position, v the hand velocity, f is a muscle-like force, g is an auxiliary variable to implement the activation dynamics' second-order low-pass filter and T and $\dot{T}$ are the target position and velocity, all at time step k in the x- and y-directions. The discrete-time system dynamics are

$$\mathbf{x}_{k+1} = \mathbf{A}\mathbf{x}_k + \mathbf{B}\mathbf{u}_k + \boldsymbol{\omega}_k, \tag{6.14}$$

where:

$$\mathbf{A} = \left[\begin{array}{cccccccc|c}
1\;0\;\delta\;0 & & & 0 & 0 & 0 & 0 & & \\
0\;1\;0\;\delta & & & 0 & 0 & 0 & 0 & & \\
0\;0\;1\;0 & & & \delta/m & 0 & 0 & 0 & & \\
0\;0\;0\;1 & & & 0 & \delta/m & 0 & 0 & & \\
0\;0\;0\;0 & & & 1-\delta/\tau_u & 0 & \delta/\tau_u & 0 & & \mathbf{0}^{8\times 4} \\
0\;0\;0\;0 & & & 0 & 1-\delta/\tau_u & 0 & \delta/\tau_u & & \\
0\;0\;0\;0 & & & 0 & 0 & 1-\delta/\tau_u & 0 & & \\
0\;0\;0\;0 & & & 0 & 0 & 0 & 1-\delta/\tau_u & & \\
\hline
\multicolumn{8}{c|}{\mathbf{0}^{4\times 8}} & \mathbf{I}^{4\times 4}
\end{array}\right], \tag{6.15}$$

$$\mathbf{B} = \left[\begin{array}{cc}
\multicolumn{2}{c}{\mathbf{0}^{6\times 2}} \\
\delta/\tau_u & 0 \\
0 & \delta/\tau_u \\
\multicolumn{2}{c}{\mathbf{0}^{4\times 2}}
\end{array}\right] \text{ and} \tag{6.16}$$

$$\boldsymbol{\omega}_k \sim \mathcal{N}(\mathbf{0}, \Omega^{\omega}). \tag{6.17}$$

We set the mass m to $1\,\mathrm{kg}$ and the muscle-filter time constant to $\tau_u = 0.04\,\mathrm{s}$ [25]. The motor noise $\boldsymbol{\omega}_k$ on the control input was zero mean with covariance $\Omega^{\omega} = \mathrm{diag}\left(0, 0, 0, 0, 0, 0, \sigma_u^2, \sigma_u^2, 0, 0, 0, 0\right)$.

The sensory feedback contains information about the hand position, hand velocity, target position and target velocity:

$$\mathbf{y}_k = \mathbf{H}\mathbf{x}_k + \boldsymbol{\nu}_k, \tag{6.18}$$

where:

$$\mathbf{H} = \begin{bmatrix} \mathbf{I}^{4\times 4} & \mathbf{0}^{4\times 4} & \mathbf{0}^{4\times 4} \\ \mathbf{0}^{4\times 4} & \mathbf{0}^{4\times 4} & \mathbf{I}^{4\times 4} \end{bmatrix} \text{ and} \tag{6.19}$$

$$\boldsymbol{\nu}_k \sim \mathcal{N}(\mathbf{0}, \Omega^{\nu}). \tag{6.20}$$

Because we do not model any information exchange through the interaction force, it is not needed to observe the interaction force $\mathbf{F}_i$ on the hand. The sensory noise $\boldsymbol{\nu}_k$ was zero-mean with covariance
$\Omega^\nu = \text{diag}\left(\sigma_p^2, \sigma_p^2, \sigma_v^2, \sigma_v^2, \sigma_T^2, \sigma_T^2, \sigma_{\dot{T}}^2, \sigma_{\dot{T}}^2\right)$.

State estimation

We implemented a Kalman filter to optimally estimate the state and target despite the motor noise and noisy sensory measurements. The Kalman filter updates the posterior state estimate $\hat{\mathbf{x}}_{k|k}$ by combining the prior state prediction $\hat{\mathbf{x}}_{k|k-1}$ with the noisy observation $\mathbf{y}_k$:

$$\hat{\mathbf{x}}_{k|k} = \hat{\mathbf{x}}_{k|k-1} + \mathbf{K}_k\left(\mathbf{y}_k - \mathbf{H}\hat{\mathbf{x}}_{k|k-1}\right), \tag{6.21}$$

where $\mathbf{K}_k$ are the Kalman gains. The prior state prediction $\hat{\mathbf{x}}_{k|k-1}$ is computed using the human's estimate of the system dynamics, $\hat{\mathbf{A}}$ and $\hat{\mathbf{B}}$, also referred to as the internal model, and a known copy of the motor command $\mathbf{u}_{k-1}$:

$$\hat{\mathbf{x}}_{k|k-1} = \hat{\mathbf{A}}\hat{\mathbf{x}}_{k-1|k-1} + \hat{\mathbf{B}}\mathbf{u}_{k-1}. \tag{6.22}$$

Because the target observation contains sensory noise, the participants determined the target position and velocity based on the noisy target motion in $\mathbf{y}_k$. To ensure that the participants estimated the target motion in the posterior state estimate $\hat{\mathbf{x}}_{k|k}$, we added a target position and velocity update noise (i.e. a random walk model of the target position and velocity) in the process noise when iterating the Kalman filter, following the approach of Izawa et al. [17]. These update noises, which were zero-mean with variance $\sigma_{T,u}^2$ and $\sigma_{\dot{T},u}^2$, respectively, represented the uncertainty of the human's target motion estimate due to the random-appearing motion of the target.

Feedback controller

The motor command $\mathbf{u}_k$ moved the hand to the target based on the current posterior state estimate:

$$\mathbf{u}_k = -\mathbf{L}_k\hat{\mathbf{x}}_{k|k}. \tag{6.23}$$

We derived the optimal feedback gains $\mathbf{L}_k$ such that the participant tracked the target with certain accuracy requirements. Because we assumed that tracking behavior was constant during a trials, we computed the infinite-horizon optimal gains (i.e., constant feedback control gains). The resulting feedback gains $\mathbf{L}_k$ minimize the cost function

$$\begin{aligned} J = \sum_{k=1}^{N} \Bigg(& w_p \left[\left(p_k^{(x)} - T_k^{(x)}\right)^2 + \left(p_k^{(y)} - T_k^{(y)}\right)^2 \right] + \\ & w_v \left[\left(v_k^{(x)} - \dot{T}_k^{(x)}\right)^2 + \left(v_k^{(y)} - \dot{T}_k^{(y)}\right)^2 \right] + \\ & w_r \left[\left(u_k^{(x)}\right)^2 + \left(u_k^{(y)}\right)^2 \right] \Bigg), \end{aligned} \tag{6.24}$$

where w_p and w_v are the weighting factors on the difference between the hand position and target position and hand velocity and target velocity, respectively. This cost function describes the task requirements: participants had to track the target with their hand as accurately as possible. Because each participant based their control on their *estimate* of the real system dynamics, we computed the optimal control gains using the internal model system matrices $(\hat{\mathbf{A}}, \hat{\mathbf{B}})$. Because we did not make the participants aware of the coupling, we did not include the interaction in the internal model system matrices.

6.2.6. Interaction model

The two partners were only coupled through a compliant connection (see Fig. 6.3); no other exchange of information through the interaction force was included in our model. We refer to this model as the 'no haptic communication' model. The physical connection between the two partners during the connected trials is implemented by introducing the compliant spring of equation 6.2 in the system dynamics (equation 6.14). We combined the state space models of both partners (denoted as partner 1 and 2) in one system:

$$\begin{bmatrix} \mathbf{x}^1 \\ \mathbf{x}^2 \end{bmatrix}_{k+1} = \left(\begin{bmatrix} \mathbf{A} & \mathbf{0} \\ \mathbf{0} & \mathbf{A} \end{bmatrix} + \mathbf{C} \right) \begin{bmatrix} \mathbf{x}^1 \\ \mathbf{x}^2 \end{bmatrix}_{k} + \begin{bmatrix} \mathbf{B} & \mathbf{0} \\ \mathbf{0} & \mathbf{B} \end{bmatrix} \begin{bmatrix} \mathbf{u}^1 \\ \mathbf{u}^2 \end{bmatrix}_{k} + \begin{bmatrix} \boldsymbol{\omega}^1 \\ \boldsymbol{\omega}^2 \end{bmatrix}_{k}, \tag{6.25}$$

where $\mathbf{C}$ is the connection matrix in which the spring is implemented (see Section D.1 for the implementation). The same connection stiffness and damping from in the experiment were used ($k_s = 150\,\mathrm{N\,m^{-1}}$ and $b_s = 2\,\mathrm{N\,m^{-1}}$). To reiterate, because we assumed that the participants were unaware of the connection, we did not include the connection dynamics in their internal model, only in the actual system dynamics.

6.2.7. Parameter estimation and simulation

To describe the tracking behavior of each participant in the single trials, we estimated the position weight w_p, velocity weight w_v and motor noise uncertainty σ_u for each participant. The control effort weight w_r was set to 1. Based on previous research [17, 25–27], we set σ_P to 0.005 m and σ_V to 0.01 m s^{-1}. The target position and velocity observation uncertainties were set to the same values: $\sigma_T = 0.005$ m and $\sigma_{\dot{T}} = 0.01$ m s^{-1} and $\sigma_{T,u}$ was set to 0.005 m and $\sigma_{\dot{T},u}$ to 0.01 m s^{-1}.

We fitted the LQG model to the last eight single trials of both the baseline and after effect blocks, resulting in 16 single trials per participant. The fit parameters were estimated such that the model resulted in similar tracking performance as the participant by matching their individual tracking performance over the 16 measured single trials. We used a genetic algorithm followed by a gradient-based search algorithm (the `ga` and `patternsearch` functions in MATLAB). The lower and upper bound were set for the baseline fit to 10^1 to 10^6 for w_p and w_v and 0 N to 1 N for σ_u.

We then used these parameter estimates to simulate the tracking behavior of each participant alone and while they were connected to the same partner as in the experiment. The resulting simulated tracking performance is then compared to the data.

6.3. Results

We performed a collaborative tracking task similar to Ganesh et al. [3], who observed that haptic interaction improved tracking performance for both partners in a pair. Participants tracked a common randomly-moving target alone in single trials and while haptically-interacting through a compliant connection in connected trials. We compared the tracking performance in the single and connected trials and confirmed that haptic interaction generally improved performance for both partners.

Why does haptic interaction with another human improve tracking performance, even when interacting with a relatively worse-performing partner? Do the participants need to estimate their partner's actions or movement goals from the interaction force to improve their own tracking performance [6]? Or can the improvement be attributed to the compliant coupling between the two partners? We first impaired the perception of the interaction force by superimposing a velocity-dependent force field on the tracking task to test whether accurate perception of the interaction was necessary to improve performance during haptic interaction. If accurate perception of the interaction force was necessary to improve performance, we would expect significantly less to no performance improvements due to haptic interaction in the force field. In the second analysis, we used a computational model that only mechanically coupled the two partners to explain the performance improvements.

6.3.1. Haptic interaction improves individual tracking performance, also when the partners interact in a force field

Figure 6.4A compares the average individual performances in the single and connected trials in the null field and force field blocks. Haptic interaction leads to small but significant performance improvements, both within the null field and in the force field blocks (dependent-samples t-tests; null field (♦): $t(19) = 8.65$, $p < 10^{-7}$; force field (▾): $t(19) = 7.11$, $p < 10^{-6}$). The improvement in the null field blocks was similar to the improvement in the force field blocks (dependent samples t-test: $t(19) = -0.44$, $p = 0.669$). Each participant's improvement depended significantly on the relative performance of the partner (see Fig. 6.4B; ANOVA on the relative partner performance factor R in the linear model of equation 6.12: $F(1, 356) = 270.52$, $p < 10^{-12}$). Interestingly, interaction with an inferior partner ($R < 0\,\%$) increased performance, but improvement benefits decreased with a progressively worse partner and seemed to converge to no improvement ($I \approx 0\,\%$) when interacting with even more worse-performing partners.

We investigated whether the force field affected the haptic interaction and subsequently its performance benefits. Besides comparing the improvements in all connected trials in the null field and force field blocks, we also included the improvements in the first three connected trials in the first force field block, in which the participants presumably only started to learn the force field perturbation (denoted as 'early force field'). Remarkably, we found similar improvements of haptic interaction in the force field, early force field, and null field (ANOVA on equation 6.12 with force field, null field, and early force field as factor levels; $F(2, 784) = 1.95$, $p = 0.144$).

If the estimation of the partner's goal from the interaction force was essential to improve performance, we would expect no or at least reduced improvement in the force field blocks. Were the participants able to accurately discriminate the interaction force from the force-field forces? To discriminate the interaction force from the force-field force (Fig. 6.2B), it is possible that participants learned and used an internal model to predict the forces generated by the force field. In the ideal case, all participants had a

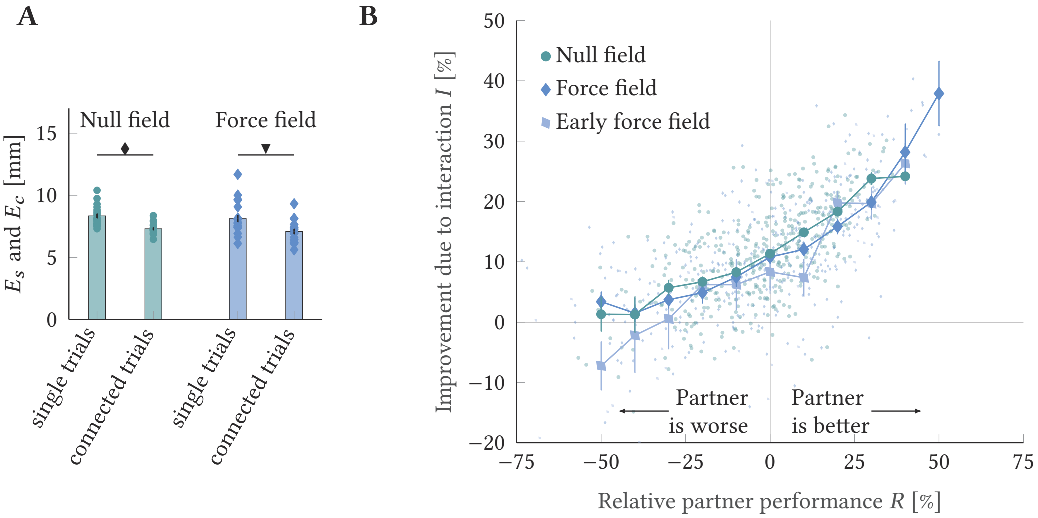

Figure 6.4. | Haptic interaction improves tracking performance. **A** Average improvement due to interaction in the null field and force field blocks. **B** Performance improvement due to interaction is a function of the relative partner performance. Haptic interaction improved motor performance equally in the force field, early force field, and when no force field was present. We grouped the improvement in bins of 10 % of relative performance wide. The mean and s.e.m. of the improvement per bin are shown.

perfect internal model of the force field. However, our compensation factor showed that participants did not fully compensate for the force field, ranging from $\alpha = 0.72$ in the first single trial up to an average $\alpha = 0.86$ with extensive practice in the force field (see Fig. 6.5A), consistent with previous work [15–18]. Because the participants learned an incomplete model of the force field, an uncompensated force-field force $\mathbf{F}_{c,u} = (1 - \alpha)\mathbf{D}\mathbf{v}$ remained that the participants did not account for. The uncompensated force-field force could bias the actual interaction force $\mathbf{F}_i$ in direction and magnitude, resulting in an incorrect perceived interaction force $\hat{\mathbf{F}}_i$ (see Fig. 6.5B for two examples).

To illustrate how the force field could bias the interaction force perception in magnitude, we calculated the time-averaged total force-field force magnitude $\bar{\mathbf{F}}_c$ (using equation 6.3), the time-averaged uncompensated force-field force magnitude $\bar{\mathbf{F}}_{c,u}$ (using $\alpha = 0.86$), and the time-averaged actual interaction force magnitude $\bar{\mathbf{F}}_i$ across all connected trials and all participants (Fig. 6.5C). The force field produced an average force of $\bar{\mathbf{F}}_c = 1.31\,\mathrm{N}$ per trial; the average interaction force was smaller: $\bar{\mathbf{F}}_i = 0.43\,\mathrm{N}$. If the participants learned a fraction of 0.86 of the force field, the average uncompensated force-field force was 0.18 N. This uncompensated force could still lead to an overestimation of the interaction force magnitude of 40 % when the two

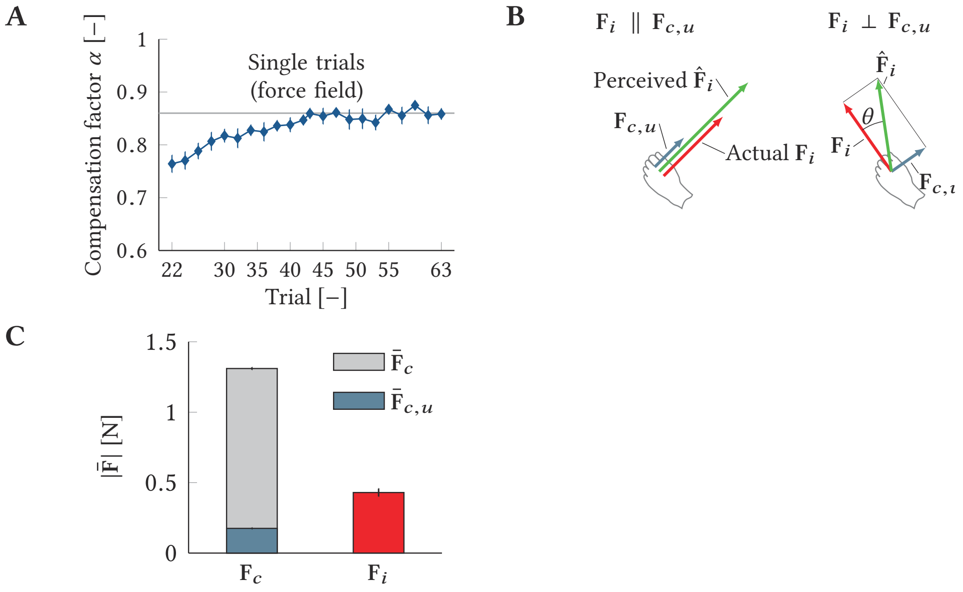

Figure 6.5. | Force field compensation factor and potential bias of the interaction force perception due to the uncompensated force-field force. **A** Force field compensation factor α of the single trials across the force field blocks (from Chapter 3). **B** Two examples illustrating how the uncompensated force-field force $\mathbf{F}_{c,u}$ can bias the perceived interaction force $\hat{\mathbf{F}}_i$ in magnitude and direction. **C** Comparison of the time-averaged total force-field force magnitude $\bar{\mathbf{F}}_c$, time-averaged uncompensated force-field force magnitude $\bar{\mathbf{F}}_{c,u}$ and time-averaged interaction force magnitude $\bar{\mathbf{F}}_i$.

forces are parallel, or a direction bias $\theta \approx 22\,\text{deg}$ when the two forces are perpendicular (e.g., Fig. 6.5B). We performed a more detailed analysis of how the uncompensated force field force could the bias the interaction force perception in magnitude and direction in Section D.4. These results indicate that accurate perception of the interaction force was impaired by the force field, even when the participants learned a significant yet incomplete internal model of the force field. Still, even though accurate perception of the interaction force was difficult and unlikely, haptic interaction improved performance similarly in the force field.

6.3.2. An interaction model without haptic communication explains the interaction improvements

Using an interaction model that only connected the hands of two partners who independently tracked the same target, we showed that no haptic communication between the two partners was necessary to explain the improvements. Instead, we propose that the error-correcting nature of the compliant connection is the primary reason for the observed performance improvements during haptic interaction. We first modeled each participant's *individual* tracking behavior in the single trials in the null field blocks using the tracking model described in Section 6.2.5. This resulted in estimates of the position and velocity cost weights w_p and w_v and the motor noise variance σ_u^2 for each participant (see Table D.1). We then coupled the two single tracking models to simulate how the mechanical coupling affects tracking performance.

The tracking model described each participant's individual tracking behavior well, which we assessed by comparing the measured and simulated time traces, power spectral densities, single motor performance and motor output variability per participant. Figures 6.6A-C show the measured and simulated time traces in the x-direction, power spectral density in the x-direction and the tracking performance of the last eight single trials in both null field

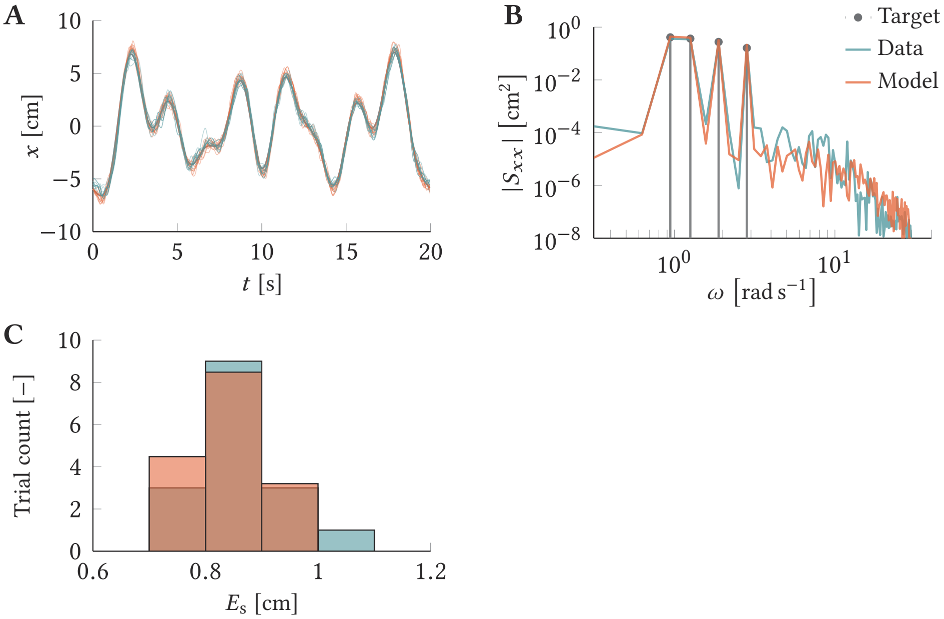

Figure 6.6. | The tracking model described individual tracking behavior during single trials in the null field blocks well. Shown are the measured tracking behavior of the last eight single trials in both null field blocks (e.g. 16 trials in total) for one representative participant in the x-direction. We simulated the tracking model for one participant with 16 different motor noise time realizations. The legend in **B** holds for all figures. **A** Comparison of the measured and modeled hand path (x-direction). **B** Power spectral density of the measured and simulated data. **C** The distribution of measured single trial performance E_s of the 16 single trials compared to the tracking model's predicted single performance for one participant.

blocks (i.e., 16 trials in total) for one representative participant. The tracking model predicted similar mean tracking behavior in the time and frequency domain for each participant; the variance-accounted-for (VAF), a measure to describe the correlation of two time-domain signals, was 97.7 % on average across all participants. The tracking model also predicted similar individual tracking performance (E_s) per participant (Fig. 6.6C). Lastly, individuals with worse mean individual tracking performance showed higher motor output variability σ_x^2 in the single trials (Fig. 6.7A). The tracking model predicted a similar increase in motor variability with increasing mean tracking error (ANCOVA with mean performance as covariate and data/model as factor showed no significant difference: $F(1, 36) = 0.04$, $p = 0.85$).

The interaction model was created by mechanically coupling the two single tracking models of the partners who also performed the experiment together (equation 6.25). By using each participant's estimated model parameters fitted to the single trial behavior, we assumed that the participants did not change their tracking behavior when coupled to their partner.

The interaction model showed similar improvements in tracking performance per participant as the data (Fig 6.8). Using the linear model in equation 6.12, we found no significant difference between the data and model ($F(1, 796) = 1.73$, $p = 0.19$). The interaction model also captured two salient features in the data: (1) interaction with a worse partner still improved performance, but (2) the improvement benefit decreased with interaction with

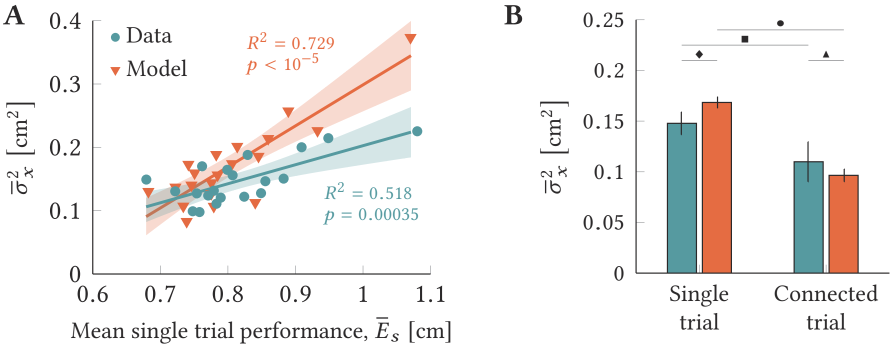

Figure 6.7. | Motor output variability analysis in the null field blocks. The legend in **A** also holds for **B**. **A** Measured and simulated motor output variability versus the mean performance of each participant in the single trials. Shown are regressed linear models ($\bar{\sigma}_x^2 = \beta_0 + \beta_1 \bar{E}_s$) to the measured data and tracking model, including the 95 % confidence intervals. **B** Comparison of the mean measured and mean simulated motor output variability in the single and connected trials for all participants combined. All statistics were done using paired-sampled t-tests. ♦: $t(19) = -1.78, p = 0.089$, ▲: $t(19) = -2.68, p = 0.023$, ■: $t(19) = 6.05, p = 8.1 \cdot 10^{-6}$, ●: $t(19) = 6.21, p = 5.8 \cdot 10^{-6}$.

a progressively worse partner. However, the interaction model predicted that haptic interaction with a worse partner would lead to a deterioration of performance for the better partner at some point ($R \approx -40\,\%$), whereas the data showed that haptic interaction still led to some improvement at a similar relative partner performance.

The data show that haptic interaction reduced motor output variability significantly on a group level (see Fig. 6.7B). The interaction model showed a similar trend, but predicted a larger reduction in motor output variability (dependent-samples t-test between data and model in the connected trials: $t(19) = -2.68$, $p = 0.023$). The similar reduction in motor output variability during interaction indicates that the compliant connection partially counteracted motor output variability, improving performance

Based on the data and model analysis, we hypothesize that haptic interaction improves performance depending on the relative performance of the participants. We split the data into the superior ($R < 0$) and inferior ($R > 0$) participants. First, we propose that superior partners still improved performance when interacting with a inferior partner because the compliant connection partially counteracted for their average motor output variability in the connected trials. To test this hypothesis, we removed each participant's motor output variability from the interaction model. Because the model's motor output variability is mainly determined by σ_u^2 (see Fig. D.1), we esti-

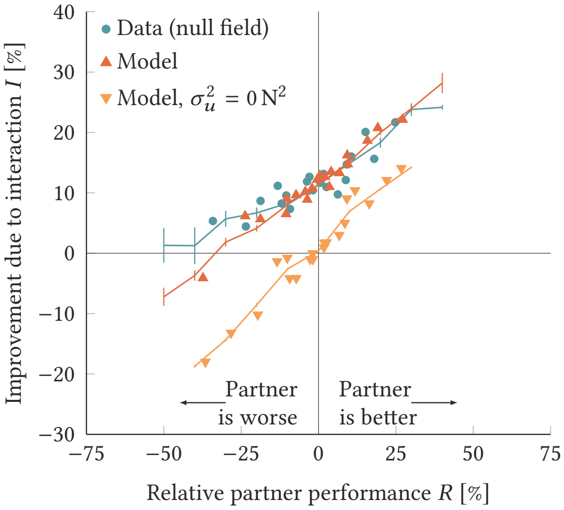

Figure 6.8. | Comparison of the measured performance improvement versus relative performance with the improvement predicted by the interaction model in the null field blocks. The markers indicate the mean relative performance and mean improvement of each participant (data and model). We also show the binned improvement curves.

mated w_p and w_v for each participant once more while constraining σ_u^2 to $0\,\mathrm{N}^2$. As a result, the model now described the average measured tracking behavior of each partner without trial-by-trial motor variability due to the motor noise. Removing the motor output variability from the single tracking models reduces the improvement benefits for all participants (Fig. 6.8) and predicts that interaction with a worse partner now deteriorates performance. In addition, when we simulated the interaction model with identical motor noise for both partners in a pair, performance improvements decreased similarly (see Section D.3 for more details). Hence, our results suggest that the reduction of motor variability by the compliant connection can explain the motor improvements when haptically-interacting with a worse-performing partner.

Second, we propose that the worse-performing partners improved performance using in two complementary mechanisms. First, haptic interaction improved their performance by partially counteracting their motor output variability, same as the mechanism we described earlier. In addition, the interaction model without motor noise showed that the worse partners still benefited from the interaction with a better partner (Fig. 6.8). Inspection of the estimated tracking feedback gains in the single trials of the two partners in a pair showed that the superior partners tracked the target with higher gains than the inferior partners (see Section D.1 and Table D.1). When connecting both partners, the better partner with stronger tracking gains likely provided haptic assistance to the worse partner. The resulting interaction force assisted the worse partner to move closer to the target, improving their performance.

6.4. Discussion

This study investigated why haptic interaction between humans through a compliant connection improved the performance of both partners in a tracking task. Data showed that both partners generally improved tracking performance during interaction. Surprisingly, haptic interaction with a worse partner also improved performance. We found through computational modeling that the participants improved performance because the compliant connection partially compensated for motor output variability for both partners. The worse-performing partners additionally benefited from the haptic guidance provided by their better-performing partner. Participants did not need to estimate their partner's actions or goals from the interaction force, as suggested by Takagi et al. [6]. We also found that when a velocity-dependent force field impaired the perception of the interaction force, performance still improved equally during interaction compared to when no force field was present, supporting our hypothesis that no haptic communication needed to occur to improve performance during interaction.

Haptic interaction with a worse partner still improved performance

An important result is that haptic interaction with a worse partner still led to performance improvements. Our results are consistent with Ganesh et al. [3], who were the first to show that haptic interaction improves performance for both partners, however, there is one crucial difference. Whereas the results of Ganesh et al. [3] suggested that haptic interaction improved your performance independent of how bad your partner was at the tracking task (for $R < 0\,\%$), we found that the improvements decreased with an increasingly worse partner. It seems that interaction with an even worse partner does not lead to deteriorated performance: the measured improvement seemed to converge to $I = 0\,\%$, although the number of data points in this region is limited (~5 % of the data is below $R \approx -40\,\%$). Our improvement results are intuitive; being coupled to progressively worse partners will eventually physically 'hold you back', even with a compliant connection, resulting in less to no performance benefits. Lastly, we found the same improvement curves in a different study with an additional twenty other participants (see Section D.2).

Interacting partners did not need to estimate each other's actions to improve performance

The interaction model provided evidence that the partners did not need to understand each other's actions or movement goals to improve performance during haptic interaction in a fast-moving tracking task. These findings are in contrast with the work of Takagi et al. [6], who proposed that participants improved performance in a similar tracking task by estimating their partner's movement goal from the interaction force and used it to improve their own estimate of the moving target. However, we question whether such accurate communication through the interaction force is possible, in particular in a fast-moving tracking task in which the interaction force continuously changes magnitude and direction because of the independently-moving partners.

To accurately estimate the partner's movement goal, Takagi et al. [6] assumed that the individuals had exact knowledge of the dynamics of the haptic connection. However, participants were not made aware of the interaction or the dynamics of the connection. Perhaps the interacting individuals learned the connection dynamics over time; humans are able to learn to manipulate unknown complex but deterministic dynamics, but only after extensive practice [28]. However, it is debatable whether individuals learned the connection dynamics accurately enough to pinpoint their partner's movement goal from the interaction force, in particular if they were unaware of the interaction. Our no haptic communication model did not require the participants to know the connection dynamics.

Furthermore, to estimate the partner's goals solely from the interaction force, the individuals need to accurately perceive the interaction force in magnitude and direction. However, human force perception likely contains systematic errors. Humans typically produce higher forces than the externally presented force, indicating that humans overestimate externally applied forces (such as an interaction force) [9, 10, 29–31]. Humans are also inaccurate at estimating the direction of a force [8, 9]. It is still unclear whether these systematic errors in force perception are because individuals indeed *perceive* the force incorrectly, but it is likely that the accuracy of any information exchanged through the interaction force in a fast-moving tracking task is limited.

Lastly, a recent study showed that haptically-interacting individuals can only exchange incomplete information to each other through an interaction force [32]. In their study, participants were haptically coupled with a compliant connection while they performed joint reaching movements. The researchers varied the amount of information that individuals received from their partner, ranging from only the interaction force to a combination of the interaction force and the visual position of their partner. When only receiving haptic information from their partner – like in our study – participants adopted interaction strategies that minimized the need-to-know about their partner; they planned their motions independently and ignored the behavior of their partner (we found similar results in our joint reaching study in Chapter 5). Only when the researchers added visual information about the partner, individuals started to estimate their partner's actions. These findings corroborate our hypothesis that accurate information exchange solely through an interaction force is unlikely to occur.

Haptic interaction resulted in similar improvements even when the perception of the interaction force was impaired

To further support our hypothesis, we found that haptic interaction still improved performance similarly even when the perception of the interaction force was impaired by a velocity-dependent force field. These results indicate that accurate perception of the interaction force was not necessary to improve performance during haptic interaction; hence, presumably, no haptic communication needed to occur.

Additional analysis showed that when we assumed that the participants learned and used an internal model of the force field to differentiate the interaction force from the force-field force, the perception of the interaction force would be biased in magnitude and direction because of an imperfectly-learned internal model. The incorrect estimate of the interaction force would yield incorrect estimates of the partner's position and movement goals. Suppose that a participant estimates their partner's location relative to their own position using $\Delta\mathbf{p} = \hat{\mathbf{F}}_i/k_s$, assuming that the partners know the connection stiffness k_s and ignoring the connection damping for simplicity. An overestimated magnitude of the interaction force would result in an overestimation of the partner's position. Any other information about the partner extracted from the interaction force that depends on the partner's location, such as their spatial movement goal, would be inaccurate as well. Therefore, the improvements of haptic interaction in the force field are unlikely to be explained by haptic communication, as discussed earlier.

Limitations of the interaction model

The no haptic communication model is not able to explain the improvements for all individuals. The model predicts that haptic interaction would start impeding performance when interacting with a partner whose performance is $\sim$40 % worse, whereas the data seem to suggest that improvement converges to $I \approx 0\,\%$. However, the number of data points in the range of relative partner performance $R < 50\,\%$ is small, so we can only speculate. The interaction model also assumed that participants used their single trial tracking behavior when interacting with their partner; we will briefly discuss this below.

Do participants adapt their control behavior during haptic interaction?

Humans have been shown to change their motor behavior when moving in a different physical environment, such as haptic interaction with a robotic device (e.g., [17, 33]). It is possible that the haptically-interacting partners changed their control behavior based on their partner's skill level. For example, a superior partner could have experienced the interaction force as a disturbance and adapted control, such as increased arm impedance through muscle co-contraction, to counteract the disturbances [21]. A worse-performing partner could have changed their control behavior, such as decreasing their physical effort to depend more on the haptic assistance of the interaction force [33]. For now, it remains unknown whether and how participants changed their motor behavior during tracking with respect to their individual behavior in the single trials, warranting further research.

Conclusion

The main conclusion of this chapter is that no haptic communication – or more specifically, no estimation of the partner's movement goals – was necessary to explain the observed performance improvements during a fast-moving tracking task. Instead, we hypothesized that both partners improved from the haptic interaction because the mechanical coupling between the participants decreased motor output variability and provided some form of haptic guidance for participants with a skill level lower than their partners'. Although we suggest that *accurate* information exchange through the interaction force is unlikely to occur, we do not rule out the possibility that some, *less accurate*, information could be communicated trough the interaction force. However, more research is necessary to better understand how useful the information communicated through the interaction force is, in particular for complex motor tasks.

References

[1] A Sawers and L H Ting. Perspectives on human-human sensorimotor interactions for the design of rehabilitation robots. *Journal of NeuroEngineering and Rehabilitation*, 11(1), 2014.

[2] R P R D van der Wel, G Knoblich, and N Sebanz. Let the Force Be With Us: Dyads Exploit Haptic Coupling for Coordination. *Journal of Experimental Psychology: Human Perception and Performance*, 37(5):1420–1431, October 2011.

[3] G Ganesh, A Takagi, R Osu, T Yoshioka, M Kawato, and E Burdet. Two is better than one: Physical interactions improve motor performance in humans. *Scientific Reports*, 4, 2014.

[4] K B Reed and M A Peshkin. Physical Collaboration of Human-Human and Human-Robot Teams. *IEEE Transactions on Haptics*, 1(2):108–120, 2008.

[5] S Gentry, E Feron, and R Murray-Smith. Human-human haptic collaboration in cyclical Fitts' tasks. In *2005 IEEE/RSJ International Conference on Intelligent Robots and Systems*, pages 3402–3407. IEEE, 2005.

[6] A Takagi, G Ganesh, T Yoshioka, M Kawato, and E Burdet. Physically interacting individuals estimate the partner's goal to enhance their movements. *Nature Human Behaviour*, 1(3):0054, 2017.

[7] L A Jones. Matching Forces: Constant Errors and Differential Thresholds. *Perception*, 18(5):681–687, October 1989.

[8] F E van Beek, W M Bergmann Tiest, and A M L Kappers. Anisotropy in the Haptic Perception of Force Direction and Magnitude. *IEEE Transactions on Haptics*, 6(4): 399–407, December 2013.

[9] F E van Beek, W M Bergmann Tiest, W Mugge, and A M L Kappers. Haptic perception of force magnitude and its relation to postural arm dynamics in 3D. *Scientific Reports*, 5(1):18004, 2015.

[10] B Onneweer, W Mugge, and A C Schouten. Force Reproduction Error Depends on Force Level, Whereas the Position Reproduction Error Does Not. *IEEE Transactions on Haptics*, 9(1):54–61, March 2016.

[11] N Gurari, A M Okamura, and K J Kuchenbecker. Perception of force and stiffness in the presence of low-frequency haptic noise. *PLoS ONE*, 12(6):e0178605–26, June 2017.

[12] K Mojtahedi, B Whitsell, P Artemiadis, and M Santello. Communication and Inference of Intended Movement Direction during Human–Human Physical Interaction. *Frontiers in neurorobotics*, 11:127–23, April 2017.

[13] R C Oldfield. The Assessment and Analysis of Handedness: the Edinburgh Inventory. *Neuropsychologia*, 9(1):97–113, 1971.

[14] R Shadmehr and F A Mussa-Ivaldi. Adaptive Representation of Dynamics During Learning of a Motor Task. *Journal of Neuroscience*, 14(5):3208–3224, May 1994.

[15] R A Scheidt, D J Reinkensmeyer, M A Conditt, W Z Rymer, and F A Mussa-Ivaldi. Persistence of motor adaptation during constrained, multi-joint, arm movements. *Journal of Neurophysiology*, 84(2):853–862, July 2000.

[16] J B Heald, D W Franklin, and D M Wolpert. Increasing muscle co-contraction speeds up internal model acquisition during dynamic motor learning. *Scientific Reports*, 8(1):3270, 2018.

[17] J Izawa, T Rane, O Donchin, and R Shadmehr. Motor adaptation as a process of reoptimization. *Journal of Neuroscience*, 28(11):2883–2891, March 2008.

[18] M A Smith, A Ghazizadeh, and R Shadmehr. Interacting adaptive processes with different timescales underlie short-term motor learning. *PLOS Biology*, 4(6):1035–1043, June 2006.

[19] M A Conditt and F Gandolfo. The motor system does not learn the dynamics of the arm by rote memorization of past experience. *Journal of Neurophysiology*, 1997.

[20] D W Franklin, R Osu, E Burdet, M Kawato, and T E Milner. Adaptation to stable and unstable dynamics achieved by combined impedance control and inverse dynamics model. *Journal of Neurophysiology*, 90(5):3270–3282, October 2003.

[21] E Burdet, R Osu, D W Franklin, T E Milner, and M Kawato. The central nervous system stabilizes unstable dynamics by learning optimal impedance. *Nature*, 414 (6862):446–449, November 2001.

[22] J R Lackner and P DiZio. Rapid adaptation to Coriolis force perturbations of arm trajectory. *Journal of Neurophysiology*, 72(1):299–313, July 1994.

[23] O Donchin, J T Francis, and R Shadmehr. Quantifying Generalization from Trial-by-Trial Behavior of Adaptive Systems that Learn with Basis Functions: Theory and Experiments in Human Motor Control. *The Journal of Neuroscience*, 23(27): 9032–9045, October 2003.

[24] M J Wagner and M A Smith. Shared internal models for feedforward and feedback control. *Journal of Neuroscience*, 28(42):10663–10673, October 2008.

[25] E Todorov. Stochastic Optimal Control and Estimation Methods Adapted to the Noise Characteristics of the Sensorimotor System. *Neural Computation*, 17(5):1084–1108, 2005.

[26] J Izawa and R Shadmehr. On-Line Processing of Uncertain Information in Visuomotor Control. *Journal of Neuroscience*, 28(44):11360–11368, October 2008.

[27] J Diedrichsen. Optimal task-dependent changes of bimanual feedback control and adaptation. *Current Biology*, 17(19):1675–1679, 2007.

[28] A J Nagengast, D A Braun, and D M Wolpert. Optimal control predicts human performance on objects with internal degrees of freedom. *PLoS Computational Biology*, 5(6):e1000419–e1000419, June 2009.

[29] S S Shergill, P M Bays, C D Frith, and D M Wolpert. Two Eyes for an Eye: The Neuroscience of Force Escalation. 301(5630):187–187, July 2003.

[30] L D Walsh, J L Taylor, and S C Gandevia. Overestimation of force during matching of externally generated forces. *The Journal of Physiology*, 589(3):547–557, 2011.

[31] W Mugge, J Schuurmans, A C Schouten, and F C T van der Helm. Sensory Weighting of Force and Position Feedback in Human Motor Control Tasks. *Journal of Neuroscience*, 29(17):5476–5482, April 2009.

[32] V T Chackochan and V Sanguineti. Incomplete information about the partner affects the development of collaborative strategies in joint action. *bioRxiv*, pages 1–21, November 2018.

[33] J F Israel, D D Campbell, J H Kahn, and T G Hornby. Metabolic Costs and Muscle Activity Patterns During Robotic- and Therapist-Assisted Treadmill Walking in Individuals With Incomplete Spinal Cord Injury. *Physical Therapy*, 86(11):1466–1478, November 2006.

Chapter 7.

General discussion

Haptic interaction between two humans performing a motor task together has been demonstrated to improve performance of both partners [1–4]. Furthermore, learning a motor task while being haptically coupled to a partner who is learning the same task has been shown to improve individual motor learning [1].

Most of these studies investigated haptic interaction in collaborative motor tasks, in which the two individuals share a common goal, but have no pre-assigned roles [5, 6]. Participants were not made aware of the interaction and could only influence each other or potentially communicate through interaction force. However, it is not clear how haptic interaction would improve performance and learning in collaborative tasks.

The goal of this thesis is to create a better understanding of whether and, if so, why haptic interactions between humans would improve individual motor learning and performance during interaction in a collaborative task. We investigated the following research questions and found the corresponding (summarized) answers:

1. Does haptic human-human interaction improve individual motor learning in a collaborative motor task and if so, why? (Chapters 3 and 4)
   Haptic interaction between two humans who are learning the same collaborative task does not improve or impede individual motor learning compared to someone who learned the task alone, neither in a force field nor in a visuomotor rotation perturbation.

2. How do rigidly-coupled partners coordinate motor actions in a joint reaching task? (Chapter 5)
   Rigidly-coupled partners accomplish joint reaching movements by relying on a pre-programmed motion plan that is independent of the partner's behavior.

3. Do individuals improve performance during haptic interaction in a collaborative tracking task by exchanging information about each other through the interaction force (also referred to as haptic communication)? (Chapter 6)
   Participants did not need to haptically communicate through the interaction force – such as estimating their partner's actions or intentions – to explain the improvements due to interaction. Instead, we suggest that both interacting partners improved because the mechanical coupling between the participants decreased motor output variability and provided assistance in the form of haptic guidance for participants with a skill level lower than their partners'.

Here we discuss these findings, their implications and our recommendations for future work. We begin by focusing on how haptic interaction influences individual motor learning (research theme I). We then discuss the results on haptic communication (research theme II), followed by a discussion on the BROS (our dual-robotic setup) and, lastly, future work and conclusions.

7.1. Motor learning through haptic human-human interaction (theme I)

7.1.1. Haptic interaction does not improve individual motor learning in collaborative tracking tasks

Ganesh et al. [1] reported that haptic interaction improved individual motor learning of tracking a moving target in a visuomotor rotation, in which the visual feedback of the hand movement was rotated with 80 deg with respect to the actual movement [7]. Interacting participants showed more individual improvement after learning and improved faster. Motivated by these results, we investigated whether haptic interaction would also facilitate learning to move in a new dynamic environment.

In our first experiment (Chapter 3), pairs tracked a common randomly-moving target in a plane, similar to the tracking task of Ganesh et al. [1]. The participants were intermittently coupled with a compliant connection, which allowed each participant to still move independently. A velocity-dependent force field was then introduced as a new dynamic environment to elicit motor learning. Participants who haptically-interacted while learning the force field did not show better individual performance or faster learning rates compared to the individuals who learned the force without interaction (see Fig. 7.1A). Haptic interaction also did not interfere with motor learning.

The benefits of haptic interaction on motor learning could have been limited because the learning task – the force field – and the interaction were in the same sensory domain. We, therefore, repeated the experiment of Ganesh et al. [1] (see Chapter 4), in which the haptically-interacting participants now learned to track the common target in the same visuomotor rotation. Ganesh et al. [1] briefly suggested that haptic interaction enabled individuals to attain additional information about the task, which would have improved learning, but they did not test this hypothesis. So, to better understand why haptic interaction would improve motor learning, we investigated how learning was influenced by the amount of time spent interacting and the strength of the interaction. In contrast to Ganesh et al. [1], haptic interaction did not

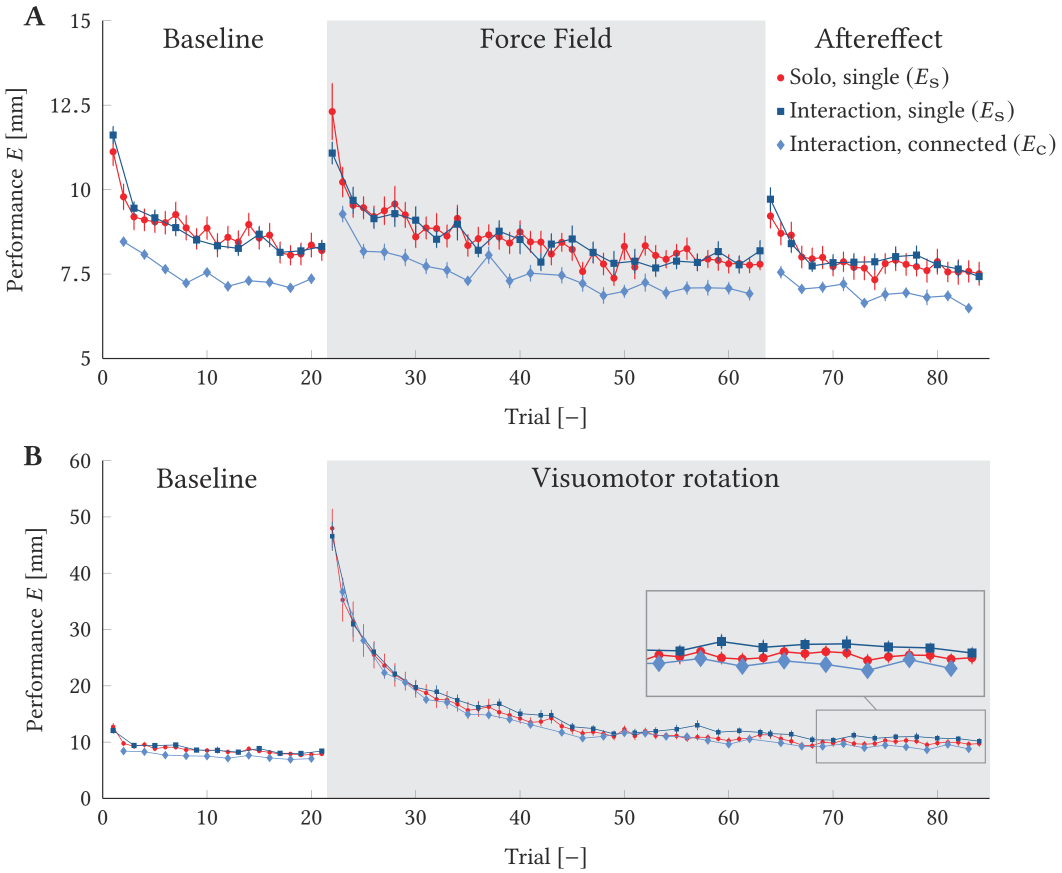

Figure 7.1. | Motor performance over the course of the force field (**A**) and visuomotor rotation (**B**) experiments. Participants performed the task alone (in single trials) or coupled to their partner (connected trials). The solo group always practiced the tasks alone. The figures are from Chapters 3 and 4, respectively.

improve individual motor learning in the visuomotor rotation (see Fig. 7.1B). More interaction time or increased interaction strength also did not lead to better individual performance or faster learning. While haptic interaction did not improve individual motor learning in our learning tasks, it also generally did not impede learning.

Why is individual motor learning in a collaborative task *not* improved by haptic interaction?

Our motor learning results are in line with observations in error-based learning and robot-assisted motor learning. The force field and visuomotor rotation are perturbations that create discrepancies between the predicted and executed hand trajectories, resulting in movement errors. These movement errors are a key training signal for a process in which humans learn to adapt to the perturbation [8–11]. The motor system minimizes the movement errors using feedback control and updates an internal model based on the experienced errors to compensate for the perturbation [9, 10, 12]. We and others (e.g., [1]) showed that haptic interaction with a partner significantly reduced movement errors in a visuomotor rotation or force field compared to someone practicing those tasks alone. Hence, purely from an error-based motor learning perspective, we would not expect any benefits of haptic interaction on motor learning.

In addition, motor variability is considered to be an important factor in motor learning, as it lets participants explore the space of possible movements and solutions [13, 14]. Wu et al. [13] found that individuals with high motor variability learn a velocity-dependent force field faster than individuals with lower levels of motor variability. Our results showed that haptic interaction significantly decreased motor variability (see Chapter 6), which could be an additional reason why haptic interaction did not speed up individual learning.

Our motor learning results are also consistent with several studies on robotic training strategies, in particular those who studied the effect of haptic guidance on motor learning [15]. Robotic haptic guidance is a training strategy in which a robot haptically interacts with an individual to guide the individual over a desired trajectory by reducing movement errors. Although robotic haptic guidance typically improves performance temporarily, there is limited evidence that it benefits individual motor learning, in particular in tasks in which require spatial accuracy (e.g., a tracking task) [16–23]. Haptic human-human interaction through a compliant spring can be regarded as a form of haptic guidance. Like robotic haptic guidance, haptic interaction gives an erroneously good impression of performance, especially when the interacting partners are unaware of the interaction, but reduces the movement errors as a driving factor for motor learning [17]. Haptic guidance could facilitate learning for initially less-skilled individuals [24]. However, we did not find any evidence that haptic interaction was more helpful for less-skilled individuals. Interaction with a better partner also did not result in more improvement for the less-skilled individual.

Another possible reason why we found no learning benefits of haptic interaction is that participants were not made aware of the interaction. If the participants extracted any task-relevant information from the interaction force to improve their motor learning, it is likely that they had to learn how to interpret the interaction forces, while they learned the force field or visuomotor rotation at the same time. Learning multiple motor processes has been shown to interfere with each other [25, 26].

Also, we did not assign roles to the partners, such as leader-follower or student-teacher. In collaborative tasks, roles emerge spontaneously or do not emerge at all (Chapter 5), and it is not certain which roles partners will assume beforehand [6, 27]. If partners first had to develop or negotiate roles, it is possible that this process counteracted the potential learning benefits of haptic interaction. Even when we allowed participants more time to haptically interact, such that they could negotiate roles or learn to 'use the force', we still did not see faster learning or better individual performance after learning (Chapter 4).

In addition, we found that partners did not need exchange information to explain the motor behaviors during interaction (Chapter 6). This could indicate that no information relevant for motor learning was exchanged (Chapter 6).

7.1.2. Motor adaptation versus motor skill learning

We used a force field and a visuomotor rotation, which are well-established paradigms to study motor adaptation, to elicit learning [7, 28]. Because our robotic setup allowed movements in a horizontal plane with limited workspace, the force field and visuomotor perturbations enabled us to evoke significant and consistent motor learning. Pilot tests showed that making the target movements more difficult – for example by adding more frequency content to the target motion – led to inconsistent learning and interaction results.

However, the applicability of the visuomotor rotation and force field tasks to real-world learning scenarios is limited [29]. Acquiring a motor skill, which involves improving performance beyond your initial skill level [30], takes a considerable amount of time and does typically not occur within a single experiment session [31, 32]. Studies on the effect of haptic human-human interaction on more complex motor tasks, such as whole-body movements, are scarce and do not report benefits on learning (e.g., [33]).

7.1.3. How should we proceed to study the potential benefits of haptic interaction for motor learning?

Next, we will discuss some possible research avenues in haptic human-human interaction that could be useful to complement the design of robotic training strategies.

Predefining roles in haptic human-human interaction, such as student-teacher or athlete-coach, in cooperative tasks is considered to be vital for effective motor education [5, 6, 15]. Surprisingly little work has been done concerning how pre-assigning roles in haptic interaction affects individual motor learning. Recently, Sawers et al. [33] investigated how a dancing couple used haptic interaction to coordinate dancing moves. The pairs were instructed to perform sequences of backward and forward steps. Roles were predefined: the leader was aware of the stepping sequence and had to guide and initiate the steps; the follower had to infer the leader's intentions from the interaction force. Stepping performance only improved over time in pairs with two experts, but not in expert-novice or novice-novice pairs. This result suggests that you have to be an expert to generate useful interaction forces, but you also need to be an expert to correctly interpret the forces to improve performance over time.

Still, little is known regarding how a teacher should apply forces onto the student to encourage motor learning [6]. Galvez et al. [34] found that experienced therapists exerted substantially different forces on individuals with spinal cord injury during physical rehabilitation. Different teachers likely use different haptic education methods for the same motor learning task. For example, one teacher might constantly correct the student, whereas another teacher might focus on providing a safe environment and lets the student learn more independently. In addition, haptic education strategies will likely need to be tailored to each specific motor task [16]. To increase our knowledge on how experts or teachers use haptic interaction to teach students, observational studies could be performed, however classifying the possible haptic education strategies will be a challenge (e.g., [27]), let alone how to implement such strategies in a robotic training paradigm. A framework on how to investigate and analyze haptic education between humans in cooperative motor tasks would be helpful but is, to our knowledge, not yet available.

Another, more scientifically structured approach would be to instruct the teacher on how to educate the student based on existing learning theories. According to the challenge point theory, the teacher could keep task difficulty appropriate for the participant's skill level to facilitate learning

[35]. In robotic training studies, haptic guidance benefits learning of initially less-skilled individuals, whereas individuals with an initially high skill level learned more when they are challenged [16, 24, 36].

Furthermore, the robotic haptic training can be beneficial for motor learning, but the benefits likely depend on the type of task. The effect of haptic human-human interaction on motor learning has only been investigated in a limited number of tasks that primarily required spatial accuracy ([1] and our own work, among others). Robotic haptic guidance has been shown to benefit learning of time-critical motor tasks [24, 37, 38]. For example, a teacher could haptically educate a student when to initiate a forehand stroke in tennis [24]. Furthermore, it is possible that haptic interaction between two humans will have benefits for learning more complex motor skills. In an unpublished study, we studied how haptic interaction with an expert – who was aware of the interaction – would influence the motor learning of novice individuals in a complex tracking task in three dimensions. The expert practiced the tracking task for twenty hours and was instructed to haptically assist the novices as he saw fit. However, despite that the novices improved during interaction, haptic interaction did not benefit their individual motor learning, similar to our other learning studies. Haptic interaction could benefit learning of complex tasks that are comprised of multiple sub-tasks; a teacher could haptically support the student in one sub-task, such that the student can focus on learning one of the sub-tasks [39].

Lastly, we only studied the effect of *haptic* interaction on motor learning; we did not assess the influence of other cognitive aspects involved in joint action (see [40] for an overview). Social interaction with another learner may also motivated partners to set more difficult goals than they normally would or attempt to outperform their partner [41]. Studies showed that playing an exercise-based game with someone else benefits the user's motivation and even rehabilitation outcome [42, 43]. Visually observing someone else learn a task can improve learning as well [41, 44–46]. Similarly, having a student observe someone else learn a motor task through haptics – hence feeling how the individual learns a new motor task – may improve learning in the student as well. Lastly, although it is important to understand how different modes of interaction affect motor control and learning by studying them in isolation, future work should assess the complementary effect of haptic interaction and other aspects of joint action, such as competition and social facilitation, on individual motor learning to help the development of more complete and effective robotic training paradigms.

7.2. Haptic communication in collaborative tasks (theme II)

7.2.1. Rigidly-coupled partners in a collaborative reaching task did not coordinate motion plans

In one of the earliest studies on haptic human-human interaction, Reed and Peshkin [2] found that pairs who rotated a crank as fast as possible to stationary targets were faster than either of the partners reaching to the target alone. They found that partners specialized into roles in which one partner accelerated while the other decelerated the crank. The authors proposed that the partners negotiated these roles through the interaction forces. How did the partners achieve such coordination, and how did the roles emerge trial-by-trial?

To answer these questions, we examined how two rigidly-coupled individuals coordinated their actions trial-by-trial during a collaborative reaching task to a common stationary target (Chapter 5). The joint reaching movements were remarkably consistent across the trials. Pairs also produced opposing forces between them that they did not minimize over trials. Using a computational model of the joint reaching movement, we found that each partner had a distinct motion plan that did not change with time. These results suggest that the rigidly-coupled pairs performed joint reaching movements by relying on pre-programmed motion plans that ignored their partner's behavior. The results also suggest that the partners did not exchange information through the interaction force – also referred to as haptic communication – to coordinate actions.

7.2.2. Is haptic communication necessary to explain the motor improvements in a collaborative tracking task?

While haptic communication was not needed to explain the motor behaviors of rigidly-coupled individuals in a joint reaching task, it does not mean that haptic communication is not necessary in other tasks. Some studies that investigated haptic collaboration in tasks that required tracking a randomly-moving target proposed that participants had to exchange information through the interaction force to explain their results [47–49]. Here we further test whether haptic communication was crucial (see Chapter 6).

Pairs performed trials in which they tracked a similar common randomly-moving target alone (single trials) and coupled to their partner (connected trials) with a compliant connection: a spring ($k_s = 150\,\mathrm{N\,m^{-1}}$) with a damper ($b_s = 2\,\mathrm{N\,s\,m^{-1}}$). The compliant connection enabled partners to exert forces onto each other, but still allowed independent movement. Importantly, like [47–49], we did not make the participants aware of the haptic interaction.

Haptic interaction with a partner in a collaborative tracking task improves motor performance

Consistent with previous work [1], we found that haptic interaction improved performance for both partners in the tracking task, also when a force field or visuomotor rotation was introduced (see Chapter 6). The amount of improvement depends on the relative individual performance of the partner (see Fig. 7.2). The data revealed two interesting findings. First, haptic interaction with a worse-performing partner still improved performance; though the interaction benefits converged to $I = 0\,\%$ when connected to an increasingly worse-performing partner. Second, when we superimposed a velocity-dependent force field on the interaction force and tracking task – impairing the perception of the interaction force – haptic interaction still improved performance similarly compared to when no force field was present (Fig. 7.2). In fact, the improvement due to interaction did not dependent on the type of task (force field, visuomotor or no perturbation); we found no significant differences between the improvement curves of both experiments (ANCOVA with relative partner performance as covariate and experiment (perturbation + no perturbation) as factor $F(3, 1413) = 1.57$, $p = 0.1947$).

Haptic communication is not necessary to explain the performance improvements due to haptic interaction in a tracking task

How does haptic interaction improve performance, especially when coupled to a worse-performing partner? To explain these results, we developed a computational model in which we mechanically coupled two partners who performed the tracking task independently (similar to the joint reaching task in Chapter 5). The model assumed that no haptic communication – such as estimating the partner's state or actions – through the interaction force occurred between the partners. The 'no haptic communication' model accurately predicted the improvement due to interaction for the majority of our data (Fig. 7.2). Additional model analysis suggested that performance was improved because the compliant connection partially compensated for the motor output variability – which includes tracking errors such as overshoots – for both partners. The worse-performing partners in a pair additionally benefited from the haptic guidance provided by their better-performing partner. Hence, the model suggested that the participants did not need to haptically communicate to improve performance.

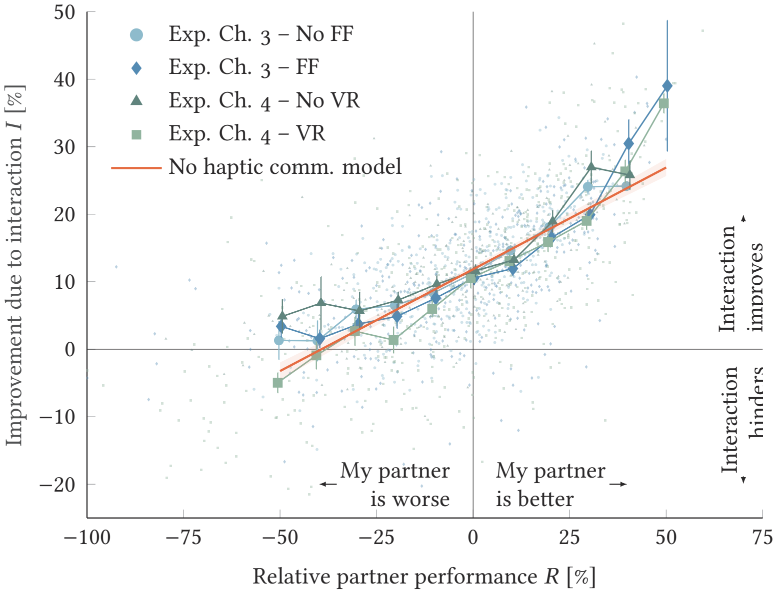

Figure 7.2. | Improvement due to interaction versus the relative performance of the partner. The relative improvement per participant is calculated as $I = 1 - E_c/E_s$, where E_c is the tracking performance in a connected trial and E_s is the performance in a single (or unconnected) trial of each participant. The relative performance $R = 1 - E_{s,p}/E_s$, where $E_{s,p}$ is the partner's single performance. We combined the data from the experiments in Chapters 3 and 4 (a total of forty participants), which included blocks with a force field or visuomotor rotation and blocks without any perturbation. The data are binned across relative performance and error bars indicate the standard error of the mean.

This conclusion is in contrast with the goal integration model of Takagi et al. [47], who hypothesized that haptically-interacting individuals exchanged information through the interaction force to improve performance in a similar collaborative tracking task. They proposed that each individual estimated their partner's movement goal solely from the interaction force and used it to improve their own visual estimate of the target movement, which is then used to enhance tracking performance.

Comparing the no haptic communication model with the goal integration model, there are important differences in the model assumptions. Our model made as few assumptions as possible about the haptic interaction: (1) the partners were unaware of the haptic interaction and had no knowledge of the connection dynamics; (2) the individuals did not estimate their partner's state, actions or goals; and (3) the partners did not need to accurately perceive the interaction force. In contrast, the goal integration model made two important assumptions about the haptic interaction, which we will discuss below.

First, Takagi et al. [47] assumed that each individual had accurate knowledge of the connection dynamics (i.e., the partners new the exact stiffness and damping of the compliant connection). However, as in our study, the participants were not made explicitly aware of the haptic interaction; they were only told that they would feel forces that would sometimes assist or resist their motion. In a post-experiment questionnaire, most of our participants indicated that they were unaware of the connection. Perhaps the partners were able to accurately estimate the connection dynamics over time. Humans can learn to move objects with complex but unknown dynamics from one point to the other, but only after extensive practice and with limited success [50]. In our and Takagi et al.'s experiments, the main source of information for learning the connection dynamics was the interaction force that depended on the position and velocity of both partners, making the estimation of the connection dynamics much more complicated. We, therefore, suggest it unlikely that the interacting individuals were able to build a representation of the connection dynamics accurate enough to be used for estimating their partner's movement goal.

The second assumption is that the individuals were able to and needed to accurately perceive the continuously changing interaction force in the fast-moving tracking task. However, when we impaired the perception of the interaction force by superimposing a velocity-dependent force field, haptic interaction still improved performance similar to when no force field was present (Chapter 6). We showed that the interaction force was biased in direction and magnitude by the force field, even when assuming that the partners learned a substantial, but incomplete internal model of the force field. These results suggested that that haptically-interacting individuals did not need to have an accurate perception of the interaction force to yield similar performance improvements during interaction.

Furthermore, several studies suggested that human force perception contains uncertainty (random errors) and systematic errors (biases). The systematic errors in force magnitude are, among others, manifested in incorrect force reproductions; humans typically produce higher forces than the externally presented force (in the range of 10 N to 20 N), indicating that humans overestimate externally applied forces (such as an interaction force) [51–54]. Moreover, when asked to reproduce a force of 10 N by moving a spring with low stiffness ($\sim 100\,\mathrm{N\,m^{-1}}$), individuals relied more on position sensory feedback than force sensory feedback, indicating that force perception is inaccurate at low force levels [54]. Humans are also inaccurate at estimating the direction of a force and perceive forces applied to the hand as smaller or larger depending on the configuration of the arm [55, 56]. It is unclear whether the aforementioned force reproduction errors are due to an incorrect force representation in the brain or because the correctly perceived force is reproduced incorrectly by our motor system [51, 53, 57]. It is still possible that systematic errors are present in force perception that biased or limited the accuracy of the information exchanged through the interaction force.

Limitations of the no haptic communication model

The no haptic communication model is not able to explain the improvements for all individuals. The no haptic communication model predicts that haptic interaction would hinder performance when interacting with a partner whose performance is $\sim 50\,\%$ worse than yours, whereas the majority of the data suggested that the improvement converges and plateaus around $I \approx 0\,\%$ (Fig. 7.2). While our data are scarce for $R < -50\,\%$ (only $5\,\%$ of the data), other studies that used similar tracking tasks and similar compliant connection dynamics found that haptic interaction with a partner in this range either slightly hindered performance or led to no improvement for individuals, depending on the task [48, 49]. To illustrate the plateau that these studies observed, we regressed an exponential function ($I = \beta_0 + \beta_1\, e^{\gamma R}$, where R is the relative partner performance) to the data and extrapolated the improvement to $R = -125\,\%$ in Fig. 7.3. The no haptic communication model shows a mismatch with the extrapolated data, underestimating the improvement when interacting with a worse partner.

The goal integration model could explain the improvements in this relative performance region ($R < -50\,\%$) [48, 49]. However, we question how the goal integration mechanism would help to improve performance for individuals that are already superior in the tracking task in this region (we will discuss this later). Furthermore, closer inspection of the data of Takagi et al. [48, 49] in this region suggested that the data density is limited in their studies as well, which questions the reliability of their regression model fits. Also, Takagi et al. [48, 49] rely on the regression model fits – quadratic linear models – to base their conclusion, while the regression model choice is debatable; binning the data, as performed by Ganesh et al. [1] and in our studies makes less assumptions about the data. Lastly, this relative performance region represents the few cases in which the performance difference between partners is very large. Although this region is important to consider, one can argue about its relevance, in particular compared to the more relevant range of $-50\,\% < R < 50\,\%$, which accurately predicted by the no haptic communication model.

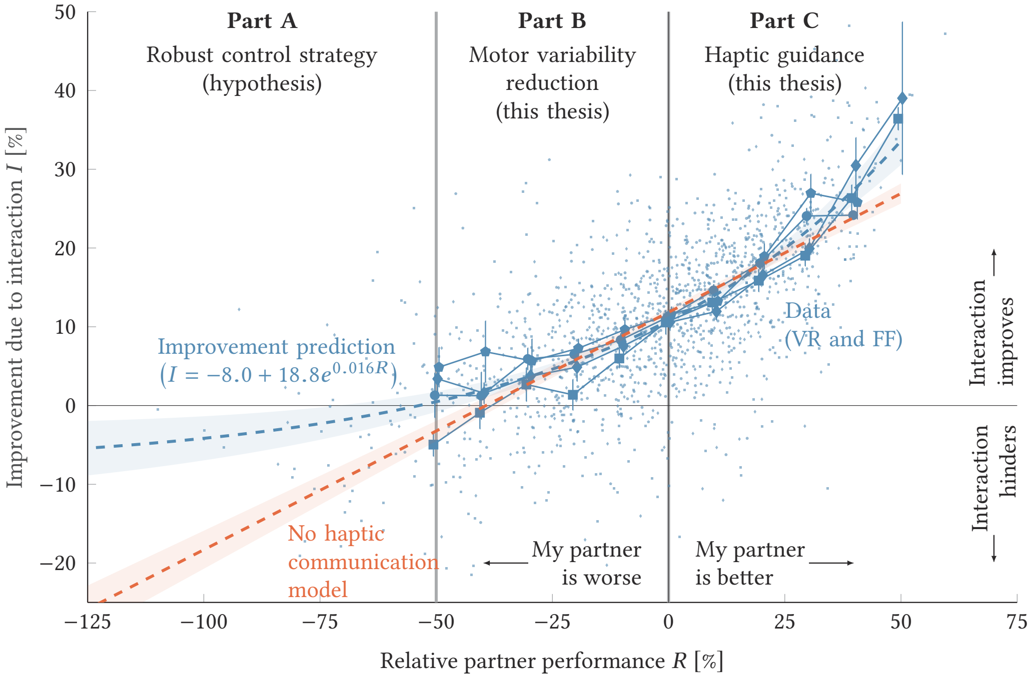

Figure 7.3. | Interacting partners likely use different interaction strategies based on the performance of their partner. We divided the figure into three parts based on the improvement and relative partner performance. The figure also shows the measured improvement data from Fig. 7.2. We added the extrapolated 'improvement plateau' when interacting with a much worse partner. Note that the data density is low for $R < -50\,\%$ to support this extrapolated improvement curve. The no haptic communication model prediction is shown as well.

7.2.3. One model fits all? Do haptically-interacting partners adopt the same or different interaction strategies?

Our no haptic communication model and the goal integration model of Takagi et al. [47] assumed that both partners did not change their control behavior based on the interaction and selected the same interaction strategy: they either both executed the task independently or they both estimated and used each other's movement goals through the interaction force. This is an important assumption that is up for debate; humans have been shown to co-adapt when interacting with adaptive robotic controllers (e.g., [58–62]), hence each individual likely modulated their control behavior and interaction strategy with respect to their partner because of the haptic interaction.

Here we hypothesize, based on the results in this thesis and findings in human motor control, how individuals adapt their control behavior and interaction strategy due to the haptic interaction with another partner in a collaborative fast-moving tracking task. We limit our discussion to three possible interaction strategies; however, many more interaction strategies are possible and individuals could use multiple strategies simultaneously. We propose that individuals adapt control behavior based on the relative performance of their partner in collaborative tracking tasks.

We split the improvement versus relative performance data into three parts based on the improvement and relative partner performance (see Fig. 7.3). Part A consists of the individuals whose partner is relatively bad at the tracking task ($R < -50\,\%$). As mentioned before, our data density is limited in this range, and we base our hypothesis on the extrapolated improvement curve. Part B consists of the range in which interaction with a worse partner still yields performance improvements ($-50\,\% \leq R < 0\,\%$). Part C includes all participants who interacted with a better partner ($R \geq 0\,\%$).

The no haptic communication model strongly suggests that the interacting partners in parts B and C chose a strategy in which they both independently perform the tracking task. Furthermore, partners did not need to exchange information about each other or the task through the interaction force to improve performance. The improvements in parts B and C are primarily because of the mechanical coupling between the partners. The individuals in part B primarily improve because the compliant connection with their partner reduced their motor variability (Chapter 6).

The relatively worse-performing individuals in part C additionally benefited from the haptic guidance provided by their better-performing partner (Chapter 6), as predicted by the no haptic communication model. However, the model seems to underestimate the performance improvement starting around $R > 40\,\%$ (Fig. 7.3). Although we found no evidence that partners estimated each other's goals through the interaction force, we do not rule out the possibility that individuals were able to extract some, *less accurate* information from the interaction force. It is possible that some individuals – who were significantly worse at the tracking task compared to their partner – could get an idea of the usefulness of the interaction force (for example, the force seems to be pointing toward the target most of the time) or participants could get an idea of the skill level of their partner. Based on this information, participants could decide to let the force help them move closer to the target to improve performance even more (e.g., similar to haptic guidance), which could explain the slightly higher improvement around $R > 40\,\%$. A stiffer connection allows the worse partner to benefit even more from the guidance of the interaction force [48], similar to a stiffer robotic haptic guidance [20].

Lastly, because the data are scarce in part A, we can only hypothesize what strategy individuals used when interacting with a much worse-performing partner. The no haptic communication model shows a mismatch with the extrapolated data in part A (Fig. 7.3), which indicates that, to improve during interaction, either information was exchanged through the interaction force (e.g., the goal integration mechanism) or that the better partner independently changed his/her control behavior. The goal integration model of Takagi et al. [47] predicted a similar improvement to their data and our extrapolated improvement trend for the individuals in this part (see Takagi et al. [48, 49]). However, how can a superior partner – who presumably already has an accurate estimate of the target – improve their target movement estimate by inferring the movement goal of their much worse-performing partner? Theoretically, following optimal multisensory integration, the superior individual's estimate of the target could be improved by using the partner's less accurate goal estimate, but only if the estimate of their inferior partner's movement goal is not biased. However, as discussed earlier, we question whether such accurate goal estimation through an interaction force is even possible in a fast-moving tracking task.

We propose an alternative, and in our view more intuitive but untested mechanism to explain the improvement in part A. Because of the substantially inferior performance of their partner, the superior partner experiences the interaction force as a disturbance. This causes the better partner to choose a more robust control strategy to counteract the force disturbance and to minimize the reliance on the partner's behavior, for example by increasing the arm impedance through muscle co-contraction [27, 63, 64]. Selecting such a strategy would minimize the hindering influence of the worse-performing partner, leading to only slightly worse performance (or no difference in performance) during interaction.

To conclude, we have only begun to understand which interaction strategies individuals could use in haptic interaction; ranging from independently executing joint reaching tasks by ignoring each other's behavior (Chapter 5) or independently performing a tracking task while being mechanically connected to someone else (Chapter 6), to using haptic communication to infer each other's motor actions (e.g., [47]). Instead of assuming that both partners use the same interaction strategy, we need to investigate whether interacting partners adopt the same or different interaction strategies, which interaction strategies they adopt, and how these interaction strategies emerge over time.

7.2.4. Can humans estimate accurate information about each other through an interaction force?

In the previous section we mentioned that it is possible that some form of haptic communication could occur in complex movement tasks, such as our fast-moving tracking task, despite the fact that our no haptic communication model suggests otherwise. We do *not* argue that no exchange of information could occur in haptic interaction. We *do* reason that the exchange of accurate information, specifically estimating the precise state, actions, and goal of the partner solely from the interaction force as proposed by Takagi et al. [47], is unlikely to occur. Of course, less accurate but still very useful information can be conveyed through an interaction force, such as a general direction in which the partner intends to move in the case of human-human interaction [65], or the boundaries of a safe operation zone by a robotic system, such as a distance-keeping system in cars [66] or a flight envelope protection system in aircraft [67].

To support our view, a recent study showed that haptically-interacting individuals can only exchange incomplete information to each other through an interaction force [68]. In their study, participants were haptically coupled with a compliant connection while they performed joint reaching movements. Chackochan and Sanguineti [68] varied the amount of information that individuals received from their partner, ranging from only the interaction force to a combination of the interaction force and the visual position of their partner. When only receiving haptic information from their partner, participants adopted interaction strategies that minimized the need-to-know about their partner; they planned their motions independently and ignored the behavior of their partner. We found similar results in our joint reaching study (Chapter 5) and tracking task (Chapter 6) for the haptic information only condition of [68]. Only when adding visual information of the partner, individuals seemed to estimate their partner's actions [68]. These findings support our reasoning that accurate information exchange through an interaction force solely is unlikely, opposing the claims by Takagi et al. [47, 48, 49].

Haptic information can be a vital information source for inferring the intentions of an agent, though the haptic information needs to be complemented with other sources, such as visual cues. Future research should investigate how much information can be exchanged through an interaction force.

7.3. BROS: the admittance-controlled multiplayer haptic robot

We designed and built BROS – the Bi-partner RObotic Setup – as a dual-robotic setup to investigate haptic human-human interaction; Chapter 2 provides a description of the design and evaluation of the setup. BROS was used for the experiments in Chapters 3, 4 and 6 and several studies by students working on their Master's degree, ranging from experiments on the effect of the haptic connection strength to haptic interaction with a virtual partner. So far, BROS has proven to be a reliable research tool: we tested over 234 participants (not counting all of the pilot tests) without any major issues.

The compact design – all sensors and actuation are integrated in each manipulandum – allows for multiple configurations of the setup. We primarily used a configuration with two manipulanda for studying haptic interaction between two humans. BROS could also be used for investigating bimanual control in this configuration (Fig. 7.4). Motor tasks that require bimanual motor control can be useful to assess upper limb motor impairment and cognitive functions [69, 70]. For example, Bourke et al. [70] used a motor task in which the participants had to hit all targets using both arms, while avoiding all the other objects, which required decision motor processes and motor action selection that could be impaired in participants with stroke. Moreover, the handle of a manipulandum can be replaced with a finger cap. By using two manipulanda, we are able to simulate objects that the user can grasp with two fingers and manipulate in three dimensions (rotate and move the object in a 2 DOF plane, see Fig. 7.4). In addition, as we built four manipulanda, we are able to investigate haptic interactions between four humans, bimanual object grasping and manipulation, or haptic interaction between two individuals who are both manipulating an object in multiple degrees of freedom.

Still, enhancements can be made to improve the performance of the manipulanda. First, the inner position control loop can be enhanced by improving the velocity estimation by adding dedicated sensors or state estimation in general. Furthermore, the low-frequency resonance of the capstan transmission, which reduced control stability margins, could be remedied by adding acceleration feedback or using higher-stiffness cables [71, 72].

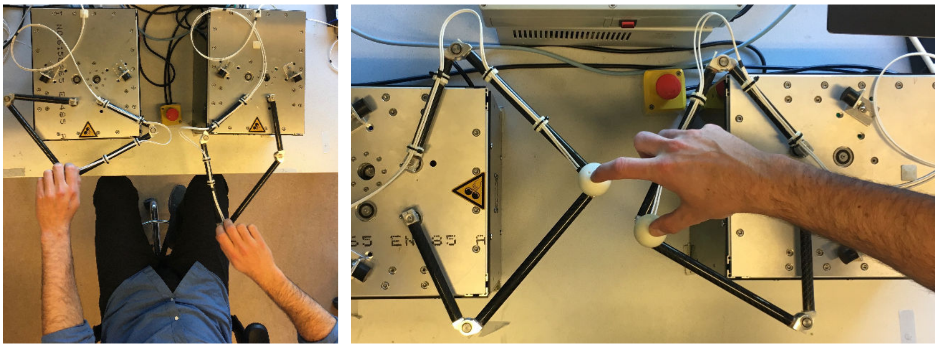

Figure 7.4. | Beside studying haptic interaction between two humans, BROS can also be used for investigating bimanual motor control or object manipulation with two fingers.

7.4. Possible applications

From a parent helping their child to ride a bike to a physiotherapist physically assisting an individual who is training to regain motor functions after a stroke, there are many anecdotal examples of how haptic interaction between humans plays a vital role in motor learning. Although we found no evidence that haptic interaction improves individual motor learning in collaborative motor tasks, there is still a lot to be learned from how two humans learn a task together. Ultimately, this knowledge could be useful to complement the development of robots that can physically interact with humans in intuitive and biologically-inspired ways for, among others, facilitate motor learning for example in physical therapy in neurorehabilitation or sports.

Furthermore, our results found that haptic interaction in a collaborative task improved performance for both participants during interaction. These findings could be useful for designing robotic assistance for tasks that require high precision, for instance in the medical field or inspection of nuclear power plants [73]. We showed that individuals both performed the task independently, and that the improvements are primarily due to the error-reducing nature of the compliant connection with the other partner. Presumably, haptic interaction with a human-like virtual agent that performed the same task independently (using the relatively simple interaction model in Section 6.2.6) could result in similar improvements compared to when two humans interact. A potential benefit of modeling robotic haptic guidance based on haptic human-human interaction is that even when the user outperforms the robotic haptic guidance, he/she will still benefit from the haptic interaction (within a certain range).

Lastly, robotic systems are rapidly becoming more intelligent and are beginning to execute certain functions autonomously while cooperating with humans. Allowing the user and robot to (continuously) haptically-interact could help the user to better and timelier understand the intentions of the robot, and vice versa, but more research is needed to find the full potential of haptic interaction.

7.5. Future work

Much more work needs to be done to better understand haptic human-human interaction and its application in human-robot interaction strategies. Although we mentioned possible research avenues throughout this discussion, we will summarize the most important recommendations for future work here.

To further investigate the potential benefits of haptic human-human interaction for learning, studies should focus on cooperative or competitive tasks in which the interacting participants are aware of the interaction and in which roles are assigned beforehand. Examples include interactions in which one partner fulfills the teacher role, assisting a student in learning a new task (e.g., haptic education) or interactions with a competitive element in exercise-based games to motivate the individuals. The complementary effects of other types of interaction, including social and verbal interaction should also be considered when investigating haptic human interactions to develop more complete (robotic) training strategies.

Researchers agree that haptics are a valuable means for bidirectional communication between two agents, but our knowledge on the underlying mechanisms of haptic communication, its limitations and benefits, and how we can promote and exploit haptic communication for more intuitive human-human and human-robot interactions remains limited. Future work should study how humans can communicate through haptics, in particular how much and what kind of information can be transferred through the haptic interaction and at which bandwidth (e.g., how well haptic interaction can continuously transfer time-critical information).

Lastly, individuals likely adopt different interaction strategies when haptically-interacting with each other. A more thorough understanding of how people co-adapt during haptic interaction, specifically which interaction strategies they adopt, is needed.

7.6. Conclusion

We investigated how haptic interaction between two humans affects each individual's motor behavior and learning during collaborative motor tasks. In summary, our results showed that haptic interaction does not improve individual motor learning of a force field or a visuomotor rotation in a collaborative tracking task. We also found that haptic interaction generally improved performance for both individuals. Interestingly, haptic interaction resulted in the same improvements when the perception of the interaction force was substantially impaired by a superimposed velocity-dependent force field. Using a computational model of two coupled individuals performing the tracking task independently, we showed that the improvements in our tracking task can be explained by the error-correcting nature of the compliant connection between the interacting partners in the range where the differences in performance between the partners is not too large ($-50\,\% < R < 50\,\%$). Combining our force field results with the model-based analysis, we suggest that participants did not need to exchange information through the interaction force to improve in our tracking task. Lastly, consistent with the previous conclusion, we found that two rigidly-coupled individuals do not coordinate actions through the interaction force in a joint reaching task.

References

[1] G Ganesh, A Takagi, R Osu, T Yoshioka, M Kawato, and E Burdet. Two is better than one: Physical interactions improve motor performance in humans. *Scientific Reports*, 4, 2014.

[2] K B Reed and M A Peshkin. Physical Collaboration of Human-Human and Human-Robot Teams. *IEEE Transactions on Haptics*, 1(2):108–120, 2008.

[3] S Gentry, E Feron, and R Murray-Smith. Human-human haptic collaboration in cyclical Fitts' tasks. In *2005 IEEE/RSJ International Conference on Intelligent Robots and Systems*, pages 3402–3407. IEEE, 2005.

[4] D Feth, R Groten, A Peer, S Hirche, and M Buss. Performance related energy exchange in haptic human-human interaction in a shared virtual object manipulation task. In *WHC '09: Proceedings of the World Haptics 2009 - Third Joint EuroHaptics conference and Symposium on Haptic Interfaces for Virtual Environment and Teleoperator Systems*. Technical University of Munich, IEEE Computer Society, March 2009.

[5] N Jarrassé, T Charalambous, and E Burdet. A Framework to Describe, Analyze and Generate Interactive Motor Behaviors. *PLoS ONE*, 7(11), 2012.

[6] A Sawers and L H Ting. Perspectives on human-human sensorimotor interactions for the design of rehabilitation robots. *Journal of NeuroEngineering and Rehabilitation*, 11(1), 2014.

[7] J W Krakauer, Z M Pine, M F Ghilardi, and C Ghez. Learning of visuomotor transformations for vectorial planning of reaching trajectories. *Journal of Neuroscience*, 20(23):8916–8924, 2000.

[8] M Kawato, K Furukawa, and R Suzuki. A Hierarchical Neural-Network Model for Control and Learning of Voluntary Movement. *Biological Cybernetics*, 57(3):169–185, 1987.

[9] K A Thoroughman and R Shadmehr. Learning of action through adaptive combination of motor primitives. *Nature*, 407(6805):742–747, 2000.

[10] R Shadmehr, M A Smith, and J W Krakauer. Error Correction, Sensory Prediction, and Adaptation in Motor Control. *Annual Review of Neuroscience*, 33(1):89–108, June 2010.

[11] K Wei and K P Körding. Relevance of error: what drives motor adaptation? *Journal of Neurophysiology*, 101(2):655–664, January 2009.

[12] M A Smith, A Ghazizadeh, and R Shadmehr. Interacting adaptive processes with different timescales underlie short-term motor learning. *PLOS Biology*, 4(6):1035–1043, June 2006.

[13] H G Wu, Y R Miyamoto, L N Gonzalez Castro, B P Ölveczky, and M A Smith. Temporal structure of motor variability is dynamically regulated and predicts motor learning ability. *Nature Neuroscience*, 17(2):312–321, January 2014.

[14] A K Dhawale, M A Smith, and B P Ölveczky. The Role of Variability in Motor Learning. 40(1):479–498, July 2017.

[15] L Marchal-Crespo and D J Reinkensmeyer. Review of control strategies for robotic movement training after neurologic injury. *Journal of NeuroEngineering and Rehabilitation*, 6(1), 2009.

[16] L Marchal-Crespo, N Rappo, and R Riener. The effectiveness of robotic training depends on motor task characteristics. *Experimental Brain Research*, 235(12):3799–3816, December 2017.

[17] L Marchal-Crespo, M Bannwart, R Riener, and H Vallery. The effect of haptic guidance on learning a hybrid rhythmic-discrete motor task. *IEEE Transactions on Haptics*, pages 1–16, January 2013.

[18] R A Schmidt and R A Bjork. New Conceptualizations of Practice: Common Principles in Three Paradigms Suggest New Concepts for Training. *Psychological Science*, 3(4):207–218, 1992.

[19] C J Winstein, P S Pohl, and R Lewthwaite. Effects of Physical Guidance and Knowledge of Results on Motor Learning: Support for the Guidance Hypothesis. *Research Quarterly for Exercise and Sport*, 65(4):316–323, December 1994.

[20] E H F van Asseldonk, M Wessels, A H A Stienen, F C T van der Helm, and H van der Kooij. Influence of haptic guidance in learning a novel visuomotor task. *Journal of Physiology - Paris*, 103(3-5):276–285, September 2009.

[21] M K O'Malley, A Gupta, M Gen, and Y Li. Shared Control in Haptic Systems for Performance Enhancement and Training. *Journal of Dynamic Systems, Measurement, and Control*, 128(1):75–11, 2006.

[22] L Marchal-Crespo, J Lopez-Oloriz, L Jaeger, and R Riener. Optimizing learning of a locomotor task: Amplifying errors as needed. In *36th Annual International Conference of the IEEE Engineering in Medicine and Biology Society*, pages 5304–5307. IEEE, August 2014.

[23] H Heuer and J Lüttgen. Robot assistance of motor learning: A neuro-cognitive perspective. *Neuroscience & Biobehavioral Reviews*, 56:222–240, 2015.

[24] L Marchal-Crespo, M van Raai, G Rauter, P Wolf, and R Riener. The effect of haptic guidance and visual feedback on learning a complex tennis task. *Experimental Brain Research*, 231(3):277–291, September 2013.

[25] P M Bays, J R Flanagan, and D M Wolpert. Interference between velocity-dependent and position-dependent force-fields indicates that tasks depending on different kinematic parameters compete for motor working memory. *Experimental Brain Research*, 163(3):400–405, April 2005.

[26] C Tong, D M Wolpert, and J R Flanagan. Kinematics and Dynamics Are Not Represented Independently in Motor Working Memory: Evidence from an Interference Study. *Journal of Neuroscience*, 22(3):1108–1113, February 2002.

[27] A Melendez-Calderon, V Komisar, and E Burdet. Interpersonal strategies for disturbance attenuation during a rhythmic joint motor action. *Physiology & Behavior*, 147:348–358, 2015.

[28] R Shadmehr and F A Mussa-Ivaldi. Adaptive Representation of Dynamics During Learning of a Motor Task. *Journal of Neuroscience*, 14(5):3208–3224, May 1994.

[29] G Wulf and C H Shea. Principles derived from the study of simple skills do not generalize to complex skill learning. *Psychonomic Bulletin & Review*, 9(2):185–211, May 2002.

[30] L Shmuelof, J W Krakauer, and P Mazzoni. How is a motor skill learned? Change and invariance at the levels of task success and trajectory control. *Journal of Neurophysiology*, 108(2):578–594, June 2012.

[31] T Kitago and J W Krakauer. Motor learning principles for neurorehabilitation. *Handbook of clinical neurology*, 110:93–103, 2013.

[32] R A Schmidt and T D Lee. *Motor control and learning: a behavioral emphasis.* Human Kinetics, Champaign, IL, 5 edition, 2011.

[33] A Sawers, T Bhattacharjee, J L McKay, M E Hackney, C C Kemp, and L H Ting. Small forces that differ with prior motor experience can communicate movement goals during human-human physical interaction. *Journal of NeuroEngineering and Rehabilitation*, 14(1):8, January 2017.

[34] J A Galvez, A Budovitch, S J Harkema, and D J Reinkensmeyer. Trainer variability during step training after spinal cord injury: Implications for robotic gait-training device design. *Journal of Rehabilitation Research and Development*, 48(2):147–14, 2011.

[35] M A Guadagnoli and T D Lee. Challenge point: a framework for conceptualizing the effects of various practice conditions in motor learning. *Journal of Motor Behavior*, 36(2):212–224, June 2004.

[36] J E Duarte and D J Reinkensmeyer. Effects of robotically modulating kinematic variability on motor skill learning and motivation. 113(7):2682–2691, 2015.

[37] D Feygin, M Keehner, and F Tendick. Haptic Guidance: Experimental Evaluation of a Haptic Training Method for a Perceptual Motor Skill. In *Proceedings 10th Symposium on Haptic Interfaces for Virtual Environment and Teleoperator Systems. HAPTICS 2002*, pages 40–47. IEEE Computer Society, March 2002.

[38] J Bluteau, S Coquillart, Y Payan, and E Gentaz. Haptic guidance improves the visuo-manual tracking of trajectories. 3(3):e1775–7, March 2008.

[39] J Klein, S J Spencer, and D J Reinkensmeyer. Breaking it down is better: haptic decomposition of complex movements aids in robot-assisted motor learning. *IEEE Transactions on Neural Systems and Rehabilitation Engineering*, 20(3):268–275, April 2012.

[40] N Sebanz, H Bekkering, and G Knoblich. Joint action: bodies and minds moving together. *Trends in Cognitive Sciences*, 10(2):70–76, February 2006.

[41] C Granados and G Wulf. Enhancing motor learning through dyad practice: Contributions of observation and dialogue. *Research Quarterly for Exercise and Sport*, 78 (3):197–203, June 2007.

[42] K Baur, P Wolf, R Riener, and J E Duarte. Making neurorehabilitation fun: Multiplayer training via damping forces balancing differences in skill levels. In *2017 International Conference on Rehabilitation Robotics (ICORR*, pages 876–881. IEEE, 2017.

[43] M Mace, N Kinany, P Rinne, A Rayner, P Bentley, and E Burdet. Balancing the playing field: Collaborative gaming for physical training. *Journal of NeuroEngineering and Rehabilitation*, 14(1):1, November 2017.

[44] C H Shea, G Wulf, and Chad Whitacre. Enhancing Training Efficiency and Effectiveness Through the Use of Dyad Training. *Journal of Motor Behavior*, 31(2): 119–125, 1999.

[45] A G Mattar and P L Gribble. Motor Learning by Observing. *Neuron*, 46(1):153–160, 2005.

[46] J R Flanagan and R S Johansson. Action plans used in action observation. *Nature*, 424(6950):769–771, 2003.

[47] A Takagi, G Ganesh, T Yoshioka, M Kawato, and E Burdet. Physically interacting individuals estimate the partner's goal to enhance their movements. *Nature Human Behaviour*, 1(3):0054, 2017.

[48] A Takagi, F Usai, G Ganesh, V Sanguineti, and E Burdet. Haptic communication between humans is tuned by the hard or soft mechanics of interaction. *PLoS Computational Biology*, 14(3):e1005971–17, March 2018.

[49] A Takagi, M Hirashima, D Nozaki, and E Burdet. Individuals physically interacting in a group rapidly coordinate their movement by estimating the collective goal. *eLife*, 8:1081, February 2019.

[50] A J Nagengast, D A Braun, and D M Wolpert. Optimal control predicts human performance on objects with internal degrees of freedom. *PLoS Computational Biology*, 5(6):e1000419–e1000419, June 2009.

[51] S S Shergill, P M Bays, C D Frith, and D M Wolpert. Two Eyes for an Eye: The Neuroscience of Force Escalation. 301(5630):187–187, July 2003.

[52] B Onneweer, W Mugge, and A C Schouten. Force Reproduction Error Depends on Force Level, Whereas the Position Reproduction Error Does Not. *IEEE Transactions on Haptics*, 9(1):54–61, March 2016.

[53] L D Walsh, J L Taylor, and S C Gandevia. Overestimation of force during matching of externally generated forces. *The Journal of Physiology*, 589(3):547–557, 2011.

[54] W Mugge, J Schuurmans, A C Schouten, and F C T van der Helm. Sensory Weighting of Force and Position Feedback in Human Motor Control Tasks. *Journal of Neuroscience*, 29(17):5476–5482, April 2009.

[55] F E van Beek, W M Bergmann Tiest, and A M L Kappers. Anisotropy in the Haptic Perception of Force Direction and Magnitude. *IEEE Transactions on Haptics*, 6(4): 399–407, December 2013.

[56] F E van Beek, W M Bergmann Tiest, W Mugge, and A M L Kappers. Haptic perception of force magnitude and its relation to postural arm dynamics in 3D. *Scientific Reports*, 5(1):18004, 2015.

[57] B Onneweer. *Is the force wIth you?* PhD thesis, February 2016.

[58] A W de Jonge, J G W Wildenbeest, H Boessenkool, and D A Abbink. The Effect of Trial-by-Trial Adaptation on Conflicts in Haptic Shared Control for Free-Air Teleoperation Tasks. *IEEE Transactions on Haptics*, 9(1):111–120, March 2016.

[59] M Khoramshahi and A Billard. A dynamical system approach to task-adaptation in physical human–robot interaction. *Autonomous Robots*, 56(8):692, 2018.

[60] Y Li, G Carboni, F Gonzalez, D Campolo, and E Burdet. Differential game theory for versatile physical human–robot interaction. *Nature Machine Intelligence*, 1(1): 36–43, January 2019.

[61] A Mörtl, M Lawitzky, A Kucukyilmaz, T M Sezgin, C Basdogan, and S Hirche. The role of roles: Physical cooperation between humans and robots. *The International Journal of Robotics Research*, 31(13):1656–1674, 2012.

[62] L Peternel, T Petrič, E Oztop, and J Babič. Teaching robots to cooperate with humans in dynamic manipulation tasks based on multi-modal human-in-the-loop approach. *Autonomous Robots*, 36(1-2):123–136, January 2014.

[63] E Burdet, R Osu, D W Franklin, T E Milner, and M Kawato. The central nervous system stabilizes unstable dynamics by learning optimal impedance. *Nature*, 414 (6862):446–449, November 2001.

[64] D W Franklin, G Liaw, T E Milner, R Osu, E Burdet, and M Kawato. Endpoint stiffness of the arm is directionally tuned to instability in the environment. *Journal of Neuroscience*, 27(29):7705–7716, July 2007.

[65] K Mojtahedi, B Whitsell, P Artemiadis, and M Santello. Communication and Inference of Intended Movement Direction during Human–Human Physical Interaction. *Frontiers in neurorobotics*, 11:127–23, April 2017.

[66] M Della Penna, M M van Paassen, D A Abbink, M Mulder, and M Mulder. Reducing steering wheel stiffness is beneficial in supporting evasive maneuvers. *2010 IEEE International Conference on Systems, Man and Cybernetics*, pages 1628–1635, November 2010.

[67] D Van Baelen, J Ellerbroek, M van Paassen, and M Mulder. Design of a Haptic Feedback System for Flight Envelope Protection. In *2018 AIAA Modeling and Simulation Technologies Conference*, page 1, Reston, Virginia, January 2018. American Institute of Aeronautics and Astronautics.

[68] V T Chackochan and V Sanguineti. Incomplete information about the partner affects the development of collaborative strategies in joint action. *bioRxiv*, pages 1–21, November 2018.

[69] L Simmatis, J Krett, S H Scott, and A Y Jin. Robotic exoskeleton assessment of transient ischemic attack. *PLoS ONE*, 12(12), December 2017.

[70] T C Bourke, C R Lowrey, S P Dukelow, S D Bagg, K E Norman, and S H Scott. A robot-based behavioural task to quantify impairments in rapid motor decisions and actions after stroke. *Journal of NeuroEngineering and Rehabilitation*, pages 1–13, October 2016.

[71] J Werkmeister and A Slocum. Theoretical and experimental determination of capstan drive stiffness. *Precision Engineering*, 31(1):55–67, December 2006.

[72] G Ellis. Cures for low-frequency mechanical resonance in industrial servo systems. *Conference Record of the IEEE Industry Applications Conference. th IAS Annual Meeting Cat. No.CH*, 1:252–258, 2001.

[73] J van Oosterhout, J G W Wildenbeest, H Boessenkool, C J M Heemskerk, M R de Baar, F C T van der Helm, and D A Abbink. Haptic Shared Control in Tele-Manipulation: Effects of Inaccuracies in Guidance on Task Execution. *IEEE Transactions on Haptics*, 8(2):164–175, 2015.

Appendices

Appendix A.

BROS
Supplementary information

Table A.1 shows the sum-of-sine excitation signal parameters which was used for evaluating the position control loop bandwidth. The excitation signal is calculated by summing 25 sines:

$$x(t), y(t) = \sum_{k=1}^{25} A_k^{(x,y)} \sin\left(2\pi f_k^{(x,y)} t + \varphi_k^{(x,y)}\right). \tag{A.1}$$

The excitation signals contained independent and non-harmonic frequencies, which were multiple integers $n^{(x,y)}$ of the frequency resolution $\delta f = 1/T_m$, where T_m is the measurement time of 30 s per repetition. Amplitudes were scaled such that the signal variance was $21.25\,\mathrm{mm}^2$. The amplitudes at frequencies above 30 Hz were reduced with a factor 2. Phases were chosen such that the resulting time traces yielded a minimum crest factor. See Table A.1 for the excitation signal parameters.

Table A.1. | **Excitation signal parameter values for evaluating the low-level position control loop bandwidth and system identification.**

#	$n^{(x)}$ [−]	$f^{(x)}$ [Hz]	$A^{(x)}$ [m]	$\varphi^{(x)}$ [rad]	$n^{(y)}$ [−]	$f^{(y)}$ [Hz]	$A^{(y)}$ [m]	$\varphi^{(y)}$ [rad]
1	5	0.167	0.005	1.200	3	0.100	0.005	4.613
2	7	0.233	0.005	1.063	8	0.267	0.005	3.099
3	11	0.367	0.005	1.389	10	0.333	0.005	−1.336
4	13	0.433	0.005	−0.191	14	0.467	0.005	−0.455
5	17	0.567	0.005	4.361	19	0.633	0.005	0.316
6	23	0.767	0.005	3.551	24	0.800	0.005	−1.543
7	29	0.967	0.005	−1.299	31	1.033	0.005	1.923
8	37	1.233	0.005	−0.010	41	1.367	0.005	3.287
9	47	1.567	0.005	1.019	53	1.767	0.005	−0.551
10	61	2.033	0.005	0.473	67	2.233	0.005	2.378
11	79	2.633	0.005	1.168	83	2.767	0.005	1.074
12	103	3.433	0.005	3.484	107	3.567	0.005	−1.422
13	131	4.367	0.005	3.250	137	4.567	0.005	2.581
14	173	5.767	0.005	1.941	179	5.967	0.005	3.603
15	223	7.433	0.005	2.594	227	7.567	0.005	0.932
16	293	9.767	0.005	1.711	307	10.233	0.005	0.818
17	379	12.633	0.005	3.758	383	12.767	0.005	1.500
18	491	16.367	0.005	3.178	499	16.633	0.005	2.751
19	631	21.033	0.005	−0.845	641	21.367	0.005	−0.286
20	821	27.367	0.005	−0.502	823	27.433	0.005	1.980
21	1063	35.433	0.0025	2.412	1069	35.633	0.0025	2.799
22	1381	46.033	0.0025	0.958	1399	46.633	0.0025	1.804
23	1787	59.567	0.0025	4.392	1789	59.633	0.0025	4.170
24	2311	77.033	0.0025	0.447	2333	77.767	0.0025	1.541
25	2999	99.967	0.0025	−1.022	3001	100.033	0.0025	1.189

Appendix B.

Haptic interaction does not improve motor learning of a visuomotor rotation Supplementary information

B.1. Target signal design

The target signal is defined as a quasi-random sum-of-sine signals which are designed following human-in-the-loop tracking signal design guidelines [1]. The target signal movement $f^{(x,y)}(t)$ in x and y was generated using

$$f^{(x,y)}(t) = \sum_{k=1}^{4} A_k^{(x,y)} \sin\left(\omega_k^{(x,y)} t + \varphi_k^{(x,y)}\right), \tag{B.1}$$

where $A_k^{(x,y)}$ is the amplitude, $\omega_k^{(x,y)}$ is the frequency and $\varphi_k^{(x,y)}$ is the phase of sine k. Both sum-of-sines in x and y consist of four sines, each with a different amplitude, frequency and phase which are listed in Table B.1.

The frequencies spanned a frequency bandwidth of $0.943\,\mathrm{rad\,s^{-1}}$ to $3.142\,\mathrm{rad\,s^{-1}}$, similar to Ganesh et al. [2]. The frequencies were multiples $n_k^{(x,y)}$ of the measurement time base frequency $\omega_m = 2\pi/T_m = 0.3142\,\mathrm{rad\,s^{-1}}$ (the measurement time for each trial was $T_m = 20\,\mathrm{s}$). The frequency multiples and frequencies are given in Table B.1.

We used a second-order low-pass filter to determine the amplitudes [3]:

$$|A\,(j\omega)| = \left|\left(\frac{1 + T_1 j\omega}{1 + T_2 j\omega}\right)^2\right|, \tag{B.2}$$

where $T_1 = 0.1\,\mathrm{s}$ and $T_2 = 0.8\,\mathrm{s}$. The amplitude set in x and y were both scaled to a variance of $12\,\mathrm{cm}^2$. The reduced amplitudes at the higher frequencies yields a target movement that is not overly difficult, but still results in quasi-random movement.

Phases were selected from a large set of randomly generated phases such that the resulting time traces of the target signal had a minimum crest factor (no excessive peaks in the time traces) [1].

Table B.1. | Target signal sum-of-sine parameter values.

k	$n^{(x)}$[−]	$\omega_k^{(x)}$[rad s^{-1}]	$A_k^{(x)}$[cm]	$\varphi_k^{(x)}$[rad]	$n_k^{(y)}$[−]	$\omega_k^{(y)}$[rad s^{-1}]	$A_k^{(y)}$[cm]	$\varphi_k^{(y)}$[rad]
1	3	0.94	2.87	−7.77	4	1.26	2.71	−0.71
2	4	1.26	2.71	−8.53	5	1.57	2.53	−3.45
3	6	1.89	2.35	−4.36	7	2.20	2.16	3.92
4	9	2.83	1.80	−3.79	10	3.142	1.64	4.93

B.2. Analysis: error after learning and improvement when connected to a better partner

We analyzed whether physical interaction with a *better* partner improves your own motor performance after learning. First, we identified the superior- and inferior-performing partner in each pair of the interaction, stiff connection and continuous interaction groups. We compared single trial performance between the partners in a pair for all single trials in blocks 2–4 using independent-samples t-tests. This resulted in two subgroups within each interaction group: (1) a group inferior performing partners which physically interacted with a better partner and (2) a group superior partners which interacted with a worse partner. Figure B.1A shows the individual error after learning for both groups, including the solo group error after learning for comparison. Interacting with a better partner seemed to lead to significantly worse error after learning compared to practicing the task alone (which is supported by a significant Kruskal-Wallis test, $\chi^2(3) = 9.94$, $p = 0.019$), however post-hoc tests showed no significant differences. Interaction with a worse partner did not influence the error after learning compared to the solo group (Kruskal-Wallis, $\chi^2(3) = 0.74$, $p = 0.86$). Similarly, we examined whether interaction with a better partner is more beneficial in terms of motor improvement (see Fig. B.1B). Physical interaction with a better partner during learning did not lead to more improvement compared to the solo group and other interaction groups (Kruskal-Wallis test; $\chi^2(3) = 0.99$, $p = 0.803$). The same held for the participants who interacted with an inferior partner: their improvement was also not significantly different between interaction groups and the solo group ($\chi^2(3) = 0.44$, $p = 0.9321$).

B.3. Analysis: improvement due to interaction versus relative partner performance

To investigate how much motor performance improvement during interaction depends on the individual performance of the partner, we calculate the relative performance between partners and performance improvement due to the interaction [2, 4]. The interaction group performed sets of connected and single trials (CS) in each block. Using the performance of the connected and single trial in each set, the performance improvement per participant due to interaction (I) is calculated as

$$I = 1 - E_c/E_s. \tag{B.3}$$

The relative performance (R) of the partner you interact with is calculated by

$$R = 1 - E_{s,p}/E_s, \tag{B.4}$$

where $E_{s,p}$ is the partner's performance during the single trial and E_s is the participant's own performance during the same single trial. We binned the improvement in bins of 10 % of relative performance wide to reveal any trend in the improvement I versus relative performance R. The mean and s.e.m. of the improvement was calculated per bin. See Fig. B.2 for the improvement due to interaction versus relative performance curve. Interaction with a better partner during a connected trial improves performance. Interaction with a worse partner also improves performance albeit less than interaction with a better partner. Improvement benefits decrease toward zero with a progressively worse partner. The improvements due to haptic interaction are similar to those of Ganesh et al. [2]. Importantly, interaction with a worse partner leads to improvement. There is one important difference between our and their data: in our data, when your partner is approximately 40 % worse at the task, you do not improve during interaction; their data suggests that you still keep improving due to interaction, even with a progressively worse partner. The data even suggest that when your partner is approximately 50 % worse than you, interaction even hinders performance.

B.4. Supplementary Figures

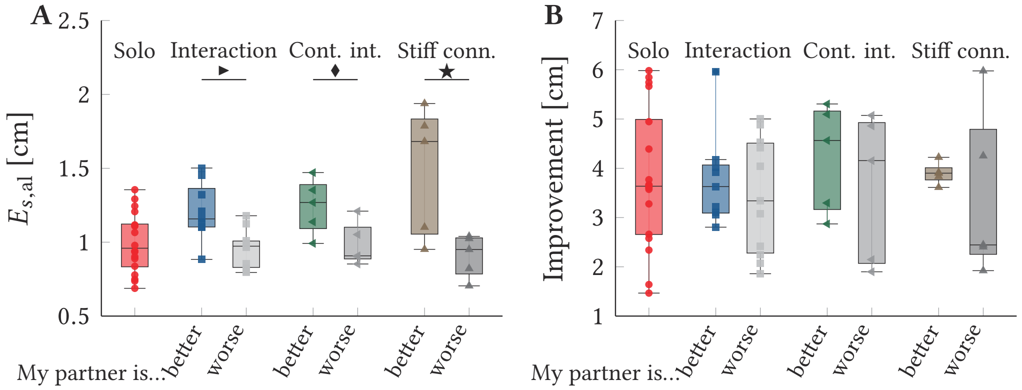

Figure B.1. | Motor performance after learning and motor improvement. **A** Error after learning of the participants who interacted with a better partner. The error after learning of the solo group is included for comparison, as well as the error after learning of the participant who were connected to an inferior partner. ►: Mann-Whitney U test, $U = 86$, $p = 0.006$. ♦: Mann-Whitney U test, $U = 22$,$p = 0.056$. ★: Mann-Whitney U test, $U = 23$, $p = 0.032$. **B** Motor improvement of the participants who interacted with a better and worse partner.

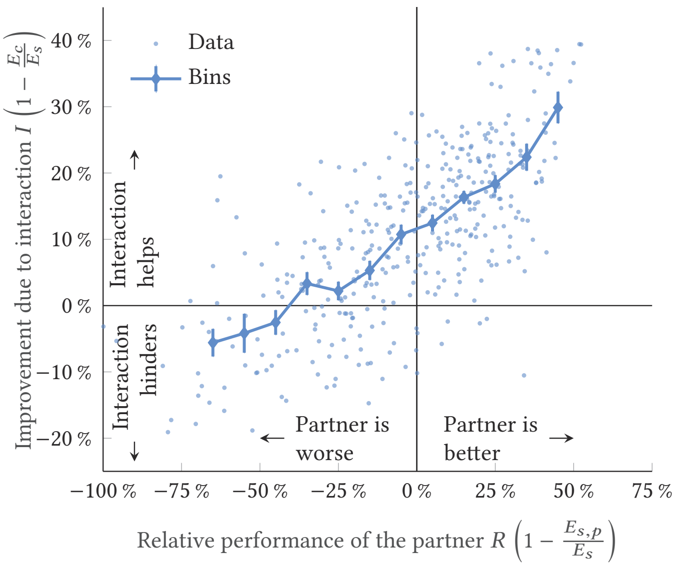

Figure B.2. | Physical interaction improves motor performance, regardless of relative partner performance. The figure shows the improvement as a function of relative performance performance.

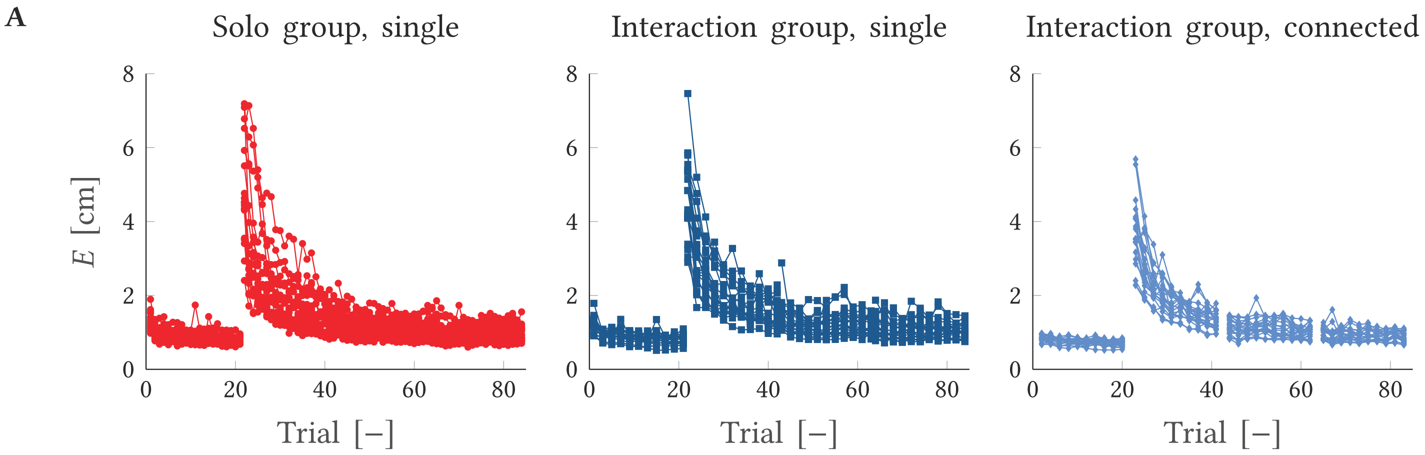

Figure B.3. | Individual performance curves for every participant for each group. **A** Solo and interaction groups. **B** Continuous interaction group. **C** Stiff connection group.

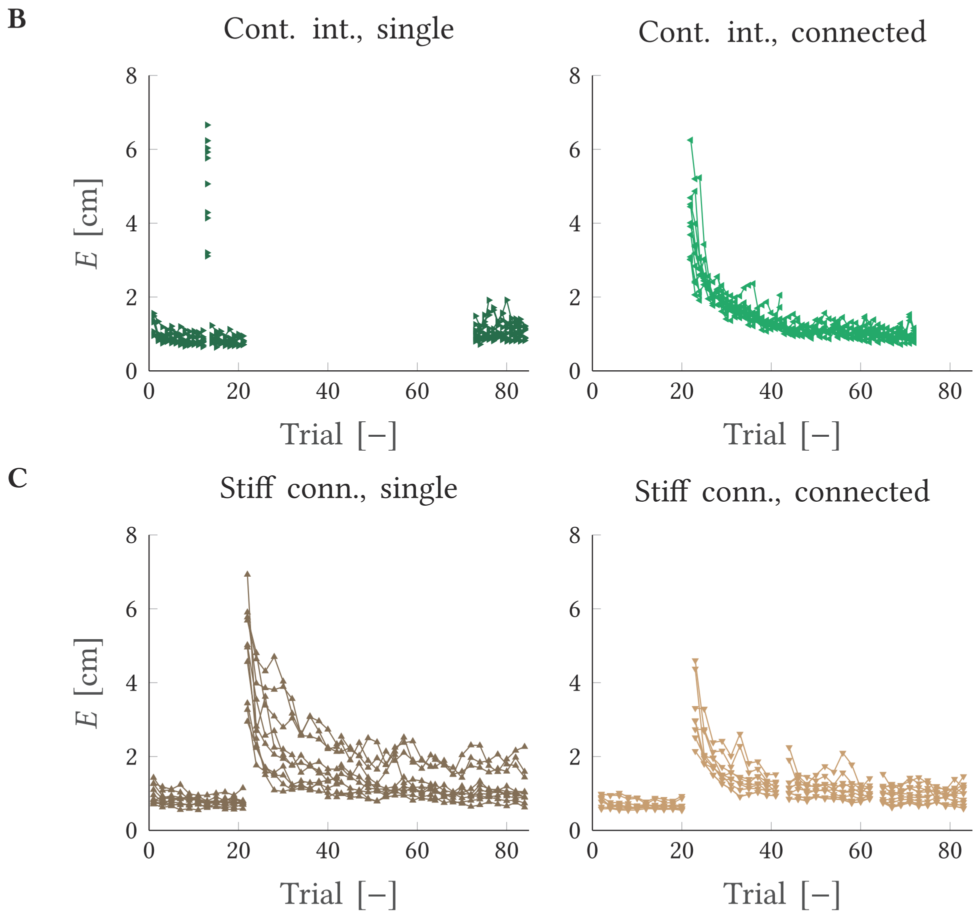

Figure B.3. | Individual performance curves for every participant for each group. **A** Solo and interaction groups. **B** Continuous interaction group. **C** Stiff connection group.

References

[1] H J Damveld, G C Beerens, M M van Paassen, and M Mulder. Design of Forcing Functions for the Identification of Human Control Behavior. *Journal of Guidance, Control, and Dynamics*, 33(4):1064–1081, 2010.

[2] G Ganesh, A Takagi, R Osu, T Yoshioka, M Kawato, and E Burdet. Two is better than one: Physical interactions improve motor performance in humans. *Scientific Reports*, 4, 2014.

[3] P M T Zaal, D M Pool, M Mulder, and M M van Paassen. Multimodal pilot control behavior in combined target-following disturbance-rejection tasks. *Journal of Guidance, Control, and Dynamics*, 32(5):1418–1428, September 2009.

[4] A Takagi, G Ganesh, T Yoshioka, M Kawato, and E Burdet. Physically interacting individuals estimate the partner's goal to enhance their movements. *Nature Human Behaviour*, 1(3):0054, 2017.

Appendix C.

Motion plans of rigidly-coupled pairs change predictably in joint reaching Supplementary information

Table C.1. | Summary of significant differences between within-dyad binned torque patterns. Some statistical differences were found between within-dyad binned torque patterns. Significant differences between bins are indicated for each dyad and each coupled and push-pull blocks as follows: first, the bins between which the differences were found are indicated, followed by the time window of the reaching movement in which the differences were found. For example, the significant difference in torque between bins 1 and 2 for dyad VIII in the coupled block (see Fig. C.1) would be indicated as: “Bin 1 – Bin 2 (0.68 s to 0.88 s)”. All the significant differences are the result of a significant F tests at a level of significance of 0.05. A dash (–-) indicates that no significant differences were found.

Dyad	Coupled	Push-pull 1	Push-pull 2
I	–	–	Bin 1 – Bin 5 (0.79 s to 1.2 s) Bin 1 – Bin 6 (0.87 s to 1.06 s) Bin 2 – Bin 5 (0.88 s to 1.2 s)
II	–	–	–
III	Bin 2 – Bin 3 (0.38 s to 0.45 s)	–	–
IV	–	–	–
V	–	–	–
VI	–	–	Bin 2 – Bin 6 (0.78 s to 0.9 s) Bin 2 – Bin 6 (0.81 s to 1.05 s)
VII	–	Bin 2 – Bin 4 (0.7 s to 1.2 s) Bin 2 – Bin 5 (0.74 s to 1.2 s)	–
VIII	Bin 1 – Bin 2 (0.68 s to 0.88 s) Bin 1 – Bin 3 (0.57 s to 1.04 s) Bin 1 – Bin 4 (0.5 s to 1.2 s) Bin 1 – Bin 5 (0.56 s to 1.08 s) Bin 1 – Bin 6 (0.69 s to 0.86 s)	–	Bin 1 – Bin 4 (0.5 s to 0.8 s 1.03 s to 1.2 s) Bin 1 – Bin 6 (0.5 s to 0.85 s 0.96 s to 1.2 s)

Table C.2. | Summary of identified state cost terms, for all blocks and all dyads.

		Coupled		Washout		Push-pull		Washout		Push-pull		Washout	
Partner		Blue	Red	Blue	Red	Blue	Red	Blue	Red	Blue	Red	Blue	Red
I	Q(1, 1)	0.54	2.17	47.17	28.48	0.19	9.01	72.24	27.13	2.58	0.79	103.58	23.75
	Q(2, 2)	0.11	0.05	1.46	1.15	0.15	0.21	1.96	1.06	0.05	0.11	1.92	1.22
II	Q(1, 1)	1.91	2.15	26.11	26.28	3.66	5.69	41.54	64.05	1.68	7.50	43.35	63.92
	Q(2, 2)	0.13	0.06	1.30	1.33	0.18	0.20	1.58	1.89	0.17	0.02	1.35	1.92
III	Q(1, 1)	7.84	5.56	29.02	49.47	6.84	0.98	21.01	40.83	1.60	11.28	24.94	118.23
	Q(2, 2)	0.25	0.15	1.46	1.43	0.01	0.40	1.31	1.47	0.34	0.30	1.42	1.20
IV	Q(1, 1)	3.16	5.13	25.58	26.47	0.30	13.12	113.60	43.74	2.82	0.97	52.63	27.51
	Q(2, 2)	0.12	0.22	1.14	1.32	0.23	0.01	1.99	1.60	0.67	1.15	1.75	1.04
V	Q(1, 1)	11.28	8.99	110.79	59.35	4.43	16.11	1118.81	152.16	21.41	1.45	58.03	47.89
	Q(2, 2)	0.01	0.45	1.70	1.82	0.09	0.57	1.66	2.09	0.01	0.34	1.80	1.45
VI	Q(1, 1)	9.72	6.55	57.35	253.77	16.77	1.28	30.96	127.77	11.12	2.13	24.88	162.88
	Q(2, 2)	0.28	0.32	2.21	2.21	0.77	0.13	1.17	2.20	1.00	0.01	1.41	2.21
VII	Q(1, 1)	2.55	1.90	55.89	22.38	0.30	5.84	22.43	21.88	7.75	0.01	19.27	26.28
	Q(2, 2)	0.01	0.19	1.87	1.37	0.01	0.42	1.54	1.74	0.35	0.04	1.98	1.16
VIII	Q(1, 1)	4.30	6.14	42.24	59.92	7.72	1.04	45.77	213.43	1.90	8.76	75.74	61.65
	Q(2, 2)	0.23	0.10	1.75	1.74	0.32	0.06	1.40	2.20	0.36	0.01	1.63	1.81

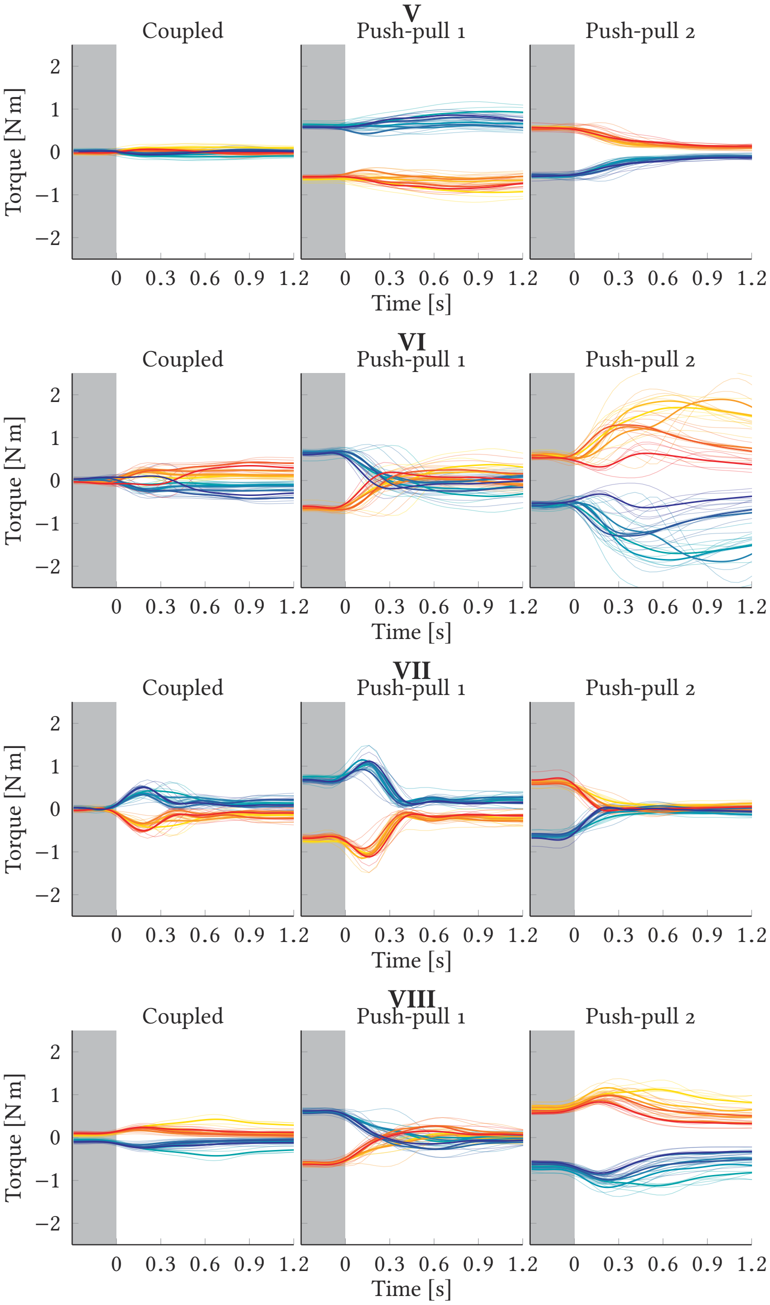

Figure C.1. | Torque patterns from dyads V–VIII in the coupled and push-pull blocks.

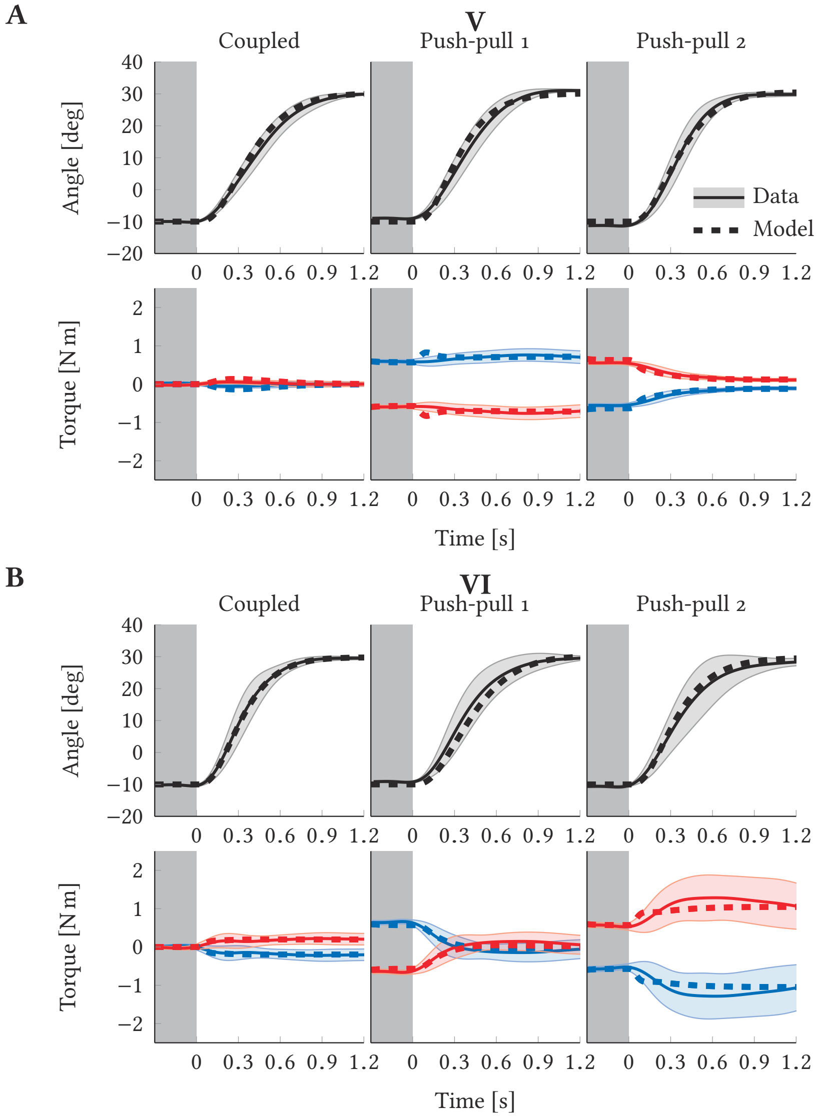

Figure C.2. | Measured and predicted trajectories and torque waveforms from dyads V–VIII in the coupled and both push-pull blocks.

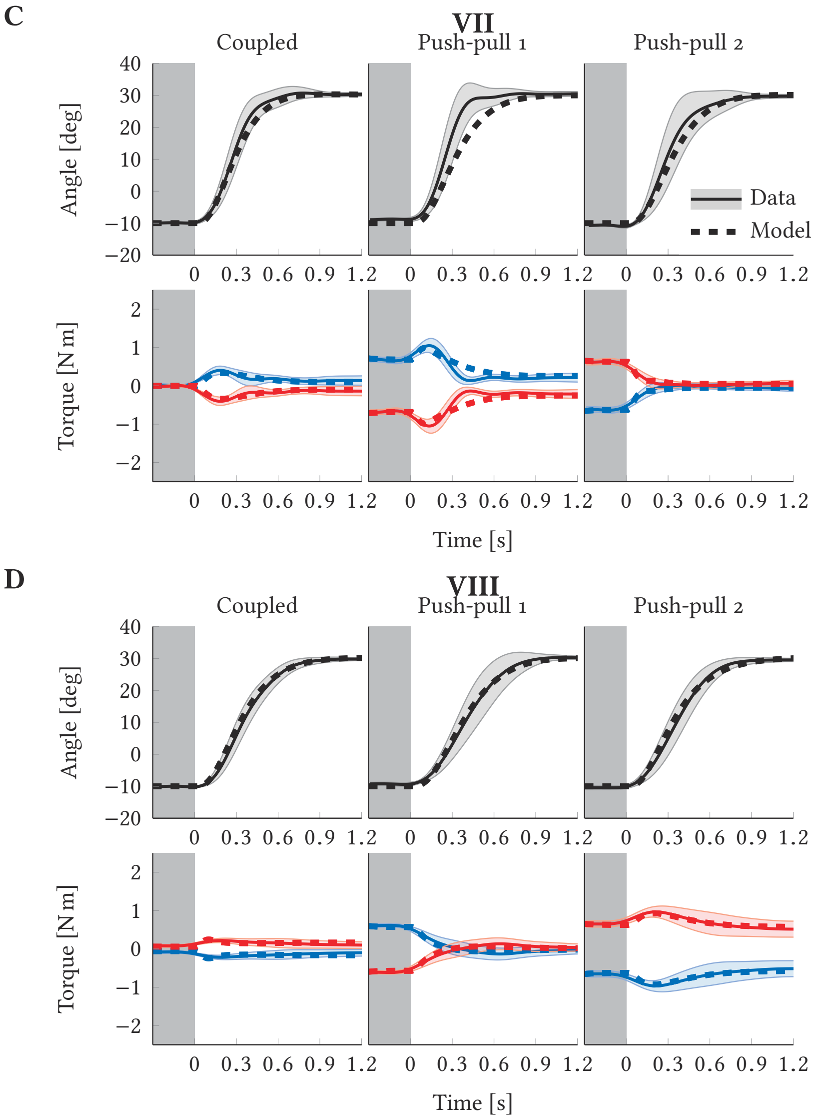

Figure C.2. | Measured and predicted trajectories and torque waveforms from dyads V–VIII in the coupled and both push-pull blocks (continued).

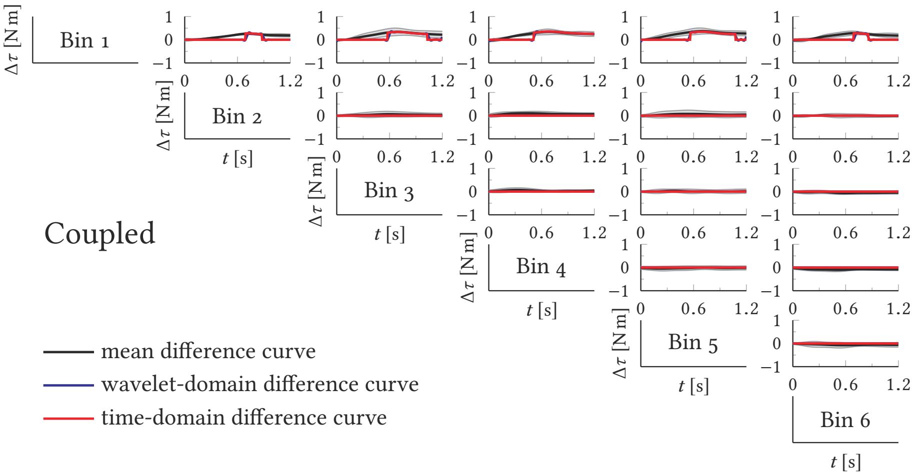

Figure C.3. | Example torque difference curves, coupled block, dyad VIII. Example of all pairwise comparisons of torque patterns between bins in the coupled block for dyad VIII. The figures show the torque difference $\Delta\tau$ between the mean torque patterns of the bins. Black traces: mean difference curves. Blue traces: statistically significant difference curves identified with wavelet-based single-factor ANOVA. When the blue trace is zero, no significant differences were found between the two bins. Non-zero values indicate significant differences. Red traces: statistically significant difference curves identified with ANOVA performed in the time domain. For dyad VIII, bin 1 showed significantly higher interaction torques compared to other bins (see the torque patterns of dyad VIII in Fig. 5.1). Other comparisons between bins were not significantly different. Statistically significant difference curves identified with ANOVA in the time-domain corroborate the wavelet-domain ANOVA results. The torque difference curves for all dyads and all connected blocks can be found online (link).

Appendix D.

Haptic communication in a tracking task Supplementary information

Here we provide the supplementary materials for Chapter 6, which includes additional information on the interaction model and estimated model parameters (Section D.1), a comparison of the improvement curves in the force field and visuomotor learning studies (Chapters 4 and 3) in Section D.2, and a detailed analysis of how the force field impaired the perception of the interaction force (Section D.4).

D.1. Interaction model

D.1.1. Connecting the two independent LQG models

The interaction model was explained in Section 6.2. Here, we describe the connection matrix C, which coupled the two independent partners (equation 6.25):

$$\begin{bmatrix} \mathbf{x}^1 \\ \mathbf{x}^2 \end{bmatrix}_{k+1} = \left(\begin{bmatrix} \mathrm{A} & \mathbf{0} \\ \mathbf{0} & \mathrm{A} \end{bmatrix} + \mathrm{C} \right) \begin{bmatrix} \mathbf{x}^1 \\ \mathbf{x}^2 \end{bmatrix}_{k} + \begin{bmatrix} \mathrm{B} & \mathbf{0} \\ \mathbf{0} & \mathrm{B} \end{bmatrix} \begin{bmatrix} \mathbf{u}^1 \\ \mathbf{u}^2 \end{bmatrix}_{k} + \begin{bmatrix} \omega^1 \\ \omega^2 \end{bmatrix}_{k},$$

The compliant connection coupling the partners, seen from each partner's perspective, is defined by (equation 6.2):

$$\begin{aligned} \mathbf{F}_i^1 &= k_s \left(\mathbf{p}^2 - \mathbf{p}^1 \right) + b_s \left(\mathbf{v}^2 - \mathbf{v}^1 \right) \text{ and} \\ \mathbf{F}_i^2 &= k_s \left(\mathbf{p}^1 - \mathbf{p}^2 \right) + b_s \left(\mathbf{v}^1 - \mathbf{v}^2 \right). \end{aligned} \qquad \text{(D.1)}$$

To implement the interaction form in connection matrix C, we divide C into four parts:

$$\mathrm{C} = \begin{bmatrix} -\mathrm{C}_p & \mathrm{C}_p \\ \mathrm{C}_p & -\mathrm{C}_p \end{bmatrix}, \qquad \text{(D.2)}$$

where $\mathbf{C}_p$ is:

$$\mathbf{C}_p = \left[\begin{array}{cccccc|c}
0 & 0 & 0 & 0 & 0 & 0 & \\
0 & 0 & 0 & 0 & 0 & 0 & \\
k_s\,\delta/m & 0 & k_s\,\delta/m & 0 & 0 & 0 & \\
0 & b_s\,\delta/m & 0 & b_s\,\delta/m & 0 & 0 & \mathbf{0}^{6\times 6} \\
0 & 0 & 0 & 0 & 0 & 0 & \\
0 & 0 & 0 & 0 & 0 & 0 & \\
\hline
\multicolumn{6}{c|}{\mathbf{0}^{6\times 6}} & \mathbf{0}^{6\times 6}
\end{array}\right]. \tag{D.3}$$

D.1.2. Estimated model parameters

Table D.1 shows the estimated model parameters (w_p, w_v, and σ_u) for the no force field blocks.

After setting the motor noise to $\sigma_u^2 = 0\,\mathrm{N}^2$, the model predicted that being connected to a better partner still improved performance and being coupled to a worse partner decreased performance. We proposed that this is because the worse performing partner benefits from the haptic guidance of the better partner. This is reflected in the estimated tracking gains (Table D.1). We compared the single performance of one partner to the single performance of the other partner in a pair using independent-samples t-tests. All highlighted $\bar{E}_s$ in Table D.1 indicate the pairs in which the single tracking performances of the partners were significantly different. The level of significance was set to 0.05 and we applied a Bonferroni correction to account for multiple testing. Comparing the mean single performance between partners in a pair and the estimated tracking gains, we generally see that the better performing partner (i.e., with lower $\bar{E}_s$) has higher tracking gains.

In the scenario where we reduced σ_u^2 to $0\,\mathrm{N}^2$ and assuming that the partners kept the same tracking gains in the connected trials, the partners with the higher tracking gains will likely assist the worse partner (pull him/her toward the target), improving their performance. The worse partner with lower tracking gains will 'drag' the better partner away from the target, deteriorating the better partner's performance.

D.2. Improvement versus relative performance: comparison of the force field and visuomotor rotation studies

Figure D.2 shows the improvement due to interaction versus the relative performance in the null field (no force field) and force field blocks of the

Table D.1. | Estimated model parameters, resulting gains and measured mean performance for each participant's single trial performance in the no force field blocks. The columns denoted with K_p and K_v are the feedback tracking gains resulting from the estimated state cost weights w_p and w_v, amongst others. The last column shows the measured mean single performance $\bar{E}_s$ per participant. The highlighted $\bar{E}_s$ indicate that the partner performed significantly different.

		w_p [−]	w_v [−]	σ_u [N]	K_p [N m^{-1}]	K_v [N s m^{-1}]	$\bar{E}_s$ [cm]
Pair 1	I	6400.9	67.1	0.306	74.75	20.14	0.945
	II	15 298.2	53.5	0.307	114.24	25.21	0.754
Pair 2	I	12 277.4	17.8	0.332	102.99	22.78	0.829
	II	9086.0	48.0	0.200	88.78	21.60	0.758
Pair 3	I	11 280.6	99.6	0.345	98.24	24.19	0.855
	II	8158.2	44.4	0.282	84.28	20.86	0.849
Pair 4	I	11 293.7	15.3	0.255	98.93	22.14	0.771
	II	10 373.1	28.6	0.372	94.83	21.92	0.909
Pair 5	I	6857.1	31.2	0.183	77.55	19.50	0.799
	II	6181.9	1.2	0.396	73.97	17.99	1.076
Pair 6	I	13 582.2	19.2	0.262	108.13	23.53	0.722
	II	7689.5	91.5	0.161	81.57	21.75	0.762
Pair 7	I	4529.3	3.2	0.161	63.57	16.40	0.883
	II	15 668.3	12.3	0.343	115.91	24.43	0.783
Pair 8	I	19 237.9	6.0	0.281	128.02	25.92	0.679
	II	19 511.9	3.5	0.355	128.92	25.98	0.748
Pair 9	I	10 745.6	97.8	0.294	95.96	23.84	0.824
	II	9315.6	89.5	0.236	89.57	22.79	0.789
Pair 10	I	9551.7	12.9	0.260	91.24	20.96	0.807
	II	10 621.4	94.4	0.264	95.44	23.69	0.779

force field study (Chapter 3) and the baseline block and visuomotor rotation blocks of the visuomotor study (Chapter 4) We fitted the same linear model as equation 6.12 to the data with block/experiment type as factor (e.g., no force field, force field, no visuomotor rotation, visuomotor rotation). We found no significant effect of block/experiment type: $F(3, 1413) = 1.57$, $p = 0.195$.

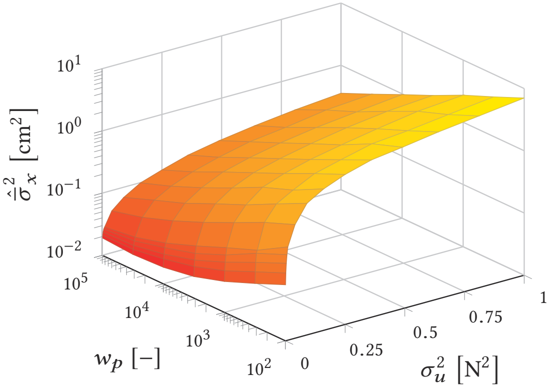

Figure D.1. | The model's predicted motor output variability $\hat{\bar{\sigma}}_x^2$ depends on the position weight w_p and motor noise σ_u^2

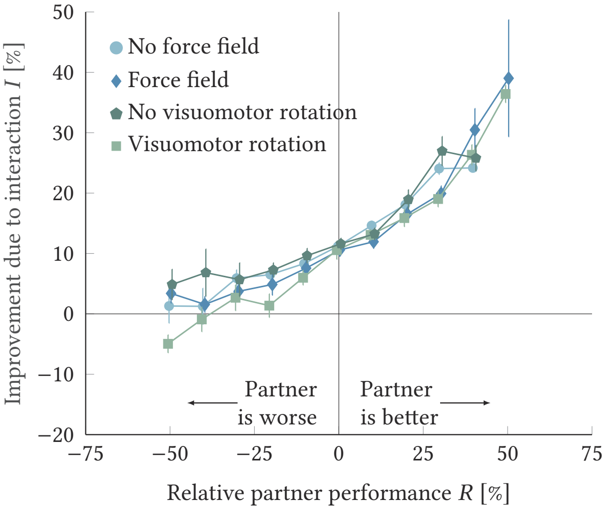

Figure D.2. | Improvement due to interaction versus relative performance; comparison between the force field and visuomotor rotation studies. The error bars indicate the s.e.m.

D.3. Improvement versus relative performance: motor variability-reducing effect of the compliant connection

In the chapter, we set σ_u^2 to $0\,\mathrm{N}^2$ to investigate whether haptic interaction improves performance by partially reducing the motor variability of each individual. To complement this approach, we also simulated the interaction model with identical motor noise time realizations for both partners to illustrate that the improvements are due to the motor variability-reducing effect of the compliant connection. Indeed, as can be seen in Fig. D.3, the improvement benefit of interacting with a worse partner disappears, indicating that the compliant connection partially counteracts the uncorrelated motor noise of each individual.

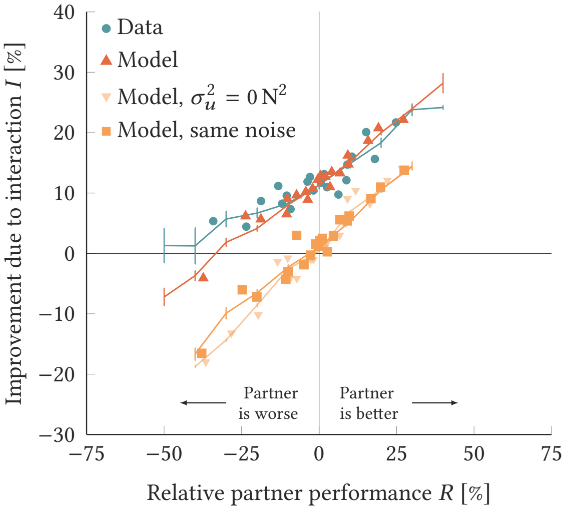

Figure D.3. | The compliant connection partially counteracts the motor variability due to (uncorrelated) motor noise. We simulated the interaction with the same motor noise for both partners.

D.4. The superimposed force field impaired the perception of the interaction force

We analyzed how the force field force impaired the perception of the interaction force. To estimate the interaction force $\hat{\mathbf{F}}_i$, participants had to decompose the perceived total force $\mathbf{F}_t$, which is the (sign-adjusted) sum of the actual interaction force $\mathbf{F}_i$ and force field force $\mathbf{F}_c$ (see Fig. 6.2B):

$$\mathbf{F}_t = \mathbf{F}_i + \mathbf{F}_c. \tag{D.4}$$

To differentiate the interaction force from the force field force, people can use an internal model of the force field (denoted as $\hat{\mathbf{D}}$) to predict the force field forces $\hat{\mathbf{F}}_c$ based on their current hand velocity ($\hat{\mathbf{F}}_c = \hat{\mathbf{D}}\mathbf{v}$) [1–5]. People generally do not fully learn the force field; studies found that humans only learn to compensate ~80 % of the perturbation [3, 5, 6]. As explained in Section 6.2, we calculated the force field compensation factor α, which served as a measure of how much each participant on average compensated for the force field forces in every single trial [4, 6]. The compensation factor α is used to model the participant's internal model of the force field: $\hat{\mathbf{D}} = \alpha\mathbf{D}$. The participant can estimate the interaction force $\hat{\mathbf{F}}_i$ as follows using equation D.4:

$$\hat{\mathbf{F}}_i = \mathbf{F}_t - \hat{\mathbf{F}}_c = \mathbf{F}_t - \alpha\mathbf{D}\mathbf{v} = \mathbf{F}_i + (1-\alpha)\,\mathbf{D}\mathbf{v}. \tag{D.5}$$

Hence, because the participant has an incomplete model of the force field perturbation resulting in a force $\mathbf{F}_{c,u} = (1-\alpha)\,\mathbf{D}\mathbf{v}$, the participant's estimate of the interaction force is biased, degrading the quality of any potential information exchange through the interaction force.

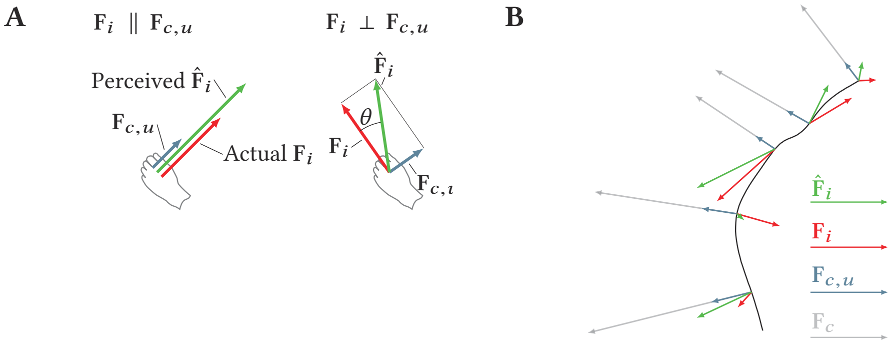

Figure D.4. | Force field compensation factor and potential bias of the interaction force perception due to the uncompensated force-field force. **A** The perceived interaction force is biased by to the uncompensated force-field force in the magnitude and direction (same as Fig. 6.5A). **B** Example of the uncompensated force-field force (calculated using the final compensation factor of the participant) and interaction force (measured) and the resulting perceived interaction force in part of the tracking task for one participant.

The uncompensated force-field force can introduce a bias in magnitude and direction in the estimation of the real interaction force; two examples are given in Fig. 6.5B. We define the magnitude bias as the ratio of the perceived interaction force with the real interaction force $\|\hat{\mathbf{F}}_i\|/\|\mathbf{F}_i\|$ and the directional bias θ as the angle between the perceived interaction force with the real interaction force, both time-averaged across every trial. Figure D.5 shows the distribution of the magnitude bias and directional bias of all participants combined. Examination of the magnitude distribution showed that the interaction force magnitude is consistently overestimated (median of $\|\hat{\mathbf{F}}_i\|/\|\mathbf{F}_i\| = 1.27$). The directional bias has a mean and standard deviation of $\bar{\theta} = 3.5\,\text{deg}$ and $\sigma_\theta = 7.5\,\text{deg}$, respectively. Hence, even if the participants learned 86 % of the force field, the resulting estimate of the force field

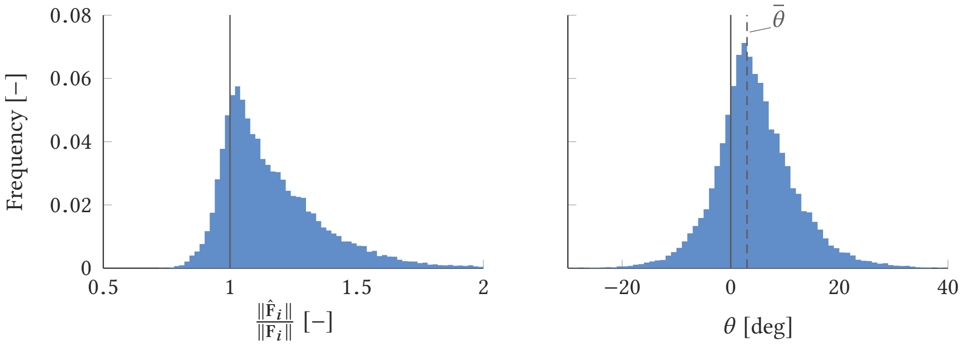

Figure D.5. | Frequency histograms of the bias in interaction force magnitude, defined as the ratio of the magnitude of the perceived and real interaction force $\|\hat{\mathbf{F}}_i\|/\|\mathbf{F}_i\|$ and the direction bias θ for all participants combined. The solid vertical lines indicate the ideal case when no bias would be present.

would still be biased in magnitude and direction, which would degrade the information that could be extracted from the interaction force.

References

[1] R Shadmehr and F A Mussa-Ivaldi. Adaptive Representation of Dynamics During Learning of a Motor Task. *Journal of Neuroscience*, 14(5):3208–3224, May 1994.

[2] J R Lackner and P DiZio. Rapid adaptation to Coriolis force perturbations of arm trajectory. *Journal of Neurophysiology*, 72(1):299–313, July 1994.

[3] R A Scheidt, D J Reinkensmeyer, M A Conditt, W Z Rymer, and F A Mussa-Ivaldi. Persistence of motor adaptation during constrained, multi-joint, arm movements. *Journal of Neurophysiology*, 84(2):853–862, July 2000.

[4] M A Smith, A Ghazizadeh, and R Shadmehr. Interacting adaptive processes with different timescales underlie short-term motor learning. *PLOS Biology*, 4(6):1035–1043, June 2006.

[5] J Izawa, T Rane, O Donchin, and R Shadmehr. Motor adaptation as a process of reoptimization. *Journal of Neuroscience*, 28(11):2883–2891, March 2008.

[6] J B Heald, D W Franklin, and D M Wolpert. Increasing muscle co-contraction speeds up internal model acquisition during dynamic motor learning. *Scientific Reports*, 8 (1):3270, 2018.

Dankwoord

Een PhD proefschrift is een *Gesamtkunstwerk*. Niet alleen omdat ik van alles geleerd heb of dat het schrijven van een proefschrift een bepaalde mate van creativiteit nodig heeft, maar voornamelijk omdat veel mensen mij geholpen hebben om alles voor elkaar te krijgen. Hier, in het meest gelezen deel van mijn boekje, ga ik mijn uiterste best doen om iedereen te bedanken. Voor het geval dat ik iemand vergeet: sorry (en ik ben je een drankje verschuldigd)!

Allereerst wil ik Herman en Edwin hartelijk bedanken voor hun begeleiding tijdens mijn promotietraject. Herman, ik kon elke vergadering weer bouwen op jouw kritische noten en nieuwe inzichten. Een van de belangrijkste dingen die ik mij zal herinneren is jouw positieve blik op mijn data: daar waar ik er flink van kon balen zag jij juist waarde. Door de vrijheid en verantwoordelijkheden die je me gaf heb ik me flink kunnen ontwikkelen. Wellicht kom ik je een keer tegen op de Haute Route!

Edwin, als goedgemutste en goedlachse copromotor stond je altijd voor me klaar. Ik zal met veel plezier terugdenken aan onze discussies en brainstormsessies waar je écht de tijd voor nam. Onvermoeibaar bleef je mijn vele schrijfsels doorlezen. Naast het wetenschappelijke werk bekommer je je ook om andere zaken omtrent je studenten, waar ik je erg dankbaar voor ben. Binnenkort nog maar eens een rondje MTB in het Nijmeegse land doen?

Arno, hoewel jij al vroeg in mijn promotietraject een andere uitdaging vond, wil ik je bedanken dat je me aan boord hebt gebracht. Je bleef me pushen om mijn onderzoek praktisch te houden. Dat is niet altijd gelukt, maar ik herken nu zeker de waarde in jouw standpunt. Bedankt!

Although my defense still has to happen as I write these acknowledgements, I would like to thank my defense committee (professors Abbink, Marchal-Crespo, Smeets, Brouwer and Buurke) for vetting my work. I am sure that you will put my feet to the fire, as is the norm in science; I look forward to it (well, at least now I still do)!

I was fortunate enough to spend some time in professor Etienne Burdet's lab at Imperial College London; one of the chapters resulted from this visit. Etienne, thank you for your hospitality and Atsushi, thank you for the collaboration and good times in and out of the lab.

Dat ik het naar mijn zin gehad tijdens mijn promotie komt mede door de leuke collega's bij de vakgroep Biomechanical Engineering. Tycho, Gijs, Victor, Joan, Serdar, Cristina, Michelle, Ronald, Guillaume, Simone, René, Kostas, Stergios, Frank, Amber, Mark, Iris, Arvid, de VICI-boys (Kyrian, Quint, Wolfie, Alan, Martijn), Claudia, Martijn Wessels, Wouter, Nikolai en nog vele anderen: bedankt voor de fijne dagen op kantoor en gezelligheid! En mogen er nog veel stiltes vallen tijdens de lunch waarin iedereen zijn of haar onderzoek overpeinst; ik zal er helaas niet meer zijn om ze ongemakkelijk te doorbreken. Islam, the latest addition to our office, thank you for your friendliness and for spoiling me with good coffee every morning. Good luck with your new lab! Daarnaast wil ik de collega's van het Symbionics project bedanken voor de nuttige discussies en gezelligheid: Ronald, Kostas, Stergios, Teun, Claudia, Laura, Bob en Nauzef, alle PI's en de sponsoren. Claudia, vanaf het begin was het gezellig bij ons op het kantoor en het is nog steeds gezellig als je op de UT bent. Dank je voor al je hulp en wijze raad. Ik heb gehoord dat de kroketjes in Rotterdam ook best goed zijn, kom je eens langs?

Ik ken maar weinig mensen met zoveel passie voor hun vak als Victor. Victor staat voor iedereen klaar met adviezen over mechatronica (en eigen over alles). Al mijn kennis over drives, sensor resoluties, signaalversterkers en EtherCAT heb ik van hem. Dankzij Victor werd ik enthousiast over mooi gereedschap (dure hobby). En hij is ook nog eens een klimmer! Het was een plezier om met je te mogen werken en je te leren kennen, Victor!

De echte supersterren van de groep zijn Lianne en Jeanine. Bedankt dat jullie er altijd voor iedereen zijn en alles soepel laten verlopen ondanks dat de groep uit zijn voegen barst. In het bijzonder wilde ik Lianne bedanken. Lianne, bedankt dat je altijd tijd voor me nam, voor alle dingen die je voor me geregeld hebt, voor al je adviezen en uiteraard voor de Twentse spreekwoorden die ik van je geleerd heb.

Als je onderzoek doet naar mens-robot interactie, heb je een robot nodig. Gelukkig kreeg ik veel hulp bij het bouwen van BROS, 'mijn' robotische opstelling. Koen is de man die mijn CAD-geknutsel (gestuntel?) om wist te toveren naar iets dat daadwerkelijk gebouwd kon worden. Bedankt, meneer Heuver! Ooit zal ik je eruit fietsen op de mountainbike. Misschien. Daarnaast kun je geen mens-robot interactie onderzoek doen zonder mensen. Ik wil daarom alle deelnemers in mijn experimenten hartelijk danken voor hun tijd en inzet.

In de ruim vier jaar tijdens mijn PhD onderzoek heb ik met een aantal gemotiveerde studenten mogen samenwerken. Harm, Demian, Mattia, Vivian, Dave, Tom, Jolein en Eline; dank jullie wel voor de leuke onderzoeken en bedankt dat jullie me scherp hebben gehouden. Daarnaast wil ik Frits, Jeanine en Ingrid bedanken voor alle uren die ze gemaakt hebben als experimentleiders om de vele gigabytes aan data te verzamelen die in de meeste hoofdstukken is gebruikt.

Hoewel een promotie een zwart gat lijkt te zijn waar al je tijd in wordt gezogen, heb ik het geluk dat ik een hoop leuke vrienden om me heen heb die voor de hoognodige ontspanning hebben gezorgd.

Martijn, wat kan ik zeggen? Goed om te weten dat er iemand rondloopt die net zo tikt als ik! Ik kan je maar al te goed ongemakkelijk maken (lekker voor je) en jij laat geen kans onbenut om mij op mijn tekortkomingen te wijzen (we leken wel een getrouwd stel af en toe). De wekelijkse klimsessies en doordeweekse Weizen ga ik zeker missen, maar als je dacht dat je eindelijk van me af was, think again...

I would also like to thank Jared and Chris. Jared – undoubtedly the most friendly Canadian in the world – thank you for all your advice, perusal of my work ("stop writing 'for example'!"), chatting about the good and bad of life and academia, and for being an overall great guy, eh. Chris – the friendliest German in Germany – the same holds for you! Always when I thought I understood statistics, you came up with another statistical model that made my head spin. Gents, I am sure we will see each other regularly.

In de gangen van onze groep hoor je wel eens: Arvid heeft bijna drie proefschriften geschreven, maar hij heeft er maar één doctorstitel voor terug gekregen. Dat zegt veel over Arvid: hij staat altijd voor je klaar om mee te denken over de meest complexe vragen. Het is bijzonder hoe snel jij dingen oppikt en op hoog niveau mee kan denken. Bedankt voor al je hulp! Maar nog belangrijker, je bent vooral een fijne kerel en goede vriend!

Liever fijne huisgenoten dan een verre buur (of zoiets). Bob! Je was een fantastische huisgenoot en ik ben blij dat ik je heb leren kennen. Je staat onwijs positief in het leven en weet mensen te enthousiasmeren; daar kan ik nog een hoop van leren. Ook superleuk dat je je droom na bent gaan jagen in Mestreech samen met Eline. Ik kom nog vaak langs bij Radium, dus zorg maar voor genoeg taartjes of andere baksels. Met Bob kwam ook Elsa (die een échte dokter wordt) bij ons in huis. Elsa, het was supergezellig met je in huis, helemaal als je weer eens schaterlachend een serie zat te kijken! Ik vond het daarom jammer toen Bob, Eline en Elsa verhuisden, maar gelukkig kreeg ik er een echte Tukker voor terug. Coen, wat ben jij een relaxt persoon, huisgenoot en vriend. Ik heb een hoop geleerd van je nuchtere en praktische kijk op alles. Mooi om te horen hoe jij binnen tien seconden naar het Twents omschakelt zodra je je familie aan de telefoon hebt. Ik weet zeker dat we elkaar nog in de mooiste (klim)gebieden gaan zien. En veel plezier (of eerder: succes?) met de altijd goedgemutste Nienke in je nieuwe huis!

En natuurlijk ook de heren van de *Luxe Woensdag*, een begrip binnen de woensdagen die luxe zijn. Hoewel ik geen planningswonder ben (sorry!), vinden jullie het nog steeds leuk als ik er weer eens bij ben. Mark, Martin, Tim en Tom, bedankt voor de leuke tijden, de goede gesprekken en het regelmatig controleren of 'het nog wel goed gaat daar in het verre oosten'.

Des te vlakker dat Nederland is, des te enthousiaster lijken de klimmers die er wonen: Martijn (niet denken, maar klimmen), Manon (puppies & ijsjes!), Erik, Nick, Boudewijn, Mariangela, Coen, Nienke, Gert-Jan en nog velen meer. Coen, Nienke, Erik en Maikel, bedankt voor de fantastische alpineercursussen mit *der Martin* (nah, das ist nicht ideal… Joa Bomber! Tip Top!). Ik heb van alle klimavonturen genoten, met name dankzij alle leuke mensen en de (sterke) verhalen over die ene route waar je je met trillende beentjes toch doorheen hebt gewerkt[1].

Dan zijn er nog een paar extra speciale mensen die me altijd hebben bijgestaan.

Mijn ouders hebben alles mogelijk gemaakt. Pap en mam, ik ben jullie eeuwig dankbaar voor al jullie steun in de leuke tijden maar ook minder leuke perioden. Dat ik niet wegloop voor een uitdaging heb ik van jullie. Hoewel mijn grijze haren hoofdzakelijk genetisch bepaald zijn, vermoed ik dat ik door deze PhD nog grijzer ga eindigen dan jullie! Mijn 'kleine' broertje Tom: het is fantastisch om te zien hoe jij je plek hebt gevonden in de afgelopen jaren (en wie had ooit gedacht dat jij Arcen zou verruilen voor de stad?)!

Als laatste: Brigit. Voor een buitenstaander lijkt het alsof ik alles uit de kast heb getrokken om zover mogelijk van je weg te blijven (eerst Boston, dan Enschede), maar niets is minder waar. Dank je voor je begrip, dat je er altijd voor me was, mij sociaal hield, voor je geduld, en voor je liefde. En aangezien iedereen dit lezen kan stop ik hier, want anders wordt het misschien nog gênant (net zoals jouw pogingen om Limburgs te praten).

Niek

Enschede, een mooie lentedag in 2019

---

[1] Mam, we weten wat we doen hoor, geen zorgen.

About me

I got my B.Sc. and M.Sc. in Aerospace Engineering at Delft University of Technology (2007 and 2012, respectively). My M.Sc. project focussed on human-in-the-loop control behavior in flight simulation at the Control & Simulation group led by professor Max Mulder, supervised by dr.ir. Daan Pool and dr.ir. Ana Rita Valente Pais. During my M.Sc., I also spent several months at TNO, performing research on spatial disorientation in the Desdemona flight simulator, and MIT, developing a search algorithm to support UAV operators in identifying objects in aerial footage.

After my M.Sc. degree, I worked as a software engineer at Simendo, where I developed virtual reality games for minimally invasive surgery in collaboration with surgeons at various hospitals. I then got accepted to MIT's Aeronautics and Astronautics graduate program in which I studied how our sensorimotor system adapts to changing gravity levels during spaceflight.

Humans interacting with robots, intelligent systems, or complex environments has interested me since my M.Sc. thesis. I, therefore, took the opportunity to research haptic human-human interaction with applications to human-robot interaction at the University of Twente for my Ph.D. under the supervision of professor Herman van der Kooij, dr. Edwin van Asseldonk, and dr.ir. Arno Stienen.

I enjoy working with students, being involved in education, and learning new skills, ranging from programming in several languages to mechanical design.

In my spare time, I enjoy rock climbing, mountaineering, hiking, and mountain biking. If only The Netherlands had some actual mountains...

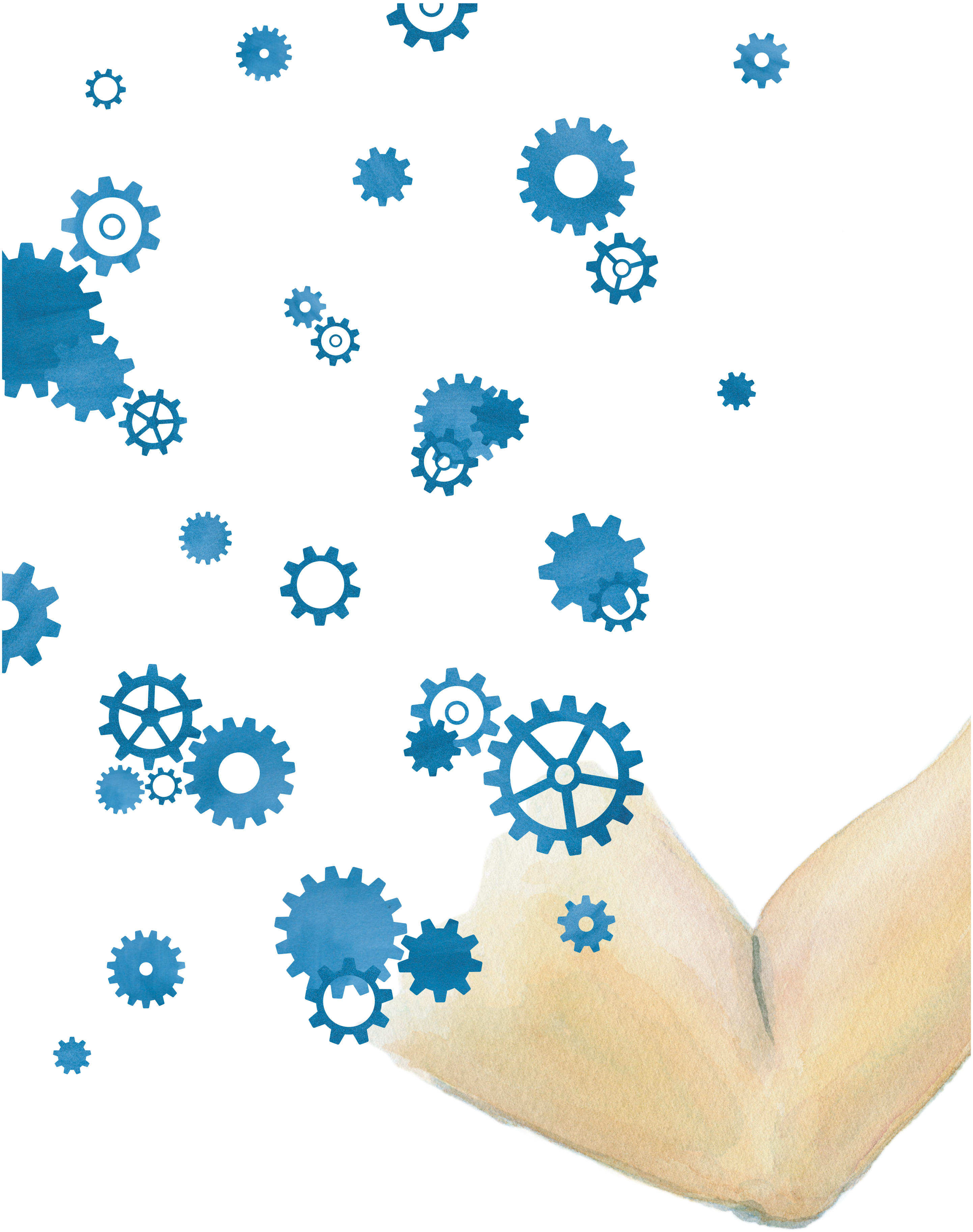

Propositions
belonging to the thesis:

Haptic human-human interaction

Motor learning & haptic communication

Niek Beckers

1. People are stubborn, they would rather hold on to their own plan at the cost of expending more energy than collaborating with a partner that they do not fully trust or understand (in haptic interaction and in real life).
2. Intuitive physical interaction strategies between human and robot cannot be designed without considering haptics, but truly intuitive and natural human-robot interaction is impossible to achieve through haptics alone.
3. To fully exploit the potential of haptics in promoting motor learning, the trainee and trainer should be aware of what is happening and what is expected of them.
4. To understand how humans collaborate, we must construct more complex models, but the more complex the model, the harder it is to understand how humans collaborate (based on Bonini's paradox).
5. Publication pressure and grant competition encourage moonshot research, which does not benefit the overall correctness of scientific output.
6. One swallow does not make a summer: if the scientific community was really serious about itself, it should stimulate and reward reproduction studies more.
7. People who refuse to accept a scientific consensus (about climate change and vaccination) and hold their own opinion as the truth should not be allowed to make decisions on those matters that affect others or the planet.
8. Selecting an optimal strategy requires its own optimal strategy.
9. Eight propositions are sufficient.

The propositions are considered to be opposable and defendable and have been approved as such by the promotor prof.dr.ir. H. van der Kooij and co-promotor dr. E. van Asseldonk.

Stellingen

behorend bij het proefschrift:

Haptic human-human interaction

Motor learning & haptic communication

Niek Beckers

1. Mensen zijn koppig, ze houden liever vast aan hun eigen plan ten koste van meer verbruikte energie dan samen te werken met een partner die ze niet volledig vertrouwen of begrijpen (in haptische interactie en in het echte leven).

2. Intuïtieve fysieke interactiestrategieën tussen mens en robot kunnen niet worden ontworpen zonder rekening te houden met haptics, maar echt intuïtieve en natuurlijke mens-robot interactie is niet haalbaar door alleen op haptics te concentreren.

3. Om het potentieel van haptics volledig te benutten voor het bevorderen van motorisch leren moeten de leerling en de leraar op de hoogte zijn van wat er gebeurt en wat van hen wordt verwacht.

4. Om te begrijpen hoe mensen samenwerken moeten we complexere modellen bouwen, maar hoe complexer het model, des te moeilijker het wordt om te begrijpen hoe mensen samenwerken (gebaseerd op Bonini's paradox).

5. Publicatiedruk en subsidieconcurrentie moedigen ‘moonshot’ onderzoek aan, wat de algehele correctheid van de wetenschap niet ten goede komt.

6. Een zwaluw maakt nog geen zomer: als de wetenschappelijke gemeenschap zichzelf echt serieus zou nemen, zou ze reproductiestudies meer moeten stimuleren en belonen.

7. Mensen die weigeren een wetenschappelijke consensus (bijvoorbeeld over klimaatverandering en vaccinatie) te accepteren en hun eigen mening als de waarheid zien, zouden geen beslissingen mogen nemen over deze zaken die anderen of de planeet treffen.

8. Het selecteren van een optimale strategie vereist een eigen optimale strategie.

9. Acht stellingen zijn voldoende.

Deze stellingen worden opponeerbaar en verdedigbaar geacht en zijn als zodanig goedgekeurd door de promotor prof.dr.ir. H. van der Kooij en de co-promotor dr. E. van Asseldonk.